Naturally grown timber elements for load-bearing structures: *Methods for modeling, structural design, and construction.*

Von der Fakultät für Architektur
der Rheinisch-Westfälischen Technischen Hochschule Aachen
zur Erlangung des akademischen Grades eines
Doktors der Ingenieurwissenschaften
genehmigte Dissertation

vorgelegt von

Kevin Moreno Gata
aus Alcalá de Henares, Spanien

Berichter: Univ.-Prof. Dr.-Ing. Martin Trautz
Univ.-Prof. Dr.-Ing. Jan Knippers
Univ.-Prof. Dr.-Ing. habil. Sven Klinkel

Tag der mündlichen Prüfung: 24. November 2025

Diese Dissertation ist auf den Internetseiten der Universitätsbibliothek online verfügbar.

Naturally grown timber elements for load-bearing structures: Methods for modeling, structural design, and construction

Kevin Moreno Gata

Doctoral Dissertation

submitted in fulfillment of the requirements for the academic degree

Doktor der Ingenieurwissenschaften (Dr.-Ing.)

at RWTH Aachen University

Examination Day: 24 November 2025

Members of the Examination Board

Chair of the Examination Board

Univ.-Prof. Dr. techn. Sigrid Brell-Cokcan
Chair of Individualized Production in Architecture, RWTH Aachen University, Germany

Supervisor

Univ.-Prof. Dr.-Ing. Martin Trautz
Chair of Structures and Structural Design, RWTH Aachen University, Germany

Additional Members of the Examination Board

Univ.-Prof. Dr.-Ing. Jan Knippers
Institute of Building Structures and Structural Design, University of Stuttgart, Germany
Univ.-Prof. Dr.-Ing. habil. Sven Klinkel
Chair of Structural Analysis and Dynamics, RWTH Aachen University, Germany

Funding Acknowledgement

This dissertation was funded by the German Research Foundation (Deutsche Forschungsgemeinschaft, DFG) under Project No. 512769030. It also received financial support from the Zukunft Bau research initiative under Project No. 10.08.18.3-22.15, as well as additional support from the Faculty of Architecture, RWTH Aachen University.

Published in: 2025

© 2025 Kevin Moreno Gata



Oak tree crown, Aachen Forest (50.678783, 6.157209)

Abstract

This dissertation investigates the potential of naturally grown timber as a structural material, focusing on its geometric and mechanical characteristics to inform architectural design. Contrary to the conventional approach of designing first and then sourcing materials, this research adopts an inverse methodology: it begins by analyzing inherent natural design patterns and subsequently applies these insights to the conception of architectural structures.

This study bridges multiple disciplines to propose a methodology that integrates tree analysis, growth pattern interpretation, scanning, geometric modeling, material characterization, and structural design across scales—from individual growth behavior to full-scale assemblies. Computational tools are employed to simulate the structural behavior of the material, enabling performance-driven design decisions that account for fabrication feasibility and resource availability.

This work contributes a multi-scalar analytical framework and a set of custom joinery strategies tailored to irregular timber geometries. Structural optimization methods are developed for both element positioning and connection design. Through case studies, prototypes, and workshops, the methodology is tested in academic and applied contexts. Overall, this dissertation promotes a material-driven design philosophy, demonstrating how raw timber can serve as a viable and sustainable alternative for load-bearing architectural applications.

Kurzfassung

Diese Dissertation untersucht das Potenzial natürlich gewachsenen Holzes als Baustoff, mit Fokus auf dessen geometrische und mechanische Eigenschaften zur Unterstützung architektonischer Entwurfsprozesse. Anstatt mit einem formalen Entwurf zu beginnen und anschließend Material auszuwählen, verfolgt diese Forschung einen umgekehrten Ansatz: Die natürlichen Gestaltungsprinzipien werden analysiert und auf die Konzeption von Tragwerken angewendet.

Die Arbeit vereint verschiedene Disziplinen und entwickelt eine Methodik, die Baumstrukturanalyse, Wachstumsmusterinterpretation, Scanning, geometrisches Modellieren, Materialanalyse und Tragwerksentwurf über Maßstabsebenen hinweg integriert – von wachstumsbedingtem Verhalten bis hin zu großformatigen Konstruktionen. Rechnergestützte Werkzeuge dienen dazu, das strukturelle Verhalten des Materials abzubilden und gestalterische Entscheidungen auf Grundlage von Leistungsfähigkeit, Fertigungstauglichkeit und Materialverfügbarkeit zu ermöglichen.

Die Dissertation liefert einen multiskalischen Analyseansatz sowie eine Reihe maßgeschneiderter Verbindungstechniken für unregelmäßige Holzgeometrien. Optimierungsmethoden werden für die Positionierung einzelner Elemente und die Detalierung der Verbindungen entwickelt. Anhand von Fallstudien, Prototypen und Workshops wird die Methodik in akademischen und praktischen Kontexten überprüft. Insgesamt plädiert die Arbeit für einen materialorientierten Entwurfsansatz und zeigt, wie roh belassenes Holz eine tragfähige und nachhaltige Alternative im architektonischen Tragwerksbau darstellen kann.

Acknowledgements

I would like to express my sincere gratitude to all those who have accompanied me on this journey — dear friends, colleagues, professors, and students.

This dissertation marks the conclusion of six years of academic work as a research associate and assistant lecturer at the Chair of Structures and Structural Design. During this time, I had the opportunity to develop, plan, and refine a methodology that supported my development as a researcher across multiple scales. The wide range of research projects at the chair, along with teaching duties, workshops, and exchanges with other institutions, have greatly influenced and enriched my work. These experiences have shaped both my academic path and the work presented in this thesis.

First, I am deeply grateful to my supervisor, Professor Martin Trautz, for giving me the opportunity to work and carry out independent research in the interdisciplinary fields of structural design, geometry modelling, and timber analysis. He placed great trust in me and supported my work, allowing me the freedom to explore new ideas — a true "sandbox" environment for both research and teaching, as a university ideally should provide.

I am also thankful to Team Trako — my colleagues at the Chair of Structures — who shared their knowledge and supported me throughout this process. What began as professional collaboration has developed into strong friendships beyond the university. I sincerely hope this continues for many years to come. In particular, I would like to thank Dana Saez, Denis Grizmann, and Alex Seiter. My gratitude also extends to colleagues and former colleagues Malik Qdeimat, Juan Musto, Andrija Pranjic, Thorsten Pofahl, and Hans-Willi Heyden for their valuable discussions and generous collaboration. My thanks also go to the student assistants — Sheldon Stephens, Raman Suliman, Viktor Wages, Tobias Grüters, and Owen Zeipelt — who shared the ambition and enthusiasm that drove this research. I am equally grateful to the many students who joined my seminars, participated in my courses, or chose me as a thesis advisor. Their curiosity and engagement were essential and reflect the core mission of the university.

I would like to thank the German Research Foundation (DFG) and BBSR Zukunft Bau for funding this research. Their support made it possible to build new academic collaborations. One key result of this was the interdisciplinary work with Professor Sven Klinkel, who co-supervised the project. From this collaboration, a long-term research partnership also began with Florian Spahn. Our many discussions on hypotheses and plant growth modelling were essential to the development of this work. I am grateful not only for the scientific exchange but also for the friendship that has grown from it — and I truly hope it continues in the future.

Special thanks go to the forestry team at Wald und Holz NRW, especially to Andreas Wintraken from the Regionalforstamt Rureifel-Jülicher Börde, Forstbetriebsbezirk Aachen, who served as our main contact for forest-related matters. His support in establishing connections — including with the Landvogt Forestry Company in Aachen-Sief and the Aachener Stadtgärtnerei on Krefelder Straße — was essential for accessing the necessary material. He also actively helped bring our research into the public sphere, notably through the installation of the Growing Bridge in Mausbach.

I would also like to thank the members of my thesis committee: Professor Sigrid Brell-Cokcan, who kindly agreed to chair the defense, Professor Jan Knippers, who travelled to take part in the examination and provided valuable feedback, and Professor Sven Klinkel, who also served on the examination committee. I am very grateful for their time, support, and evaluation of this work.

I also wish to thank my great friend and guiding influence, Professor Felix Amtsberg, who introduced me to a deep and lasting interest in academic research on digital fabrication in architecture during our first meeting at the Digital Structures Lab (Professor Caitlin Mueller, MIT) — a fortunate encounter that not only shaped the direction of my work but also inspired me to pursue a doctoral degree. Our long-standing friendship and shared curiosity have been a continuous source of both academic and personal support.

Finally, I owe my deepest gratitude to my partner, fiancée, and constant source of support, Kateryna Babiichuk. Her understanding, advice, and encouragement — especially her belief in me and her conviction that I could commit to and complete this work — were essential during the final stages of this journey. I also dedicate this achievement to my parents, Remedios Gata Gamero and Antonio Moreno Ato, to my sister, Sofía Moreno Gata, and to my aunt, Isabel Gata Gamero, for their steady belief in me.

Contents

1 Introduction **1**

1.1 Overview . . . 1

1.2 Hypothesis . . . 1

1.3 Research Context . . . 2

1.4 Personal background and motivation . . . 2

1.5 Research questions . . . 3

1.6 Research Objectives . . . 3

1.7 Thesis Structure . . . 4

1.7.1 Thesis Domains . . . 4

1.7.2 Projects . . . 6

1.8 Methodology . . . 10

1.8.1 Process Structure . . . 10

1.8.2 Research Methods . . . 13

2 State of the art **15**

2.1 Integrating Naturally Grown Timber . . . 16

2.1.1 Context of Timber Structures . . . 16

2.1.2 Advances in Timber Construction Techniques . . . 17

2.1.3 Overview of Naturally Grown Timber . . . 17

2.1.4 Historical Context and Traditional Techniques . . . 18

2.1.5 Current Trends . . . 18

2.2 Computational Frameworks . . . 20

2.2.1 Architectural Geometry and Engineered Timber Systems . . . 20

2.2.2 Manufacturing and Fabrication Processes for Raw Timber . . . 21

2.2.3 Matching Algorithms for Material Allocation . . . 22

2.2.4 Limitations in Design-to-Simulation for Naturally Grown Timber . . . 23
2.3 Structures by Nature . . . 23
2.3.1 Interdisciplinary Foundations and Biomimetics . . . 24
2.3.2 Structural Adaptation in Trees . . . 25
2.3.3 Formal Modeling of Growth Processes . . . 26
2.3.4 Tree-Like Structures and Living Construction Systems . . . 26
2.4 Data Acquisition — Scanning Techniques . . . 27
2.4.1 Basis of Scanning . . . 27
2.4.2 Image-Based Methodologies . . . 27
2.4.3 Non-Invasive Physical Scanning Methods . . . 28
2.5 Tree Growth and Forest . . . 29
2.5.1 Tree Growth and Forest Area . . . 29
2.5.2 Determinants of Tree Growth and Tree Differentiation . . . 31
2.5.3 Tree Growth Observations . . . 33
2.5.4 Timber Supply Chain and Grading Rules . . . 34
2.6 Material Properties . . . 37
2.6.1 Tree Growth and Mechanics . . . 37
2.6.2 Reaction Wood and Material Differentiation . . . 37
2.6.3 Summary: MOE–Density Correlation in Central European Hardwoods 38
2.7 Potential Approach for a Supply Chain and Timber Analysis . . . 38

3 Geometric Methods and Modeling 41
3.1 Tree Growth . . . 42
3.1.1 Types of Tree Growth . . . 42
3.1.2 Observation Strategies of the Tree Growth . . . 45
3.2 Methods for Geometry Adquisition . . . 48
3.2.1 Geometrical definitions . . . 48
3.2.2 3D Acquisition: Scanning and Image-Based Methodologies . . . 49
3.2.3 Datasets . . . 51
3.2.4 Tree Data Adquisition . . . 54
3.2.5 Mesh generation and topology process . . . 56
3.3 Tree Modeling . . . 60
3.3.1 Tree Geometry Model . . . 61

3.3.2 Analysis . . . 66
3.4 Three-Dimensional Raw Timber . . . 69
3.4.1 Pre-processing . . . 69
3.4.2 Geometrical Analysis for Raw Timber Elements . . . 70
3.4.3 Segmentation of 3-Dimensional Raw Timber into 2-Dimensional Elements . . . 74
3.5 2D Raw Timber . . . 76
3.5.1 2D Object Scanning Methodologies . . . 76
3.5.2 Data Acquisition from Raw Photos . . . 76
3.5.3 2D Automation Based on Processed Photos . . . 76
3.6 Subdivision Modeling . . . 78
3.6.1 Subdivision Model for Bifurcated Elements . . . 81
3.7 Conclusions on Geometrical Analysis and Modeling . . . 83

4 Growth and Material Mapping **85**
4.1 Geometric-Relevant Material Properties . . . 86
4.1.1 Acquisition of Material Properties . . . 87
4.1.2 Definition of the Material-Integrated Model . . . 88
4.2 Tree Growth Analysis for Raw Timber Assessment . . . 93
4.2.1 Branch-Level Structure . . . 93
4.3 Mechanical Properties . . . 97
4.3.1 Material Characterization . . . 97
4.4 Non-destructive Testing for Raw Timber . . . 100
4.4.1 Testing Approach . . . 100
4.4.2 Preliminary Considerations . . . 100
4.4.3 Construction of the Testing Setup . . . 103
4.5 Conclusions on Material Mapping . . . 108

5 Structural Design With Raw Timber **111**
5.1 Structural Design . . . 112
5.1.1 Definition of Structural Elements . . . 113
5.2 Structural Optimization Methods . . . 115
5.2.1 Matching methodology . . . 116

5.2.2 Joint Positioning Optimization For Bar-Type Structures 121
5.3 Simulation of Structural System 125
5.3.1 Simulation of Structural Elements 125
5.4 Geometrical Growing Simulation 127
5.5 Conclusion 127

6 Construction Methods **129**
6.1 Modeling Construction Applications 130
6.1.1 Classification of Construction Integration of Naturally Grown Timber . 130
6.1.2 Scalability, Geometric Constraints, and Cross-Sectional Analysis . . . 134
6.2 Construction Design 135
6.2.1 Modeling Joints 135
6.2.2 Connections Catalogue: Custom Joinery for Naturally Grown Timber . 136
6.2.3 Design of Structural LRS Panels 140
6.2.4 Fabrication and Assembly Techniques 143
6.3 Case Studies and Built Demonstrations 144
6.3.1 Case Study Design 1: Forest Pedestrian Bridge 144
6.3.2 Case Study 2: Sandwich Panel Application — The ReGrowth Pavilion . 153

7 Conclusion **161**
7.1 Overview 161
7.2 Restatement of Aims 161
7.3 Summary of Findings 162
7.3.1 Geometrical Modeling 162
7.3.2 Material Mapping 162
7.3.3 Structural Design 162
7.3.4 Construction Methods 163
7.3.5 Demonstrative Constructions 163
7.3.6 Interdisciplinary Workflow 163
7.4 Answering the Research Questions 163
7.5 Limitations 165
7.6 Perspectives and Future Outlook 165
7.6.1 Supply Chain 165

7.6.2 Tree Growth Model and Simulation . . . 165
7.6.3 Construction Demonstrations . . . 166
7.6.4 Agenda for Naturally Grown Timber Research . . . 166

References **167**

List of Figures **195**

List of Tables **197**

A Appendix **199**
A.1 Geometrical Growth Simulation . . . 199
A.1.1 Self-Formation Geometry Optimization . . . 199
A.2 Design of a Testing Machine . . . 203
A.2.1 Calculation of Test Span and Diameter Limits . . . 203
A.3 Growing Experiments . . . 205

B Technical Material **207**
B.1 Overview . . . 207
B.2 List of Technical Applications and Plugins . . . 207
B.3 Attached in Chapter 3 . . . 209
B.3.1 Results of Tree Global Growth Analysis . . . 209
B.3.2 Results of Tree Geometry Analysis and Library . . . 211
B.3.3 Raw Timber Library. Geometrical Analysis . . . 217
B.3.4 Raw Wood Library 2D Segmentation . . . 218
B.4 Attached in Chapter 4 . . . 219
B.4.1 Micro-CT Scan Overview . . . 219
B.4.2 Macro-CT Scan Overview . . . 220
B.5 Attachments in Chapter 5 . . . 221
B.6 Attached in Chapter 6 . . . 223
B.6.1 Construction Details . . . 223
B.6.2 Built Prototypes . . . 224
B.6.3 Growing Bridge . . . 227
B.6.4 reGrowth Pavilion . . . 233
B.6.5 Academic Works . . . 236

C Research & Academic Projects **237**

C.1 Research Projects 237

C.2 Contributions to Academic Projects and Thesis 238

C.3 Scientific Results 240

C.3.1 Peer-Reviewed Journals and Book Chapters 240

C.3.2 Peer-Reviewed Conference Papers 241

C.3.3 Conference Proceedings and Other Contributions 242

Indices and Acronyms

Latin Indices

Symbol	Unit	Meaning	from Page
a	–	base line in a bifurcation or in a curved element	72
A	–	point in a base line	74
b	–	base line in a bifurcation	72
B	–	point in a base line	74
c	–	base line in a bifurcation	72
c_g	–	center curve of geometry	58
c_G	–	center curve of growth or pith	91
c_M	–	center curve of mass	91
C	–	point in a base line	72
C_g	–	center of geometry	49
C_G	–	center of growth	49
C_M	–	center of mass	49
$\lvert\vec{d}\rvert$	mm	deformation during testing	107
D	m	diameter	95
$\mathcal{D}$	m	cost matrix	119
f_m	$\mathrm{kN\,cm^{-2}}$	characteristic bending strength	101
F	kN	force	99
$\vec{g}$	–	weight vector direction	66
G	–	geometry element	120
$\mathcal{G}$	–	geometry matrix	120
h	m	height or thickness	74
i	–	count, number of sections in a timber element	116
I_z	$\mathrm{m^4}$	second moment of area	96
j	–	count, number of sections in a target element	118
K	cm	curvature or % curvature coefficient	62
k_{mod}	–	modification factor	103
L	m	length	63
LC	–	load case	146
m	–	count or number in a target element	118
M	$\mathrm{kN\,m}$	moment	147
$\vec{M}$	–	moment field	118
$\vec{m}$	–	moment vector direction	119
n	–	count or number in a timber element	117
O	–	origin or centroid	69
$\vec{p}$	–	growth vector	94
R	m	radius	92
s_i	–	section (cross-section index)	63
$\vec{t}$	–	tropism vector direction	43
T	–	target element	120
$\mathcal{T}$	–	target matrix	120
u	–	parameter subdivisions	116
v	–	parameter subdivisions	118
w	m	width / deflection	136
W	$\mathrm{m^3}$	section modulus of inertia	95
x, y, z	m	spatial coordinates	70

Greek Indices

Symbol	Unit	Meaning	from Page
α, β, γ	$^\circ$	dihedral angle	72
γ_M	–	safety factor	103
π	–	coplanar plane	72
$\lvert\vec{\delta}\rvert$	mm	displacement from pith	79
θ	$^\circ$	dihedral angle in a polar system	74
λ	$\mathrm{g\,cm^{-3}\,m}$	material density	91
σ	$\mathrm{N\,mm^{-2}}$	stress	95
ϵ	–	threshold dihedral angle difference	74
ζ	mm	vector growth amplitude	200
ζ, η, ξ	–	longitudinal, tangential and radial parameters in a GS-BIGA model	126

Acronyms

Acronym	Meaning	from Page
AEC	Architecture, Engineering & Construction	2
AGB	Aboveground Biomass	32
CAO	Computer-Aided Optimization	25
CAD	Computer-Aided Design	41
CLT	Cross-Laminated Timber	17
CNC	Computer Numerical Control	17
CT	Computed Tomography	29
DBH	Diameter at Breast Height	32
DLT	Dowel-Laminated Timber	17
ELDAT	Elektronischer Datenaustausch Holzdaten	35
FEA	Finite Element Analysis	26
FSC	Forest Stewardship Council	34
Glulam	Glue-Laminated Timber	17
IBMR	Image-Based Modeling and Rendering	27
L-System	Lindenmayer System	26
LRS	Leafy-Raw Wood Sandwich	140
LiDAR	Light Detection and Ranging	32
MFA	Microfibril Angle	37
MOO	Multi-Objective Optimization	121
MRI	Magnetic Resonance Imaging	28
MS	Matching Score	119
NeRFs	Neural Radiance Fields	28
NGT	Naturally Grown Timber	1
NURBS	Non-Uniform Rational B-Splines	13
NRW	North Rhine-Westphalia	52
PEFC	Programme for the Endorsement of Forest Certification	34
QSM	Quantitative Structural Model	33
RVR	Rahmenvereinbarung für den Rohholzhandel in Deutschland	34
RWTH	Rheinisch-Westfälische Technische Hochschule	i
GSBIGA	Generalised Scaled Boundary Isogeometric Analysis	126
SFB TRR	Sonderforschungsbereiche & Transregios (TRR)	24
SIA	Statisch Integrierte Abschätzung	33
SKO	Soft Kill Option	25
SubD	Subdivision Geometry	49
TLS	Terrestrial Laser Scanning	52
UAV	Unmanned Aerial Vehicle	32
LAP	Linear Assignment Problem	119

Chapter 1

Introduction

1.1 Overview

This dissertation investigates the use of naturally grown timber (NGT) as a load-bearing material in contemporary construction. As the construction and engineering industries shift toward bio-based materials, wood is gaining attention for its sustainability and resource efficiency. Unlike conventional timber, irregular components such as tree-branch segments offer unique structural potential but are often overlooked due to their complexity and non-standard geometry. This work proposes a systematic methodology for modeling these natural elements—first by analyzing their intrinsic geometry and growth, then by evaluating their applicability in construction. The goal is to develop practical workflows that enable the integration of naturally grown timber into sustainable architectural and structural design.

1.2 Hypothesis

This dissertation hypothesizes that naturally grown timber elements—particularly in their round, unprocessed form—can be effectively integrated into load-bearing structures by leveraging their anisotropic characteristics and inherent geometric features. The natural curvature and fiber orientation of such elements may offer structural advantages for load distribution and stability. To enable their practical use, a systematic methodology for selection, geometric analysis, and structural modeling is essential. Despite their irregularity, the application of advanced imaging and simulation tools makes their integration into architectural and engineering practice both feasible and beneficial.

1.3 Research Context

This research is situated within the growing demand for environmentally responsible materials in architecture and construction. Timber has re-emerged as a key material in the AEC (Architecture, Engineering, and Construction) sector due to its favorable strength-to-weight ratio, carbon-sequestering properties, and compatibility with prefabrication techniques. However, conventional timber supply chains—particularly those dependent on softwoods—face increasing challenges due to climate change, pest outbreaks, and rising material costs. Softwoods, in particular, are less suited to warmer climates, affecting their long-term viability.

As a result, interest has shifted toward native and locally grown hardwood species, as well as irregular tree components from crowns, which are typically excluded from direct engineering applications. Although these elements offer structural potential, they pose challenges due to their non-standard geometries and variable material properties.

This context aligns with principles of bionic and biomimicry design and natural structures, as proposed by Frei Otto [1], which advocate for construction approaches inspired by natural growth processes. The use of naturally grown, irregular timber supports this paradigm by moving away from standardization and toward material-led design.

Recent advances in digital workflows—integrating image-based methods and parametric modeling—now enable the analysis and integration of non-standard timber into architectural practice. Cross-disciplinary collaboration between forestry, materials science, and computational design is generating new opportunities to valorize materials previously considered waste.

1.4 Personal background and motivation

The design of medium-scale constructions is influenced by a persistent interest in natural materials, especially hardwood. Architectural designs may reflect wood's natural variability, utilizing its differences in texture and growth direction to improve both its aesthetic and functional aspects. Practical experience with hardwood species has resulted in an awareness of their structural potential, which, when understood, can inspire innovative construction techniques.

The investigation of tree growth mechanisms and their adaptation to environmental factors provides significant insights for structural design and engineering. Collaboration across forestry management, material science, and computational design has led to the development of the digital modeling and fabrication techniques presented in this dissertation.

Modern timber construction, which primarily relies on standardized products and cross-sections, often overlooks the structural potential that naturally grown wood can offer. Additionally, broad-leaf trees, due to their spatial growth patterns, often result in roughly 50% of the tree being suitable for these standardized products, with the rest being discarded at the initial stages of processing. This serves as a key motivation for this research, aiming to bridge the gap between sustainable concepts in tree and forestry research and their effective integration into structural design practice.

1.5 Research questions

- How can the inherent irregularities and growth patterns of naturally grown timber be systematically documented, analyzed, and modeled for integration into load-bearing architectural structures?
- What design and simulation methodologies are most effective for evaluating the mechanical capabilities of naturally grown hardwood in structural applications?
- How can advanced digital techniques, such as photogrammetry, 3D laser scanning, and finite element analysis, facilitate the adaptation of non-standardized timber components into standardized construction workflows?
- What are the specific structural advantages and limitations of using naturally grown timber in comparison to conventional engineered wood products, especially in terms of load distribution and material efficiency?
- How can naturally grown timber, or indeed tree crowns, be incorporated into circular and sustainable design practices to reduce material waste, particularly for species and tree parts traditionally overlooked in timber construction?
- What fabrication and assembly techniques are necessary to accommodate the unique geometries of naturally grown timber in a way that optimizes their load-bearing capabilities?

1.6 Research Objectives

This research aims to develop a process for studying wood within trees and exploring its application in construction. The objectives of the thesis are structured into three main areas:

Objective 1: To Identify, Document, and Evaluate Naturally Grown Timber Elements

- Identify the right tree branches and their corresponding diameters for use in structural applications.
- Digitally capture the geometry of the selected elements using photogrammetry and 3D laser scanning.
- Evaluate geometric properties and growth patterns in relation to material behavior.
- Assess mechanical and physical properties through non-destructive and destructive testing to understand structural potential.

Objective 2: To Develop Digital Modeling and Structural Analysis Methods

- Construct digital models that represent the geometry of natural wood elements.
- Analyze load paths and explore strategies for optimizing joints and connections.
- Apply structural analysis to evaluate the performance of natural timber in engineering applications.

Objective 3: To Design and Fabricate Scaled Prototypes and Demonstrators Integrating Irregular Timber

- Develop construction, fabrication and assembly methods for integrating irregular timber into bar-type or sandwich-panel systems.
- Design and construct scaled prototypes—such as canopies, bridges, roofs, and wall panels—to demonstrate feasibility in modular construction.

1.7 Thesis Structure

This thesis is developed through a series of overlapping projects conducted over a six-year period at the Chair of Structures and Structural Design (Trako), each situated within distinct experimental domains. Owing to the interdisciplinary nature of the research, the projects span multiple fields and locations. Following this section, the research methodology is presented. The thesis starts with a review of the state of the art in computational design, with a particular focus on timber construction methods, identifying the primary research trajectories. Subsequent chapters describe the conducted work and experimental approaches. The thesis concludes with an analysis of the constructed prototypes, addressing the research questions and outlining broader future perspectives, thereby proposing directions for continued exploration.

The overall structure is organized around the intersection of various disciplines, illustrated in Figure 1.1. Their integration is distributed across Chapters 3 to 6 and is explored at varying levels of depth, contributing both to the formulation of answers to the research questions and to the development of additional concepts for future investigations.

1.7.1 Thesis Domains

The domains of the thesis are divided into four main pillars, developed through an interdisciplinary approach of a funded research project [2], primarily hosted by the Trako Chair, with support from colleagues at LBB (Chair of Structural Analysis and Dynamics) and IBG-2 (Institute for Bio- and Geosciences Plant Sciences) from Jülich Research Center, and in collaboration with external institutions such as the foresters of NRW (Landesbetrieb Wald und Holz NRW) and additional support from Uni Stuttgart and Uni Göttingen:



Figure 1.1: Interaction between disciplines. The themes are addressed at varying levels of depth throughout the thesis.

- **I. Geometric Analysis** focuses on creating a comprehensive geometric framework for modeling naturally grown timber, particularly complex forms such as curved and bifurcated elements. This digital and geometric domain is essential for integrating these forms into various disciplines, enabling further material analysis and simulation.
- **II. Growth Mapping** involves evaluating essential material properties of the established timber geometries, including density, growth direction, and internal structure. It uses non-destructive testing methods for acquiring material data without compromising the material.
- **III. Structural Design** defines key structural principles for application. It is supported by optimization methods such as matching algorithms and joint positioning strategies.
- **IV. Construction Methods** explores practical applications across multiple proposals, including joint details, fabrication processes, and assembly techniques.

1.7.2 Projects

The themes arise from experimental projects within the mentioned domains, which are interconnected and multi-faceted. The following chapters of the thesis explore these aspects, providing a complete picture and establishing their interconnection.

Modeling Raw Timber



The modeling of raw timber allows extensive analysis of its geometric and material parameters, and thus its mechanical behaviour. This process forms the basis for many of the projects cited in this work and facilitates interdisciplinary collaboration.

Self-Formation Simulation

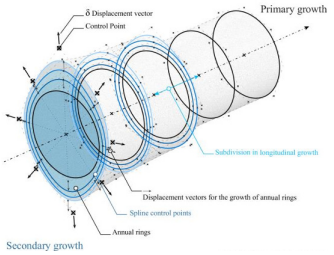

Growth simulation makes it possible to estimate how cross-sections have developed in the tree based on geometric considerations. These considerations also help to determine how a tree's cross-section grows depending on the loads it must bear.

Tree Structure Modeling

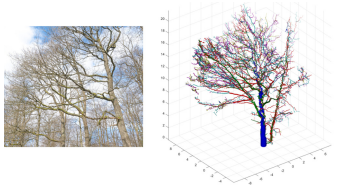

Structural tree models break down the tree into its hierarchical elements, providing a detailed understanding of its structure. This aids in organizing and analyzing the tree before felling, enabling digital tracking of its growth and development. The work is done in collaboration and datasets from the Spatial Structures and Digitization of Forests group at the University of Göttingen.

Growth Experiments

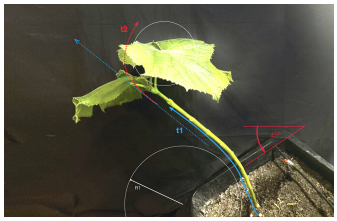

Experiments with growing plants help to understand the conditions for natural, controlled growth. Passive growth, like that caused by tropisms, happens naturally, while active growth is induced by applying external forces to shape growth patterns. This is visible in the secondary growth near the stem's base.

Non-Invasive Analysis

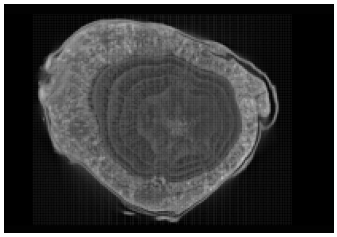

Documentation methods based on scanning techniques—such as 3D scanning, photogrammetry, or non-invasive medical imaging (CT or MRI)—enable the acquisition of material properties like density and fiber orientation without damaging the specimens. This work was carried out in collaboration with colleagues from the Jülich Research Centre, IGB-2.

Material Analysis

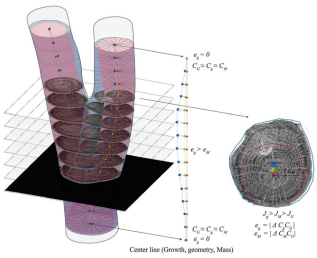

As a next step after imaging, material properties can be mapped in three dimensions by combining them with advanced geometric models. This enables the analysis of local density variations through the integration of CT data with geometric features, providing deeper insight into the distribution of density and biomass within the specimens.

Non-destructive testing

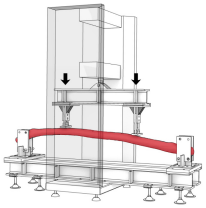

A load testing design is developed for the mechanical behavior analysis of previously collected and scanned elements. This setup allows us to perform a basic check of how the elements resist or elastically deform without breaking or reaching failure.

Mechanical Simulations

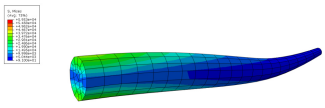

A basic finite element mechanical simulation provides an initial validation of how the timber element may behave under specific loads. This is done by defining the boundary conditions as well as the properties and orientations of the orthotropic material.

Scaled Boundary Isogeometrical Analysis

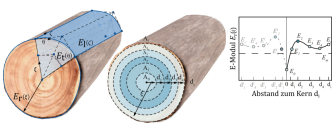

In collaboration with civil engineering colleagues (LBB), a finite element mechanical model based on isogeometric analysis theory was developed. This model enables accurate mechanical formulation using NURBS, building on the geometric models developed in previous projects.

Course: Tree-based constructions

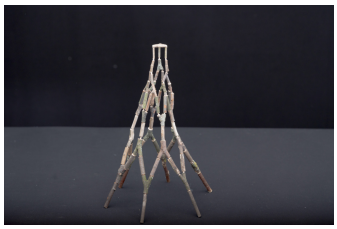

In an architectural course, structural typologies that can be used in constructions are investigated, also providing a foundation for designs that can later be studied or developed into full-scale demonstrations. Various typologies were explored, including towers, shells, and vaults, among others. Additionally, 1:1 scale prototypes of furniture elements were constructed.

Course: Shaped in the Forest



In an interdisciplinary course, structural typologies are investigated from both an architectural and civil engineering perspective. Geometries of local trees from the forest are acquired and transformed into structures, which are later simulated using mechanical models.

Off-knot Timber Joint Design

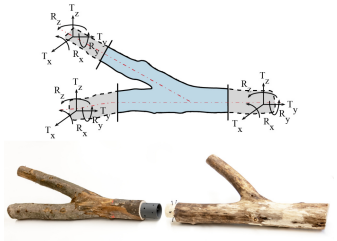

Placing structural nodes in connection elements is common in timber design, but it complicates detailing for large timber structures without metal components. Offsetting the nodes to the bars simplifies the joints and maximizes the mechanical potential of raw timber.

Hybrid Raw Timber: Construction Prototypes



The combination of timber elements continues the off-knot joints approach, where multiple curved branches form constructed bifurcations, connected with fully threaded screws. This enables tailored design solutions and allows for different wood species based on structural needs.

Prototype Sandwich Panels



This project is a constructive timber proposal where raw elements, particularly hardwood, are integrated into the structural core of sandwich panels. These are individually designed to allow for the distribution of specific loads, aligned with the stress patterns provided by the arrangement of the branches.

Exhibition at Zukunfbau Pop-up Campus



The exhibition took place in Aachen in September 2022, where many of the constructive prototypes shown here, along with other scale models and furniture elements, were displayed. The main exhibition piece was the construction of the Canopy Regrowth Pavilion.

Demonstrator reGrowth



The demonstrator was designed using the logic of sandwich panels. An elliptical canopy was created, incorporating various raw elements collected that same year from the Aachen forest. This pavilion was built in cooperation with colleagues from the Institute for Computational Design and Construction (ICD) at the University of Stuttgart, employing augmented reality to assist in the assembly process.

Demonstrator Growing Bridge



As part of a circular construction approach and the use of forest resources, a pedestrian bridge was designed to be installed directly in the forest, spanning over a stream. Various raw timber elements collected from the forest were used, which were scanned and CNC-fabricated on two axes.

Domain	Project
Geometric Analysis	Modeling Raw Timber Tree Structure Modeling Non-invasive Analysis
Growth Mapping	Growth Experiments Material Analysis Non-destructive Testing
Structural Simulation	Self-formation Simulation Mechanical Simulations Scaled Boundary Isogeometric Analysis
Construction Methods	Off-knot Timber Joint Design Hybrid Raw Timber Constructions Sandwich Panels Demonstrator reGrowth Demonstrator Growing Bridge

Table 1.1: Overview of domains and associated projects.

1.8 Methodology

This dissertation applies a **practice-based**, iterative approach to integrating naturally grown timber into load-bearing structures, following a **feedback-driven methodology** that aligns design, modeling, fabrication, and experimental validation. The methodology is grounded in state-of-the-art research to develop new methods and integrate data acquisition, multi-scalar modeling, and collaborative processes among agents to develop, analyze, and refine timber-based structural prototypes.

1.8.1 Process Structure

Feedback Design Chain

The methodology follows a feedback-driven design chain, emphasizing continuous iteration and collaboration across design stages:

- **Early Stage Design:** Begins with a conceptual understanding of naturally grown timber's unique forms and properties, integrating them into initial design ideas.
- **Design Development:** Refinement of digital models based on material characteristics, structural requirements, and aesthetic considerations.

- **Material Analysis:** Involves insights into the material's structural potential.
- **Engineering and Simulation:** Structural performance is analyzed using mechanical simulations to assess load paths and stress distribution.
- **Construction Documentation:** Digital models are adapted for construction detailing, with precise processes prepared to account for timber irregularities.
- **Fabrication and Assembly:** Final fabrication and assembly processes are guided by CNC milling and sensor calibration based on point clouds.
- **Experimental Validation:** Assembled structures undergo testing for real-world load-bearing capacity, providing empirical data to refine and adapt the methodology.

This iterative process supports continuous feedback, allowing each stage to inform and improve subsequent phases.

Agent Participation and Roles

This research involves multiple agents, each contributing specialized knowledge throughout the methodology:

- **Material Scientists (Physics and Material Properties):** Provide insights into timber's physical and mechanical behavior, such as fiber orientation and density, ensuring accurate digital representation.
- **Tree Growth Specialists (Forestry and Ecology):** Contribute expertise on tree development, environmental factors, and sustainable harvesting, identifying underutilized parts like crowns and branches for structural use.
- **Designers and Modelers:** Develop and refine digital models, adapting irregular timber forms into buildable structures while preserving natural geometry.
- **Structural Engineers:** Perform simulations and structural analysis at various scales to ensure performance and compliance with load-bearing requirements.
- **Fabrication Specialists:** Use wood working and milling techniques to fabricate components, translating digital models into accurately shaped timber elements.
- **Educators and Researchers:** Lead workshops and seminars, engaging students and practitioners in modeling, simulation, and fabrication.

This collaborative setup supports a feedback loop, where contributions from each agent improve the overall design and construction process.

Multi-Scalar Modeling Framework

A multi-scalar modeling framework is used to address the complexity of applying naturally grown timber in structural systems, covering interconnected scales. This approach ensures that insights from each scale contribute to the final structural design.

- **Micro Scale (Material Properties):** Analyzes growth orientation, density, and mechanical properties, enabling control over load and biomass distribution.
- **Meso Scale (Timber Elements):** Models individual timber components, accounting for natural geometry, branching, and curvature. This scale supports structural analysis and optimization.
- **Macro Scale (Structural System):** Assesses the full assembly, including construction design, load paths, and overall stability, ensuring performance as a load-bearing system.

Prototype Development and Demonstration

Prototype development is a necessary component of the methodology, providing tangible insights into naturally grown timber's structural capabilities:

- **Scaled Models:** Small-scale prototypes are developed to test the feasibility of digital-to-physical processes, offering insights into joint behavior, detail solutions, and the practicality of fabrication techniques.
- **Full-Scale Demonstrators:** Structures such as research pavilions are constructed to assess timber's real-world application in structural assemblies. These demonstrators provide essential performance data, validating both the timber's strength and the accuracy of simulation models.
- **Project Mapping and Documentation:** All prototypes are documented to track performance data, structural feedback, and any necessary modifications, ensuring that insights from prototypes directly inform future models and full-scale applications.

Educational Initiatives: Seminars and Workshops

Alongside technical research, workshops and seminars engage students and professionals in hands-on, material-driven approaches to design and construction. These formats promote awareness of natural geometries, local resources, and non-standard fabrication, encouraging a shift toward resource- and material-first thinking.

Participants are introduced to digital modeling and mechanical simulation with irregular timber; gain practical experience from material sourcing to CNC-based fabrication and adaptive joinery; and explore sustainable construction methods focused on circular material strategies and low-impact techniques. These initiatives challenge conventional design approaches by encouraging alternatives to standardized systems.

1.8.2 Research Methods

Data Acquisition and Digitization

High-resolution data are collected from raw timber using photogrammetry and laser scanning to capture detailed surface geometries. Recently, Neural Radiance Fields (NeRF) have been introduced to generate accurate 3D reconstructions using machine learning techniques applied to photo sequences.

Post-Processing, Topology and Modeling

The captured data are processed into mesh models and converted into Non-Uniform Rational B-Splines (NURBS), enabling smooth and flexible geometric manipulation.

Simulation Methods

NURBS-based models are used in simulation workflows with colateral impact of this dissertation, including Finite Element Analysis (FEA) and Isogeometric Analysis (IGA), to evaluate structural performance.

Application to Construction Elements

Simulation results guide the refinement of timber element geometry, inform digital fabrication through precision milling, and support physical load testing to verify real-world performance.

Experimental Validation

Digitized, simulated, and fabricated elements are assembled into 1:1 structures, with their performance evaluated through experimental setups to support iterative improvement. Additionally, this integrated approach combines modeling tools with load testing to establish a reliable method for extracting material properties.

Forest as a Raw Material Provider

Forests provide a valuable source of raw material, especially from underutilized components often excluded from standard supply chains. This thesis explores the potential of a *digital forest* through tree geometry analysis, enabling precise documentation of volume and growth over time.

Material acquisition areas were defined in collaboration with forest officials from Wald und Holz NRW, Regionalforstamt Rureifel-Jülicher Börde, Forstbetriebsbezirk Aachen [3]. These

include both private and public forests. Examples include Schmithof (Landvogt Forestry Company, Aachen-Sief, coordinates: 50.683672, 6.157928) and Zweifall, Spießweg, Stolberg (coordinates: 50.714893, 6.287604).



(a) Tree crown (b) Logs and crown branches (c) Reclaimed raw timber

Figure 1.2: Forest and material acquisition.

Tree Growth Control and Maintenance

In urban settings, tree maintenance for landscaping and safety leads to the routine removal of excess parts, typically discarded at municipal dumping sites. With the expansion of green infrastructure, this practice presents a potential raw material source.

In collaboration with local forestry professionals and the tree maintenance team in Aachen, access was granted to the dumping site at *Aachener Stadt-Gärtnerei*, Krefelder Str. 295, 52070 Aachen. This enabled systematic collection and assessment of discarded timber for sustainable construction applications.



(a) Collection of branches (b) Sorting and shredding (c) Wood chips for pellets

Figure 1.3: Stages in dumping site recycling.

Chapter 2

State of the art

The research discussed in this dissertation stands at the intersection of various fields, as reviewed in this chapter, including architectural geometry and parametric modeling, material analysis, and construction engineering.

Timber construction has seen renewed interest, particularly in exploring raw timber for structural use. This review begins with examples of architectural projects that integrate naturally shaped timber, highlighting its potential in built environments. It then examines how theoretical and computational approaches are applied in practice, with a focus on the challenges posed by non-standardized elements. To address these challenges, the literature proposes strategies for modeling irregular timber, including digital methods enabled by advances in parametric design. Recent work explores schematic modeling and image-based data acquisition to capture material and geometric properties non-invasively. The review concludes with a discussion on timber sourcing and grading, emphasizing in hardwoods; and experimental methods for assessing material properties.

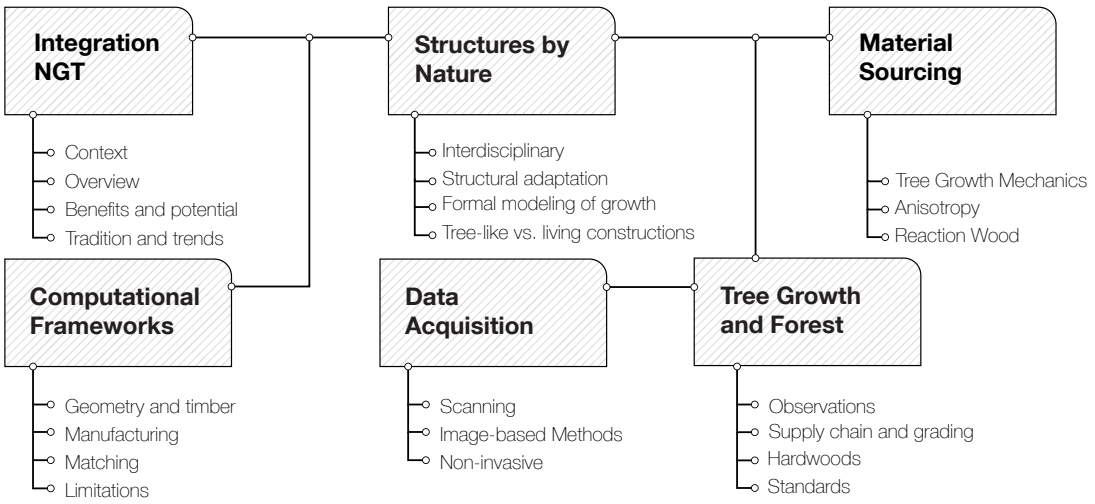

Figure 2.1: Chapter Diagram: Overview of the domains covered in the state-of-the-art review.

2.1 Integrating Naturally Grown Timber

The use of raw and minimally processed timber in architectural structures has long-standing historical and theoretical foundations. In De Architectura, Vitruvius describes how early humans, driven by the discovery of fire and the need for collective protection, built shelters using materials found in nature—mainly trees and branches. These simple constructions, shaped by natural conditions and human reasoning, are considered the first intentional architectural forms and mark a transition from nature to built space [4]. In Book II, Vitruvius also discusses different species of trees, noting how their material and mechanical properties influenced their suitability for architectural use.

A similar idea appears in Marc-Antoine Laugier's Essay on Architecture (1755), where he presents the "primitive hut" (*la petite cabane rustique*) as a basic model of architecture. For Laugier, the hut represents architecture reduced to its essential parts: column, entablature, and pediment. Its value lies in its simplicity, functionality, and connection to natural materials [5]. This idea of the primitive hut also appears in the work of other theorists, who viewed it either as a structural model or as a symbol of cultural and material origins [6]. Some authors pointed to traces of timber construction in ancient Egyptian and Greek architecture, interpreting them as symbolic elements that preserved the memory of earlier wooden structures [7].

In summary, the integration of naturally grown or raw timber into architectural theory and practice reflects a long-standing effort to connect architecture with natural materials, simple construction methods, and symbolic clarity. This historical perspective offers a strong foundation for reconsidering naturally grown timber as a relevant material for contemporary design—one that responds to environmental concerns and recalls architecture's earliest forms.

2.1.1 Context of Timber Structures

Timber has been an essential material in construction for centuries, valued for its natural abundance, versatility, and sustainability. As a renewable resource, timber plays a critical role in sustainable building practices, aligning with global efforts to reduce carbon footprints and environmental impacts [8, 9]. Timber structures, ranging from simple residential homes to complex architectural masterpieces, demonstrate the material's capacity to provide strength, durability, and aesthetic appeal [10, 11]. The resurgence of timber in modern construction is driven by its ecological benefits, including carbon sequestration, low embodied energy, and the potential for sustainable forestry management [12, 13]. As the construction industry seeks to innovate and adapt to environmental challenges, timber's relevance and importance continue to grow, highlighting its role in creating resilient and sustainable built environments.

Another significant advantage of timber is its suitability for prefabrication processes. Due to its relatively soft nature, timber is easy to process and transform, making it ideal for extensive applications in prefabricated construction [14, 15].

2.1.2 Advances in Timber Construction Techniques

The advancement of timber construction techniques has transformed how the material is applied in modern architecture and engineering. Prefabrication enables the efficient production of complex components, facilitating rapid on-site assembly and reducing labor costs. It also improves precision and quality control, contributing to overall sustainability. Innovations in digital design and fabrication further support material efficiency, reduce waste, and enhance structural performance [16]. Techniques such as cross-laminated timber (CLT), glue-laminated timber (glulam), and dowel-laminated timber (DLT) have expanded the possibilities for timber construction, allowing for larger spans, greater load-bearing capacities, and more complex geometries [15, 17]. In parallel, hybrid systems that combine timber with reinforced concrete or steel, for example in composite floor slabs, are increasingly used to improve stiffness, acoustic performance, and fire resistance while still reducing the overall environmental footprint. Advances in timber grading, treatment, and preservation have improved the durability and service life of timber structures. The integration of Building Information Modelling (BIM) and computer numerical control (CNC) machining has further streamlined the design-to-fabrication process, ensuring accuracy and consistency in timber construction projects. Taken together, these technological developments are driving a renewed interest in timber and support a broader adoption of timber-based and hybrid systems as viable alternatives to conventional materials such as concrete and steel, particularly in the context of environmentally responsible building practices.

2.1.3 Overview of Naturally Grown Timber

Naturally grown timber refers to timber that is harvested with minimal processing and used in its natural form, leveraging the inherent shapes and properties of tree growth [18]. This approach contrasts with conventional timber processing, which often involves extensive cutting, shaping, and treating [10]. Naturally grown timber capitalizes on the organic growth patterns and structural adaptations of trees, which have evolved to withstand environmental stresses [19, 20]. This method promotes the use of underutilized parts of trees, such as branches and crooked trunks, which are typically discarded in traditional timber production [21, 22].

Structural and Environmental Benefits

The utilization of naturally grown timber in construction presents both structural and environmental advantages. Structurally, the material retains the natural fiber orientation of the tree, enhancing load-bearing capacity and resilience against stress. Studies indicate that round timber is approximately 50% stronger than milled lumber of equivalent size and exhibits superior fire resistance compared to steel and conventional timber products [23]. Additionally, its organic morphology allows for optimized structural performance, particularly in applications where curvature and bifurcations contribute to load distribution [19, 20].

From an environmental perspective, this approach reduces material waste by incorporating irregularly shaped tree components that are often discarded in conventional forestry practices [24, 25]. By using more of the tree, the overall efficiency of timber harvesting improves, contributing to sustainable forest management and reducing the demand for high-impact processing techniques such as milling and gluing [10].

2.1.4 Historical Context and Traditional Techniques

Beyond its structural performance, naturally grown timber has long offered unique architectural possibilities—particularly in its curved or minimally processed form. Its use spans from early Neolithic settlements to pre-industrial and neoclassical architecture [26, 6]. Early self-built structures were often based on direct observation of nature, with communities adapting available timber into functional forms such as shelters, bridges, and fortifications. These early techniques frequently relied on intuitive processes and the availability of local materials, resulting in construction systems closely aligned with natural geometries [27].

In the European context, pre-industrial log constructions exemplify the systematic use of raw timber. Minimally processed wood was also applied in the fabrication of tools, cranes, and large-scale sailing ships [28]. In Anglo-Scandinavian and medieval contexts, archaeological evidence shows a craft-based understanding of material behavior in both domestic and maritime structures [29]. Notably, Viking-age builders selected curved tree parts—branches and roots—for ship components [30], aligning wood grain with expected stress paths to maximize mechanical performance [31]. These practices are also documented in early timber merchant manuals [32]. Later, similar principles were echoed in the joinery of medieval stave churches in Norway, particularly in elements such as “knees” used to enhance bending resistance.

In the early modern period, forest management practices in Central Europe began to formalize the cultivation and conservation of native timber species [33]. This led to the development of lightweight timber structures, including the iconic timber-framed houses (Fachwerkhäuser) [34]. These buildings often incorporated naturally curved timber elements and joinery techniques, including S-shaped braces, as seen for example in the Glockenstuhl of the Münster zu Konstanz. Such methods persisted until the 18th century, when increasing standardization and the importing of straight-grained timber species began to replace local irregular forms.

Vernacular practices like these have continued into the modern era, often as adaptive responses to material scarcity [35]. Drawing on local resources and context-specific knowledge, they continue to inform contemporary innovation in design using naturally grown timber.

2.1.5 Current Trends

The organic form of raw timber has found a place in contemporary architectural design, where its shape supports bio-inspired (biomimetic) concepts that merge with natural landscapes, enabling the creation of structures that integrate seamlessly into their surroundings—a theme later presented in Section 2.3.1. Nevertheless, when it comes to raw timber, the work done

at Hooke Park [36, 37], the Architectural Association School's woodland campus in Dorset, UK, is among the earliest noteworthy modern examples that remains relevant today. One of the most exemplary constructions using juvenile straight round wood, also built as an on-site construction experiment, is the cafeteria originally designed by Richard Burton of ABK Architects and Frei Otto. Later, the Woodshop, in the form of a tent [38], was also designed by Burton and Otto together with the engineers Buro Happold in 1989. It used green spruce wood from the surrounding forest and remains in use today by students of the *Design & Make* master's programme. This motivation and those principles can be seen in the new buildings in the park, which continue to use minimally processed wood and carry forward these design and fabrication ideas [39].

This approach aligns with biophilic design principles, enhancing the human connection with nature by incorporating raw, unprocessed materials into the built environment [27]. Moreover, the aesthetic qualities of naturally grown timber introduce an expressive dimension to architecture. Each element retains the unique growth history of the tree, resulting in visually dynamic structures that contrast with the uniformity of conventional timber construction. This variability, rather than being a limitation, becomes an asset, inspiring new methodologies in digital fabrication and parametric design that adapt to the intrinsic characteristics of each timber piece [22].

The digital approximation drives the current trends in research and experimental applications in rural or forest landscapes. One of the earliest digital examples of raw timber, also at Hooke Park, by Self and Vercruysse [21], showcases how multiple timber elements can be combined. Other authors, such as Bukauskas et al.[40], further explored these possibilities with their work on whole tree constructions, highlighting the structural potential of irregular timber. This approach has also been developed as the technology called Structural Round Timber (SRT) by the company Whole Trees in Madison, USA[41]. Vestartas et al. [42, 43] presented a comprehensive design-to-fabrication workflow for whole timber structures, including several automation strategies and open-source software packages built on the Open3D library [44], which provides a range of tools for mesh and point-cloud analysis and is wrapped into domain-specific components for raw timber. However, as in many geometry-driven workflows, their approach relies mainly on the external mesh representation and leaves the modeling of internal material and structural properties aside. Similarly, Cousin et al. [45, 46] modelled irregular timber inventories with a focus on geometric complexity and stock allocation, without explicitly integrating material properties or internal fibre structure, so that the internal topology of the elements remains only indirectly represented. In a related line of work, Allner et al. [47] explored sculptural designs using visually random timber structures, although their approach offered only limited precision in the geometric documentation. Kerezov et al. [48] focused on the use of natural tree forks in gridshell structures, again with an emphasis on geometric configuration rather than internal material description. Tamke et al. [49] and Larsen et al. [50] proposed workflows that model tree growth for digital fabrication and explored a wide range of joinery strategies and design alternatives. Chai et al. [51] took a different approach by combining 3D scanning with robotic fabrication. However, across these works, material behavior is not

explicitly incorporated into the simulations, which limits their applicability for performance-oriented analysis.

Computational design has revolutionized the application of non-standard timber elements in architecture, particularly in reusing and upcycling found objects, including raw timber components. Sun et al. [52] provide a comprehensive review of 142 projects (some of them cited in this Section) and identify key strategies, including heuristic and metaheuristic algorithms, as well as physics-based and AI-driven methods, that optimize the integration of geometrically irregular materials into architectural design. The research highlights naturally grown timber as a primary category of "linear branching" found objects, promoting circular construction practices and expanding the expressive capacity of architectural forms.

2.2 Computational Frameworks

Contemporary architectural practice increasingly relies on computational frameworks to bridge the gap between irregular natural materials and standardized design methodologies. In the context of naturally grown timber, these frameworks integrate digital design, simulation, and fabrication workflows to address geometric variability, material behavior, and performance constraints. This section outlines core methods—from geometric modeling to algorithmic matching—that support the integration of non-standard timber components into architectural systems.

2.2.1 Architectural Geometry and Engineered Timber Systems

Modeling techniques in timber construction have traditionally focused on standardized planar and three-dimensional (3D) elements derived from processed or engineered wood. Planar components are especially prevalent in prefabricated systems, where timber is cut into uniform boards or panels and arranged along one or more axes. These elements integrate seamlessly into digital design environments, where NURBS curves or parametric splines accommodate minor geometric variation while maintaining consistent cross-sectional properties. The simplicity of planar modeling facilitates its use in design-to-fabrication pipelines and structural simulation workflows.

Planar Modeling and Agent-Based Optimization

In addition to standard modeling approaches, agent-based modeling has been applied in design-oriented workflows. Here, rule-based systems guide the static placement of geometric elements according to predefined constraints, enabling optimization in layout and material usage. Unlike dynamic simulations, these methods focus on static configurations for constructability and efficiency. Applications include monolithic timber slabs [53] and modular multi-storey timber frames [54, 55], as well as pattern-oriented planar systems [56, 57].

3D Modeling and Material-Aware Workflows

Three-dimensional timber elements introduce an additional spatial axis, allowing for curved geometries and more complex structural topologies. These elements are often realized using glue-laminated timber (GLT), which enables free-form applications such as gridshells and twisted beams. This lineage can be traced to Otto Hetzer's early 20th-century lamellae-based patent (Patent Nr. 197773), which laid the groundwork for large-span engineered timber structures. More recently, researchers such as Svilans [58] have explored the integration of material-specific properties into parametric modeling workflows, especially in the context of reusing discarded or reclaimed timber. These material-aware approaches account for dimensional variation, mechanical heterogeneity, and the unique characteristics of reused wood components.

Pattern-Based Design and Stress-Oriented Form Finding

A further line of research emphasizes pattern-based design strategies aimed at enhancing structural efficiency or aesthetics. These approaches often take inspiration from natural systems, where material distribution is governed by performance. In architecture, this has led to techniques that align geometry with load paths or optimize the placement of material according to structural demands [59]. Such bio-inspired ideas are elaborated in Section 2.3.1.

Relevant examples include stress-aligned rib structures that concentrate material along principal stress directions, such as those used by Pier Luigi Nervi [60]. Similarly, Musto's dissertation [61, 62] presents form-finding strategies for shell structures in which design topologies are directly informed by load conditions.

Current manuals on multi-storey timber buildings [63] illustrate the increasing refinement of laminated timber systems, especially in horizontal components such as ribbed slabs. These elements are often designed using stress-aligned geometries to optimize structural performance [64].

While the strategies outlined above define the current state of engineered timber construction, they rely heavily on the predictability and uniformity of industrially processed wood. In contrast, the integration of naturally grown timber—characterized by curvature, fiber orientation variability, and irregular joints—requires more adaptive computational frameworks that can accommodate non-standard geometries and material behavior.

2.2.2 Manufacturing and Fabrication Processes for Raw Timber

The fabrication of raw naturally grown timber components—such as round logs, forks, and curved branches—poses unique challenges due to their organic geometries and anisotropic properties. Conventional manufacturing techniques are being adapted to align with emerging fabrication workflows that integrate sensory input and real-time data. In this context, advanced CNC milling and robotic systems [50, 65] are increasingly used to adjust toolpaths according to the specific geometry and material characteristics of each naturally grown timber ele-

ment. These technologies enable greater responsiveness to irregular forms and anisotropic behavior, facilitating the precise processing of components such as round logs, forks, and curved branches.

Other research emphasizes responsive joinery with flexible tolerances. Larsen et al. [66] propose adaptive joints fabricated through iterative prototyping. A notable contribution in this area is the Joinery Solver developed by Vestartas et al. [42], a robotic workflow that computes and fabricates interlocking joints for complex reticular assemblies using round timber. This system exemplifies how digital tooling can adapt to irregular geometries while producing repeatable and structurally robust outcomes.

Fabrication strategies now span from fully automated robotic assembly—as in the cooperative scanning-to-fabrication pipeline of Chai et al.[51]—to mixed-reality-assisted workflows. For example, Cousin et al. [46] employed augmented reality for on-site joint positioning and manual fitting, combining visual guidance with human labor.

Together, these approaches contribute to a growing ecosystem of hybrid workflows that blend craft expertise with robotic precision, enabling the integration of irregular timber components in high-performance structures.

While robotic and manual fabrication workflows focus on shaping and assembling irregular components, a crucial preceding step involves determining how such elements can be logically assigned to structural roles. This task is addressed through matching algorithms, which serve as the computational bridge between material inventories and design intent.

2.2.3 Matching Algorithms for Material Allocation

Once irregular timber components are digitized and prepared for fabrication, a key challenge remains: how to assign them efficiently within a design system. Matching algorithms have emerged as effective tools for this allocation process. These computational strategies support circular construction principles by enabling the reuse of reclaimed or non-standard timber elements—thereby reducing waste and minimizing embodied carbon. By aligning available stock with design parameters such as length, curvature, or branching angle, matching algorithms help extend the lifecycle of existing materials while streamlining design-to-fabrication workflows.

Bukauskas et al. [67] proposed form-fitting strategies based on the *Greedy search algorithms*, which prioritize best-fit heuristics to optimize element placement [51]. Huang et al.[68, 22] applied the Hungarian algorithm to match reclaimed beams to structural roles, balancing geometric compatibility with mechanical constraints. Tomczak et al. [69] emphasized early-stage design efficiency by matching components based on minimal transformation requirements, supporting low-carbon goals. Recent developments, such as those by Warmuth et al. [70], integrate matching logic into broader form-finding workflows. Their approach combines geometric layout optimization with stock allocation, enabling flexible structural systems shaped by material availability. Implementations in parametric design platforms like Grasshopper [71] have further lowered the barrier to adoption, allowing designers to—iteratively—test and refine configurations based on real-world material inventories.

Collectively, these algorithmic approaches mark a shift toward inventory-aware design. Matching algorithms not only advance sustainability efforts but also provide greater control over structural articulation in projects involving naturally grown or reclaimed timber.

However, while effective in managing geometric variability, these strategies often focus solely on spatial fit. Most workflows rely on assumed or idealized material properties, limiting their utility in structural performance analysis. As a result, even advanced matching systems must be supplemented with methods that address timber's mechanical heterogeneity—particularly for naturally grown elements with unpredictable internal structure, as mentioned in [68, 70]. This becomes critical when moving from design to simulation, where structural reliability depends on accurate material characterization.

2.2.4 Limitations in Design-to-Simulation for Naturally Grown Timber

Although current methodologies excel in geometric modeling and digital fabrication, they lack integration with material properties essential for structural analysis. Timber's anisotropic nature—its variability in strength and stiffness—means that geometric representations alone are insufficient for load-bearing simulations. Furthermore, no standardized workflow currently links geometric modeling across all phases of the design process, from material analysis and simulation to prototyping and structural implementation.

This gap underscores the need for comprehensive workflows that embed material behavior into the modeling process, enabling more holistic and structurally reliable timber construction methods. These objectives align with the goals of the research conducted by Trautz et al. [2].

Addressing these limitations may require interdisciplinary collaboration beyond architecture and engineering. Natural systems offer models of adaptive growth and structural optimization that could inform new modeling paradigms—integrating geometry, material variability, and performance at the early stages. The following section explores such bio-inspired strategies, illustrating how insights from biology, material science, and computational design can converge to support structures shaped both by and with nature.

2.3 Structures by Nature

Natural systems—both living and non-living—have long served as models for architectural thinking, informing structural principles, material strategies, and design methodologies. The observation of how organisms grow, adapt, and resist external forces has led to a wide range of architectural interpretations—from formal mimicry (mimesis), to biologically informed construction strategies (bio-based or biostructured), and even to systems in which living organisms are directly involved in the formation of built structures (biogenetic) [72]. These nature-derived strategies have found renewed relevance today, as architecture confronts resource scarcity, high embodied carbon, and material waste.

In response to growing environmental concerns, recent developments in architecture emphasize the practical implementation of biologically inspired strategies for sustainable construction. Material systems such as bio-based composites and design technologies like parametric modeling have enabled the creation of low-entropy, adaptable structures [73]. These innovations underscore the significance of interdisciplinary approaches, which now form the foundation of bio-informed and computationally integrated design research.

2.3.1 Interdisciplinary Foundations and Biomimetics

The integration of biology and architecture gained momentum in the 1980s through initiatives such as the Research Center SFB 230 "*Natürliche Konstruktionen*." Led by figures like Frei Otto and Johann-Georg Helmcke, this program established a framework for interdisciplinary exploration and introduced the term *Selbstbildung* (self-formation) to describe material and structural behaviors observed across scales—from microscopic organisms to full-scale construction [74]. One of the center's main objectives was to investigate biological structures through engineering analysis, particularly the mechanical behavior of trees under static loads.

In parallel, experimental practices in the 1980s and 1990s—such as those of Cervera and Pioz—developed architectural and urban proposals inspired by the flexibility, adaptability, and energy efficiency found in biological systems [75]. Their research led to the formulation of concepts of "Bio-Structure" or "Bionic Tower," which redefined construction through the logic of natural growth and adaptation.

These ideas were further developed in the 2000s and 2010s by researchers seeking to establish systematic theoretical and methodological links between biology and architecture. Nachtigall and Pohl [76] provided a comprehensive framework for biomimetic principles in architectural design. They emphasized that while nature cannot be directly replicated, biological systems offer rich analogies for generating sustainable and innovative building solutions. Their work outlined the role of abstraction—from biological understanding to digital modeling and prototyping—as a key process in translating natural principles into design outcomes.

These ideas were further developed in the 2000s and 2010s by researchers seeking to establish systematic theoretical and methodological links between biology and architecture. Nachtigall and Pohl [76] provided a comprehensive framework for biomimetic principles in architectural design. They emphasized that while nature cannot be directly replicated, biological systems offer rich analogies for generating sustainable and innovative building solutions. Their work outlined the role of abstraction — from biological understanding to digital modelling and prototyping — as a key process in translating natural principles into design outcomes.

In parallel, the first and second "digital turns" in architecture, as discussed by Carpo [77, 78], fundamentally changed both the ways designers think and the ways they make. From the late 1990s into the 2010s, the introduction of parametric modeling, algorithmic design, and file-to-factory workflows reshaped design practice. These developments provided the computational and fabrication infrastructure needed to handle complex geometries and multiscale data,

thereby creating a fertile ground for biomimetic approaches that translate biological principles into architectural form and construction systems.

This interdisciplinary transfer of knowledge is central to the field of bionics, which brings together biologists, engineers, chemists, and architects to study natural systems and develop technical solutions. As summarized by Knippers et al. [79], bionics bridges the gap between observation and application, moving from natural phenomena to abstraction and eventually to construction. Through computational modeling and iterative prototyping, biological insights are transformed into architectural strategies.

The legacy of SFB 230 continued in the SFB-TRR 141 "Biological Design and Integrative Structures," which investigated natural morphologies, material systems, and load-bearing mechanisms within contemporary engineering contexts [74]. More recently, this line of inquiry has been further advanced in architectural and engineering practice through initiatives such as the Cluster of Excellence IntCDC "Integrative Computational Design and Construction for Architecture" at the University of Stuttgart [80]. Together, these research efforts demonstrate how biological knowledge has become a catalyst for innovation in structural form-finding, material optimization, and sustainable construction methodologies, as well for the development of integrative, computation-based planning and building workflows in architecture and engineering.

2.3.2 Structural Adaptation in Trees

These ideas of interdisciplinarity were applied in the area of mechanical growth of trees. Among the key contributors to this discourse were Lothar Wessolly and Claus Mattheck, who developed analytical models rooted in tree biomechanics. Mattheck proposed five core principles of self-optimization in trees [20, 81]:

- Trees reduce lever arms through asymmetric growth patterns.
- Adaptive growth smooths stress concentrations.
- Grain orientation aligns with force flow.
- Mechanical properties adapt locally to stress intensity.
- Internal growth stresses counteract external loads.

These observations align with the concept of self-formation, as introduced in earlier interdisciplinary research. Trees adapt their internal structure over time to maintain favourable stress distributions, optimising material efficiency while ensuring structural resilience.

These principles have influenced a range of engineering tools, including Computer-Aided Optimization (CAO) and Soft Kill Option (SKO) methods, which brought some of the first applications of Finite Element Analysis (FEA) to simulate material distribution for nearly uniform stress alignment. In these approaches, the load-bearing volume is iteratively adapted so that stress becomes more homogeneously distributed throughout the structure, an idea closely related to volume equalisation in tree growth [82]. Such tools reflect a growing interest in translating tree-based adaptation strategies into architectural design and structural engineering.

2.3.3 Formal Modeling of Growth Processes

Beyond material mechanics, biological growth patterns have also influenced formal modeling strategies. The mathematical theory of biological development initiated by Aristid Lindenmayer in the 1960s introduced *L-systems*—axiomatic rules to simulate plant topology [83]. Prusinkiewicz later expanded this work into a computational framework that allows the visualization and simulation of fractal and branched morphologies in real-time [84]. These models support the study of tropism, branching, and internodal growth.

Jirasek et al. [85] further explored these dynamics by simulating bending in plant stems based on modular reorientation, although secondary thickening and environmental stimuli were not included. More recent work by Pranjic et al. [82] combines the concept of growth with parametric shape optimization to generate stress-informed geometries. Their approach integrates finite element analysis (FEA) into a generative workflow to produce a structure-based 2D model of a branch, following the principle of stress equalization using isotropic material with the von Mises criterion.

2.3.4 Tree-Like Structures and Living Construction Systems

The formal and symbolic reference to trees has long inspired architectural structure. Frei Otto's experiments in structural biomorphism [1] included tree-like branching supports, some of which were realized in architectural projects such as the Stuttgart Airport Terminal (1991). These structures were classified by stress zones in analogy to trees, though they simplified mechanical complexity by ignoring bending, relying instead on planar roof elements as the primary structural plane.

Beyond metaphor, actual living trees have also been incorporated into built form. Since the Middle Ages, Central European settlements cultivated *Tanzlinden*—linden trees guided to support elevated platforms used for music and gatherings. These culturally embedded techniques anticipated modern practices in *Baubotanik* (construction botany).

Contemporary projects in construction botany—such as those by Ludwig [86]—explore hybrid structures where living trees are trained to grow into architectural forms, often combined with artificial supports. These experiments involve controlled environmental conditions (e.g., irrigation, pruning, structural scaffolding) to merge natural growth with construction logic. However, practical limitations remain due to slow growth cycles, material unpredictability, and the long time frames needed for structural maturity.

Further developments in the application of structural adaptation to living tree structures explore the formation of hybrid joints through self-growing connections between interconnected trees. Wang [87] introduces a method for creating biologically integrated nodes that facilitate self-stabilization in urban tree environments. By applying controlled bracing between young stems, trees are guided to grow in contact, eventually fusing at key junctions. Over time, these fusion zones develop continuous vascular tissue and shared load paths, enabling both nutrient transfer and mechanical cooperation between the connected trunks. The research highlights

how induced bracing can lead to structurally active, self-reinforcing networks of trees, offering a living alternative to conventional rigid tree joints in urban green infrastructure.

2.4 Data Acquisition — Scanning Techniques

Accurate data acquisition is a fundamental step in capturing the geometry of irregular materials such as naturally grown timber. Various scanning techniques enable the detailed documentation of timber elements, which are subsequently used in design and fabrication workflows. This section outlines key scanning methodologies employed in timber construction.

2.4.1 Basis of Scanning

The core principle behind scanning is the conversion of physical objects into digital models. This involves capturing surface geometry through tools such as cameras, laser scanners, or structured light systems. These techniques produce point clouds or mesh data that serve as the foundation for modeling timber elements within architectural workflows. Accurate scanning ensures geometric fidelity throughout the design and fabrication stages.

2.4.2 Image-Based Methodologies

Image-based methodologies primarily encompass surface scanning techniques used to reconstruct natural forms, such as trees. These techniques rely on capturing multiple 2D images from different viewpoints and generating 3D geometry through software-based reconstruction.

Image-Based Modeling and Rendering (IBMR)

One of the foundational techniques in this category is Image-Based Modeling and Rendering (IBMR), which creates 3D models by aligning a sequence of 2D photographs [88]. The process estimates camera positions and orientations to compute spatial relationships, producing point clouds or mesh-based geometry. It is grounded in the principles of multi-view geometry, as detailed by Kang et al. [89].

This method has been applied to vegetation modeling. For example, Quan et al. [90] developed a semi-automatic system that combines image segmentation with generative modeling to recreate individual leaves and tree structures. Due to the self-similarity of branching patterns, this approach is effective for leaf-scale modeling. However, its applicability to full-scale timber elements remains limited.

Terrestrial Laser Scanning (TLS)

Laser scanning, particularly terrestrial laser scanning (TLS), has become a widely adopted tool for high-precision documentation. It operates by projecting laser beams onto surfaces to

generate dense point clouds. TLS has proven especially valuable in forest and land studies, where it is used to scan complex and irregular environments and to enable detailed forest data analysis [91]. In the context of naturally grown timber, TLS provides accurate, non-contact data acquisition for tree modeling.

Photogrammetry and Neural Radiance Fields (NeRFs)

Photogrammetry is another standardized image-based approach that reconstructs 3D geometry from overlapping 2D photographs or video frames. Recent advancements include Neural Radiance Fields (NeRFs), which employ neural networks to represent and render volumetric scenes from multi-angle images [92]. These techniques are well suited for capturing irregular forms and offer cost-effective alternatives to conventional scanning hardware, since they rely only on cameras rather than specialized sensors. However, they still face limitations in robust scale estimation and metric accuracy, which constrains their direct use in structural analysis.

Real-Time Visualization with Gaussian Splatting

Gaussian splatting is a recent development for visualizing point clouds and radiance fields in real time. Rather than rendering individual points, this technique represents data as overlapping Gaussian splats with density control, enabling smooth and efficient visualization of complex geometries [93]. Software and mobile platforms such as Luma AI, Polycam, and Scaniverse make these image-based reconstruction workflows accessible on consumer devices and provide straightforward export and data conversion for 3D models, thereby lowering the barrier to adoption in design and research contexts [94, 95, 96].

Low-Cost Tracking Using RGB Data

Emerging research has also focused on lightweight tracking methods for forestry applications. Steininger et al. [97] introduced a system for documenting and identifying logs using only RGB image data and manual annotations. This approach removes the need for complex sensors, offering a scalable and accessible solution for timber tracking in situ.

2.4.3 Non-Invasive Physical Scanning Methods

In addition to image-based techniques, non-invasive physical scanning methods are used to reveal the internal structure of timber and trees. These approaches—primarily computed tomography (CT) and magnetic resonance imaging (MRI)—offer valuable data for assessing wood quality, grain orientation, and structural anomalies without damaging the material.

Computed Tomography (CT)

CT scanning is the most widely adopted technique for internal timber analysis and was originally adapted from medical imaging. It is commonly used to detect internal features such as knots, cracks, and fiber orientation—key data points for sawing optimization and structural evaluation. A leading research program in this field is CT Wood at Luleå University of Technology, which has conducted systematic scanning of logs for over two decades [98]. The resulting datasets have supported predictive modeling of tree structure [99], fiber direction analysis, and stiffness evaluation at both macro and micro scales [100].

Industrial applications have also integrated CT technology. For example, the CT Log scanner developed by Microtec enables real-time reconstruction of log interiors for cutting optimization and automated quality sorting [101].

CT has additionally been applied to the analysis of critical tree features such as bifurcations and branch-stem junctions. These areas, often visually inaccessible, exhibit conical fiber structures that enhance mechanical performance. Recent studies have shown how such natural junctions effectively redistribute stress, inspiring biomimetic strategies for fiber-reinforced composite materials [102].

Magnetic Resonance Imaging (MRI)

Although less commonly used in timber construction, MRI has been adapted from plant sciences to study living plant tissue. Unlike CT, MRI can visualize internal processes dynamically, such as water transport and root growth. This makes it suitable for analyzing growth patterns and structural evolution in real time [103]. While CT provides high-resolution structural imaging, MRI offers greater insight into internal dynamics. Recent studies demonstrate that combining CT and MRI yields a more comprehensive understanding of plant development, making this hybrid approach particularly promising for the study of living trees and biologically integrated structures [104].

2.5 Tree Growth and Forest

Tree growth is a complex process influenced by a multitude of factors that contribute to the uniqueness of each tree within a forest ecosystem. The interaction of these factors determines not only the growth rate but also the structural differentiation of individual trees, making each one unique in its form and function.

2.5.1 Tree Growth and Forest Area

Forests cover approximately 38% of the European land area, providing critical ecosystem services and renewable resources [105]. In Germany, about 32% of the national territory is fores-

ted [106], while in the federal state of North Rhine-Westphalia (NRW), the forest area constitutes approximately 27% [107].

The forests of North Rhine-Westphalia (NRW) exhibit a diverse species composition shaped by both ecological conditions and forest management practices. According to data from the *Landesbetrieb Wald und Holz NRW*, approximately 58% of the forest area is covered by broadleaf (deciduous) species, while coniferous species account for the remaining 42% [108]. Among the broadleaf species, European beech (*Fagus sylvatica*) represents 19%, and oak species (*Quercus robur* and *Quercus petraea*) around 17% of the forested area. The most dominant conifer is Norway spruce (*Picea abies*), which covers 30% of the area, followed by Scots pine (*Pinus sylvestris*) at 8%, with other conifers comprising an additional 4%. Other deciduous species constitute approximately 22% of the forest cover.

Although spruce remains the most widespread species, its proportion has significantly declined in recent years due to climate-induced stressors such as drought and bark beetle infestation. These developments highlight the growing importance of promoting native hardwood species to enhance ecological resilience and ensure sustainable material sourcing in timber construction. In addition, this distribution contrasts with national timber production trends, where softwoods from conifers dominate the industry, representing around 80% of the total harvested volume, whereas hardwoods, including broad-leaf species, contribute only 20–30% [106]. This disparity reveals an underutilized potential for regional hardwoods, especially given their abundance in areas like NRW.

Tree Growth Conditions

The 2023 forest condition survey revealed continued high levels of defoliation across all major tree species. In NRW, 43% of oak trees and 39% of beech trees exhibited significant crown thinning (*Schadstufen 2–4*), reflecting persistent stress factors such as drought and rising temperatures. Among conifers, 32% of pines and 33% of spruces were similarly affected. These findings align with national trends, where 36% of trees across all species were classified within the higher damage categories, and only 20% showed no visible crown loss.

The high defoliation rates, especially among older trees over 60 years of age, suggest long-term vulnerability and reduced resilience to climatic disturbances. Beech and oak, which dominate NRW's forested areas, show consistent signs of declining vitality. This situation calls for a reassessment of species selection and forest management practices.

Wood Quality in Trees

Wood quality is a multifaceted concept that cannot be defined in absolute terms but must always be contextualized according to the intended application. From a technical perspective, wood quality results from the interaction of intrinsic characteristics, external attributes, and internal defects, all of which determine the material's suitability for specific products and processing chains [109]. Additionally, economic factors such as market pricing and processing yield play

a substantial role in evaluating quality. Wood quality tends to encompass all attributes that influence the material's performance and value throughout the manufacturing process [110].

Among these attributes, stem form—particularly *crookedness* and *curvature*—has been extensively investigated in recent years due to its direct impact on harvesting and processing efficiency. Crooked or curved stems are often related to internal defects such as reaction wood and eccentric pith, which reduce mechanical reliability and complicate processing in standardized timber production. Consequently, such forms are generally downgraded in traditional quality grading systems. European standards, such as EN 1316 for hardwoods, explicitly consider stem curvature, sweep, and other geometric deviations as classification criteria for roundwood quality [111, 25].

Despite the growing use of advanced tools such as terrestrial laser scanning and photogrammetry, which enable objective and scalable assessment of visual stem features, a gap remains in understanding the correlation between external geometry and internal wood quality [109]. This limitation underscores the difficulty in predicting end-use performance only based on visible information in standing trees. Current research efforts, including protocols developed to improve visual assessment methodologies across European National Forest Inventories (NFIs), focus on measurable indicators such as branch diameter, crookedness, crown height, and stem slenderness [112]. However, fully integrating these assessments into standardized quality grading frameworks remains an ongoing challenge due to the difficulty of evaluating entire trees, particularly when accounting for small branches and complex volumetric structures.

2.5.2 Determinants of Tree Growth and Tree Differentiation

Forest Competition and Ecosystem Dynamics

According to Wang et al. [113], forest competition is a crucial factor in forest dynamics and stand structure, significantly impacting tree growth and environmental changes. The study highlights the complexity of ecological processes involved in competition, emphasizing the importance of considering temporal variations and environmental conditions to understand tree interactions and their responses to environmental fluctuations.Wang suggests a network-based approach to studying tree competition, emphasizing interactions among trees to better understand forest ecosystem dynamics. Similarly, Morin et al. [114] argue that such a perspective reveals the interconnections between trees and their influence on overall forest behavior. Morin's study underscores the significance of interactions at multiple scales, suggesting that network models can effectively capture the complex relationships that drive ecosystem changes.

Environmental Factors and Tree Growth

Tree growth serves as a critical indicator of forest health and structural change. Recent work demonstrates this clearly: for example, Jin et al. [115] use ground-based LiDAR point clouds to estimate larch growth at various scales, providing insights into how light and mechanical

loads influence growth responses. Their study shows that growth patterns reflect changes in forest structure and condition, underscoring the value of precise environmental monitoring.

Similarly, the relationship between terrain and tree development has been explored by Tang et al. [116], who studied Eucalyptus trees to reveal how factors like forest age, slope, and site conditions shape growth dynamics. Using UAV stereo imagery, they monitored seasonal changes in structural features such as height, crown width, diameter at breast height (DBH), and aboveground biomass (AGB), confirming these with field measurements. Their findings show that trees on gentle slopes grow faster in spring and autumn than those on flat terrain, emphasizing the importance of static environmental parameters in timber resource management.

Many of these environmental influences and their impacts on tree growth can be effectively documented through advanced technologies such as LiDAR and Unmanned Aerial Vehicle (UAV) imaging. These tools enable precise monitoring of growth patterns and structural changes in trees, providing valuable data for forest management and ecological research. Smart forest monitoring platforms enhance this process by offering real-time data and predictive insights [117]. Recent advances also include the use of augmented reality tools for field applications [118] and the automation of roundwood stack measurement processes [119].

Broad-Leaf Forest Resources

Broad-leaf forests play a vital role in sustainable resource management, yet factors like material availability and resource sustainability are often overlooked [120]. The industry increasingly seeks species that meet specific requirements, prioritizing rapid growth and minimal irregularities [121]. These factors are closely tied to the overall considerations of tree growth and resilience discussed earlier, which highlight the importance of species selection and growth conditions for achieving desirable timber qualities.

Grading rules typically focus on trunk diameter, straightness, and species to determine wood value [25]. The diameter is a critical factor as it often correlates with the structural strength and volume of usable wood. Straightness impacts the ease of processing and the potential uses of the timber. These criteria help define the economic value of timber, guiding the selection process for species best suited for various applications. However, these rules often overlook crown wood, which varies greatly across species and is generally not suitable for massive timber elements [122].

Selecting climate-adapted and native species over invasive ones is crucial for sustainable forestry [123]. This selection supports biodiversity and ecosystem resilience while reducing risks associated with invasive species. Forest management and conservation must adapt to these challenges to maintain healthy forest ecosystems [124]. In Germany, efforts are underway to diversify forests with a mix of conifer and broad-leaf trees to enhance ecological balance and timber availability [24].

Efficient extraction of tree volume, currently at 40-50% [125], is essential for optimizing resources. This involves utilizing not only the trunk but also incorporating irregular elements that

can be processed into valuable products. With the growing demand for sustainable timber construction, broad-leaf species are increasingly being considered for their potential to meet both ecological and architectural needs, providing an opportunity to utilize diverse forest resources more effectively.

2.5.3 Tree Growth Observations

Tree Stability

Tree stability is influenced by structural factors and environmental conditions. Tools such as the Statistisch Integrierte Abschätzung (SIA) – or Statistically Integrated Estimation– developed by Dr.-Ing. Lothar Wessolly, provide a theoretical basis for assessing the mechanical stability of trees [126]. Additional methods evaluate internal hollows and support tissues, aiding in the comparative analysis of tree safety [127, 128].

Broad-Leaf Growth, Deviations, and Quantitative Structure Models

Broad-leaf forests offer significant potential for sustainable timber construction, but understanding the growth patterns and deviations of these species is essential. Digital tools are increasingly used to analyze tree volume, structures, and deviations [129, 130]. These analyses help identify opportunities to incorporate crown wood and other irregular elements into construction designs.

Quantitative Structure Models (QSM) are employed to examine tree growth and inform new construction designs that incorporate crown wood for standardized elements. These models provide geometric accuracy and volumetric estimation, offering insight into usable biomass from branches and bifurcations.

By leveraging these models, the industry can better utilize the available resources in broad-leaf forests, enhancing both sustainability and efficiency in timber production.

Simulation and Growth Models

Simulating tree growth mechanically requires accounting for continuous material accretion, anisotropic behavior, and internal stresses [131]. External factors such as wind, moisture, temperature, and nutrients must also be considered [132].

Modeling Plant Morphogenesis

Modeling plant morphology, especially in trees, presents challenges due to the complexity of adaptive growth. Prusinkiewicz and Lindenmayer developed early models combining pattern generation and simplified biomechanics [133]. Cellular modeling addresses adaptive spatial growth and venation, essential for nutrient distribution.

Table 2.1: Key Concepts in Tree Biomechanics:

Concept	Description
Mechanical Loads	Wind and gravity influence growth
Biomechanical Adaptation	Structural changes increase resilience
Growth Resistance	Internal stress and material accumulation
Elastic Resistance	MFA and lignin affect stiffness
Simulation Conditions	Accretive growth and environmental factors

Branching architecture has been modeled using recursive logic [84]. Earlier work by Ulam, Cohen, and Sachs examined tree competition and spatial distribution [134]. Jirasek [85] introduced models where mechanical forces shape branch cross-sections.

Although molecular-level simulations offer detailed insights, they are excluded here due to their complexity.

Abstraction and Modeling Strategy

A key decision in plant modeling is the level of abstraction: whether to simulate mechanical responses alone or model the plant as a continuous structure [135].

Table 2.2: Overview of Plant Growth Modeling Approaches:

Aspect	Description
Modeling Complexity	Trees adapt dynamically, making simulation difficult
Simplified Topological Approaches	Models by Prusinkiewicz and Lindenmayer combined biology and geometry [133]
Cellular Patterns	Address spatial growth and venation
Branching Architecture	Recursive systems show hierarchical structure [84]
Spatial Competition	Studies by Ulam (1962), Cohen (1967), Sachs (1995, 2004) on tree competition for space [134]
Mechanical Growth Models	Jirasek modeled growth influenced by mechanical stress [85]
Abstraction Level	Simulations must balance detail related to tissues, lignification, and biological evidence with practical application in modeling [135]

2.5.4 Timber Supply Chain and Grading Rules

The European timber supply chain is supported by regulatory frameworks and certification systems that promote sustainable forest management, ensure traceability, and uphold quality standards. Key systems include the Programme for the Endorsement of Forest Certification (PEFC) [136], the Forest Stewardship Council (FSC) [137], and the EU Timber Regulation (EUTR) [138]. These frameworks verify that timber products are legally sourced and managed in line with environmental and social standards.

In Germany, these principles are applied through the *Rahmenvereinbarung für den Rohholzhandel* (RVR) [25] –or Framework agreement for the trade in raw timber–, which provides national guidelines for timber classification and supports transparency from the outset of the supply chain.

Regulatory Considerations

PEFC and FSC offer international certification schemes that assess forest products based on sustainability criteria and support responsible sourcing through Chain of Custody certification. The EUTR complements these by requiring due diligence to prevent illegally harvested timber from entering the EU market.

These systems account for natural geometric variations in timber—such as curvature, bifurcations, and irregularities—and provide guidelines for classification based on structural suitability. Timber with major deviations is typically assigned to lower quality classes, ensuring appropriate application and marketability.

Framework Agreement for the Raw Timber Trade (RVR)

The RVR sets standardized procedures for grading and labeling raw timber in Germany [25]. It classifies timber by species, dimensions, and visual features, with particular emphasis on trunk diameter and straightness. Timber is sorted into quality classes (A to D), where class A denotes the highest visual and structural integrity, while curvature and defects may place timber in classes C or D (see Table 2.3).

The classification process distinguishes assortments such as roundwood and industrial wood and applies uniform reference keys using the Elektronischer Datenaustausch Holzdaten (ELDAT) standard. This facilitates electronic data exchange, enhances traceability, and ensures consistency throughout the supply chain. Figure 2.2 outlines this process from forest management through quality assessment.

Table 2.3: Quality Classes for Timber Sorting according to RVR:

Criteria	**Class A**	**Class B**	**Class C**	**Class D**
Classification	Logs	Logs/ Industrial	Industrial Wood	Energy Wood
Curvature (cm/m)	≤ 1.0	≤ 1.5	≤ 2.0	≤ 3.0
Diameter (cm)	$\geq$ 35, consistent	20 - 35, moderate	20 - 35, varied	$<$ 20, inconsistent
Minimum Length (m)	≥ 3	≥ 3	Variable	Variable
Thickness	High	Moderate to High	Moderate	Low to Moderate
Knots	Few, small	Moderate	Many, larger	Extensive, large
Insect Damage	None	Minimal	Visible	Extensive
Fungal Decay	None	Minimal	Moderate	Extensive
Straightness	Very straight	Mostly straight	Curved	Highly curved
Surface Defects	Minimal	Some	Noticeable	Prominent

In the German timber sorting framework, raw wood is classified into three main categories: *Stammholz*, *Industrieholz*, and *Energieholz*.

- Stems, or logs, refers to high-quality timber that is suitable for construction and structural applications. This category includes wood that meets strict criteria for straightness, diameter, and minimal defects, making it valuable for building and carpentry purposes.
- Industrial wood, includes timber that is not of the highest quality but is still suitable for industrial processing, such as the production of paper, pulp, or engineered wood products. This category allows for more defects and variations in size.
- Energy wood, consists of lower-quality timber primarily used for biomass and energy production. This wood often has significant defects and smaller diameters, and it is not suitable for structural applications.

Timber with a diameter between 10 cm and 20 cm, while not qualifying as Logs, is typically collected for use as firewood or chipped for energy production, ensuring that forest resources are utilized efficiently. Wood that does not meet these classifications, especially timber with a diameter of less than 10 cm, often remains on the forest floor. This unclassified wood decomposes naturally, contributing to nutrient cycles and biodiversity within the forest ecosystem. Additionally, the labeling and identification of raw wood require precise marking to maintain traceability throughout the supply chain. Each piece must be marked with details such as species, quality class, and dimensions to facilitate accurate valuation and compliance with industry standards. By adhering to these stringent grading rules, the German forestry industry aims to optimize resource utilization, support sustainable forest management practices, and ensure the production of high-quality timber suitable for various applications, including construction.

This supply chain, see in Table 2.4 provides a clear view of the steps involved in maximizing timber value according to the RVR framework, emphasizing the strategic processes that contribute to efficient timber management and marketing.

Table 2.4: Timber Supply Chain Based on RVR:

Supply Chain Step	**Description and Impact**
Forest Management and Planning	Implementing sustainable strategies to ensure timber production, and evaluating resources for efficient harvesting.
Harvesting	Selective logging based on quality and sustainability criteria, minimizing environmental impact.
Initial Sorting and Classification	Quality grading based on diameter, straightness, and defects to assign classes (A, B, C, D) using the ELDAT standard for consistency.
Transportation	Organizing efficient logistics to minimize costs and carbon footprint, while maintaining traceability from forest to processing facilities.
Processing	Converting logs into timber products based on demand, with waste management practices for recycling sawdust and off-cuts.
Secondary Sorting and Quality Control	Ensuring products meet specifications and standards, with labeling and certifications to enhance marketability.
Market Distribution	Collaborating with distributors for timely delivery, providing transparency and product information to consumers.
Feedback - Monitoring	Evaluating supply chain efficiency and customer satisfaction, using insights for continuous improvement.

2.6 Material Properties

Understanding the mechanical behavior of naturally grown timber is essential for its integration into structural applications. Unlike standardized, sawn timber, naturally curved elements such as branches and forks possess highly heterogeneous, anisotropic properties that vary by species, moisture content, and anatomical direction [139, 140].

Recent research indicates that round timber can exhibit up to 50% higher strength compared to milled sections, primarily due to the preservation of natural fiber continuity and unaltered cross-sectional geometry [23]. Whole-tree studies and material testing confirm that tree bifurcations and branch–stem junctions exhibit enhanced strength due to their conical interlocking structures and gradual fiber orientation transitions. These biologically optimized geometries serve as inspiration for structurally efficient timber applications.

2.6.1 Tree Growth and Mechanics

Adaptation to Mechanical Loads

Mechanical forces such as wind and gravity significantly influence tree growth and timber quality [141]. Studies on species like Norway spruce show how stress affects both structural development and wood properties. Trees adapt to these external forces by modifying their internal architecture, as discussed by Niklas [142], which has implications for both forestry and timber utilization.

As trees mature, they accumulate layers of wood with varying internal stress, resulting in mechanically optimized structures [131]. The deposition of cellulose and lignin further enhances stiffness and resistance [132].

Elastic Resistance and Anisotropy

Elastic resistance is influenced by the microfibril angle (MFA), density, and lignin content. Smaller MFAs yield stiffer and stronger wood [132]. Environmental factors such as light, water availability, and mechanical loading also contribute to material variation [131].

Due to its anisotropy, wood exhibits direction-dependent mechanical performance: the longitudinal axis provides the highest strength and stiffness, while the radial and tangential directions exhibit reduced mechanical properties [10]. This anisotropy must be considered in structural applications, particularly when using irregular or curved timber.

2.6.2 Reaction Wood and Material Differentiation

Tree growth itself is a structural response to environmental loading. Through the formation of reaction wood—tension wood in hardwoods and compression wood in conifers—trees adapt their morphology and internal composition to resist mechanical stresses [143, 144, 145, 146].

Compression wood, typically found on the lower side of leaning conifers, is marked by high lignin content and eccentric growth. In contrast, tension wood in hardwoods contains high cellulose concentrations aligned with tensile grain directions [147]. These internal asymmetries influence both form and mechanical performance, offering a natural model for stress-responsive material systems.

2.6.3 Summary: MOE–Density Correlation in Central European Hardwoods

This section reviews the relationship between modulus of elasticity (MOE) and density in three common Central European hardwoods—birch, beech, and oak—across anatomical directions and loading conditions. All data refer to air-dry states, assuming moisture content below $10\,\%$, which is critical for reliable structural assessment.

Birch (*Betula pendula*):
Moderate density ($\sim 625\,\mathrm{kg\,m^{-3}}$); $\mathrm{MOE_L} \approx 11\,\mathrm{GPa}$ to $13\,\mathrm{GPa}$. Strong correlation between MOE and density. Transverse moduli are significantly lower: $E_\mathrm{R} \approx 5\,\%$ to $8\,\%$ and $E_\mathrm{T} \approx 4\,\%$ to $5\,\%$ of E_L.

Beech (*Fagus sylvatica*):
High density ($\sim 715\,\mathrm{kg\,m^{-3}}$); $\mathrm{MOE_L} \approx 14\,\mathrm{GPa}$. Strongest MOE–density correlation among the three species (R^2 up to 0.84). $E_\mathrm{R} \approx 10\,\%$, $E_\mathrm{T} \approx 5\,\%$ of E_L.

Oak (*Quercus robur/petraea*):
High density ($650\,\mathrm{kg\,m^{-3}}$ to $800\,\mathrm{kg\,m^{-3}}$); $\mathrm{MOE_L} \approx 11\,\mathrm{GPa}$ to $14\,\mathrm{GPa}$. Moderate MOE–density correlation ($R^2 \approx 0.6$). Transverse values are higher due to ray tissue: $E_\mathrm{R} \approx 15\,\%$ to $16\,\%$, $E_\mathrm{T} \approx 7\,\%$ of E_L.

Across all species, density consistently predicts stiffness in clear, defect-free wood, with MOE values in tension and compression closely aligning with those from bending tests.

2.7 Potential Approach for a Supply Chain and Timber Analysis

Based on the outlined regulatory frameworks and the potential for reusing underutilized materials, this thesis proposes integrating timber from various classes as solid wood in construction. The extended supply chain approach presented here is centered on digitalization, including sorting, geometric analysis, simulation, and digital fabrication. This process is illustrated in blue in Figure 2.2.

Moreover, this approach contributes to CO_2 savings by avoiding processes such as shredding or gluing, which typically require more energy. By preserving the internal structure of the material, it also facilitates integration into future reuse cascades.

These steps are incorporated into the supply chain model and form part of the state-of-the-art approach defined in this thesis.

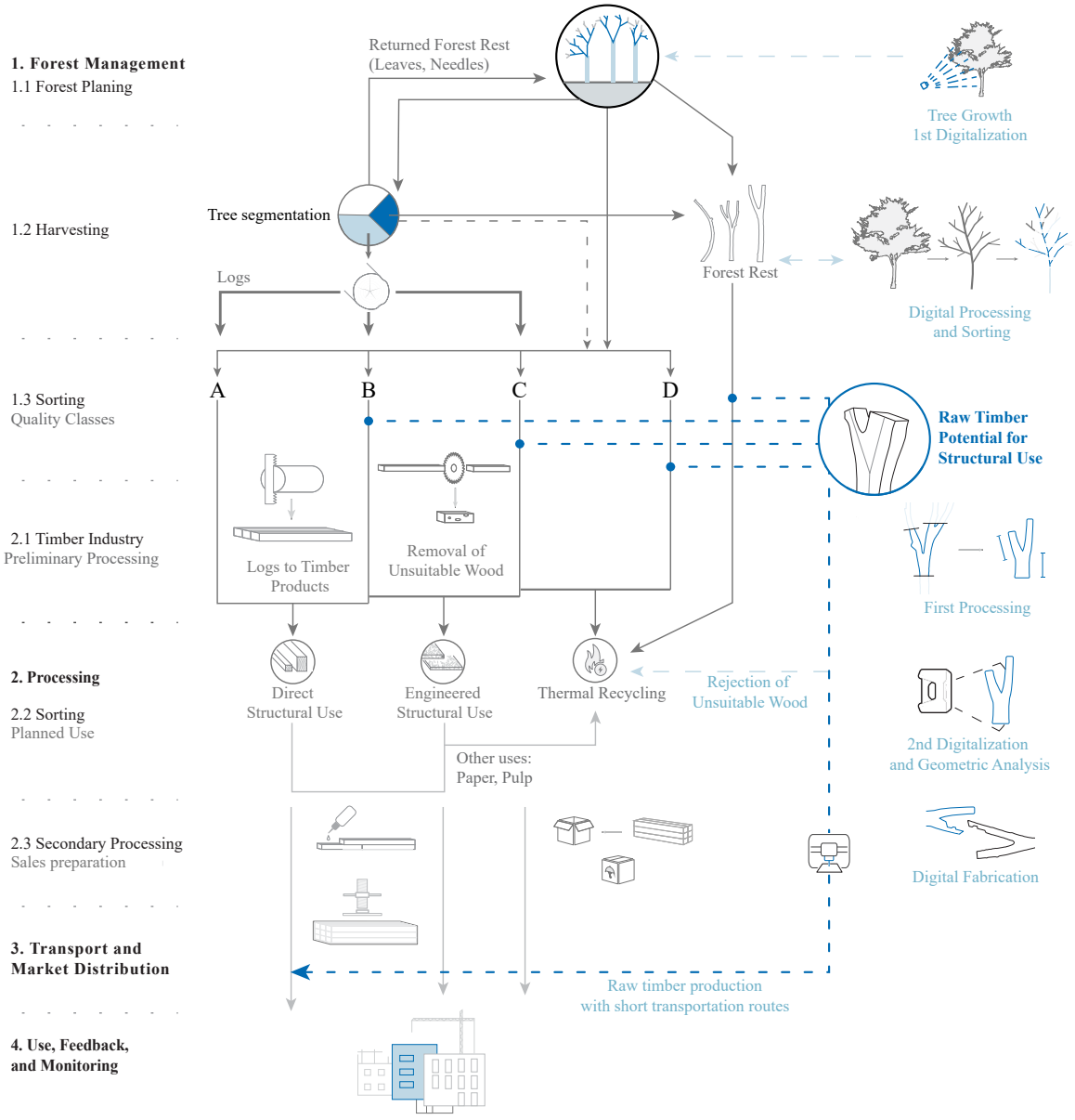

Figure 2.2: Integration of the thesis (in blue) into the existing supply chain to optimize the use of raw wood in the construction industry.

Chapter 3

Geometric Methods and Modeling

Theoretical Foundations and Advanced Data Acquisition

This chapter introduces the methodology for analyzing the geometry of raw timber, outlining an integrated approach that connects tree structures to the individual timber elements used for construction applications. This approach defines several methods adapted to different scales and types of available data. Multiple data acquisition techniques are discussed, including point clouds, photogrammetry, and LiDAR scanning.

The following sections present key definitions together with geometric analysis methods, focusing on their application to 2D and 3D timber elements. In addition, several advanced modeling techniques are introduced, with emphasis on Non-Uniform B-Splines and Subdivision Surfaces—based on standard practices in computer graphics and CAD. These methods form the foundation for a geometric model that supports future implementations throughout this dissertation.

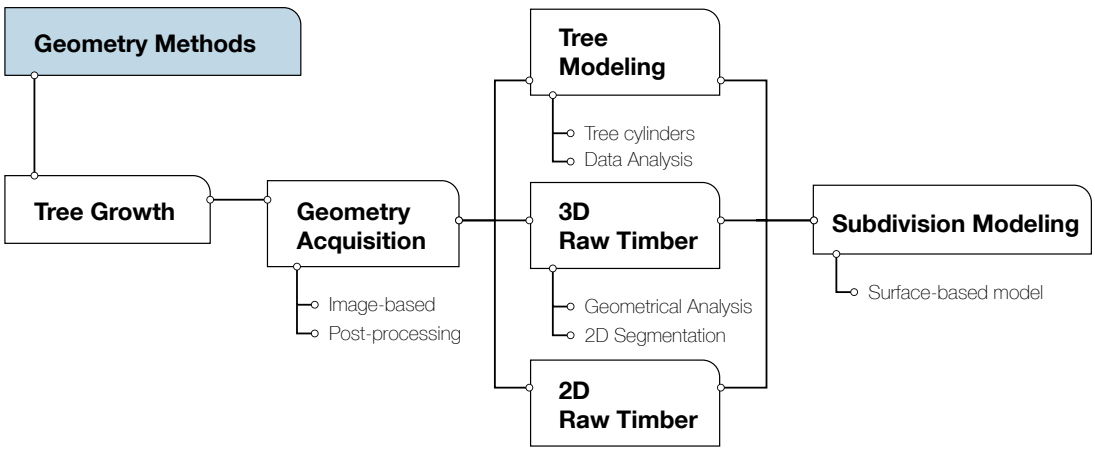

Figure 3.1: Chapter Diagram: Determination of areas and the connection.

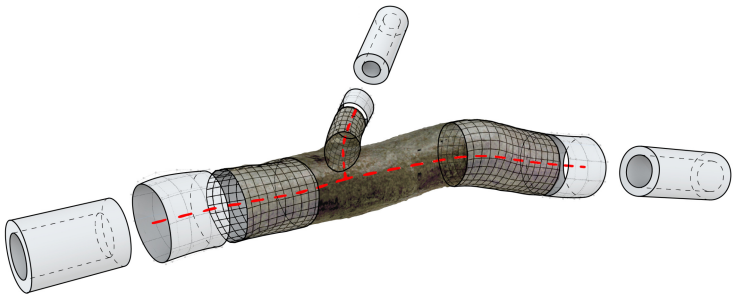

Figure 3.2: From raw timber branch geometry to structural application. Transition from natural form acquisition to construction-oriented modeling.

3.1 Tree Growth

This section provides a detailed examination of tree growth, focusing on trees with visible asymmetrical growth patterns. Various image-based documentation strategies are employed to assess the geometric and material properties of trees, enabling a deeper understanding of their load-bearing capacity. Based on growth observations, methods to estimate structural properties are applied. These observations help address irregularities in tree growth and guide the modeling process.

3.1.1 Types of Tree Growth

Tree growth occurs in two forms: primary growth and secondary growth [148]. Primary growth refers to axial elongation along the tree's main axis, whereas secondary growth involves radial expansion in the cross-section. These growth types play distinct roles in the structural development and adaptability of trees, as illustrated in Figure 3.3.

The focus here is to illustrate different methods for visualizing growth in the cross-section and longitudinal growth, in order to better understand how each contributes to the tree's overall structural performance. Figure 3.3 highlights the well-recognized volumetric growth that occurs in the cross-section as a form-optimization process. This phenomenon is based on the principle of maintaining constant maximum stress during growth [19], and is represented through a mesh structure.

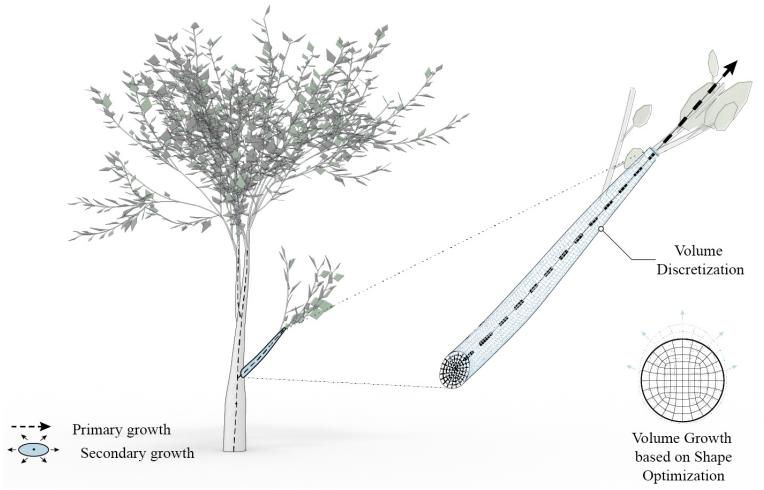

Figure 3.3: Illustration of primary and secondary growth types in trees, including volume growth. Adapted from [148].

Primary Growth

Primary growth, also known by several authors as global growth, is the initial expansion of the main stem and branches of the tree. This growth typically follows a branching pattern represented by the L-system model [83, 84, 133], which takes into account global tropisms—growth influences that affect the tree's development. In the adaptation shown in Figure 3.4, the axis of the tree extends longitudinally, with each segment growing according to the L-system rules.

The algorithm for this longitudinal growth interprets a sequence of actions represented by the letters "F" and "X". Here, "F" denotes longitudinal growth, while "X" considers variations in growth due to tropisms, such as gravity $\vec{g}$ or light $\vec{t}$ vectors. In this model, the vector $\vec{g}$ represents the self-weight of each cross-sectional part, applied in every growth iteration to account for the natural weight distribution throughout the tree structure.

Each iteration amplifies the sequence according to a substitution rule, $X \rightarrow FX$, which governs the longitudinal growth pattern. Each segment length l increases incrementally with each iteration. External forces, represented by the vector $\vec{F}$, account for influences such as wind or punctual loads; however, for simplification, these forces $\vec{F}$ are not considered in the current model. The primary growth model instead focuses on simulating global environmental factors like water, nutrients, and sunlight, incorporating these as vector quantities. This makes it possible to realistically simulate global growth patterns influenced by climate conditions such as humidity and temperature. An example of a 2D growth simulation following these rules can be found in [82].

Secondary Growth

Secondary growth refers to the local expansion of the tree's cross-section, allowing an increase in diameter and structural stability over time. This type of growth is influenced by local

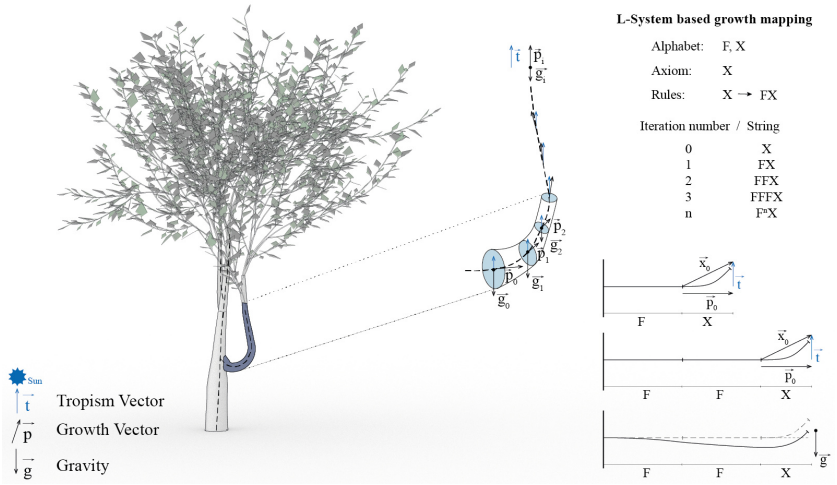

Figure 3.4: Illustration of primary growth logic based on the L-System defined in [84].

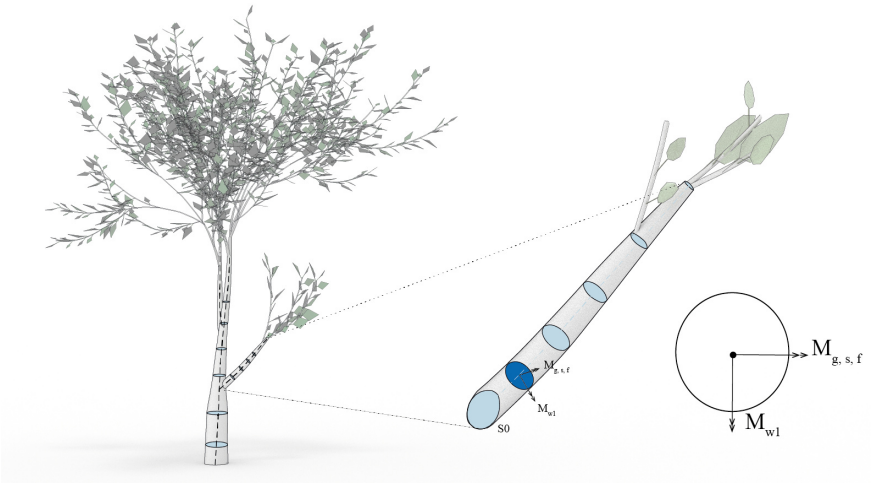

Figure 3.5: Secondary growth illustrated through thickening of the cross-section based on the moment of inertia for each segment of the tree.

loads that vary the shape and stiffness distribution within each cross-section. To document this growth, layers are distinguished along the cross-section, resembling annual rings. Each ring represents a stage in the tree's development, contributing to its increasing structural capacity.

Using cross-sectional analysis, as shown and adapted in Figure 3.5, the moment of inertia provides insight into the formation of tension and compression wood, characteristic of deciduous and coniferous trees, respectively. Mapping this secondary growth aligns with the geometric analysis of the tree structure (see Fig. 3.6), where the center of mass shifts as biomass increases. This approach offers a basis for observing volume growth over time, emphasizing how structural adaptation occurs within the tree as it matures.

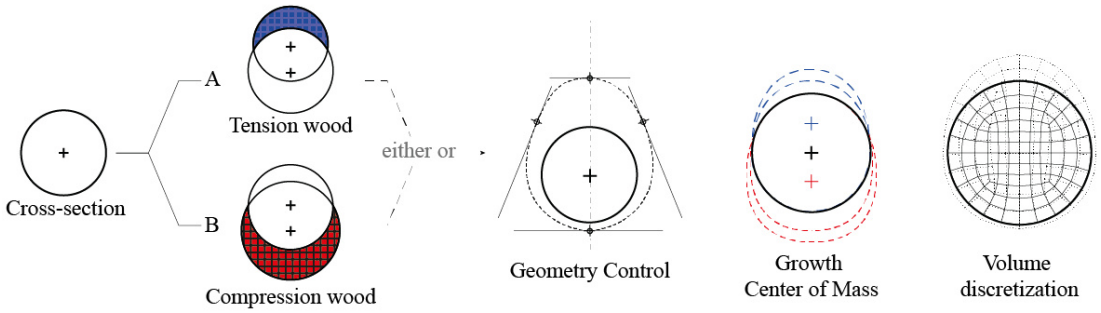

Figure 3.6: Tension and compression wood distribution across a tree cross-section, illustrating shifts in center of mass and structural adaptation as biomass increases.

3.1.2 Observation Strategies of the Tree Growth

The most commonly used methods for observing tree growth are standard practices in the fields of tree care and maintenance. In Wessolly et al. [149], several image-documented points highlight the most critical growth areas to observe. These observations allow for an assessment of whether a tree is growing *healthily*, meaning that it is producing sufficient biomass in the necessary areas to maintain its structural integrity. By observing cross-sectional growth and considering the tree species (broadleaf or conifer), it is possible to understand growth patterns. For example, in broadleaf trees, areas under tension should ideally grow proportionally to the tree's primary structural growth. Figure 3.7 illustrates the different growth zones for observation, including areas related to self-stabilization based on proportional cross-sectional growth (in light blue). When these proportional growth conditions are not met, practical interventions to support tree parts, described in [150], can be implemented for static and maintenance purposes.

Growth Constraints

Various tree growth patterns are utilized by tree-care experts to observer and protect to the tree and its surroundings from potential hazards.

Images 3.8 illustrate how this growth occurs naturally. Signs of restricted secondary growth—due to biological or soil chemical limitations—indicate structural vulnerabilities in the tree, which may lead to branch breakage or diseases that compromise wood quality. In Figures 3.8(a) and 3.8(b), healthy growth patterns are evident, showing proportional growth in tension and compression zones.

These tree-care strategies highlight the importance of documented monitoring and a thorough understanding of tree statics, a task traditionally performed manually through field notes. In certain regions, particularly forested areas, advancements have been made through the application of image-based modeling methods and LiDAR scanning, enabling more detailed statistical analyses. Meanwhile, problematic timber growth, which is sometimes removed due to regulated growth control measures, is discussed in Section 1.8.2.

For further analysis and comparison of material characteristics, refer to Section 4.3.1, where raw wood samples from different sources are examined and evaluated alongside reference data from resources such as the "*Insidewood-Database*" [151], highlighting typical growth patterns found in timber.

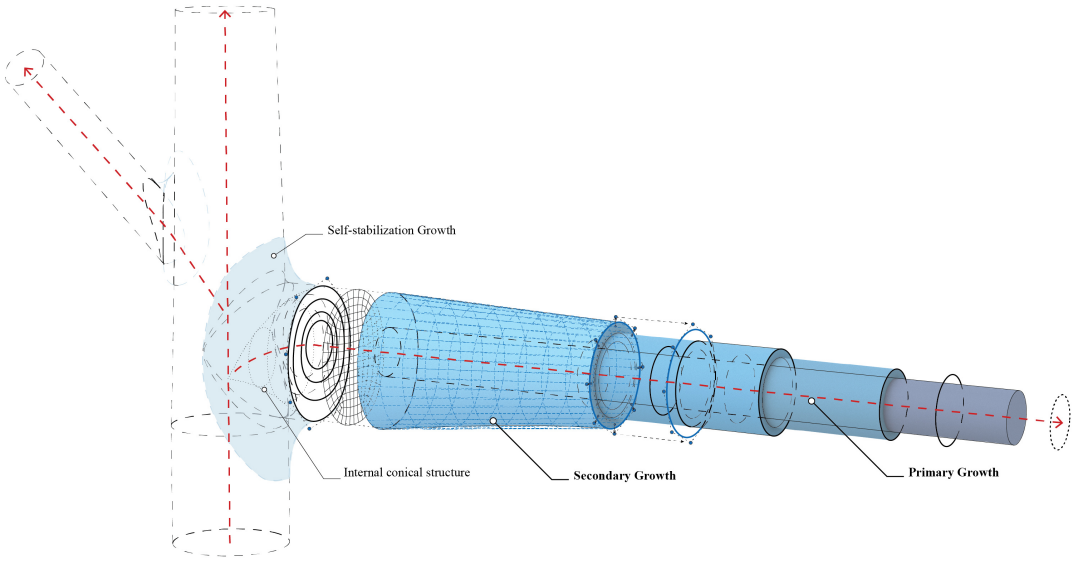

Figure 3.7: Observation of growth areas related to tree statics in a "Conifer-like" scheme. Picture adapted from [148].



(a) Tension wood in a plane tree



(b) Compression wood in a pine

Figure 3.8: Comparison visible reaction wood growth zones in trees.

Growth Geometries

In addition to observations on growth constraints, a fundamental geometric analysis of tree structures is essential for distinguishing branches and assessing their potential. Currently, no standardized methods are widely adopted for geometric analysis; instead, practical intuition is often applied in timber utilization and grading rules [25], as detailed in Section 2.5.4. These rules primarily classify elements based on criteria such as straightness, diameter, and appearance, rather than intrinsic geometric properties.

This work examines the key geometrical characteristics of naturally grown timber elements, concentrating on the distinctive morphology of curved and bifurcated forms. These forms, especially those found in the crown, are of significant geometric interest and require detailed documentation and statistical analysis to capture their variability. This approach enables the classification of elements into straight, curved, or bifurcated components, as illustrated in Figure 3.9.

A crucial aspect of this analysis is the study of primary growth, where the main axis is defined and anchoring points are identified to determine the diameters of individual elements. These parameters provide a foundation for the modeling processes discussed in subsequent chapters.

In the modeling of natural timber, the geometric properties of these elements play a critical role in determining their usability and quality. Curved or bifurcated timber parts, typically ranging from $5\,\mathrm{cm}$ to $25\,\mathrm{cm}$ in diameter, present both challenges and opportunities in timber processing. While often excluded or downgraded in traditional grading systems, these elements can offer distinct advantages in architectural design and bespoke fabrication, where natural forms are valued for both structural and aesthetic purposes.

Curved timber is defined by its deviation from a straight axis, often measured as curvature over a given length. Bifurcated timber, by contrast, features divisions where the main stem splits into two or more branches. Both geometrical forms influence the mechanical behavior of timber elements, affecting its load-bearing capacity and suitability for different applications.

Processing such non-standard forms requires specialized handling and cutting techniques to optimize yield and reduce material waste. In many cases, selecting cut locations that follow the natural grain and curvature enhances both the functional and visual qualities of the material.

Further discussion on *regulatory considerations* related to the use of such geometries can be found in Section 2.5.4.

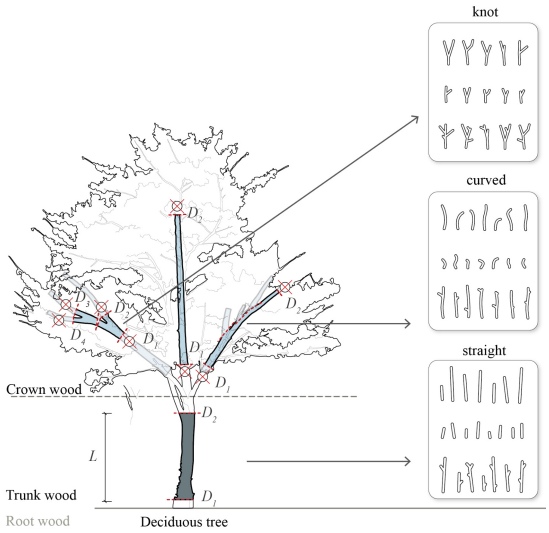

Figure 3.9: Classic tree diagram: differentiation of *knots/forks* or bifurcations, *crooked* or curved, and straight branches.

3.2 Methods for Geometry Adquisition

3.2.1 Geometrical definitions

Fundamental Geometric Representations

Geometry management involves the structured processing and transformation of geometric data—whether scanned or computationally generated—into analytically efficient and performance-optimized models. The workflow typically moves from raw spatial data to refined representations suitable for advanced analysis or design. Bellow are some definitions for producing the geometrical representations:

Point Cloud:
A *PointCloud* is a collection of discrete points defined by three-dimensional coordinates. It frequently includes additional attributes such as normal vectors and color data. Serving as raw input from scanners or volumetric captures, point clouds form the initial representation in geometric workflows.

***Gaussian Splattings*:**
The *Gaussian Splattings* [93] is a rendering technique that enables direct visualization of volumetric data without requiring surface or line conversion. It operates on point cloud-like data, where points are enriched with color in the form of splats, providing a fast visualization alternative to meshes without explicit volumetric representation. The splats are computed based on the color or intensity range of neighboring points, resulting in smooth visual transitions and continuity.

***Quantitative Structure Models (QSM)*:**
As defined in the relevant literature 2.5.3, QSM is an open-source method applied in this section to analyze tree morphology and extract structured data from a Pointcloud, see Fig 3.22(c).

The methodology enables an automated and systematic approach to tree segmentation, data classification, and the generation of exportable datasets.

***Mesh*:**
A *Mesh* represents surfaces through interconnected polygons, as triangles or quadrilaterals, created by linking points from a point cloud. Meshes facilitate efficient computational processing and visualization, widely adopted in graphical applications and numerical simulations.

***Subdivision Surface (SubD)*:**
SubDs represent smooth surfaces generated recursively from a coarse polygonal control mesh (Cage). Through iterative subdivision—applying averaging rules to refine the initial cage—SubD balances computational efficiency with smoothness, making it suitable for modeling organic forms. Prominent subdivision schemes include *Catmull–Clark*[152] (quad meshes), Loop [153] (triangular meshes), and Doo–Sabin [154] (general polygons). In practice, software implementations such as Rhinoceros' SubD [71], Realize Shape [155], T-Splines [156], and Imagine & Shape [157] leverage these algorithms to facilitate intuitive organic modeling. SubDs can be converted into networks of NURBS patches that reproduce the limit surface; around *extraordinary vertices* the conversion algorithms lets the designer choose the desired geometric continuity, balancing shape fidelity and smoothness.

Non-Uniform Rational B-Splines (*NURBS*):
NURBS explicitly describe curves and surfaces through rational parametric equations [158]. They provide exact, mathematically-defined geometries ideal for precision engineering and manufacturing tasks. A *B-Spline* (Basis Spline) is a special case of a NURBS curve or surface in which all weights are equal—typically set to 1—resulting in uniform influence of the control points.

3.2.2 3D Acquisition: Scanning and Image-Based Methodologies

The acquisition of three-dimensional data is performed using various adaptations of standard methods such as photography and laser scanning (LiDAR). These techniques enable the physical capture of objects in 3D, with implementations varying in terms of geometric precision and application. They generate highly accurate point clouds, which can be used to model complex timber structures. Although more resource-intensive, 3D scanning offers high precision and is particularly suitable for capturing fine details in naturally grown timber.

The overarching goal of this exploration is to develop a unified model (see Fig. 3.10) that not only simulates timber geometries but also incorporates material properties. This is achieved by combining various data acquisition techniques and integrating them through NURBS modeling to provide a comprehensive representation. Additionally, this section introduces the different centerlines used in the modeling process—corresponding to the geometric center (C_g), growth center (C_G), and mass center (C_M)—emphasizing their significance in accurately capturing the natural characteristics of timber.

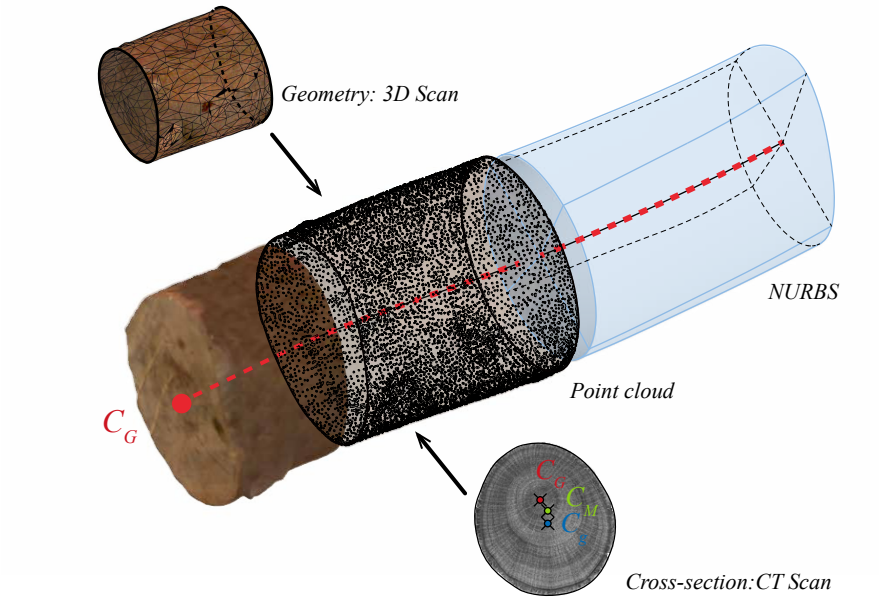

Figure 3.10: Integration of Image-Based Data Acquisition and NURBS Modeling.

Image-Based Modeling Overview

Image-based modeling refers to the acquisition of 3D geometry from photographs [159], or within hybrid workflows [160], for the creation of 3D models from 2D images. This involves distance estimation and geometric analysis using techniques such as photogrammetry and laser scanning. In architecture and computational design, image-based modeling plays a crucial role in capturing complex geometries and natural materials [161], such as irregularly grown timber. These digital models enable engineers to represent and analyze non-standard shapes, supporting structural design, fabrication, and visualization [162]. By recording precise details, image-based modeling enhances design accuracy and reduces material waste—particularly important when working with organic geometries and their integration into digital workflows.

For irregular materials like naturally grown timber, image-based modeling is essential. Such materials often exhibit non-standard forms, making conventional construction methods challenging. Techniques such as photogrammetry and laser scanning are capable of capturing the geometric complexity of these materials, enabling their integration into load-bearing structures.

Improvements in photogrammetry, such as Neural Radiance Fields (*NeRFs*) [92] make a next step in the application opportunities. *NeRFs* are a deep learning-based technique for generating highly detailed 3D models from 2D images. NeRFs are particularly effective for capturing fine surface textures and irregular shapes, making them especially valuable for modeling naturally grown timber.

Different techniques have been investigated and implemented at different scales: photogrammetry and NeRFs for large-scale tree modeling, and LiDAR scanning for detailed acquisition of raw timber elements.

3.2.3 Datasets

Tree Dataset 1: Digital Forest

To complete the information on forest development and assessment (see Subsection 2.5.1), additional efforts involving statistical data analysis have been implemented. The Digital Forest is an initiative aimed at developing real-time monitoring systems to assess climate impacts on forests. The project builds upon foundational research conducted by Seidel et al. [163, 164], which established initial methodologies for high-resolution data acquisition using LiDAR.

The studies cited above include the first dataset collected from a 0.5-hectare forest area (approximately 80 × 80 meters, including buffer zones) near Hainich, Germany. The database was generated through a point cloud processing system designed for individual tree separation, consisting of 50 million points obtained via laser scanning from 35 different positions.

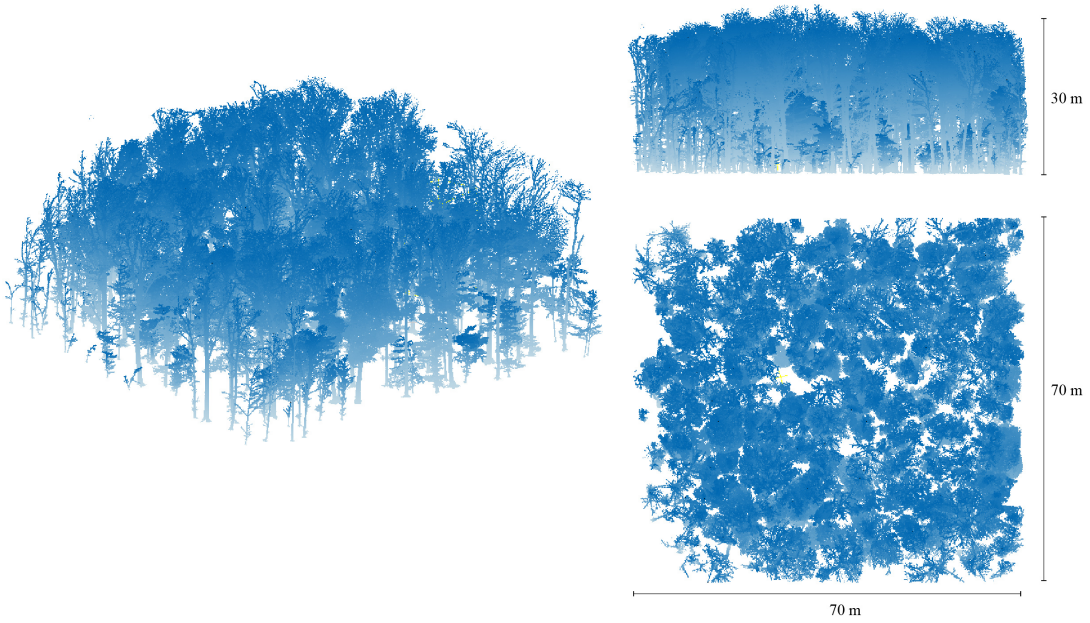

Figure 3.11: Point cloud database from Hainich [163, 164], visualized with color height map.

This dataset was further processed to facilitate *Quantitative Structure Models* in the next phase, enabling calculations of branch volumes, crown height, crown surface area, crown radius, and tree complexity metrics. The statistical analyses derived from these parameters contribute to understanding forest dynamics and structural diversity.

The motivation behind this research aligns with the *management for complexity* approach [165], an increasingly relevant concept in silviculture. By analyzing tree structural complexity, researchers can derive positive ecosystem function effects, enhance species diversity, and improve forest resilience and resistance [166]. Additionally, findings indicate that large and old trees are not only crucial for biodiversity conservation but also exhibit high structural complexity, making them a focal point for advanced forest management strategies.

The dataset contains segmented tree data following the terrestrial laser scanning (TLS) methodology described in [91, 163]. The predominant species include *European Beech* (*Fagus sylvatica*) with 176 specimens, *European Ash* (*Fraxinus excelsior*) with 30 specimens, *European Hornbeam* (*Carpinus betulus*) with 3 specimens, and *Sycamore Maple* (*Acer pseudoplatanus*) with 6 specimens. The trees were processed to extract structural metrics. The resulting dataset shows an average tree height of approximately 20 m and a mean diameter of 30 cm.

For this study, trees with wide crowns were selected to analyze branch development and hierarchy. A total of 20 trees from this inventory were chosen for further analysis in the next phase, focusing on structural form variations.

Tree Dataset 2: Tree Growth in the Region

The regional forest of North Rhine-Westphalia (NRW) is classified as a biodiversity forest, with 83% certified under the PEFC standard (see standard in Chapter 2.5.4). It covers a total certified forest area of 752,452 ha, distributed as follows: 126,389 ha (16%) state and federal forests, 119,698 ha (15%) municipal forests, 192,465 ha (25%) private forests, and 313,900 ha (41%) cooperative forestry associations [167]. Publicly available data provide additional insights into biodiversity and species composition.

In the vicinity of Aachen, particularly around the *Eifel Nature Park*, research has been conducted to obtain local timber for study, as well as to analyze tree growth dynamics. This section focuses on growth analysis, considering both interior forest trees and edge trees. Collaboration with *Wald und Holz NRW* and the *Regional Forestry Offices* of the Aachen district has facilitated the study and authorized extraction of material from selected locations. The following study sites were visited:

- **Aachen-Sief Forest** (Private forest, Landvogt Forstbetrieb, near Schmithof, Aachen). Coordinates: 50.683914, 6.160285. Visited between 2021 and 2023 to obtain raw material, primarily red beech, oak, birch, and hornbeam.
- **Zweifall Forest** (Cooperative Forestry Association, near Zweifall, Stolberg). Coordinates: 50.716532, 6.285789, see Fig. 3.12. Visited for analyzing tree growth, primarily focusing on edge trees. Data collection in these areas is planned for 2024 and 2025, targeting 12 trees using applied photogrammetry, and NeRFs for point cloud acquisition. A subset of 7 selected trees 3.13 will undergo further analysis.
- **Mausbach Forest** (Cooperative Forestry Association, near Mausbach, Stolberg). Coordinates: 50.746831, 6.294383. Designated as a construction prototype exhibition site due to its proximity to a high-traffic hiking area in the Eifel region.

Specimens Dataset 1: Raw timber specimens from the forest

Between 2021 and 2023, raw timber specimens were collected from the Aachen-Sief forest. In areas designated by forest management groups, elements with varied geometries were selected,

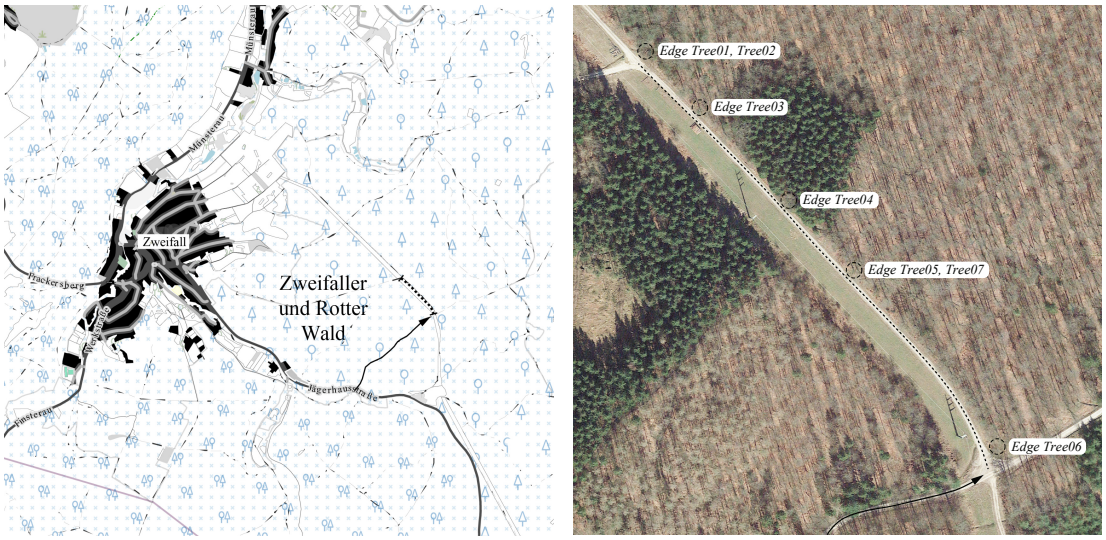

(a) Forest area in Zweifallwald (b) Forest street with edge trees in Zweifall

Figure 3.12: Mixed forest study locations.

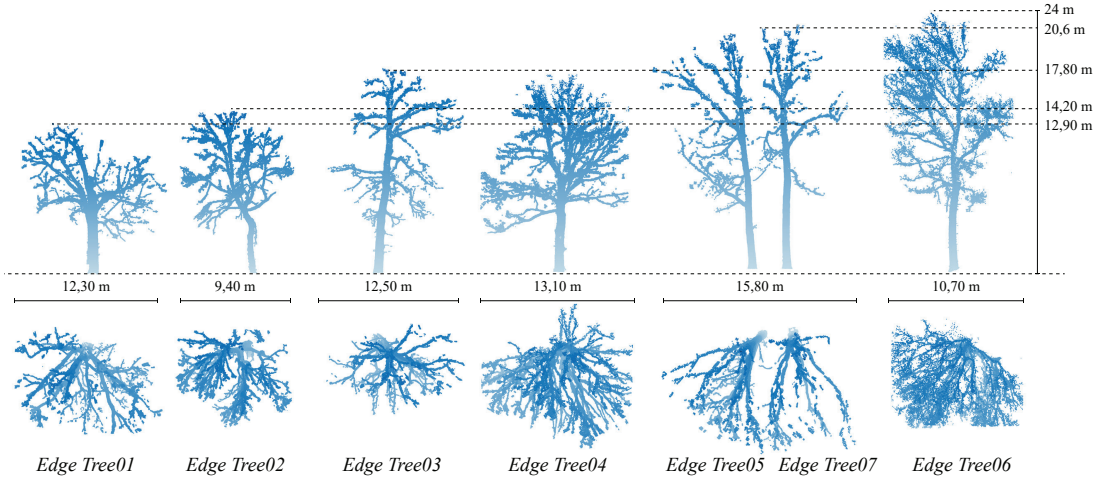

Figure 3.13: Point cloud dataset of edge trees.

typically up to 2 meters in length and with diameters ranging from 7 to 15 cm. These specimens were used in the initial geometric modeling experiments, as presented in Section 3.4, and in the construction demonstrations discussed in Chapter 6.

As shown in Figure 3.14, the raw timber elements were evaluated and pre-cut, providing average dimensions for the design of the demonstrative structure described in Section 6.3.1.

Specimens Dataset 2: Raw Timber from Dumping Site

In addition to timber extracted from the forest, raw timber elements sourced from urban areas in the city of Aachen were also utilized. These specimens were recovered from the Aachen North

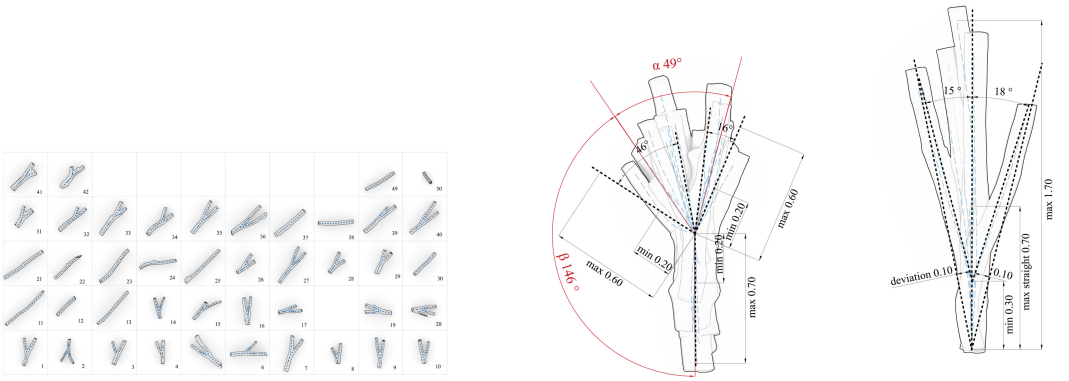

(a) Collected timber library

(b) Geometric variations in forks and curved elements (length in meters)

Figure 3.14: Overview of raw timber specimens used in modeling and construction studies.

dumping site (see Fig. 1.8.2). They were primarily used in construction experiments conducted as part of academic studies, projects, and seminars held at the Faculty of Architecture between 2024 and 2025, as presented in Appendix B.6.5. Furthermore, these elements were employed in mechanical testing and simulation experiments, which are discussed in Section 4.3.

3.2.4 Tree Data Adquisition

For the acquisition of raw data from naturally grown trees, point clouds generated through LiDAR scans are not the only viable approach. Advances in photogrammetry, particularly with NeRF technology, see Fig. 3.15, facilitate the use of photographs or simple ground-level video recordings, making data collection in forest environments more accessible. Additionally, two markers are introduced for scan calibration, positioned at a predefined distance.



(a) Gaussian splatting visualization

(b) Point cloud

(c) Processed Mesh

Figure 3.15: Example of a state of the art process of 3d acquisition of a pine tree (*Example 01*) in the Entrepeñas reservoir using the Photogrammetry NeRFs Luma software [94] (date July 9, 2024).



(a) Defined reference distance (b) Trunk view with calibration markers (c) Full tree

Figure 3.16: Scan of the oak tree *Edge Tree06*, located in the Zweifall forest, obtained using Polycam software [95] and visualized through Gaussian Splattings (date March 19, 2025).

TreeQSM Method and Data Processing

Following processing with the Quantitative Structure Model (QSM) method, the scanned trees are converted into cylindrical models to assess and evaluate tree geometries. The QSM-based data acquisition adheres to a structured workflow to ensure accurate representation of tree morphology. This includes the segmentation of individual tree components, fitting of cylindrical primitives to point cloud data, and hierarchical ordering of branches. The resulting models provide the geometric foundation for further structural and material analyses.

1. **Point Cloud Generation**:
    - 3D scanning of trees using photogrammetry or LiDAR.
    - Noise reduction and pre-processing of raw point cloud data.
2. **Segmentation and Hierarchical Structuring**:
    - Identification of primary, secondary, and tertiary branches.
    - Computation of cross-sectional diameters along branch lengths.
3. **Automated Data Export**:
    - Generation of structured files containing tree morphological data.
    - Export formats compatible with further analysis and visualization.

3.2.5 Mesh generation and topology process

Representation Selection Criteria

The choice among following geometric representations is dictated by specific application requirements: *Point Clouds* for raw geometry capture and preliminary processing; *Meshes* for discrete, computationally manageable representations; *Subdivision Surfaces (SubD)* for flexible, editable, smooth modeling of complex organic shapes; *NURBS* for mathematically rigorous, precision-controlled surface definitions suitable for structural engineering analysis and manufacturing processes.

Understanding these fundamental geometric representations and their properties is critical in developing optimized workflows in computer graphics and computational modeling.

Mesh generation

The normal vectors of tree point clouds must be carefully estimated. Using a local quadratic surface model, also called a height function, helps improve the accuracy when dealing with curved surfaces [168]. This approach improves surface reconstruction (see Fig. 3.17(a)), producing a watertight mesh from scattered points. While effective, this method often requires a retopology step to reduce mesh complexity, ensuring smoother integration into digital workflows—especially for large or highly detailed trees and branch elements.

Several implicit functions can be used for surface reconstruction, including the Poisson function, the Discrete Smooth Interpolation function, and Radial Basis Functions (RBF). Among these, the *Poisson reconstruction method* [169] is the most widely used for generating a mesh from a point cloud. This approach reconstructs surfaces without relying on heuristic spatial partitioning or blending techniques, which can introduce inconsistencies and artifacts.

Once the normals are calculated and the reconstruction is finished, the process generates a mesh M with different levels of detail (see Fig. 3.17(b)). This figure visualizes surface density distribution, where red indicates areas of high point density with more information, while blue represents regions with lower data availability. This distribution, automatically generated by the *Poisson* algorithm, introduces some uncertainty, often requiring retopology to smooth specific areas and create gradual transitions in regions with lower information density.

Retopology

Retopology refers to the process of optimizing the geometry of a scanned object by simplifying its mesh M while retaining essential surface details. This step is essential for converting high-resolution scans, from *PointClouds* PC, into usable models that can be seamlessly integrated into geometrical workflows. For timber structures, where naturally grown elements often have irregular and complex geometries, retopology ensures that models are computationally efficient for structural analysis and digital fabrication, without losing important geometric features that are critical to the integrity of the design.

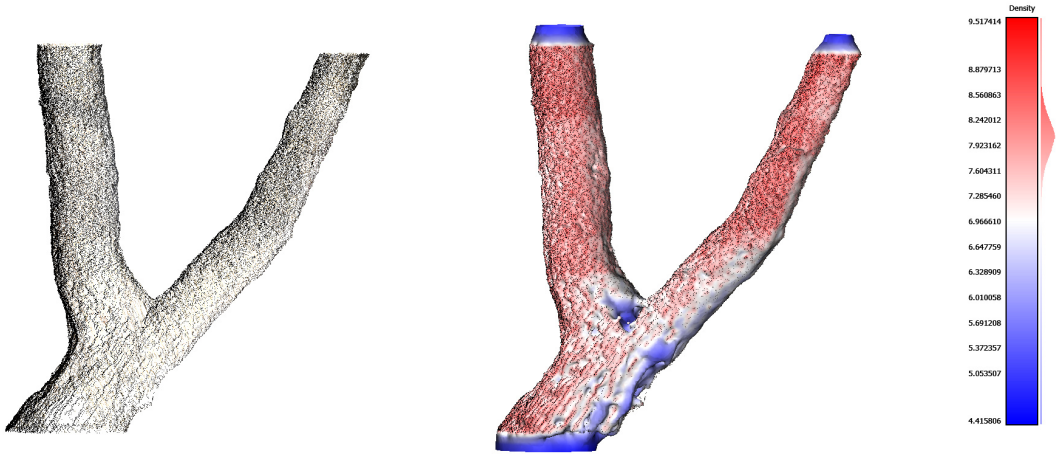

(a) Section of the Point Cloud (b) Mesh computation with surface density information

Figure 3.17: Poisson surface mesh computation of *Example 01* in Fig. 3.15.

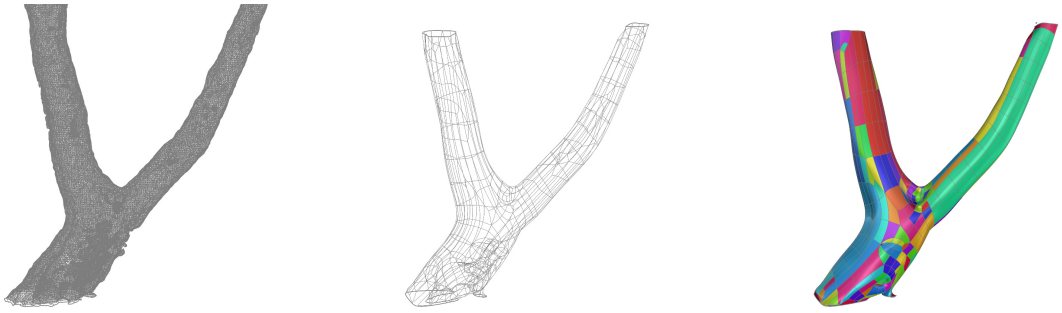

(a) Original Mesh (b) Quad Retopology in Wireframe (c) Topology with packed faces

Figure 3.18: Mesh retopology and packed faces hierarchy.

Retopology to NURBS and SubD Conversion

After retopology (see Fig. 3.18), additional processes such as reverse engineering and mesh-to-NURBS conversion can take place. Mesh-to-NURBS conversion is particularly useful for transforming a polygonal mesh M into a mathematically precise surface, such as a CAD model, for high-precision applications like structural simulations or CNC-based fabrication. However, this process is computationally expensive and often struggles with the organic and irregular shapes typical of raw timber.

For smoother workflows involving organic geometries, SubD geometries offer a more flexible alternative to traditional NURBS. SubD maintains control points similar to NURBS but is better suited for handling soft, irregular forms. The *Mesh-to-SubD* function, which is based on a *Quad Remeshing* process, serves as the foundation for generating a SubD geometry. This

method balances modeling flexibility and curvature precision, allowing the entire geometry to be analyzed while preserving its organic features.

Despite the potential of SubD geometries, a midstep is often needed to make these models usable for simulation or analysis. A key issue is the *packed faces* function in SubD (see Fig. 3.18(c)), which clusters geometry in a way that does not correspond to the natural form of raw timber, complicating the integration of material properties. Since timber's anisotropic properties, like varying strength and stiffness in the growth directions, are essential for accurate simulations, the geometric model must be adjusted to reflect these characteristics, ensuring reliable performance evaluations.

Modified Retopology based on *Packed Faces*

Once the retopology methods have been applied, there are still various random patterns that do not conform to the hierarchy required for future analyses. To address this, a hierarchical retopology subprocess is performed. This technique is based on applying processed curves from the cylindrical tree model, see Fig. 3.19(a), where centerlines are utilized as guiding curves c_g^n. These curves direct the generation of packed faces, ensuring alignment with the hierarchical structure and achieving the desired discretization.

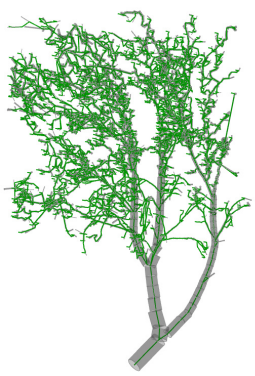

(a) QSM cylindrical tree

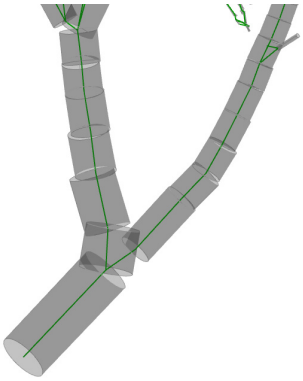

(b) QSM cylindrical tree in detail



(c) Hierarchical retopology

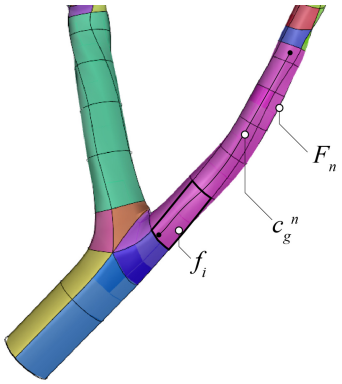

(d) Hierarchical retopology in detail

Figure 3.19: Hierarchical retopology based on packed faces.

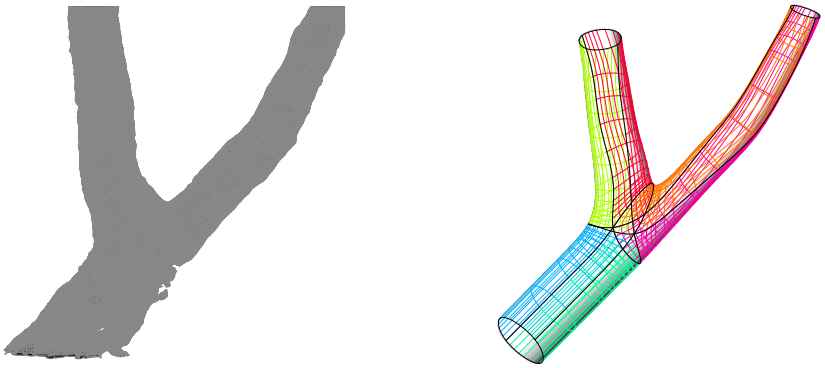

(a) Original mesh from 3d scan

(b) NURBS patches following packed faces

Figure 3.20: Processed NURBS from the QSM hierarchy applied to of *Example 01* in Fig. 3.15 with basic modeling.

The process follows a structured transformation where a given SubD geometry is converted into a Brep while preserving a hierarchical subdivision of faces.

This process is defined by a retopology function, implemented in C#, which operates on the SubD surface, a set of guiding curves c_g^n, and a Boolean parameter that controls the face-packing strategy. The output includes a new SubD topology and, optionally, a set of randomly assigned face colors C_f for visualizing patch continuity across SubD faces.

The resulting SubD face set F_n is formed as the union of individual faces f_i, each associated with a guiding curve c_g^n. The number of faces per curve is denoted by k. This hierarchical retopology clusters adjacent faces around each guiding curve to maintain geometric coherence and enhance mesh discretization quality.

The hierarchical retopology ensures that each face aligns with the corresponding structural subdivision, improving geometric consistency and enabling more precise computational analysis. This functionality has been implemented as a *plugin* for packing geometries within the QSM structure in *Grasshopper*, providing automated and structured retopology (see Appendix B.2).

Finally, the simplified geometry can be converted into surfaces. As shown in Fig. 3.20(b), the previously scanned example is represented as NURBS patches. The model has been downscaled from its original dimensions due to the use of cylindrical elements derived from the tree's Quantitative Structure Model (QSM). However, this approximation does not reflect the tree's original surface geometry. Therefore, for tasks requiring precision, a more detailed geometric analysis is necessary. As shown in Fig. 3.20, the retopology process demonstrates the potential of this modeling approach.

It is important to notice that default geometry construction often results in volume reduction and surface simplification, which compromise the fidelity of the original form. A more advanced modeling strategy enables a structured and precise representation. This is further examined in Section 3.6, which presents in-depth investigations into computational methods for advanced SubD modeling of raw timber elements.

3.3 Tree Modeling

This section presents a tree modeling methodology based on data acquisition, aimed for analysis, potential assessment, or segmentation into elements later used as structural components. The methodology is summarized in the diagram shown in Figure 3.21, which outlines a workflow covering data acquisition, and geometry analysis. The process is organized hierarchically to retain the position of the branches in the tree and to describe the spatial connections between the tree and its surrounding environment, as growing directions.

See the example in Figure 3.22, shows an example that illustrates the transition from a point cloud to a Quantitative Structure Model (QSM). This example demonstrates the pipeline introduced in the diagram, starting from a tree at the forest edge and resulting in a quantifiable model.

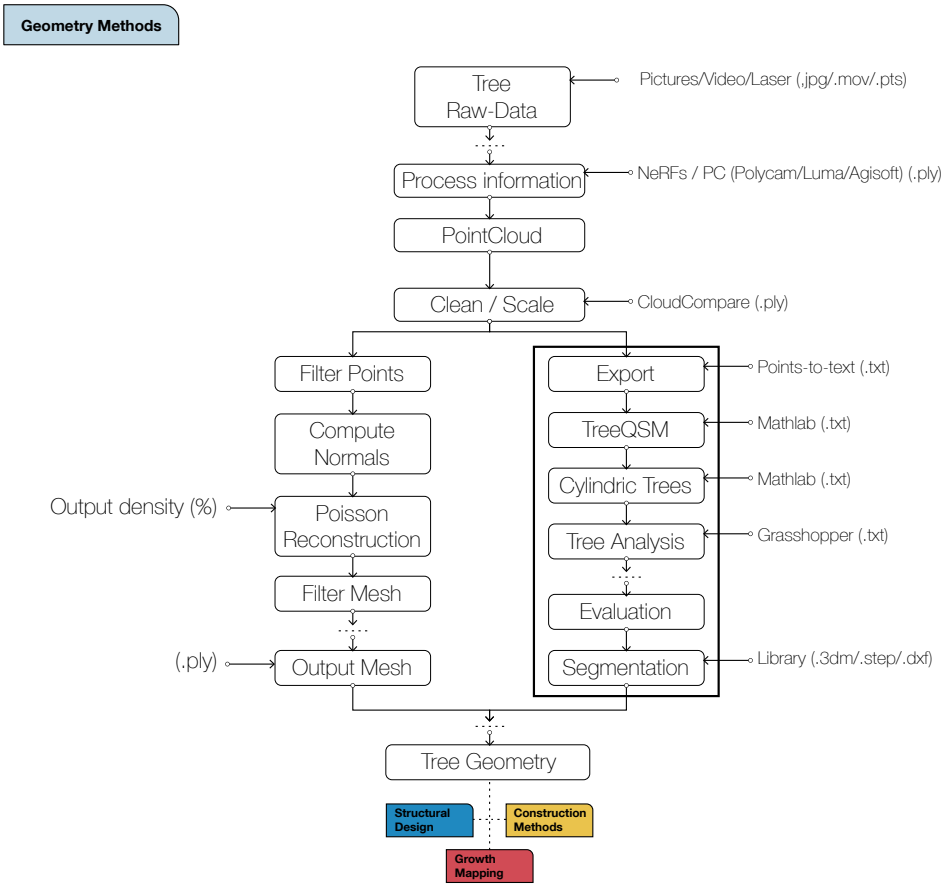

Figure 3.21: Design workflow of the tree modeling process.



(a) Forest edge tree (b) Tree point cloud (c) Tree QSM computation

Figure 3.22: Computation of forest trees. Example from PointCloud in Figure 3.13.

3.3.1 Tree Geometry Model

The geometric data obtained from QSM processing is evaluated to extract three-dimensional information for the complete tree, individual sections, or isolated elements. Using a dedicated algorithm, features such as curvature types, radii, volumes, and growth directions can be analyzed. These parameters are assessed to extract specific geometric information.

Hierarchical Structure and Tree Classification

The hierarchical structure of the tree, visualized in Figure 3.23, is derived from the TreeQSM model, which organizes the branching system by order. Branch order is assigned relative to the main stem: order {0} corresponds to the main stem itself, followed sequentially up to a maximum of {4}. Within each defined order, branches are indexed from bottom to top as {*,0} to {*,N}, where N is the total number of branches in that order. Here, the symbol {*} denotes the corresponding parent order, starting from the first-order branches.

For the identification of grown timber elements, minimum and maximum diameter thresholds are defined. The stem typically includes larger diameters—up to $25\,\mathrm{cm}$—while branches with diameters below $10\,\mathrm{cm}$ are classified as harvest residue, i.e., material that, according to forestry regulations [25], remains on the forest ground. Automation methods are relatively accurate in detecting the first two branching orders. However, smaller branches (e.g., orders {3} to {4} shown in red in Fig. 3.23)—despite their frequency and contribution to total volume—are more difficult to process and are not modeled with the same precision. This limitation, however, is not critical for the purposes of geometric analysis.

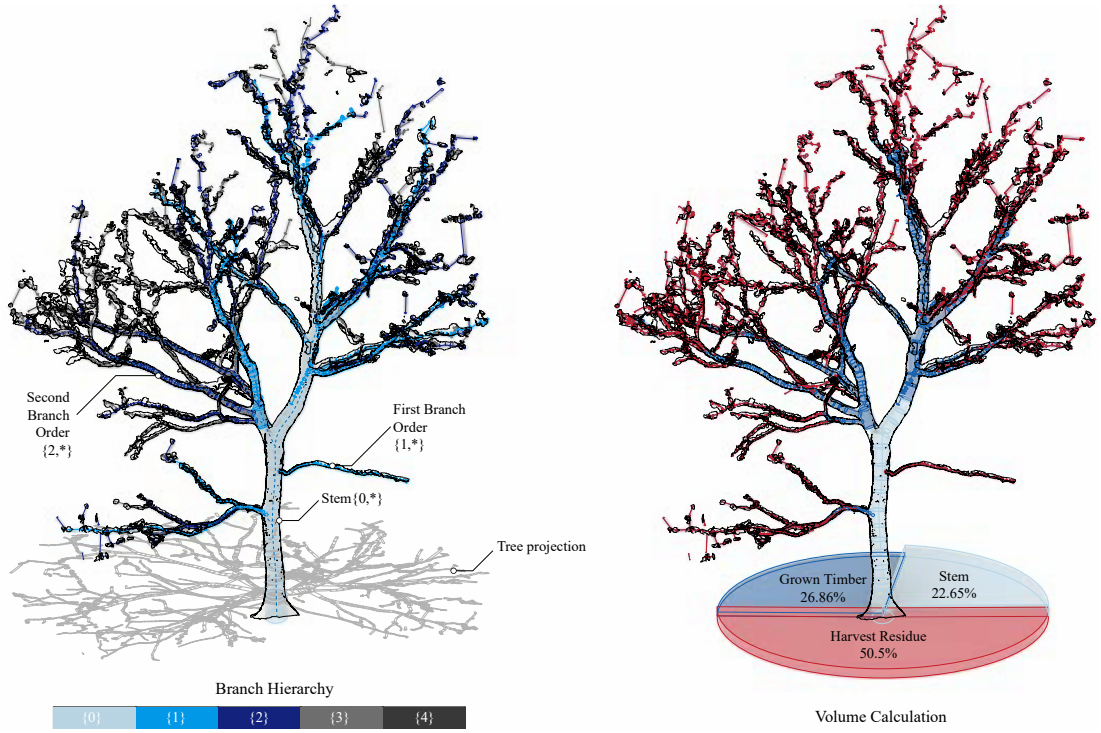

Figure 3.23: Hierarchical structure of the tree on the left, showing branch orders from 0 to 4. On the right, classification of tree parts according to their volume: stem, grown timber, and harvest residue. The tree geometry shown was extracted from a specimen of a free-standing oak located in the botanical garden at coordinates 55.966000, -3.212000.

Geometric Calculations

The analysis methods follow a set of geometric considerations illustrated in Figure 3.24, which also shows the hierarchical structure and codification used in the tree model. These considerations are based, with certain adaptations, on the *Framework Agreement for the Raw Timber Trade in Germany (RVR)* [25].

Curvature

Curvature is defined as the maximum deviation of the curve from a straight line connecting its endpoints. It is measured along the central axis of the curve. The curvature, as a percentage $K_{\%}$ is calculated as:

$$K_{\%} = \frac{K}{L} \times 100 \tag{3.1}$$

The K represents the maximum perpendicular distance from any point on the curve to that line measured in cm, and L denotes the lenght of the line segment. This normalization allows curvature to be consistently compared across segments of varying scale.

Diameter

The curve c_g is divided into segments, producing cross-sections s_i for diameter analysis. For each section s_i, a minimum bounding rectangle is computed to enclose the cross-sectional curve, from which the maximum and minimum diameters (D_{max} and D_{min}) are derived. The *taper* is a parameter related to the diameter variation along an element, calculated as:

$$Taper_{\%} = \frac{D_{0,\text{max}} - D_{i,\text{min}}}{L}$$

where $D_{0,\text{max}}$ is the maximum base diameter, $D_{i,\text{min}}$ is the minimum diameter at section i, and L is the segment length. This metric, expressed in $\mathrm{cm\,m^{-1}}$, supports the evaluation of both biomass distribution and tree statics, which are further explored in subsequent chapters.

Eccentricity

From each calculated s_i sections, the largest inscribed circile tangen to the curve in one point is calculated, defining the secondary cross-section s_{i-j}. The centroids of s_i is denoted as C_g, and the centroid of s_{i-j} is denoted as C_G. The distance between C_g and C_G is defined as eccentricity, and it is calculated in percentage as:

$$e_{\%} = \frac{e}{\left(\frac{D_{\text{min}}+D_{\text{max}}}{2}\right)} \times 100 \tag{3.2}$$

These metrics can be visualized in Figure 3.24(a) and in Figure 3.24(b).

Bifurcation Angle Calculation

The bifurcation is the point that occurs when a new branch is created. In that case, the bifurcation point C_g serves as a segmentation point: as the last point of the initial curve, and first one of the same branch order. That point is also coincident with the start point of a new branch order. Figure 3.24(c) illustrates the evaluation of final angles at a bifurcation. Resultant vectors are first computed based on the directionality of connected segments. For this purpose, three vectors are defined:

- $\vec{a}$ as the sum of the last three vectors preceding the bifurcation,
- $\vec{b}$ as the sum of the first three vectors following one branch,
- $\vec{c}$ as the sum of the first three vectors along the second branch.

These vectors are calculated according to:

$$\vec{a} = \sum_{i=n-3}^{n-1} \vec{a}_i, \qquad \vec{b} = \sum_{i=0}^{2} \vec{b}_i, \qquad \vec{c} = \sum_{i=0}^{2} \vec{c}_i$$

Where n is the total number of points in each curve. From these sequences, the terminal points A_{n-3}, B_2, and C_2 are extracted and used to define an approximated bifurcation plane π. This

plane is constructed geometrically and serves as the reference for computing the divergence angles between vectors.

The angles are defined as follows: α is the angle between vectors $\vec{b}$ and $\vec{c}$, and β is the angle between vectors $\vec{a}$ and $\vec{c}$, both measured within the plane π established by the three points.

These angular relationships are essential for characterizing fork geometry and analyzing directional growth tendencies in naturally bifurcating timber structures.

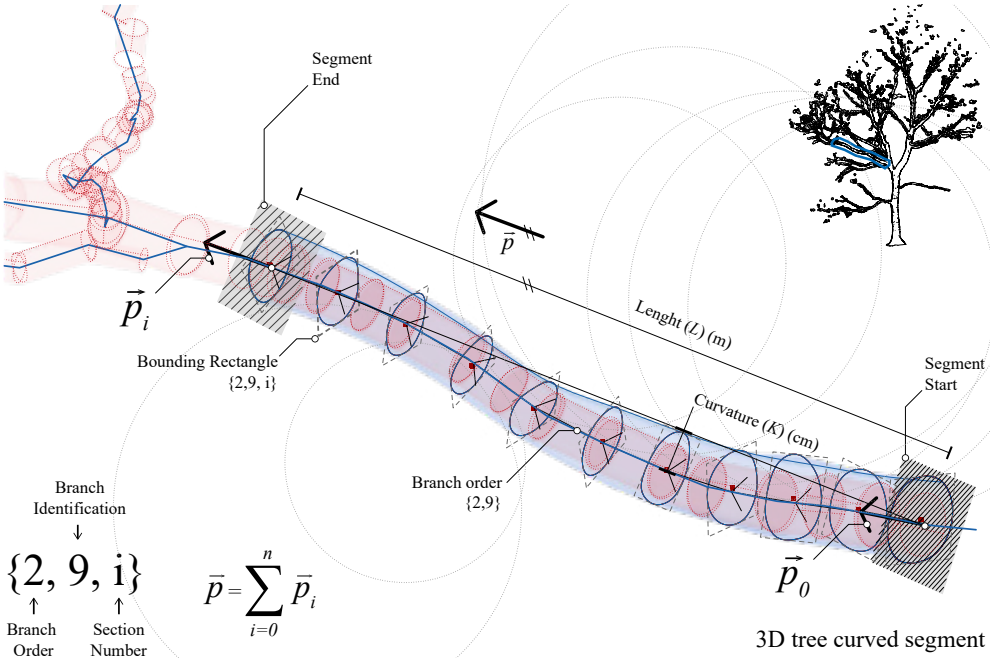

(a) Reference for branch geometry: segmentation and curvature calculation.

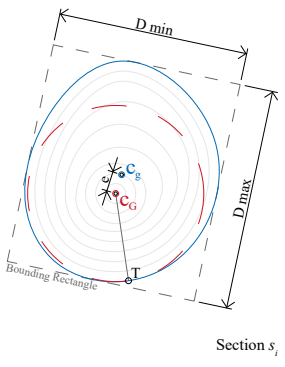

(b) Reference cross-section: Eccentricity calculation.

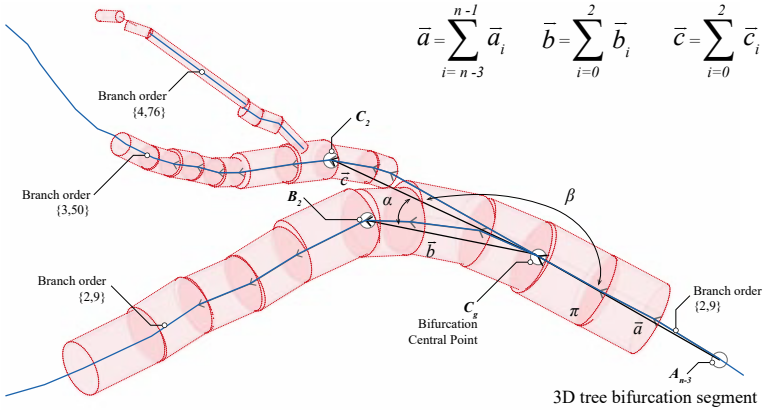

(c) Reference bifurcation geometry: Angle calculation.

Figure 3.24: Geometric reference calculations: branch-level segmentation and curvature; cross-sectional diameter and eccentricity.

Algorithm Design

The analysis algorithm builds upon the parameters described in the previous section. It is implemented as an automated workflow designed to apply these methods to the entire tree, enabling both detailed analysis and accurate segmentation. The general structure of the algorithm is shown in Figure 3.25.

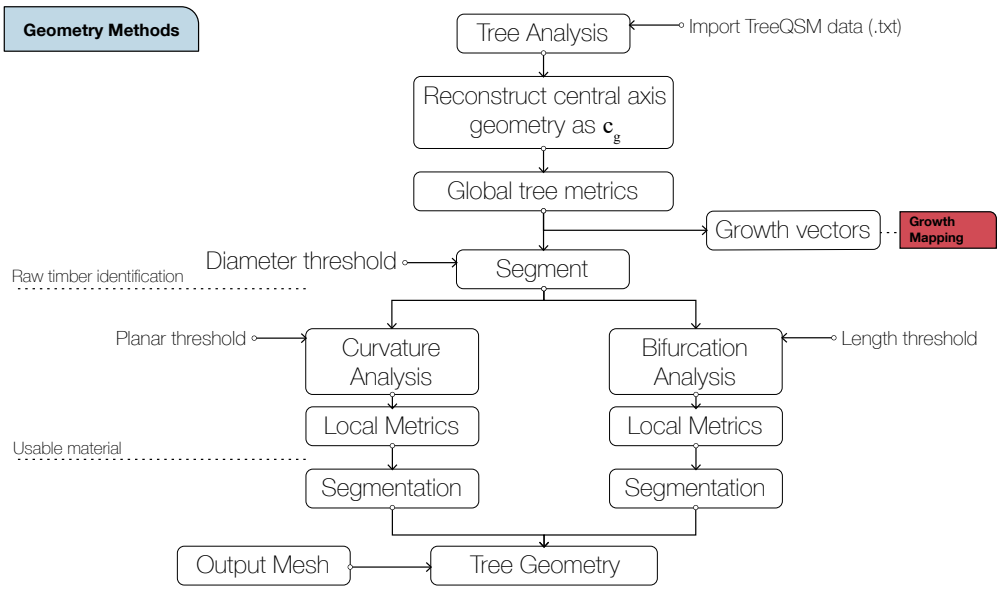

Figure 3.25: Workflow diagram of the analysis algorithm for geometry segmentation and metric extraction.

The process is automated through the import of TreeQSM data, which is pre-processed in MATLAB to enable structured geometric analysis. The model is reconstructed using the computed central axis geometry, which is segmented into straight elements with corresponding diameter values.

In the first stage, the algorithm segments the tree based on diameter thresholds. In the second stage, the selected elements are evaluated for curvature and further divided into planar components with simplified 2D curvature. This enables the creation of a raw timber element library for future analysis or applications.

The algorithm also extracts global metrics from the tree model, such as curvature variation by branch hierarchy, diameter variation across orders, and bifurcation angles at branch junctions. Additionally, it computes overall tree volume, which can be analyzed by branch hierarchy or through detailed diameter parameters.

Individual tree-level analyses are also performed. Among them is the automatic generation of growth vector diagrams, calculated by summing vectors associated with each branch order and projecting them onto the XY plane. This provides a view of the tree's primary growth direction, from which tropisms such as heliotropism ($\vec{t}$) can be inferred.

Another extracted metric is the analysis of individual elements. As illustrated in Figure 3.23, the growth direction $\vec{p}$ of each branch allows the derivation of local tropism vectors $\vec{t_n}$ and $\vec{g_n}$, characterizing directional tendencies at the element scale.

3.3.2 Analysis

Global Tree Data Export

This section presents the exported dataset for individual trees, structured through an automated process. The export includes key geometric and structural information such as:

- Tree height and total volume.
- Number of branches classified by order.
- Average and maximum branch lengths.
- Cross-sectional variation along branches.

The automated process enables large-scale analysis across multiple trees or forest sectors. This ability supports pre-harvest assessments, origin tracking, and the identification of naturally grown timber elements for specialized applications.

Several case studies included in this dissertation demonstrate the versatility of the dataset. These examples cover global tree metrics, volume comparisons, and detailed element-level analyses. While this subsection focuses on general characteristics, detailed analyses of individual elements are addressed later in this chapter (see Section 3.4).

The global tree analysis offers a comprehensive overview of structural variability, growth morphology, and segmentation logic based on the QSM model output. This forms the basis for downstream comparisons, statistical evaluations, and potential integration into fabrication-oriented workflows.

Tree Volume Analysis

The dataset reveals significant differences in volume and growth architecture among trees. These variations are observed both in the general dataset (3.11) and through specific analyses of edge trees (3.13). QSMs were applied to extract branch cylinders.

The preliminary classification distinguishes stem wood (minimum diameter of $20\,\mathrm{cm}$) in light blue, fine branches in red, and remaining branch structures in dark blue.

The analysis indicates that straight timber, primarily from stem sections, accounts for approximately 45% of the total volume in a typical interior forest tree, while this proportion drops to about 25% in edge trees. In contrast, irregular branch structures (marked in dark blue) contribute substantially to raw timber applications—comprising around 25% of the volume in interior trees and up to 45% in edge trees. The average total volume is estimated at $7\,\mathrm{m}^3$ for interior trees and $6.5\,\mathrm{m}^3$ for edge trees.

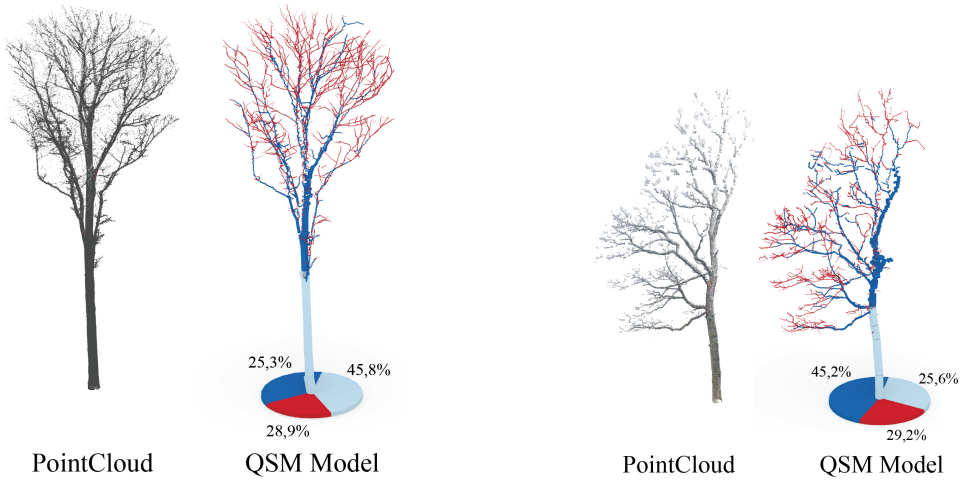

(a) Forest interior tree

(b) Forest edge tree

Figure 3.26: Comparison of extracted volumes from point cloud data using QSM for branch volume calculation.

Forest Quadrat Analysis

Analyzing a forest quadrat allows for the extraction of global growth directions, which can support modeling of tree development and its spatial structure. In the selected area, a group of 8 trees was studied to evaluate dominant growth orientations and patterns. These data help understand how environmental factors—such as sunlight exposure, slope direction, and inter-tree competition—influence directional growth trends.

The global growth direction is computed by summing all individual growth vectors of branches, either across the entire tree, per branch, or by hierarchical branch order. The resulting vectors are projected onto the horizontal plane to visualize dominant growth tendencies across the forest stand.

- Global growth vectors projected onto the horizontal plane.
- Tropic tendencies at the forest stand level.
- Mean curvature direction and orientation bias.
- Distribution of hierarchical branch orders.

The results are provided in the appendix B.3.1 of the thesis.

Individual Tree Analysis

A detailed analysis was performed on a selected group of edge trees, shown in Figure 3.26, that exhibit a high volume of grown branches. These trees were chosen for segmentation, growth evaluation, and structural analysis. Full results are available in Appendix B.3.2.

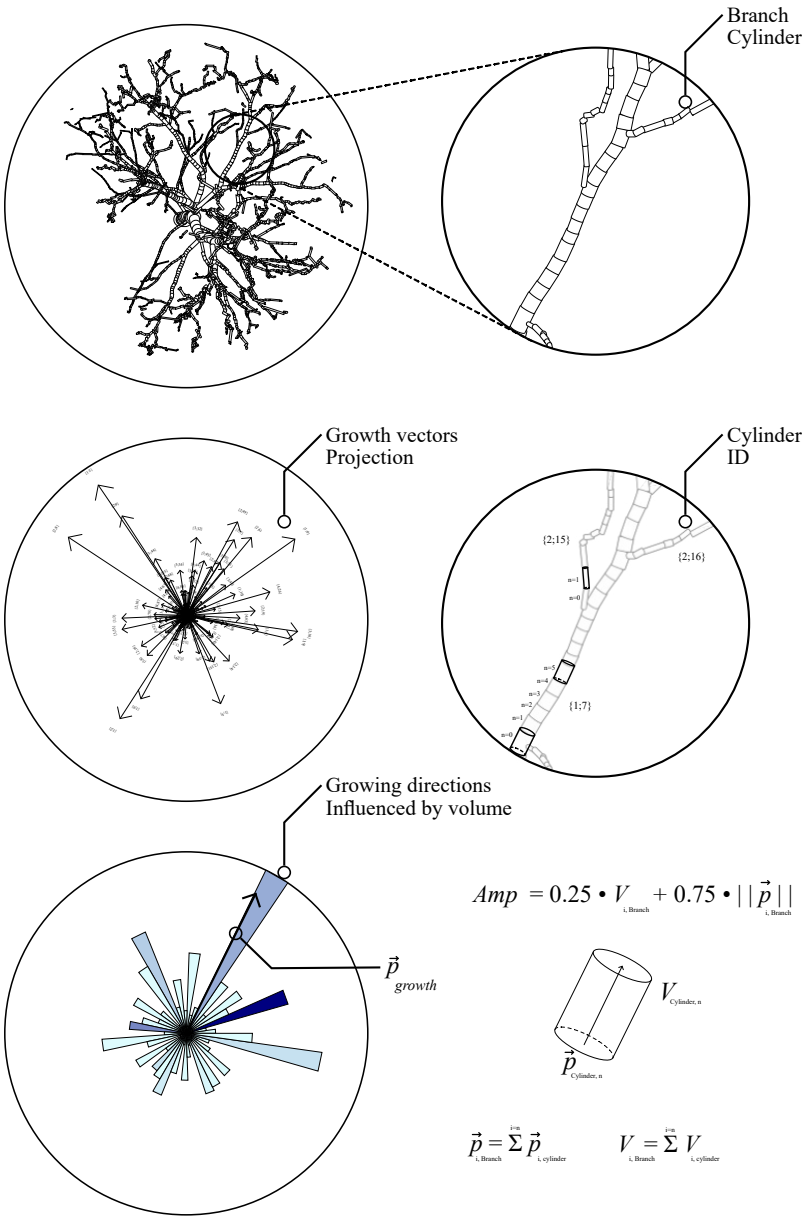

Figure 3.27: Visualization of growth vectors projected onto the horizontal plane, scaled according to tree volume. The figure displays directional growth tendencies extracted from forest quadrat analysis.

Key metrics extracted include:

- High-resolution point cloud data.
- Growth vector diagrams across hierarchical levels.
- Branch count per branching order.

- Volume distribution and curvature characteristics.
- Automated extraction of segments for the raw timber element library.

The corresponding results are documented in Appendix B.3.2. These allow the estimation of extractable volume relative to diameter and support traceability within the tree for raw material acquisition.

3.4 Three-Dimensional Raw Timber

3.4.1 Pre-processing

This section focuses on the development of analytical techniques for reclaimed individual raw timber specimens.

The processing of these elements requires a defined procedure to manage and evaluate pointclouds and mesh generation, outlined in Section 3.2.5. A simplified mesh with appropriate topology is extracted, serving as the basis for subsequent operations. This mesh is pre-processed to contribute to a materials library, with an initial reorientation step required for standardization and future data management.

Reorientation

Different 3D scanning techniques vary in accuracy when capturing the irregular geometry of timber elements. A critical step in the workflow is the calibration of scanned models by aligning the coordinate system with the volumetric distribution derived from the scan. This alignment ensures an accurate representation of the spatial dimensions and structurally relevant axes of the timber element.

Through digital modeling, dominant spatial axes are identified to determine the symmetry planes of the element, facilitating its integration into planar or three-dimensional structural configurations. Bounding boxes, as illustrated in Figure 3.28, define the minimal enclosing volume of each timber component and allow for the assessment of geometric deviation, and enables proper alignment of the model's geometric centerline (c_g).

Reorientation as Planar Alignment

Given a 3D mesh M, the reorientation process aims to align its base with a global workspace plane. This is achieved through a three-step transformation:

1. **Rotation around the local origin O:** The mesh M is iteratively rotated around its own axes (XY, XZ, YZ) to explore a range of orientations. For each configuration, the volume

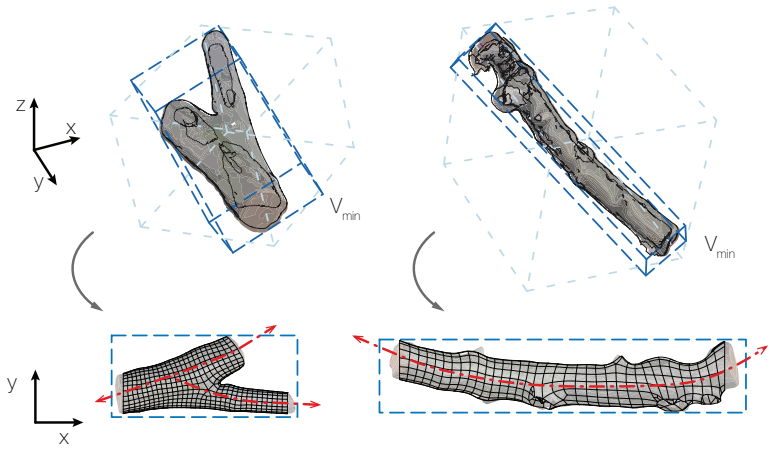

Figure 3.28: Automation of Bounding Boxes with Minimal Volume and 2D Realignment. Global and local coordinates.

of the axis-aligned bounding box $\mathcal{B}$ is computed. The optimal rotation R^* is the one that minimizes the bounding volume.

This step is implemented using a genetic solver that evaluates multiple angle combinations.

2. **Translation to the global reference point:** Once the mesh is optimally oriented, it is moved from its local centroid O to a target location O' in the global workspace. This is done with a translation vector $\vec{t}$.

3. **Reorientation to the global plane A':** Finally, the base plane of the oriented bounding box, denoted A, is aligned with a global reference plane A'. This is done by computing a plane-to-plane transformation that maps the local basis vectors of A (i.e., $\vec{X}, \vec{Y}, \vec{Z}$) to the global coordinate system $(\hat{i}, \hat{j}, \hat{k})$.

The full transformation T is thus a composition of rotation, translation, and plane alignment, applied to the entire geometry:

$$T(M) = \text{Align}_{A \to A'}(R^* \cdot (M - O) + O')$$

3.4.2 Geometrical Analysis for Raw Timber Elements

This section defines a geometric analysis methodology for parameterizing individual timber elements in accordance with their respective growth directions. A generic approach is presented, applicable to elongated curved elements, along with a modified procedure for bifurcated forms. The methodology is published in [170], where the geometric nomenclature used in this work is also formalized and adapted.

Geometrical Analysis of a Generic Curved Element

Following the pre-processing phase—which includes image-based mesh extraction, repositioning, and reorientation—the mesh volume is subdivided into transverse sections parallel to a relocation plane α_i, defined by the vertical vector $\vec{h}$ and a normal vector $\vec{a_i}$. This subdivision yields sectional slices s_i, each associated with a geometric center point A_i, later generalized as C_g. These center points collectively define the geometric centerline c_g. The construction rules are defined as follows:

$$\alpha_i = \{A_i, \vec{a_i}, \vec{h}\}$$
$$c_g = \{A_0, A_1, \ldots, A_i\}$$

This geometric information is then hierarchically structured for NURBS surface loft construction. Each cross-section s_i is further reduced to a set of up to *four* representative points S_i, which define segmented boundaries. These segments serve as the basis for constructing a *degree-3* transition surface. The process is illustrated in Fig. 3.29. The resulting 2D surfaces—referred to as patches—are generated in conjunction with the geometric centerline and are exported for subsequent mechanical simulations, see Section 5.3.1.



(a) Photo of a curved elongated element



(b) 3D mesh generation

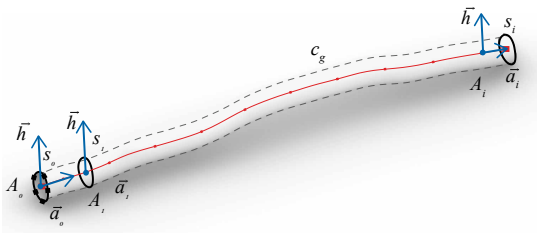

(c) Geometric construction rules

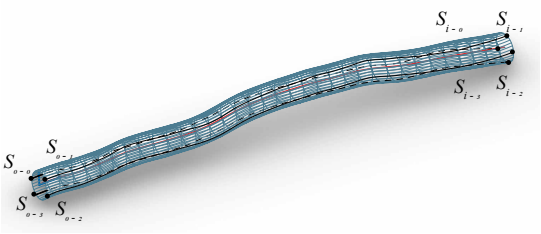

(d) Patches definition and NURBS

Figure 3.29: Geometric analysis workflow of a naturally curved timber element.

Generic Model for Bifurcations

The geometrical processing of bifurcated elements extends the generic model through integration along three axes. The oriented model, represented as a 3D mesh, interprets a bifurcation

with three central lines, a, b, and c, which are discretized along their lengths, producing direction vectors $\vec{a_0}$, $\vec{b_0}$, and $\vec{c_0}$ at their respective initial segments, originating from the bifurcation point. In this configuration, curves a and b are related to the main stem or principal growth direction, while curve c corresponds to the bifurcation. The selection between curves b and c is automated by interpreting their radii, $R - b_i$ and $R - c_i$; the curve associated with the larger radius dimension is identified as continuing the main direction, while the other is assigned to the bifurcation following the criterion $R - b_i > R - c_i$.

This process generates cross-sections s_{A-0}, s_{B-0}, and s_{C-0}, whose centroids (A_0, B_0, C_0) define the plane π. This plane π has an associated normal vector $\vec{h}_\pi$.

The combination of vectors $\vec{a_0}$, $\vec{b_0}$, and $\vec{c_0}$, together with the vertical vector $\vec{h}$ and the central geometric point C_{g-0}, defines the cutting planes α, β, and γ, which intersect the 3D mesh volume.

The plane π is defined as:

$$\pi = \{A_0, B_0, C_0\}$$
$$\vec{h}_\pi = \{\vec{h}_1, \vec{h}_2, \vec{h}_3\}$$

And the planes α, β, and γ are defined as:

$$\beta = \{C_{g-0}, \vec{h}_\pi, \vec{a}_0 + \vec{c}_0\}$$
$$\alpha = \{C_{g-0}, \vec{h}_\pi, \vec{c}_0 + \vec{b}_0\}$$
$$\gamma = \{C_{g-0}, \vec{h}_\pi, \vec{b}_0 + \vec{a}_0\}$$

The subsequent steps—defining surface patches and constructing NURBS—follow the same methodology as in the generic model. Here, the division of cross-sections s_i corresponds to the regions defined by the cutting planes. The resulting surfaces are then exported for subsequent mechanical simulation. To ensure a smooth curvature transition, a subdivision geometry element (Sub-D) is employed in the next section.



(a) 3D mesh of a bifurcation

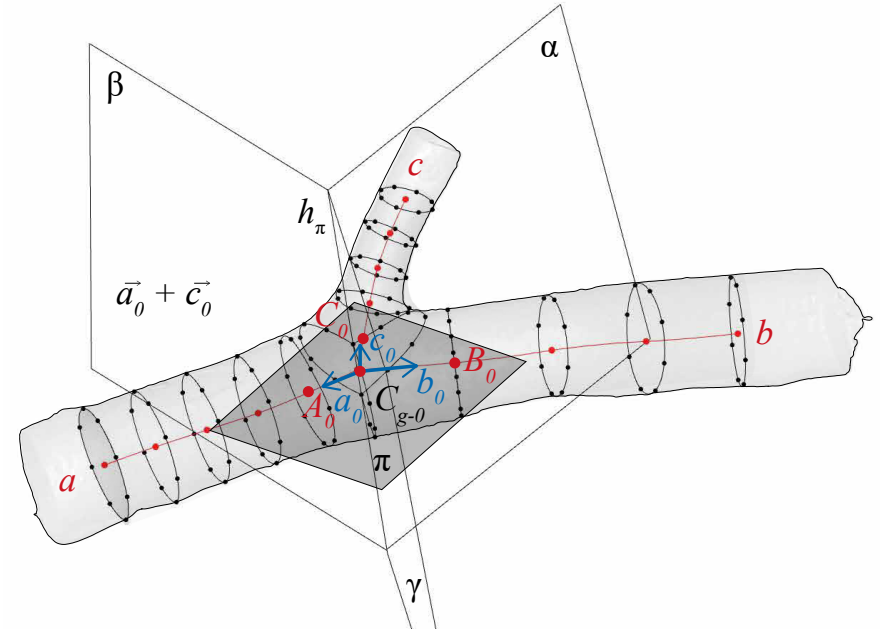

(b) Geometric construction

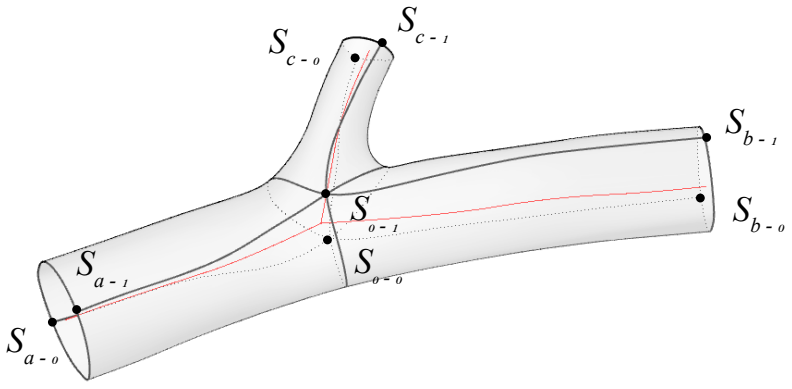

(c) Patches definition as NURBS

Figure 3.30: Geometric analysis workflow a naturally bifurcated timber element.

3.4.3 Segmentation of 3-Dimensional Raw Timber into 2-Dimensional Elements

During the development of applications for integrating raw timber into construction elements, it has proven both valuable and practical to disaggregate and segment 3D elements into 2D-like segments. This segmentation facilitates a easier implementations into construction elements—discussed in Chapter 6— like trusses or planar systems, including structural sandwich panels.

Timber elements are analyzed to extract their pith, represented as a longitudinal geometric centerline c_g, which summarizes the overall curvature of the element. This centerline c_g approximates the biological growth curve c_G. In plant algorithm theory, the growth curve is conceptualized as a directed, straight axis that determines branching at bifurcation points. These growth rules can be modeled in a two-dimensional scheme, such as axial trees [84]. Although this rule is followed during natural tree development, the growth axis often tends toward three-dimensional curvature due to adaptive responses such as tropisms. By using a geometric analysis algorithm, this three-dimensional curvature can be analyzed to identify timber segments that are predominantly two-dimensional.

In this process, the curve c_g is first segmented at regular intervals, generating a sequence of points $A_0, A_1, \ldots, A_i$. From these points, direction vectors $v_1, v_2, \ldots, v_n$ and the successive angles θ between them are computed. The angular difference is tracked, and when it exceeds a threshold value ϵ, the segment is considered non-coplanar. At this point, segment a ends, and a new segment b begins at $A_n = B_0$. The threshold ϵ therefore determines the coplanarity of points along the curve. Finally, a thickness range $(-h,\ h)$ is established and the upper and lower surfaces are planed accordingly. This segmentation process is repeated across all timber elements, contributing to the development of an image-based segment library, see in Fig 3.32.

$$\begin{aligned} \vec{v_n} &= A_n - A_{n-1} \quad (n = 1, 2, ..., n) \\ \theta_1 = \arccos\left(\frac{\vec{v}_1 \cdot \vec{v}_2}{|\vec{v}_1| \cdot |\vec{v}_2|}\right); &\quad \theta_n = \arccos\left(\frac{\vec{v}_n \cdot \vec{v}_{n+1}}{|\vec{v}_n| \cdot |\vec{v}_{n+1}|}\right) \end{aligned} \tag{3.3}$$

$$\begin{aligned} |\Delta\theta_1 - \theta_n| \geq \epsilon \quad &\rightarrow A_n = B_0 \\ \alpha = \{\vec{v'}_1, B_0\}; \quad &l = |A_0 A_n| \end{aligned} \tag{3.4}$$

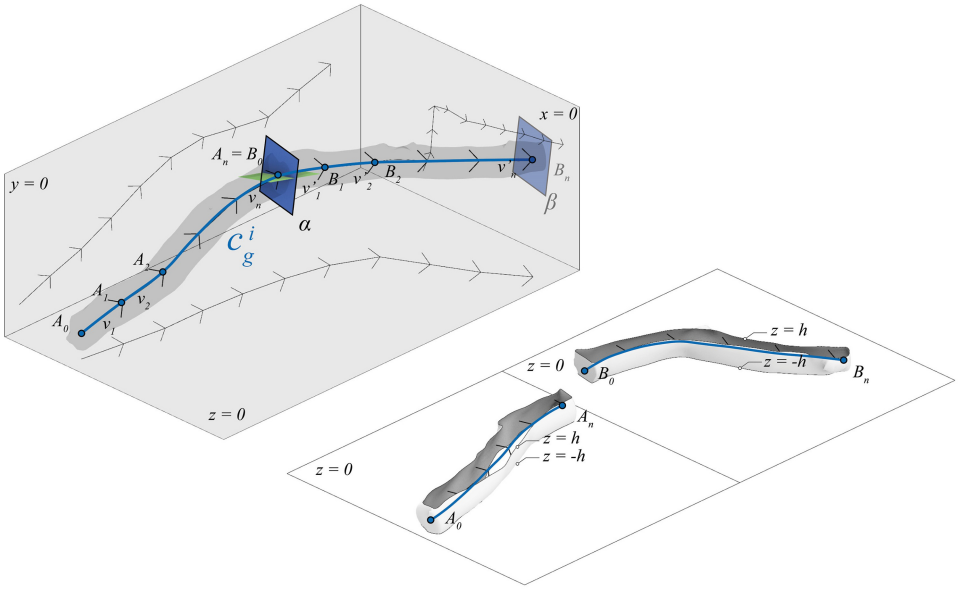

Figure 3.31: 3D Timber element segmentation for 2D elements, followed by planning their top and bottom.

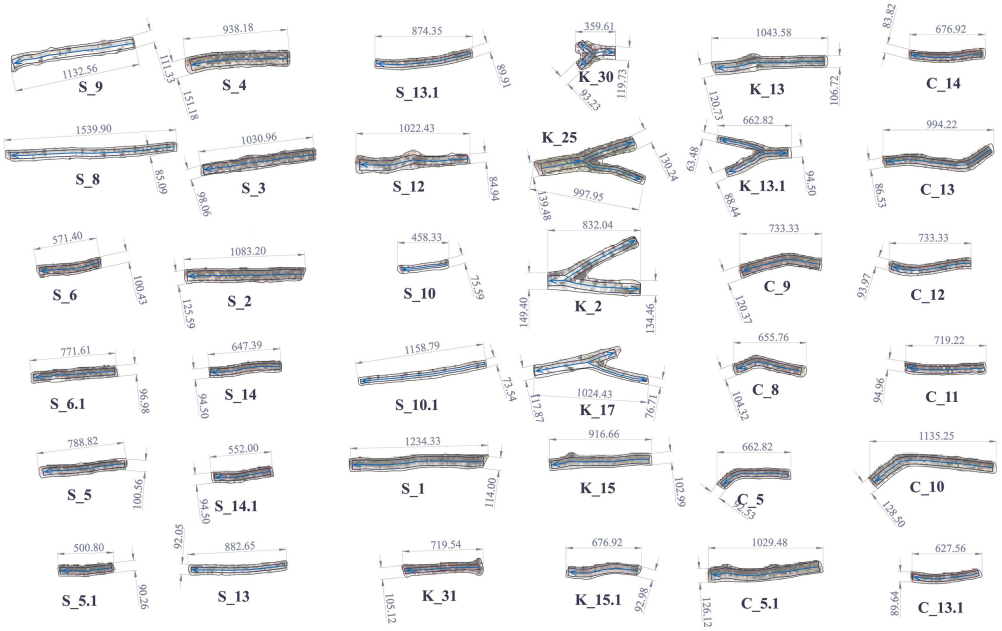

Figure 3.32: Geometric analysis applied to multiple timber elements c_g^i and conforming the image-based library, where the names S mean straight, C is curved, and K is knot.

3.5 2D Raw Timber

In many cases, the geometric analysis processes discussed in the previous sections prove unnecessarily complex when the available material is, at first glance, predominantly two-dimensional. This section builds on that premise to document 2D raw timber elements for potential applications in planar components.

3.5.1 2D Object Scanning Methodologies

2D scanning methods, such as simple photography, capture the basic shape and surface geometry of objects, focusing on their exterior form from a single angle. These methods employ tools like flatbed scanners or optical cameras to document the outline and surface texture of materials. Although they provide only surface-level data, 2D scans are essential for creating initial design templates based on the available material. For example, when documenting flat or minimally curved timber elements, 2D scanning enables the recording of precise dimensions and contours that can be used in preliminary designs. This process is particularly effective for simpler timber geometries where full 3D modeling is unnecessary, or even after minimal processing—such as dividing 3D branches into relatively flat elements—as described in the previous section and illustrated in 3.31.

In the context of this research, 2D scanning can be a first step in the documentation process, allowing estimations of available material, volumes, and approximate cross-sections before moving to more complex analyses. In the reGrowth Project (see 6.3.2), this method was used due to its speed in documenting relatively flat objects. The process starts with taking photographs, which are then processed to create discrete digital models of the timber elements.

3.5.2 Data Acquisition from Raw Photos

To illustrate this process, a relatively simple setup is proposed: a DSLR camera with a 55mm lens is placed at a height of 3 meters, perpendicular to the ground, in front of a green screen and a reference object of known size (Fig. 3.33). Each element to be documented is positioned sequentially, and an image of each is taken (Fig. 3.33(b)). These images are automatically processed by a macro in photo editing software [171], which removes the background, adjusts contrast, scales the images, and saves them in a raster image format (as RAW_i).

These images are stored and prepared for the next step in the analysis, which is the generation of planar computational models.

3.5.3 2D Automation Based on Processed Photos

The automation process is an iterative procedure in which the processed images (RAW_i) are imported for automated modeling. This operation is performed by an algorithm that runs sequentially, based on the number of image elements i to process. First, a bounding rectangle is



(a) Set up (b) Raw photo (c) Processed RAW_i

Figure 3.33: Process for macro editing the raw photos.

defined with absolute length and width $L \times W$, which serves as the projection surface. Next, the images are imported as the "IMG" parameter, projecting each image onto the surface at the correct scale with a specified mesh resolution ($Mesh_{Res}$). The white pixels are removed, while the remaining colored pixels are retained.

This step is treated as a flat point cloud, which is used to generate a Delaunay mesh—a triangulation of the given points that represents the raw geometry. The outer edge of the mesh is extracted and defines the periodic polyline RAW_{pol} (see Fig. 3.34(a)).

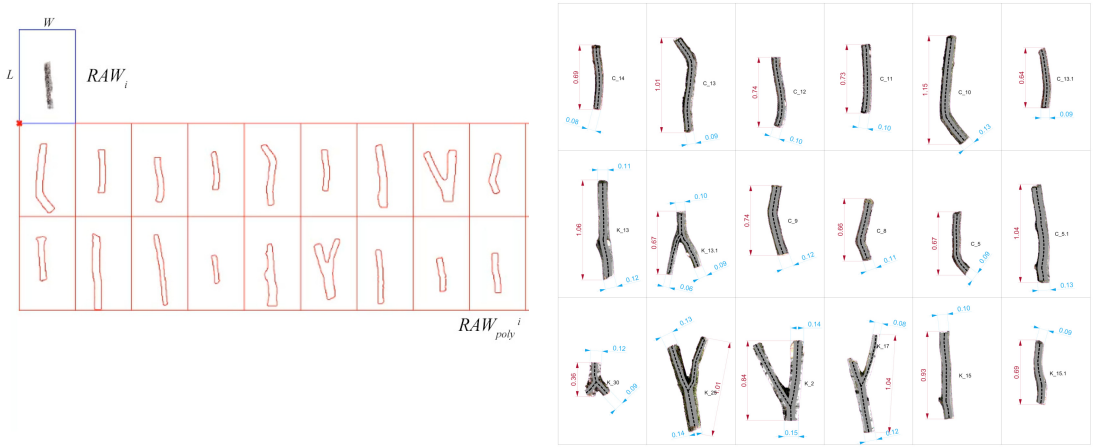

(a) Plotted perimeter polyline (b) Final elements, with dimensions and stock

Figure 3.34: 2D Automation.

The next step involves a minimal manual intervention to define the start and end points of each timber element. This step is necessary as it also serves to monitor and assess the condition of the branches (e.g., visible cracks or asymmetric cuts). It is carried out by tracing a transverse line across RAW_{pol}. This defines A_0 as the starting point and A_n as the endpoint. A straight line $A_0\bar{A}_n$ is drawn, along which divisions are made to define the α cut planes. The intersection

points of these planes with the polyline RAW_{pol} determine the central NURBS curve c_{g1} (see Eq. 3.5). This process is typically repeated three times to approximate the final centerline c_g.

This curve allows for the measurement of the distance to RAW_{pol} at each position, yielding an approximate perimeter and diameter. Based on this measurement, a 2 cm sapwood offset is applied. The process concludes by automating dimensional measurements, defining the material stock, and recording metadata such as average thickness, size, and curvature (see Fig. 3.34(b)).

$$c_g = \bigcup_{i=1}^{\alpha} (P_\alpha \cap RAW_{poly}) \tag{3.5}$$

Where:

- $P_\alpha = A_0 + \left(\frac{A_n - A_0}{\alpha} \times i\right)$ - The union $\bigcup_{i=1}^{\alpha}$ represents the set of all intersection points along the polyline RAW_{poly} defined by each cut plane P_α.

This tool is available in the attachment B.2.

3.6 Subdivision Modeling

This chapter concludes with the presentation of a more advanced modeling method, intended for cases where complex simulation techniques are required—though it is not essential in all applications, such as certain construction contexts. Instead, this approach serves as an extended modeling framework that enhances the capabilities of previously developed models, particularly by enabling growth simulation and further geometric control.

To this end, the geometric information described is managed within an abstract model that operates on surface-level data, represented as a *SubD*—a subdivision surface (see geometric definitions in Section 3.2.1).

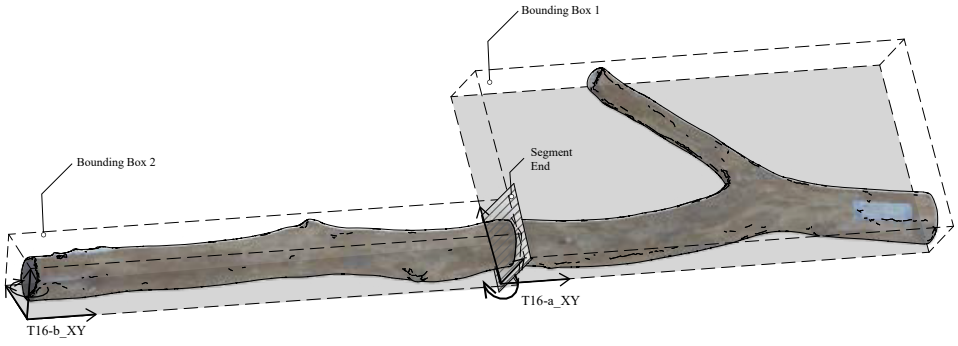

Figure 3.35: Segmentation of branch T-16 (beech specimen) based on bounding box computation. The geometry is divided into two elements using a plane aligned with the working XY plane. This plane, derived from the minimal bounding box, defines 2D working geometry for further analysis and modeling.

Computational Implementation and Control Cage Definition

A custom computational tool has been developed to automate the creation of subdivision geometries from irregular timber elements. The process begins with the segmentation of the raw mesh into discrete sections s_i, based on geometric analysis. For each segment, the largest inscribed circle tangent to the cross-sectional boundary is computed, allowing the determination of the geometric center C_G, denoted here as A_i.

To determine the point A_i, a set of sample points $P_{x,y}$ is evaluated within the domain enclosed by each section s_i. For each candidate point $P_{x,y}$, the minimal distance d_{min} to the boundary curve is computed as

$$d_{min}(P_{x,y}) = \min_{q \in s_i} \parallel P_{x,y} - q \parallel,$$

where q denotes any point on the boundary curve of the section s_i.

The center of the maximal inscribed circle corresponds to the point whose minimal distance to the boundary is maximal among all sampled points:

$$A_i = \operatorname*{argmax}_{P_{x,y} \in \Omega_i} d_{min}(P_{x,y}),$$

and the radius of the circle is therefore

$$r_i = d_{min}(A_i).$$

From these central points, a tubular subdivision mesh is defined with a fixed number of subdivisions in the radial (u) and longitudinal (v) directions. This forms an initial reference cage, with control points denoted as A_i^0, which circumscribes the sequence of segment centers.

Each point A_i^0 is then projected outward along its local normal vector until it intersects with the external surface of the raw mesh. The resulting set of intersection points defines the control cage of the SubD geometry, denoted A_i^1. An offset operation is applied iteratively to expand this cage until the volume of the resulting SubD approximates that of the original mesh.

This method is fully automated, enabling parameterization of the number of u- and v-level subdivisions, as well as the conversion of selected patches into NURBS surfaces depending on design or fabrication constraints.

Additionally, the displacement vectors $\vec{\delta_i} = A_i^1 - A_i^0$ can be mapped across the surface to visualize the geometric deviation between the control cage and the idealized circular cross-section. This deviation is rendered as a color gradient on the SubD surface, highlighting regions where the profile is significantly distorted or oblate—providing insight into zones of geometric complexity or material irregularity.

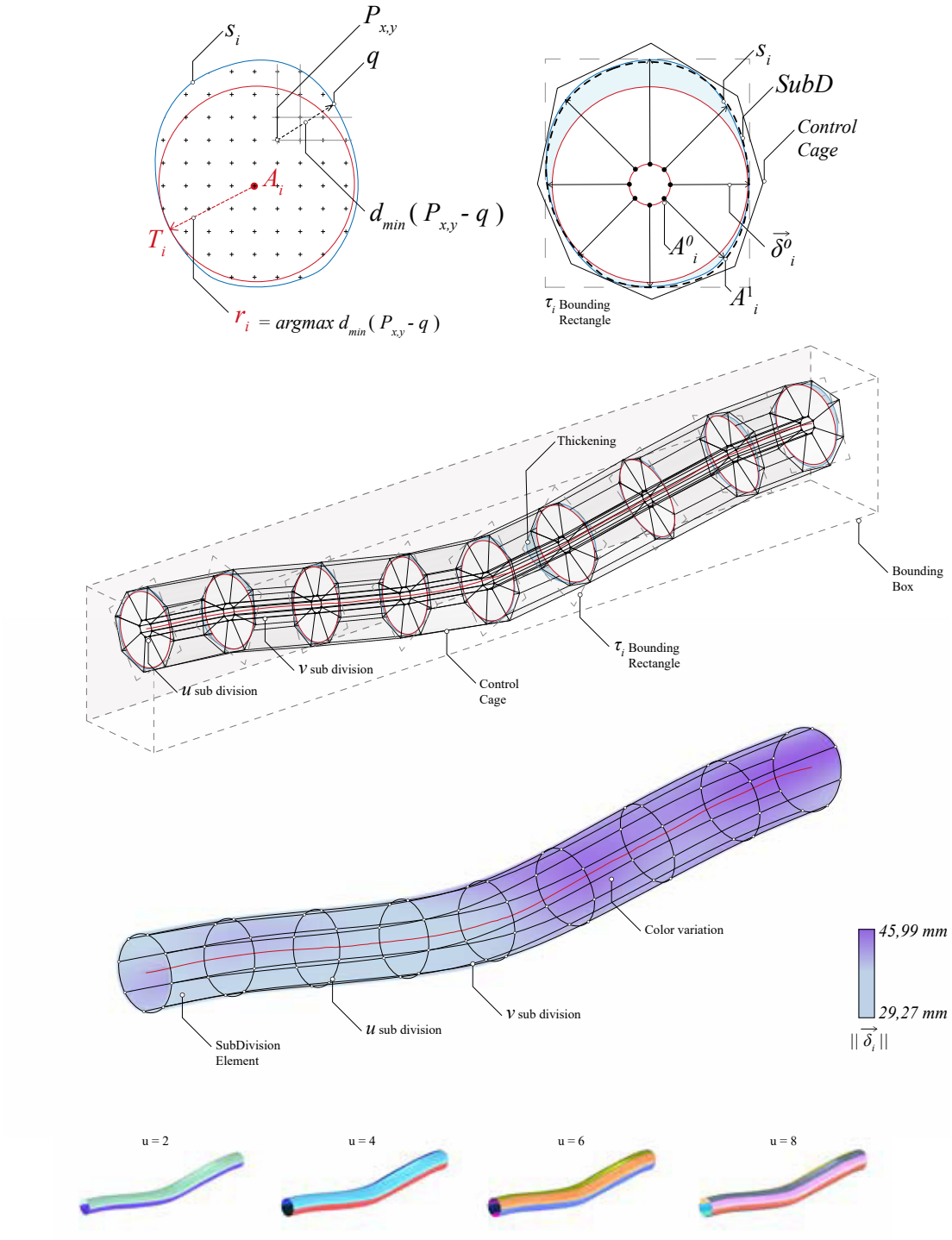

Figure 3.36: Subdivision geometry generation from raw timber elements (Specimen T-16b). The process begins with the computation of center points A_i from the largest inscribed circles along segmented cross-sections. An initial reference cage (A_i^0) is defined, followed by normal projection to intersect the mesh surface, yielding the final control cage (A_i^1). The color gradient represents displacement vectors $\vec{\delta}_i$, indicating deviation between the idealized circular profile and the actual surface geometry.

Geometry Adjustment

This step enables the optional local transformation of the control cage governing the SubD geometry, using bounding rectangles as τ_n. Each rectangle defines a local polar coordinate system that facilitates rotation via matrix R_n and translation via vector $\vec{t}_n$, both derived from the subdivision geometry along the longitudinal direction v.

Each associated control point $A^1_{v,i}$ is transformed as follows:

$$A^1_{v,i}{}' = R_v \cdot A^1_{v,i} + \vec{t}_v \tag{3.6}$$

To extend this transformation across the entire SubD model, all control points are compiled into a matrix $P \in \mathbb{R}^{M\times 3}$, where M is the total number of control points. Each row is transformed according to its corresponding longitudinal segment $v(i)$:

$$A^{1\prime}_i = R_{v(i)} \cdot A^1_i + \vec{t}_{v(i)} \qquad \text{for } i = 1, \ldots, M \tag{3.7}$$

This framework provides a basis for subsequent iterations in which the geometry can be adjusted—displaced, rotated, or scaled—using the reference planes τ_n. It offers flexibility for simulating longitudinal and cross-sectional geometrical growth. See this approach in A.1.

3.6.1 Subdivision Model for Bifurcated Elements

The modeling of bifurcations follows the same principles as described previously. However, due to the presence of three axes, the model is constructed from three separate SubD segments joined along a common seam. Subdivision modeling enables precise control over edge and vertex behavior. For this configuration, specific settings must be applied: the seam edges should be defined as *smooth, exterior*, and the three coinciding central vertices should be set to *smooth*. This ensures a continuous curvature transition between patches when the SubD model is later converted to NURBS surfaces. This process is illustrated in Figure 3.37.

The central part of the figure shows an exploded view of the welded seam that forms the junction joint between branches. All meshes are constructed using quadrilateral topology. A top view is included to aid visualization, as the three-dimensional form of the bifurcation is complex and not easily understood from a single perspective.

Additionally, the figure includes a color visualization of the magnitude of displacement vectors δ, indicating geometric deviation between control points and surface intersections.

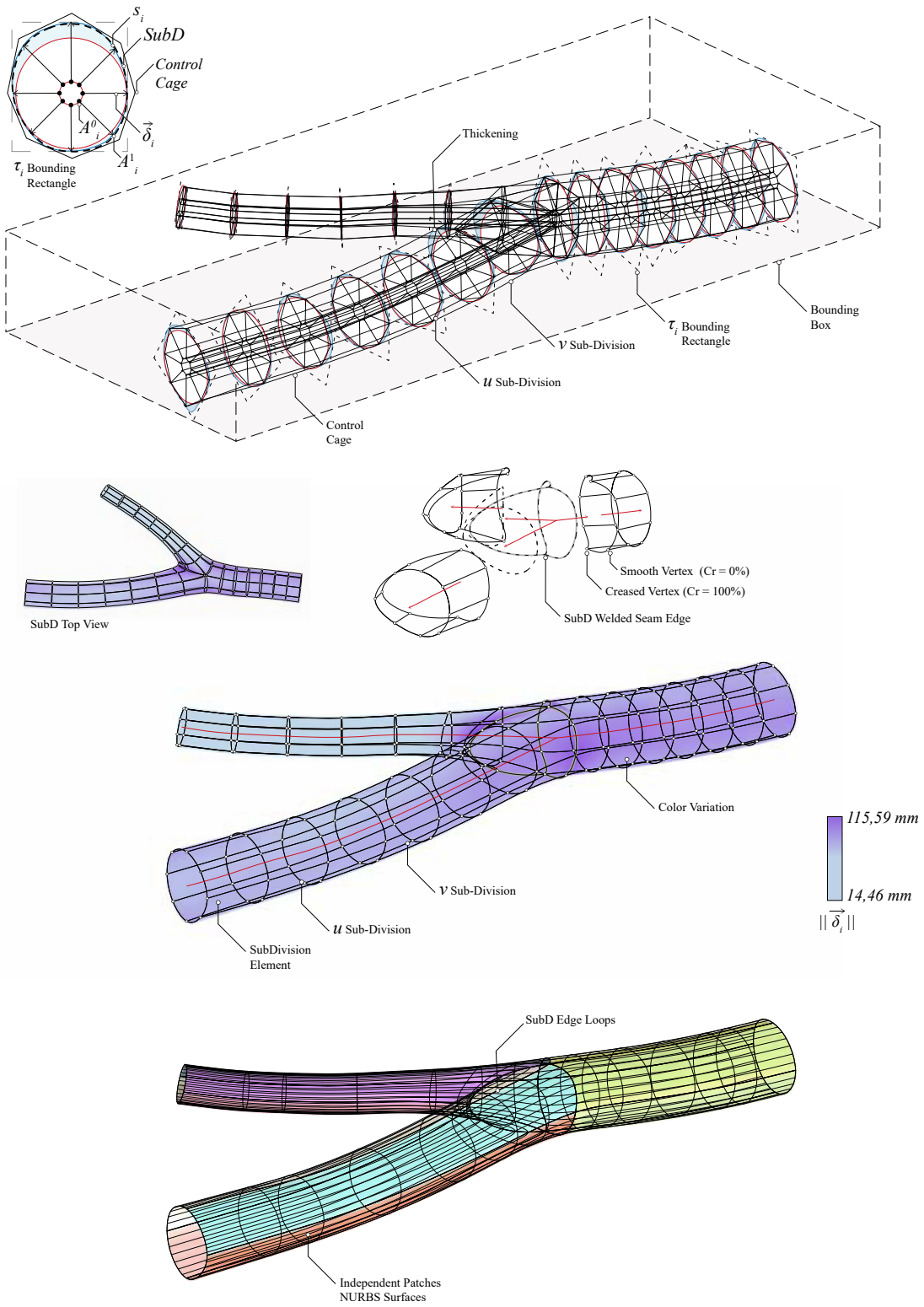

Figure 3.37: Subdivision modeling of a bifurcated timber element (Specimen T-16a). Three SubD elements are joined via a smooth welded seam to model the bifurcated geometry. The figure shows the quadrilateral topology, seam alignment, deviation magnitude (δ) as a color gradient, and finally the NURBS patches.

3.7 Conclusions on Geometrical Analysis and Modeling

This chapter presented a comprehensive framework for the geometric analysis of natural timber, covering scales from full-tree surface data acquisition to the modeling of individual segments and branches.

A hierarchical approach was introduced for managing point cloud data from trees. This enabled geometric analysis across multiple levels and supported the evaluation of curvature, bifurcation, and volumetric properties. The method also established a structured pathway from raw data acquisition to model generation.

Three complementary strategies were proposed for analyzing individual branches. First, 3D scanning techniques were used to extract modeling axes from surface geometries. Second, a segmentation method converted 3D curved elements into planar 2D segments for structural integration. Third, a fast modeling technique based on 2D image processing was applied to flat timber elements, streamlining the overall workflow.

The chapter concluded with an advanced modeling approach using subdivision surfaces. This technique allows for continuous curvature transitions across mesh patches and provides greater geometric control for future applications.

Collectively, these methodologies establish the geometric modeling foundation for the application of grown timber, developed in Chapters 4, 5, and 6.

Chapter 4

Growth and Material Mapping

From Geometry to Growth and Material

Mapping and characterizing material properties of wood is a complex task due to the inherent physical and biological variability—an aspect that makes wood science interdisciplinary. In the context of raw timber, such variability, combined with the specimen's geometric configuration, plays a crucial role in determining material behavior.

This chapter introduces an analytical methodology for material mapping that builds directly on geometric principles discussed in the previous chapter. It focuses on key properties, including material density and fundamental mechanical characteristics. By linking geometric and mechanical domains, the chapter integrates surface-level material assessment with non-invasive techniques, particularly computed tomography (CT), and progresses toward non-destructive mechanical testing. Overall, it outlines how these complementary methods can be unified within a geometry-based framework for the analysis of raw timber.

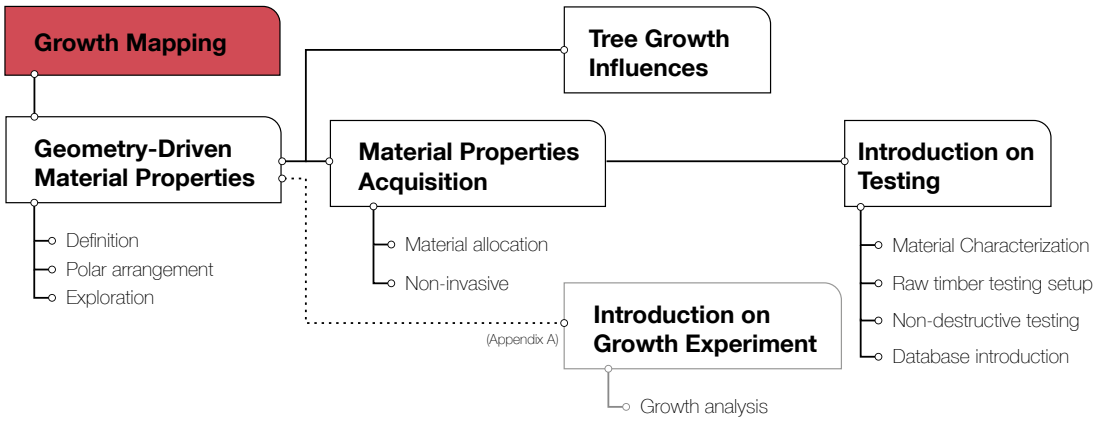

Figure 4.1: Chapter Diagram: Linking geometry, growth patterns, and material properties.

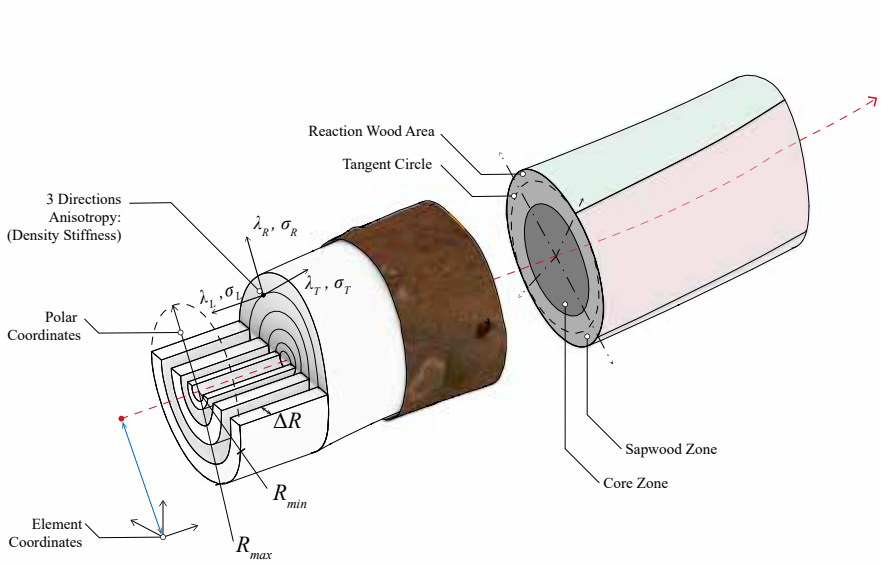

Figure 4.2: Representative macroscopic features relevant to timber geometry.

4.1 Geometric-Relevant Material Properties

This chapter identifies material properties with strong geometric relevance. While the structural centerline (c_g) was previously defined based on surface-level assumptions, the focus now shifts to the growth center (c_G), corresponding to the tree's pith. Unlike earlier approximations, the current c_G is derived from imaging techniques, such as computed tomography, enabling more accurate internal localization. This biologically grounded reference point supports the development of polar coordinate frameworks aligned with the anisotropy of wood. Key descriptors include fiber orientation, ring curvature, and the orthotropic directions—longitudinal, radial, and tangential.

According to established literature [172, 173], the structure of wood spans three hierarchical scales: macro-, micro-, and submicrostructure:

At the macroscopic level, geometrically relevant features include cutting direction, fiber angle, heartwood–sapwood distribution, ring width and curvature, color variation, and reaction wood (see Fig. 4.2).

In the layered structure of wood cell walls, the secondary wall comprises three sublayers: S_1, S_2, and S_3. The S_2 layer is the thickest and most mechanically significant, comprising about 80% of the wall thickness. Its low microfibril angle and high cellulose content strongly influence axial stiffness and tensile strength, making it central to the anisotropic mechanical behavior of wood.

At finer scales, the microstructure includes tissue distribution (e.g., xylem vessels), fiber length and wall thickness, resin canals, and fiber trajectories. Submicrostructural parameters include

fibrillar arrangement, microfibril angle (notably in the S_2 layer), lignification level, and cell wall thickness. These features interact across scales, contributing to wood's biological and mechanical complexity.

This chapter focuses on the macroscopic scale to enable the mapping of visible features. A geometry-based approach is adopted to evaluate material behavior through descriptive parameters, supporting model-driven analysis.

4.1.1 Acquisition of Material Properties

The multiscale nature of wood structure allows targeted acquisition strategies at different resolutions. These methods may be classified as invasive—such as destructive sampling or chemical contrast agents—or non-invasive. Micro- and submicrostructural scales require high-resolution imaging techniques, including micro-computed tomography (micro-CT) or ultrasonic tomography, which allow detection of defects such as fungal damage, knots, or insect infestation [174]. Such imaging also facilitates visual assessment of trunk quality.

For the macroscopic scale, which is accessible to the naked eye, information can be acquired through imaging and mechanical testing. In particular, CT scanning is increasingly used to assess internal wood properties and support grading efforts [175]. These techniques bridge the gap between macroscopic and microscopic scales by revealing internal structural features. Most notably, they provide detailed material density distributions, which in turn support geometric analysis and spatial modeling.

CT Imaging and Dataset Acquisition

Non-invasive imaging datasets were collected through macro- and micro-CT scanning of tree specimens described in Section 3.2.3:

- **Macro-CT:** Conducted at Delft University in December 2024 using a Siemens Somatom Definition dual-beam scanner, typically employed in medical imaging. Timber elements up to 1.7 m in length and 12 cm in diameter were scanned at a resolution of 0.3 mm.
- **Micro-CT:** Performed at Forschungszentrum Jülich in July 2023 using high-resolution imaging (0.034 mm isotropic). Small specimens, approximately 10 cm in length and 5 cm in diameter (small branches), were scanned.

Each imaging approach provides access to distinct structural scales. Macro-CT facilitates a broader assessment of density distribution and general annual ring configuration. Micro-CT, by contrast, captures the fine internal architecture of growth rings. Scan times ranged from 3–4 minutes for macro-CT and 15–18 minutes for micro-CT. Additionally, magnetic resonance imaging (MRI) was employed to analyze fluid content, relevant for greenwood analysis and the identification of xylem vessels.

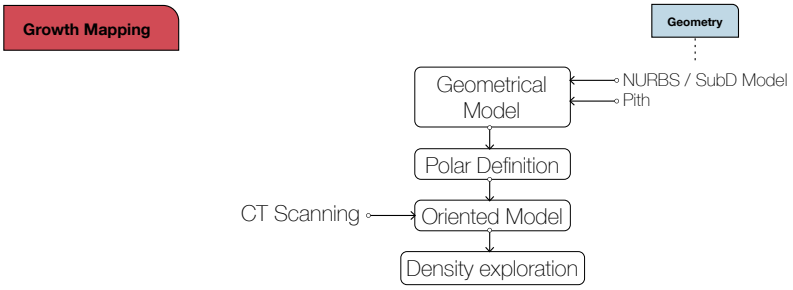

Figure 4.3: Workflow from geometry to material exploration.



Figure 4.4: Example of a bifurcated specimen exhibiting reaction wood. Left: density distribution from CT imaging. Right: CT longitudinal section showing internal density variation along the diameter.

4.1.2 Definition of the Material-Integrated Model

The second section builds upon the premise of integrating a geometric model with material properties. These properties may be obtained from literature-based databases, material surveys, or experimental tests. The model aims to couple geometric parameters with mechanical and physical properties to enable a more comprehensive analysis of timber structures.

Figure 4.5(b) illustrates the hypothesis of combining geometric descriptors with material property distributions. This approach has been explored in previous studies to assess longitudinal variations in timber quality along the trunk axis [176]. Such studies emphasize the relevance of polar modeling from the pith (c_G), capturing not only the variation of mechanical properties but also the geometric distribution of reaction wood [177]. In these examples, polar representations are employed to describe material property changes as a function of radial and angular coordinates. Parameters such as density have been shown to vary with cardinal direction. In some species, higher density regions were consistently observed along the eastern axis of the trunk, while in others the distribution showed species-dependent variability yet remained constant longitudinally.

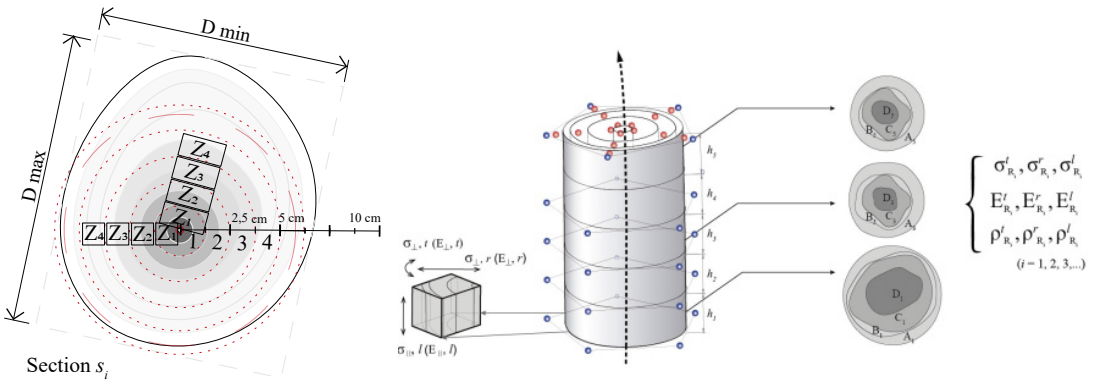

(a) Cross-section of timber zones and sampling of test specimens

(b) Parametric material model, extracted from [2]

Figure 4.5: Parametric model diagram integrating material properties and geometric zones. Left: timber cross-section identifying zones. Right: model implementation identifying strength, stiffness, and density variations. Graphic based on [176] pp 109.

Growth-induced material properties

The distribution of biomass material within a tree exhibits a polar pattern influenced by its natural growth. Understanding and accurately representing this distribution is crucial for creating comprehensive mechanical models, especially for raw timber elements, in case of twisting growth. The described methodology involves calibrating 3D-scanned components by aligning system axes with volume distribution obtained from CT scans. This calibration ensures an authentic representation, capturing complete spatial dimensions and effective spatial axes. This results in an enriched model with superficial two-dimensional representation and internal information. It allows for preliminary studies on the implications of asymmetry in curved and bifurcated grown elements. To comprehensively analyze trees, it would be necessary to supplement the work with information from sources, such as MRI or data with varying water content.

Polar definition of the cross-section

A significant challenge in this context is accurately determining the center line, also known as the growth central axis, often mistakenly assumed to be the geometric central axis. This center line is formed by the union of growth centers C_G, currently only obtainable through visual information or CT data. The center C_G represents the tree's initial growth center, located at the central point of the annual rings. In a straight element with a circular cross-section, the geometric centroid C_g and growth center C_G tend to coincide. However, in irregular elements, such as oval-shaped cross-sections primarily generated by reaction wood or in a bifurcation, the deviation becomes more pronounced. This is supplemented with the center of mass C_M, representing the sum of all masses within the section. In rectilinear elements, it tends to coincide with C_G and C_g. For irregular elements, determining its location requires a density variation

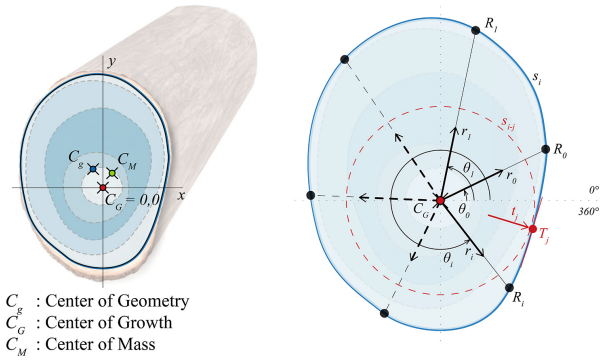

Figure 4.6: Definition of the three centers of the cross-section: Geometric center –centroid–, Growth center, and Center of mass. Polar ray (r) positioning for cross-section analysis.

study. This center allows observing biomass displacement throughout growth, helping to analyze eccentricities and center shifts along the tree length (see Fig. 4.6).

Development of the polar system

Log cross-sections are commonly analyzed using a polar coordinate system, where the growth center C_G serves as the reference point. The analysis follows these steps:

1. *Reference Circle Definition :*
A reference circle s_{i-j} is generated with center C_G and radius t_j, defining a tangent point T_j with the external perimeter s_i.

2. *Radial Rays and Intersection Points*
Rays r_i are projected from C_G at fixed angular intervals θ_i, searching for intersections with s_i:

$$R_i = (x_i, y_i) = (x_G, y_G) + t_j(\cos\theta_i, \sin\theta_i) \tag{4.1}$$

where x_i and y_i are the coordinates in the plane of the cross-section.

3. *Intersection with the Perimeter*
The intersection points R_i are found where:

$$R_i = s_i \cap r_i \tag{4.2}$$

4. *Angular Growth Orientation*
- The angles θ_i increase counterclockwise.
- The reference point R_0 is defined within a polar coordinate system ranging from $0°$ to $360°$.

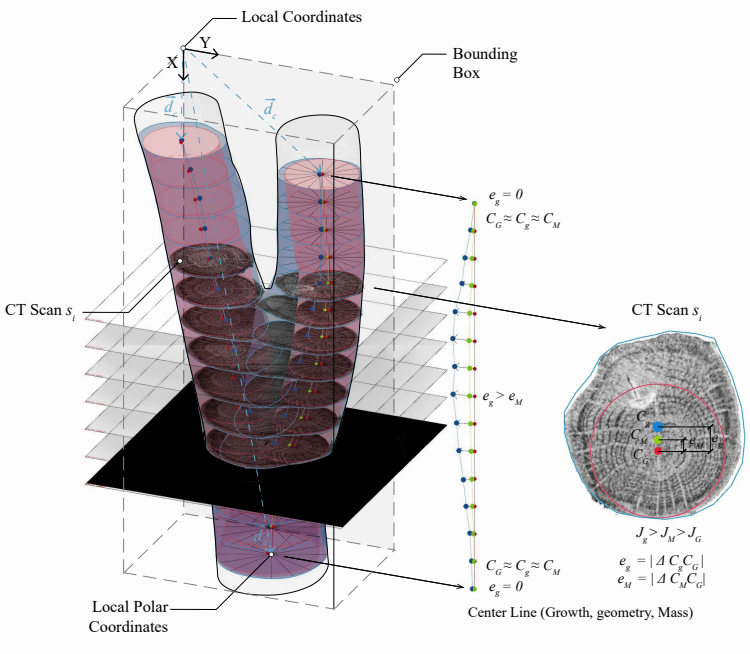

Figure 4.7: Visualization of the bifurcation of a small specimen of oak. In red: reference tangent circular geometry with c_G, assuming the tree grows straight. In blue: grown geometry with eccentric displacement of c_g. The production of tension wood can be seen in blue. c_M calculated after applying the derived polynomial density function.

Once this formulation is analytically defined, it can be applied to the study of a specific branch along its longitudinal growth. For this purpose, cross-sectional planes α_i are defined along the growth trajectory a, as detailed in Chapter 3, Section 3.4.2. The curve a is discretized into points $A_0, A_1, \ldots, A_i$, where each A_i represents a cross-section positioned along a.

To describe the longitudinal variation of the cross-sectional properties, a function $R_i(\lambda)$ is introduced, where λ is the parametric coordinate along the curve a:

$$R_i(\lambda) = A_i + t_j(\lambda)(\cos\theta_i, \sin\theta_i, 0) \tag{4.3}$$

where $R_i(\lambda)$ defines the spatial coordinates of the cross-sectional perimeter at each plane α_i. The function $t_j(\lambda)$ represents the varying radius of the section at different positions along a, allowing the study of growth asymmetries along the tree.

This formulation enables further investigations into material distribution, structural anisotropy, and density variation along the tree's growth trajectory.

Growth-induced mass displacements

The mass displacement can be observed in the model (see Fig. 4.7). For visualization, a tubular volume with variable radius $|\mathbf{t_j}|$ is traced along the central growth line as a reference. This tube

is determined at each cross-section, taking the smallest modulus of all $|\mathbf{r_i}|$. This defines a circle s_{i-j}, with a tangent T_j at s_i. Using this method, it is possible to visualize an approximation of the volume generated by the tree as reaction wood. In the example in Figure 4.7—based on a reference oak specimen— it can be recognized how the added volume in growth corresponds to tension wood. Furthermore, one central line of a bifurcation element has been extracted. With the C_G of each section in a straight line, one can observe the quantitative difference in geometric eccentricities, which increase along with the tension in the wood.

The last part of this section outlines the application of the polar method for analyzing density variations within the volume. These techniques are instrumental in detecting higher density zones, such as heartwood. The relevant eccentricities are then defined. The eccentricity e_g of the central axis, is calculated as the distance between C_g and C_G. After calculating the C_M, with the help of the density distribution (in Fig. 4.8) the e_M can be found. This is relevant for a mechanical understanding of the tree, as it has implications on the moment of inertia of each section s_i. In Figure 4.7 the cross-section on the right illustrates the variation in moment of inertia due to geometrical J_g, in comparison to a moment of inertia reference due to growth J_G. For instance, in a straight-grown tree with a perimeter s_{i-j} –delineated in red–, its J_G would be much lower than the actual J_g. This consideration requires complementing with a calculation of the mass moment of inertia J_M.

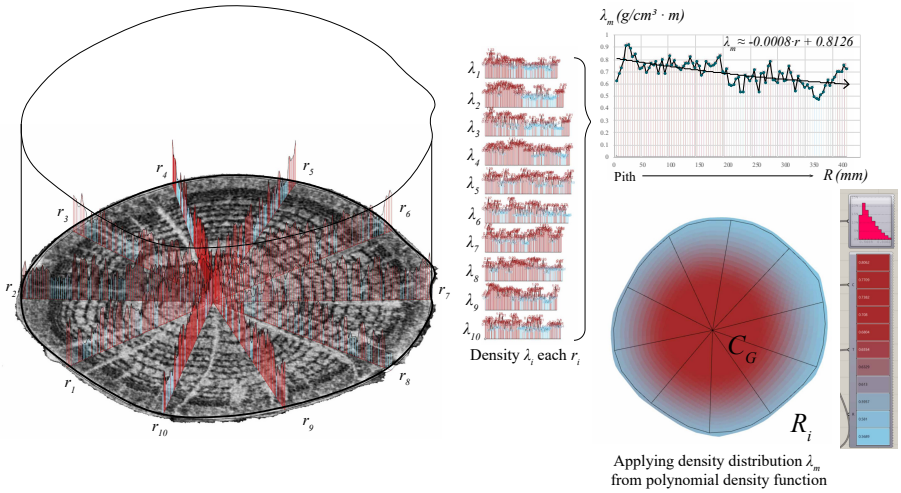

Figure 4.8: CT material density variation λ along the radius R. λ_i corresponding to every r_i, and λ_m represents the resulting density in the cross-section. Using a polynomial, a formula can be derived, which can then be reapplied to the cross-section from C_G to R_i.

Exploration of Material Stiffness

The polar coordinated system has been used to determine the moments of inertia and densities, as discussed above. In addition, there are more properties that vary along the radius, starting from C_G, such as strength and stiffness. Studies have shown that there is a relationship between density variation and strength. Matsuo et al. [178] shows that in Japanese cedar –softwood–, its

modulus is higher in the center and decreases in the radial direction (see Fig. 4.9); in contrast, in deciduous trees –hardwood–, the modulus is lower in the center and increases radially, which can be compared with the density variation study in the previous section (see Fig. 4.8).

The integration of material properties and the E modulus, based on material tests, can be employed for further analytical methods and simulations. Although the calculation of E is not addressed in this thesis, it can be taken into account and stored within the polar coordinate system. Subsequent academic work has been conducted to investigate these principles [179], initiating a base application and conducting preliminary testing further defined in the Section 4.3.

In Figure 4.9, a general formulation of area distribution proposes how to numerically analyze the variation of stiffness and the inertia moment J along the radius, where A_i is the area of each growth ring accumulation, J_i the moment of inertia, and E_i the Young modulus.

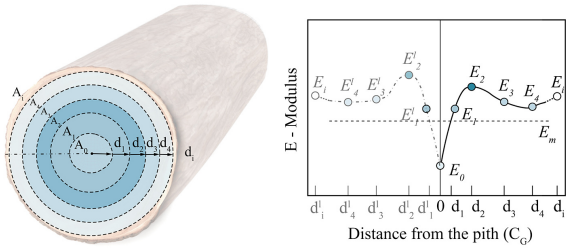

Figure 4.9: Symmetrized variation of the E-modulus over the cross-section according to [178], in a softwood. Picture extracted from [180].

4.2 Tree Growth Analysis for Raw Timber Assessment

The principles introduced by early mechanical analyses of trees [181] have guided the development of static analysis methods based on growth patterns. The core idea is that, if the growth or loading history of a tree can be understood or mapped, then its growth response can also be analyzed—allowing the identification of cross-sectional areas where reaction wood has developed, for example. Static analysis applied directly to the tree or at the branch level can therefore be useful both before felling and retrospectively, as such patterns are recorded in the variation of growth rings.

4.2.1 Branch-Level Structure

Based on the workflow illustrated in Fig. 4.10, the objective of this section is to extract geometric information from a documented tree model. The process begins with a hierarchical representation in which tree elements and their corresponding segments are identified using NURBS curves, cylinders, and subdivision elements. After a static estimation is performed, these components can be exported for structural design or for use in construction methods.

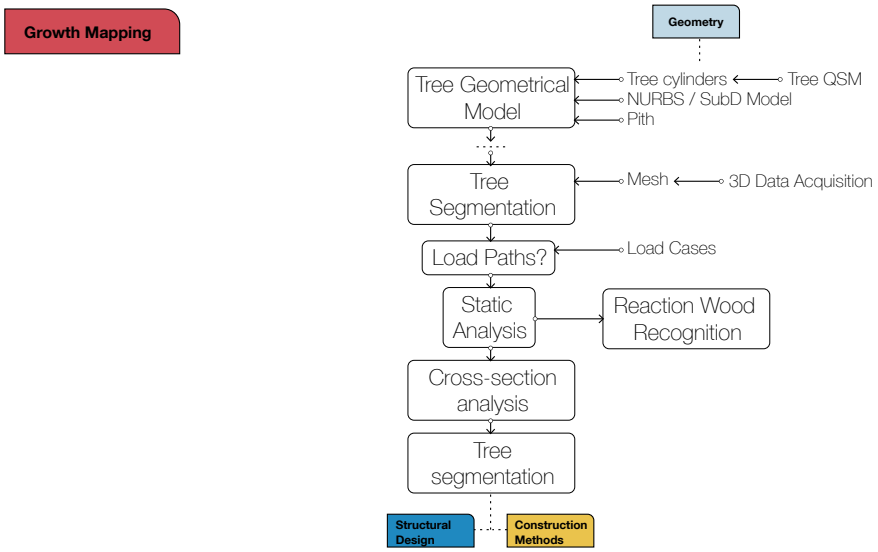

Figure 4.10: From tree geometry to growth analysis and cross-section analysis.

Tree Crown-Level Growth Direction and Geometry Setup

From the analysis presented in Section 3.22, statistical data can be extracted, such as the overall growth vectors of the tree. These data can be used to identify the main growth directions. It is also useful to apply the method to specific elements or sections of the tree. For example, it allows the mapping of the growth direction of an individual branch or the calculation of its lever arm for static considerations, such as allowable stress σ_{adm}.

An initial point P_0 and a final point P_i are defined, which determine the central curve c_g (see Fig. 3.24). The following information is used:

- The mesh or point cloud provides the cross-sections $s_0, \ldots, s_i$.
- The initial section s_0 is defined as the fixed support of the branch, with constraints in all degrees of freedom.
- The final section s_i is the location where loads are applied.
- Load paths: Load Case 1 ($\vec{LC}1$) includes self-weight and the weight of growing branches at P_i; Load Case 2 ($\vec{LC}2$) accounts for moving loads, such as wind, applied at P_i and variable angle θ_{wind}. Both Load Cases are applied as bending moments, defined by $\text{Moment} = \text{LC} \cdot L_{\textbf{arm}}$ at P_i.
- The sum of all vectors originating from point P_i defines the local growth direction at that point as $p_{\vec{\text{growth}}}$.

Bending Moment and Stress Estimation

Using this information, bending moments are calculated around the central axis c_g, and stress is evaluated across the cross-sections from s_0 to s_i.

To simplify the evaluation of flexural stress σ along the growth axis c_g, each cross-section s_i is approximated as a circular section based on its minimum bounding diameter D_{min}. This assumption enables a direct analytical estimation of stress using the section modulus W_i for a solid circular profile, defined as

$$W_i = \frac{\pi D_{\text{min}}^3}{32}.$$

The bending moment M_i acting at section s_i, derived from self-weight or external loads applied at P_i, yields a maximum tensile or compressive stress computed as:

$$\sigma_i = \frac{M_i}{W_i} = \frac{32 \cdot M_i}{\pi D_{\text{min}}^3}.$$

Finally, changes in bending moments can be visualized, enabling the identification of tension and compression zones within the cross-section. These zones are naturally defined by the tree itself—tension zones in hardwoods and compression zones in softwoods—corresponding to the formation of reaction wood. Figure 4.11 illustrates this principle, highlighting how internal stress gradients align with directional growth and result in species-specific patterns of reaction wood: typically located on the lower (compression) side in softwoods and the upper (tension) side in hardwoods.

Based on these static considerations, assumptions can be made regarding the admissible loads for a specific branch section in future structural applications or growth simulations. Moreover, it is possible to analytically determine which regions of the cross-section are influenced by the presence of tension wood. This simplification enables an efficient, geometry-based mapping of stress distribution along the tree axis, facilitating the identification of structurally active regions without the need for detailed meso-scale finite element simulation or complex material modeling.

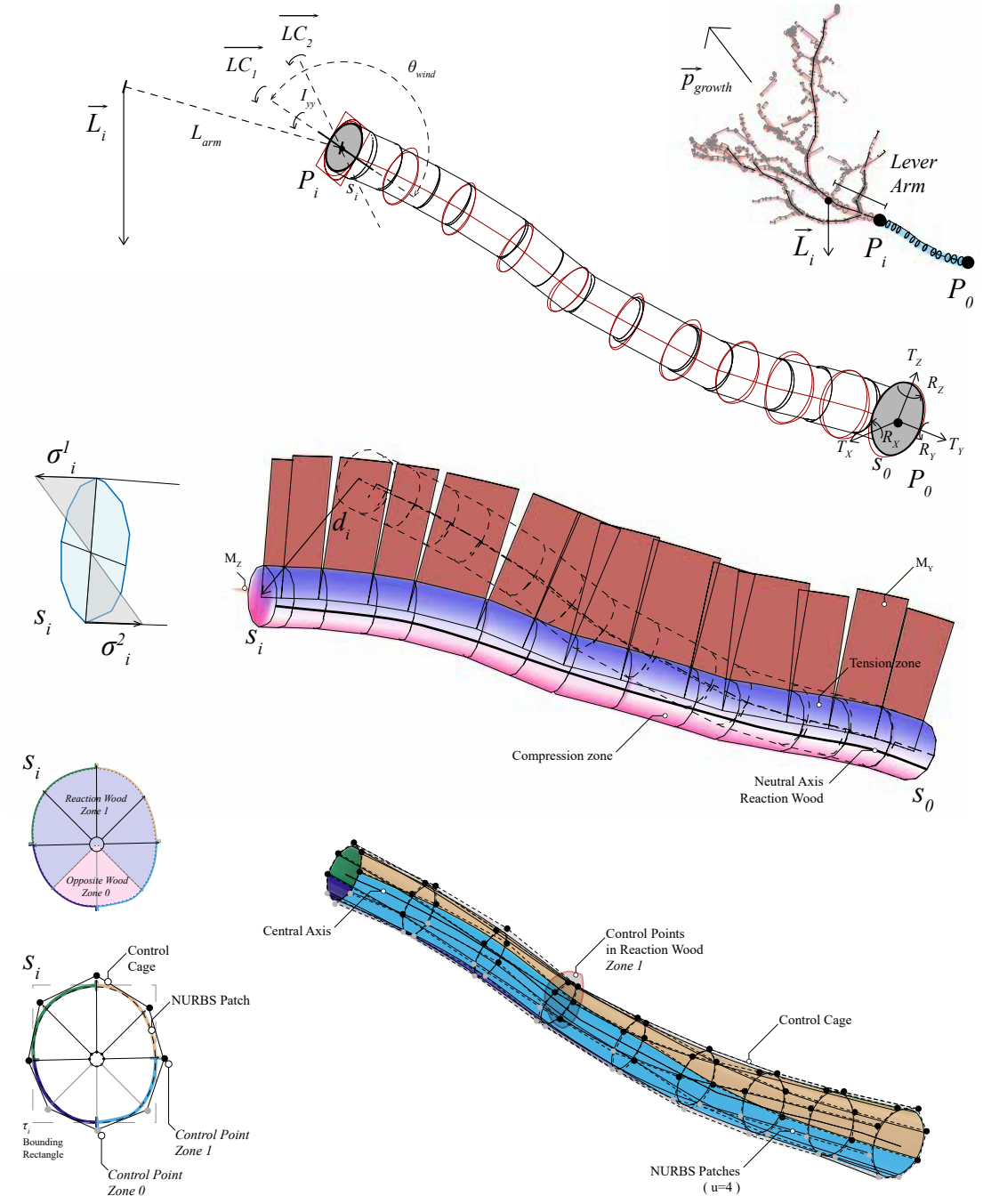

Figure 4.11: Directional growth and internal stress zones —tension and compression— leading to reaction wood formation in a tree structure.

4.3 Mechanical Properties

4.3.1 Material Characterization

Acquisition of Raw Material

After selecting specimens for testing, a preliminary material characterization test was conducted to obtain basic mechanical data and compare it with existing literature. Off-cuts from the specimens were used for this purpose, as shown in Fig. 4.13. These off-cuts, typically measuring 10–20 cm in length, are often discarded due to the presence of cracks in the wood. However, they provide sufficient material for the preparation of specimens for compression, tension, and bending tests. The extraction of these specimens was carried out using a superimposed layout fabrication process. With the aid of a milling machine (*Shaper Origin*), the pieces were precisely aligned and fabricated.

Sample Zones Determination

The zones for sample extraction were determined based on the polar position of the branch pith. Three main zones were defined, see also in Fig. 4.5(a):

- **Zone 1**: The pith, theoretically the hardest area, formed during initial growth.
- **Zone 2**: The area up to $25\,\mathrm{mm}$ from the center, which is the most structurally significant.
- **Zone 3**: The area from $25\,\mathrm{mm}$ to $50\,\mathrm{mm}$, often exhibiting sapwood, which produces less consistent mechanical results.

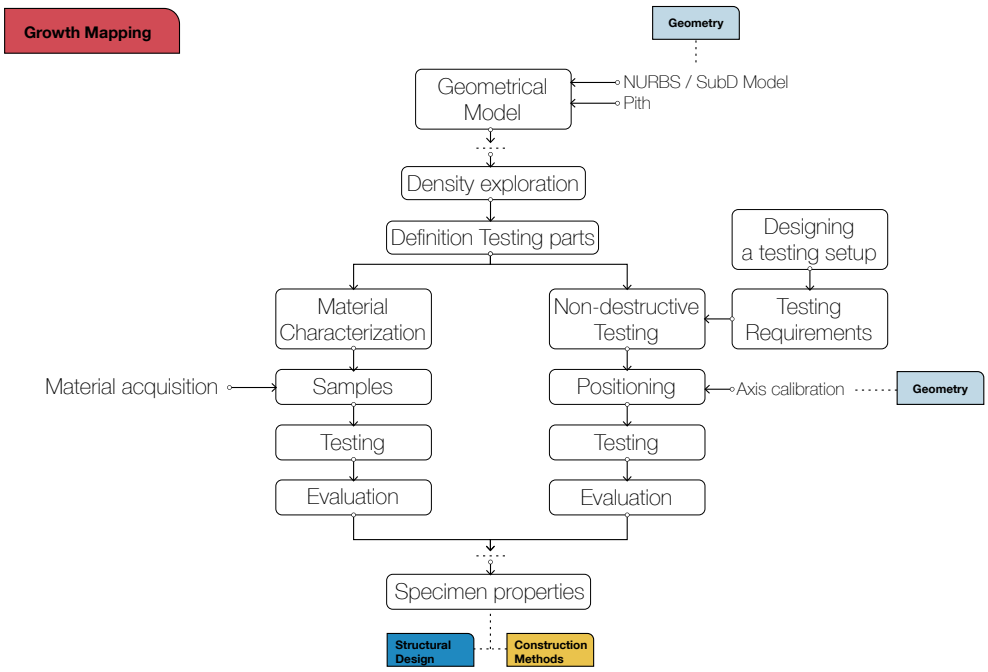

Figure 4.12: Testing workflow: From raw timber geometry to specimen properties.

For thinner specimens (10 cm in diameter), Zone 2 was identified as the most critical due to its higher reliability for standardized results. Samples were taken from different cross-sectional positions: at least five samples from Zone 2, one or two from Zone 1, and one or two from Zone 3.

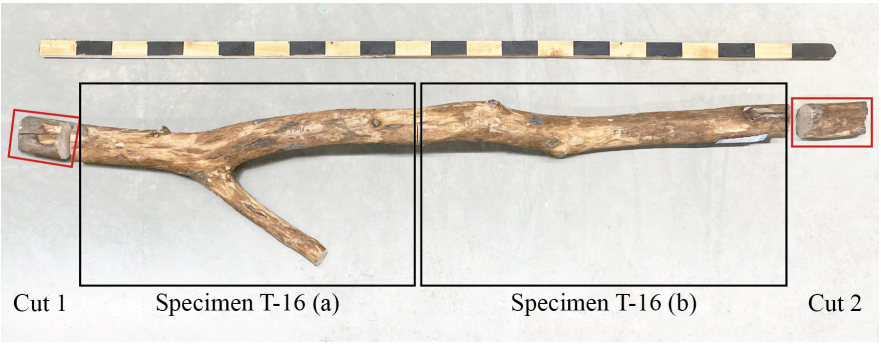

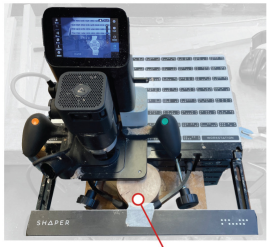

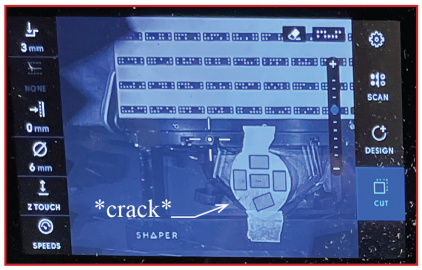

Samples for material characterization

Figure 4.13: Selection of specimens for testing. Above: the global timber element divided into two specimens for non-destructive testing and off-cuts. Below: extraction of testing samples for material characterization from different zones.



Figure 4.14: Photographs of the acquired samples.

Types of Tests

The characterization procedure included compression, tension, and bending tests conducted according to DIN EN 408 and DIN EN 14251 [182, 183].

The dimensions of the specimens were defined as follows:

- Compression tests: $20 \times 20 \times 30\,\mathrm{mm}$.
- Tension tests: $10 \times 10 \times 40\,\mathrm{mm}$.
- Bending tests: $20 \times 20 \times 40\,\mathrm{mm}$.

The specimens were mounted on a universal testing machine and loaded at a rate of $500\,\mathrm{N\,min^{-1}}$ until reaching defined deformation limits. The objective was to determine key mechanical properties, including the modulus of elasticity.



(a) Compression testing setup. (b) Specimen after testing.

Figure 4.15: Material characterization tests. Specimen in Zone 2.

To calculate the reference modulus of elasticity, the following formulation from DIN EN 408 was applied:

$$E = \frac{(F_2 - F_1) \cdot l_0}{(u_2 - u_1) \cdot A} \tag{4.4}$$

where $F_2 - F_1$ is the load increment, $u_2 - u_1$ the corresponding displacement increment, l_0 the initial length, and A the cross-sectional area.

Experimental Results

Each specimen was labeled T-1 through T-18, with the number of tests per type also indicated. The results of the experiments, including maximum forces recorded during compression, tension, and bending tests, are available in [179].

4.4 Non-destructive Testing for Raw Timber

This section outlines the design and rationale behind the proposed testing method, which aims to extract key mechanical parameters from raw timber while preserving the material's integrity and enabling its reuse in subsequent structural applications.

4.4.1 Testing Approach

The setup follows the general framework defined in DIN 52186 [182], which provides foundational guidelines for mechanical testing of wood. However, raw timber in its round and irregular geometry—as addressed partially in DIN 14251 [183]—poses challenges for standard testing protocols. In particular, the three-dimensional form, grain orientation, and curvature of naturally grown specimens deviate from the idealized conditions assumed in DIN 408 [184] or DIN 68364 [185]. These geometric factors significantly influence the mechanical response and must be addressed individually.

To bridge the gap between standardized methods and complex geometries, a tailored experimental approach is developed. This combines four-point bending tests with detailed material characterization and mechanical simulations, allowing for calibration of elastic parameters through inverse modelling. The mechanical test rig and procedure were developed within this dissertation, while data acquisition and structural interpretation were carried out in collaboration with the Chair of Structural Analysis and Dynamics (LBB).

4.4.2 Preliminary Considerations

Timber specimens range from $50\,\mathrm{mm}$ to $120\,\mathrm{mm}$ in diameter, representing relatively slender cross-sections for raw hardwood elements. A maximum load of $50\,\mathrm{kN}$ was chosen to ensure that tests remain within the non-destructive regime.

A four-point bending configuration was selected to generate a constant moment region between load points. This setup is standard in structural timber testing and has been previously applied to raw timber in [186], primarily using straight elements. A complementary study in [187] investigated compressive behavior of round hardwood specimens.

The test rig accommodates straight, curved, and bifurcated forms. It includes adjustable support spans up to $1.5\,\mathrm{m}$, with two load application pins that span up to $0.75\,\mathrm{m}$. Loads are transferred through custom load-distribution inserts to reduce local shear. Specimens are allowed vertical displacement but restrained in rotation using edge-guiding vertical plates. Figure 4.16 illustrates the axonometric design of the setup, emphasizing modularity and geometric adaptability.

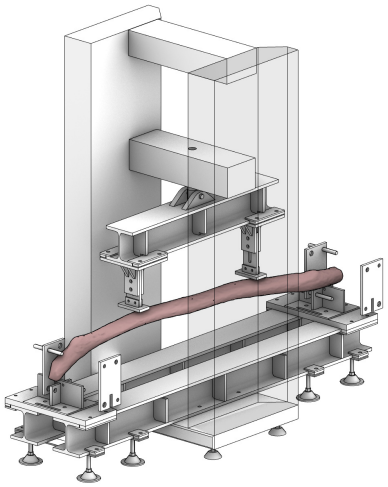

Figure 4.16: Axonometric view of the testing machine setup, illustrating movable parts and load application points.

Design of the Testing Setup

The four-point bending test setup is designed around a standard load-testing machine with a maximum load capacity of $F_{\text{max}} = 50\,\text{kN}$. The specimen is positioned between the machine's columns, which are fixed at a span of $S = 800\,\text{mm}$.

The specimen can be placed with variable alignment in both width (X) and length (Y) directions to accommodate natural curvature. The supports along the Y-axis must be adjustable to allow for angular deviations when symmetrical placement in the XY plane is not feasible. However, the projected angle must not result in a deviation greater than $1\,\%$ of the specimen's total length. For a specimen of $1\,\text{m}$, this corresponds to a maximum lateral offset in Y of $10\,\text{mm}$. Additionally, the compression elements along the Z-axis must also be adaptable to conform to the curved geometry of the specimen. To achieve this, relatively wide contact plates should be used to compensate for the projected angular deviation and ensure that the applied force is uniformly transmitted to the timber element.

The geometric constraints of the setup are illustrated in Fig. 4.17. A critical parameter is the maximum span L_{max} that can be achieved within the spatial limits of the apparatus, considering the global geometry of the specimen projected in the XY plane. The specimens tested in this experiment are assumed to have a circular cross-section with a variable diameter D, ranging from $50\,\text{mm}$ to $150\,\text{mm}$.

Estimating Test Length Based on Maximum Admissible Bending Stress

The bending test assumes a characteristic bending strength f_m, used as a reference for the maximum expected stress in a specimen prior to failure. Since the primary objective of the experiment is to conduct non-destructive testing (NDT), the setup is designed to allow incremental

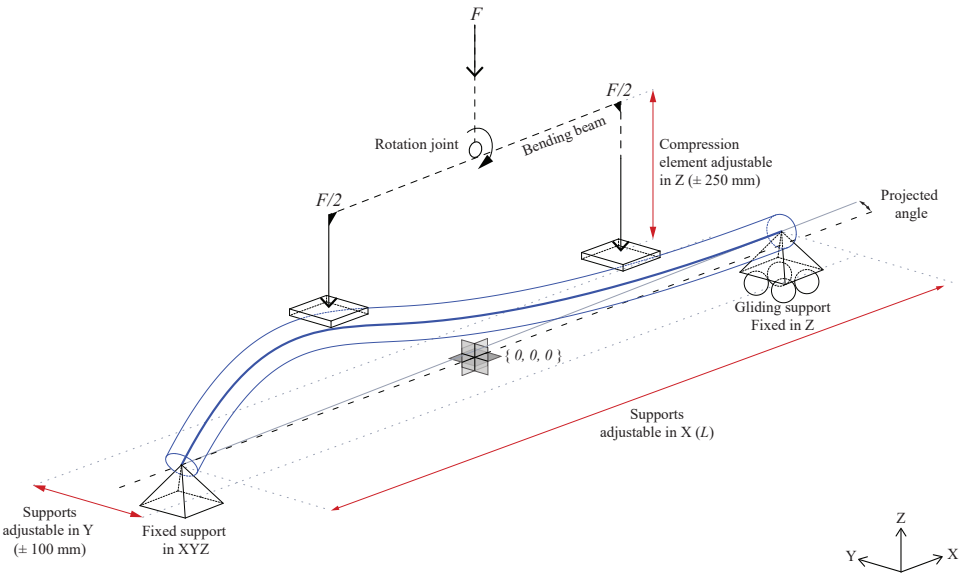

Figure 4.17: Geometric constraints of the bending setup.

loading up to approximately *65% of the theoretical failure load*, ensuring that the specimen remains within the elastic range. If desired, the loading can continue beyond this point until failure, in order to experimentally determine f_m. Based on this dual strategy, the parameters of the load case are defined to balance specimen geometry with theoretical material limitations and machine constraints.

As shown in Fig. 4.18, a four-point bending configuration was initially selected due to the presence of a constant bending moment M in the central region. Additionally, three-point bending is considered as a reference configuration. Future extensions of the study may incorporate alternative setups, including those for irregular geometries such as bifurcations (see Fig. 4.19).

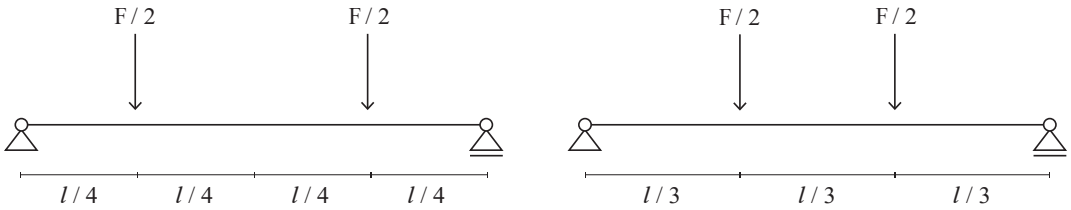

Figure 4.18: Four-point bending test configurations.

To determine the span length l, the maximum bending stress σ in the region of constant moment is derived from:

$$\sigma = \frac{M}{W_y}, \quad W_y = \frac{\pi D^3}{32}, \quad M = \frac{F \cdot l}{8}$$

Substituting leads to:

$$l = \frac{\pi D^3 \sigma}{4F}$$

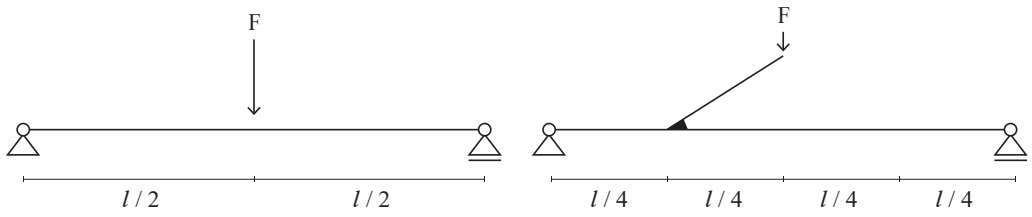

Figure 4.19: Three-point bending and three-point bending testing for bifurcations.

The design stress is calculated using:

$$\sigma = \frac{f_m}{\gamma_M} \cdot k_{\text{mod}}$$

The values used in this formulation are based on material properties and testing constraints. The characteristic bending strength $f_m = 6.0\,\text{kN}\,\text{cm}^{-2}$ corresponds to medium-strength European beech, as documented in standardized data sets [188]. The partial safety factor $\gamma_M = 1.5$ and modification factor $k_{\text{mod}} = 0.8$ are consistent with Eurocode 5 guidelines for short-term loading under standard climatic conditions. A reference load of $F = 5\,\text{kN}$ ensures elastic behavior, whereas the maximum machine capacity of $F_{\text{max}} = 50\,\text{kN}$ defines the upper boundary for specimen testing. Additionally, the test bench imposes a maximum span of $l = 1.5\,\text{m}$, which limits the geometric extent of the bending configuration.

With these parameters, the admissible design stress becomes $3.2\,\text{kN}\,\text{cm}^{-2}$. This results in a span $l = 0.50\,\text{m}$ for a specimen with $D = 10\,\text{cm}$ under a load of $F = 5\,\text{kN}$. The setup permits testing of specimens with diameters up to approximately $D_{\text{max}} < 30\,\text{cm}$ without exceeding structural or mechanical limits.

The detailed calculations underlying these estimations are presented in Appendix A.2.

4.4.3 Construction of the Testing Setup

The testing setup is custom-designed to accommodate the specific types of timber pieces identified in the preliminary study. The setup includes adjustable supports and load-bearing elements, providing flexibility for various timber shapes and sizes.

Set-up Informed by Design

The positioning process is informed by design constraints defined through the placement parameters of each element, as shown in Figure 4.21. The process begins with the automated generation of the bounding box for each specimen, which is referenced to its local coordinate system and matched to the machine's center coordinates. This vector defines the positioning, which is automated so that each grip element of the machine contacts the specimen appropriately.

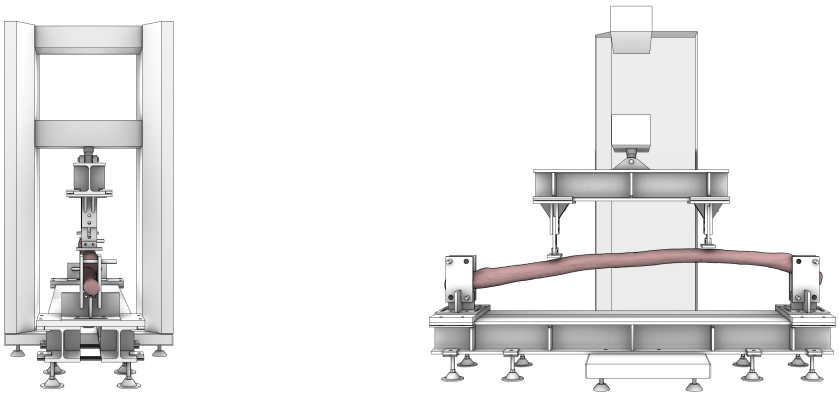

(a) Front view of the testing setup.

(b) Side view with specimen in position.

Figure 4.20: Testing setup with adjustable supports and loading components.

Each part of the setup is color-coded. Initially, points A_1 and B_1 define the experimental span and guide the placement of C_1 and D_1. A custom optimization algorithm is then used to determine the optimal configuration—referred to as the *finding parameters*. Additionally, height-adjustable load pin parameters L_4 and R_4 are computed. These values are calibrated using compression blocks inserted into the rail system of the load pin blocks, allowing the setup to adapt to each specimen's geometry and displacement range. These calibrated values also serve as reference points for manual fine-tuning.

This configuration is replicated in Abaqus mechanical simulations. The NURBS models are exported in IGES format, including their respective coordinate systems, for accurate simulation of the setup.

Calibration for the initial experiments was performed using a 3D-scanned point cloud to verify positioning accuracy. This process achieved a tolerance of less than $1\,\mathrm{cm}$, which was adjusted in the digital model. Most importantly, the centerline alignment of the specimen remained accurate.

Figure 4.23 shows photographs of the physical testing setup, highlighting the configuration and alignment of key components. The setup ensures consistency and repeatability for each specimen tested.

Additionally, the placement of deformation measurement devices is automated. As illustrated in Figure 4.21, a cross-sectional analysis is automatically generated at three key locations: at the center of each load pin and at the midpoint of the specimen. This configuration simplifies the calculation of the elastic modulus and the moment of inertia for each section. These positions determine where the strain gauges are installed, using digital measurement devices to document the deformations accurately and consistently.

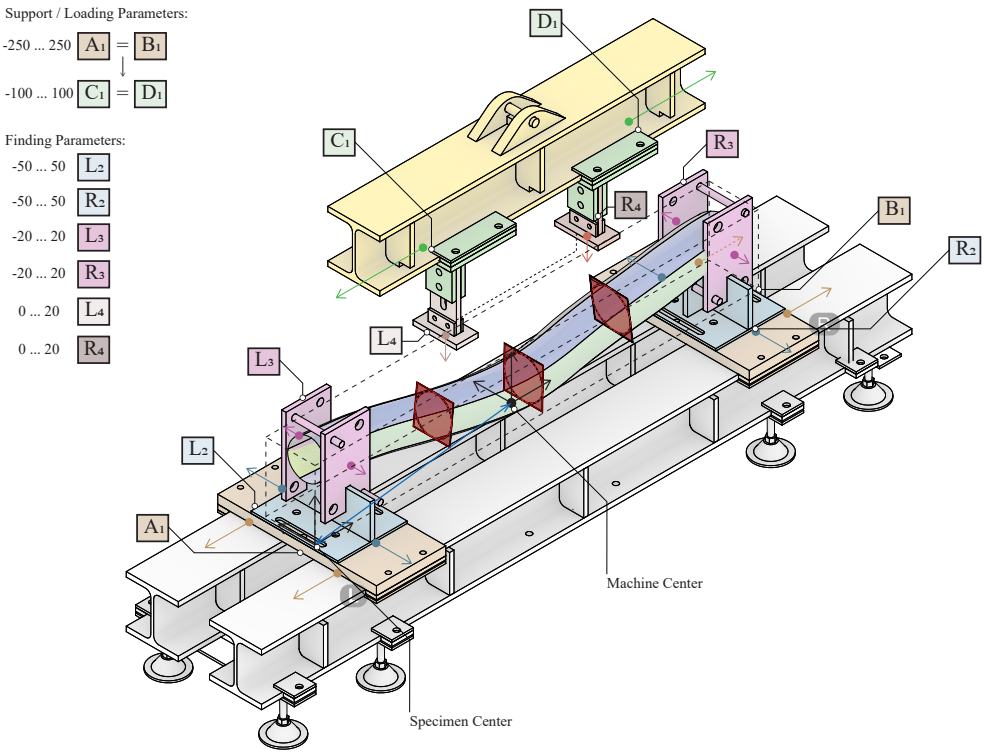

Figure 4.21: Parametric configuration of the testing setup, including bounding box alignment and load pin positioning.

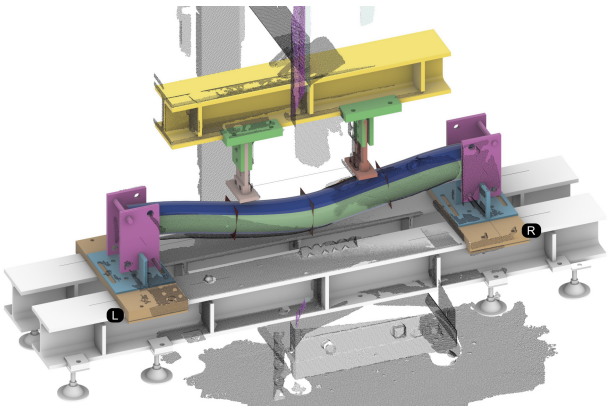

Figure 4.22: Point cloud-based calibration of the testing setup.



(a) Beech specimen with digital gauges.

(b) Setup overview.

Figure 4.24: Testing setup with digital gauges placed at defined cross-section locations.



(a) Testing specimen. (b) Detail view: Glider support.

Figure 4.23: Photographs of the testing setup.

This process is also extended to bifurcations, which can be positioned within the testing setup in a similar manner. In this case, a three-point bending configuration is adapted to apply loading on one branch of the bifurcation.

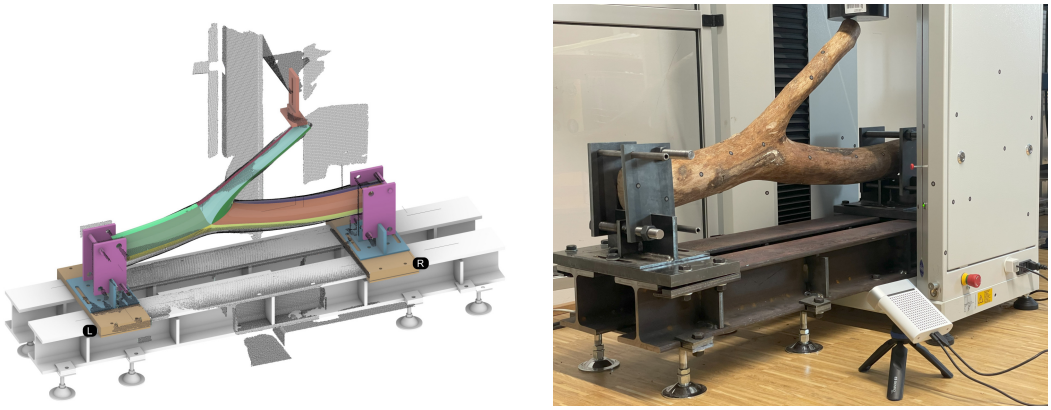

(a) CAD model and automated setup with point cloud data (b) Experimental setup for bifurcation testing.

Figure 4.25: Three-point bending setup applied to a bifurcated timber specimen.

Sensory-Informed Measurements with Volumetric Capture

A next iteration of the experimental setup was made to address the need for spatial deformation data. Since individual digital gauges only provide point-based readings, a volumetric capture sensor was introduced to support mechanical simulation calibration. Several sensor types were tested, and the Azure Kinect was selected for its development packages and real-time visualization capabilities via a custom plugin in Rhino [189].

The sensor was positioned at approximately a 45° angle to the front of the specimen. Preliminary scans established 3D alignment with the geometric model. Point clouds were captured at intervals during loading.

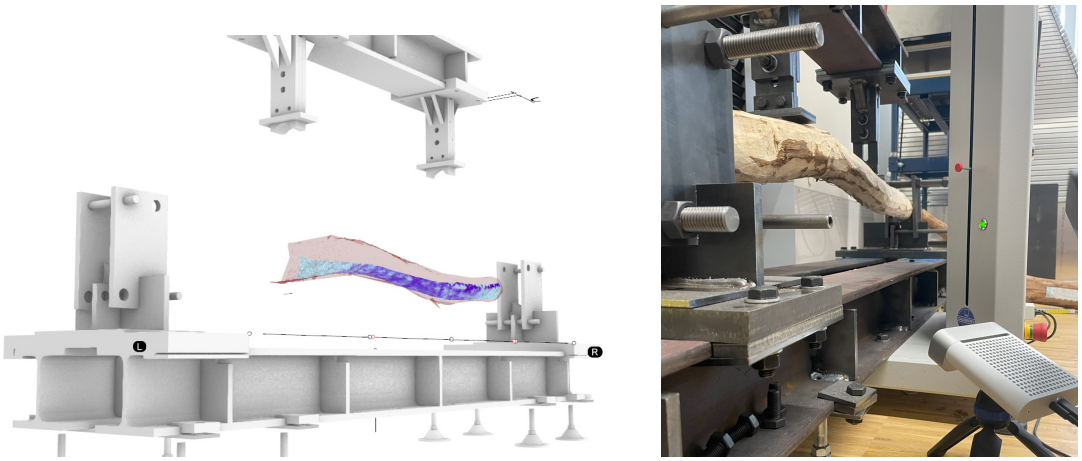

(a) Displacement mapping in a rectangular region of interest. (b) Testing with sensor during loading.

Figure 4.26: Volumetric data acquisition setup using Azure Kinect sensor for real-time displacement tracking.

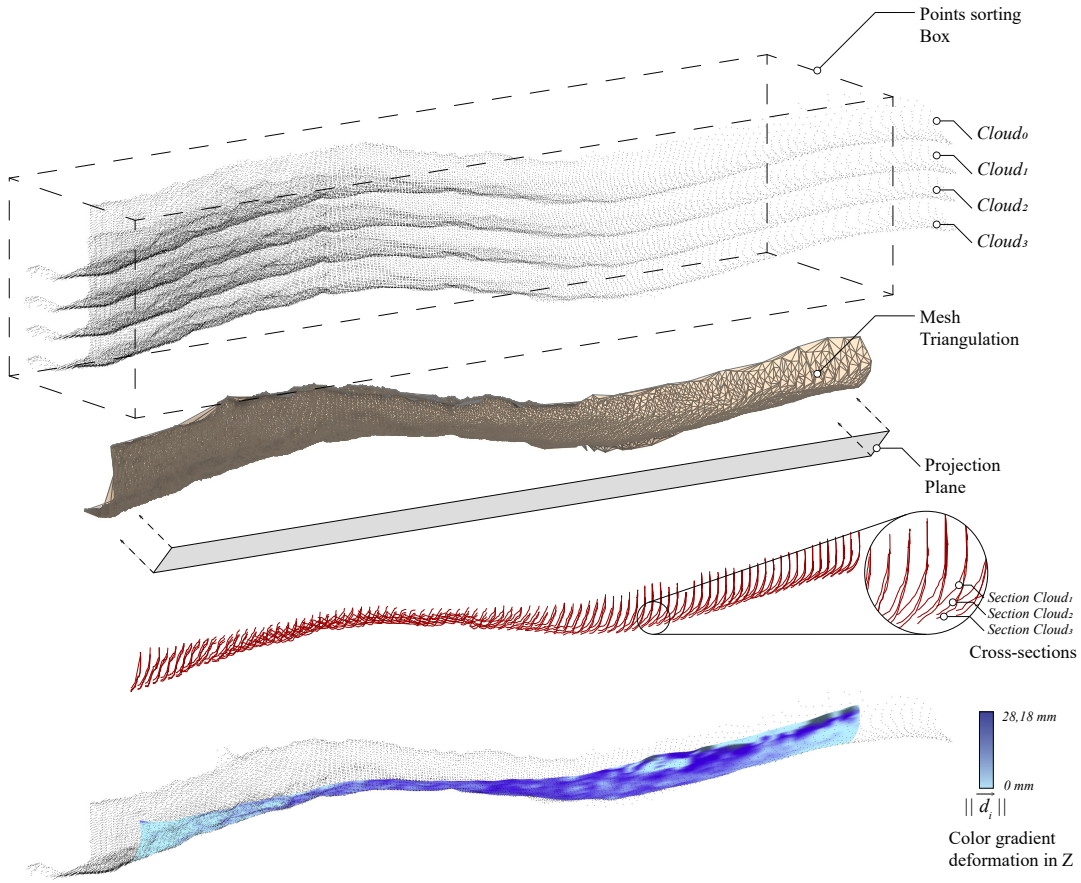

Figure 4.27: Workflow for point cloud deformation analysis.

Point Cloud Processing and Deformation Evaluation

The recorded point clouds are processed through a structured analysis pipeline. As illustrated in Figure 4.27, the workflow begins with the import and spatial alignment of sequential point clouds captured during the loading process. These datasets are cropped to a rectangular region of interest and sorted for consistency.

A reference mesh is generated from the initial scan using Delaunay triangulation. Subsequent point clouds are compared against this reference to evaluate deformation. Cross-sectional slices are extracted from each mesh, and displacement is computed as the vertical distance between corresponding points. This difference is visualized through color grading, providing a clear representation of local deformation over time.

Preliminary Tests

Preliminary tests were performed using a non-destructive setup to assess the mechanical response of timber under controlled loading. Loading cycles ranging from $5\,\mathrm{kN}$ to $10\,\mathrm{kN}$, depending on the cross-section, were applied up to four times within the elastic range without compromising the specimens. Torsional behavior was monitored to prevent unwanted rotation along the main centerline, and moisture content was recorded.

The test series focused on small to medium-diameter specimens ($50\,\mathrm{mm}$–$120\,\mathrm{mm}$), subjected to four-point bending following adapted principles from DIN 52186 [182]. Results are documented in [179]. Support positions were automatically adjusted to fit each specimen's geometry.

Displacement measurements were acquired via sensors and processed in MATLAB for comparison with reference data. These tests confirmed the potential for extracting reliable deformation data from curved raw timber without damaging the material, supporting its integration in subsequent mechanical and structural analysis workflows.

4.5 Conclusions on Material Mapping

This chapter consolidates the integration of physical and mechanical properties into digital models of naturally grown timber. The goal is to embed material behavior directly into structural simulation workflows, enabling more informed design applications. The proposed mapping method connects experimental data and geometric models, bridging irregular biological forms with engineering-level analysis.

The approach combines non-destructive testing, 3D scanning, and directional property assignment to represent internal and external structure. Localized elastic parameters are embedded into NURBS-based geometries, enabling simulation of anisotropy, heterogeneity, and growth-induced variation.

Material data was collected from seven Central European species (beech, oak, birch, spruce, pine, hornbeam, plane), conditioned to 12% moisture content. Properties were mapped directionally—longitudinal, radial, tangential—highlighting intra-specimen variability, especially in curved and bifurcated elements. This variation reinforces the need for property localization rather than uniform constants.

The values derive from combined sources: material characterization, DIN norms (DIN 68364 [185], DIN 52186 [182], DIN 14251 [183]), and literature [190, 172, 191, 192].

Tailored testing setups were developed for irregular shapes. These methods were refined in Dupre's Bachelor thesis [179], which applied a four-point bending test with simulation feedback to confirm longitudinal modulus estimates and emphasize sensitivity to boundary setup. His results validated the general trends observed in this thesis and pointed to improvements in sensor calibration.

A volumetric deformation tracking system was also introduced using real-time point cloud capture, further connecting physical testing with digital material representation. Together, these methods provide a basis for characterizing irregular timber for design integration.

Chapter 5

Structural Design With Raw Timber

Structural Systems, Static Analysis and Finite Element Analysis for Load-Bearing Applications

This chapter covers geometric concepts and material analysis, focusing on their application to load-bearing structures in architecture and construction. It establishes a link between structural design and the analysis of structural systems. At the meso-scale, finite element analysis (FEA) is used to examine individual structural elements, while at the macro-scale, bar-type and shell-type FEA modeling is applied to analyze entire structural systems, primarily composed of bar and plate elements. Structural optimization techniques are then employed to refine the designs. Finally, state-of-the-art matching methods are used to integrate previously studied timber elements into the proposed structural systems.

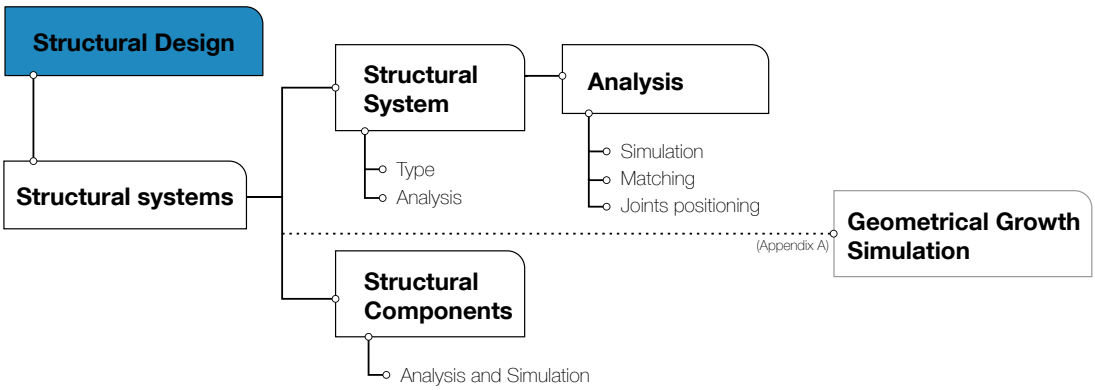

Figure 5.1: Chapter Diagram: Structural Design and Simulation.

5.1 Structural Design

This section examines the transition from individual naturally grown timber elements to their integration within larger structural systems. It emphasizes structural element modeling, structural typologies, and connection strategies, and subsequently addresses data management for simulations, structural design methodologies, optimization techniques, and analytical approaches. The structural design process, including the evaluation of results, follows the workflow illustrated in Fig.5.1. The workflow decomposes the interrelated steps into a structured sequence, integrating concepts introduced in previous chapters, as shown in Fig.5.2. Once a structural system has been conceptualized, two scales of analysis are distinguished.

First, at the macro scale, the static diagram of the overall structure is developed, serving as a framework into which the raw timber elements are integrated. This stage includes tasks such as element matching and the allocation of geometrically defined elements supplemented with corresponding material properties. Second, optimization in joint positioning. These include modifications to the static system based on the element library, and static considerations such as node displacements along the growth axis.

The process ends in a finite element analysis (FEA), which not only evaluates the global structure but also refines the mechanical assessment of individual elements at the macro scale. The results are evaluated at both scales to determine potential iterations and are cross-checked against the raw timber specimens in cases where detailed construction adjustments or subprocess modifications are required.

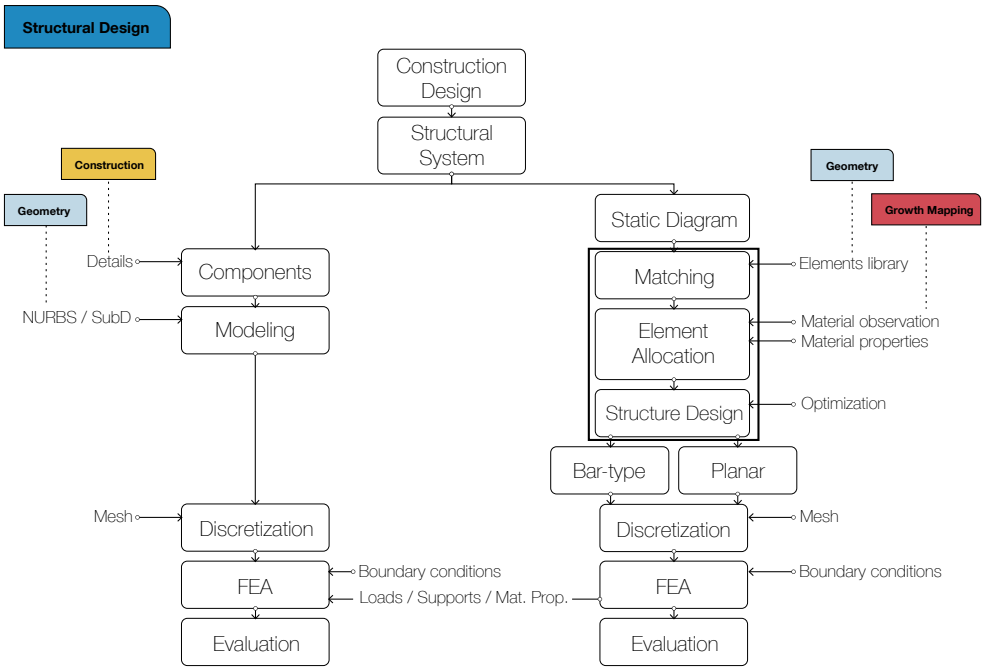

Figure 5.2: Workflow of the structural design process.

5.1.1 Definition of Structural Elements

The analyzed and documented elements provide a basis for estimating the load-bearing capacities of the components based on their geometry. These components—which include straight, curved, and bifurcated pieces—can be integrated either individually or collectively into structural systems.

As shown in Figure 5.3, the specimens can be classified as elements with undetermined connections, which are defined to form the structural system. Following the logic of the *off-knot* strategy, the type and location of joints are positioned along the growth axis of the timber elements. These axes are geometrically defined, as described in Chapter 3. This setup enables a optimization in terms of matching, in which these elements are placed within the structural system. The joints—as point P—can then be adjusted along the element's axis. For example, joint locations can be shifted toward zones of near-zero bending moment (see Section 5.2.2).

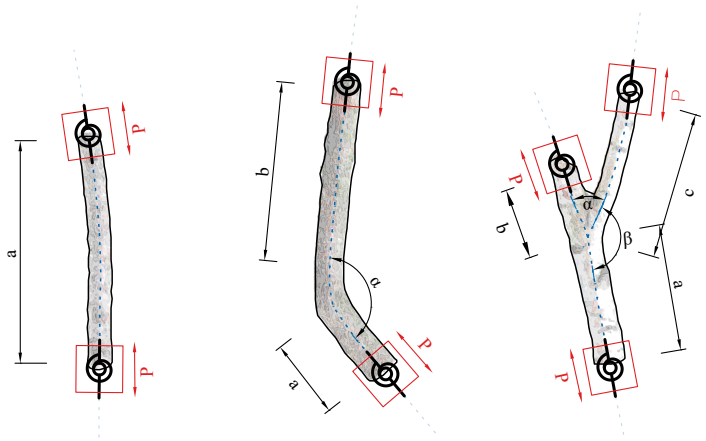

Figure 5.3: Element definitions: straight, curved, and bifurcated. Parameters include endpoints P (modeled as rotational springs), axes (A, B, C), and angles α, β.

Systems

In an initial phase, various types of structural systems can be defined, derived analytically from construction methods discussed in Chapter 6.1.1. These methods are categorized through case studies, classifying structures according to single-axis, multi-axis, planar, or spatial configurations. Based on this classification, a simplified abstraction is derived using bar-type elements (see Figure 5.4) or planar elements. These structures are analyzed statically by assuming that their joints allow rotation or behave as semi-rigid, spring-like connections. This leads to the definition of structural components, which can be analyzed in a subsequent phase to assess whether they meet the requirements imposed by the structural system.

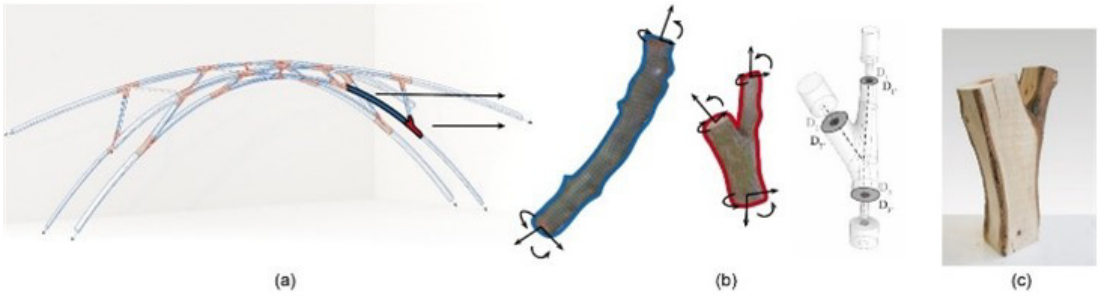

Figure 5.4: a) Structural system; b) Structural components as curved bars or bifurcated nodes; c) Structural component made from raw timber.

Components

Structural components are defined based on the timber elements, but here in terms of constructive definition, which includes determining the types of joints required. These are refined through successive iterations involving manufacturing constraints and CAD-based joint modeling. These components—as illustrated in Figure 5.4(c)—are analyzed in greater detail at the end of this chapter. At this stage, volumetric finite element analysis (FEA) may be applied, with boundary conditions defined by the global structural system.

Structural Modeling

The structural modeling of bar elements is based on the assembly of longitudinal components aligned along their central axes. Their joints are defined in the finite element analysis (FEA) environment as rotational springs—an approach implemented using the Karamba software [193], which is recognized as a standard tool in early-stage design.

Planar Systems Modeling

The structural modeling of board-based systems requires a simplified method, particularly suitable for early design phases. FE-Shell elements are used either to represent reference plates—extracting principal bending moments and converting them into design patterns— and to simulate sandwich panels with raw timber core (see Figure 5.5(c)).

In this figure, two horizontal reference meshes are shown, along with vertical sub-meshes representing raw timber components. The structural model connects horizontal and vertical layers using articulated joints, simulating the role of fully threaded screws typically used in construction. The thickness assigned to each raw timber shell element corresponds to the minimum diameter D_{min} of the respective timber sections. The spacing between the two horizontal meshes matches the height defined in the geometric model and corresponds to the intended length of the raw timber components.

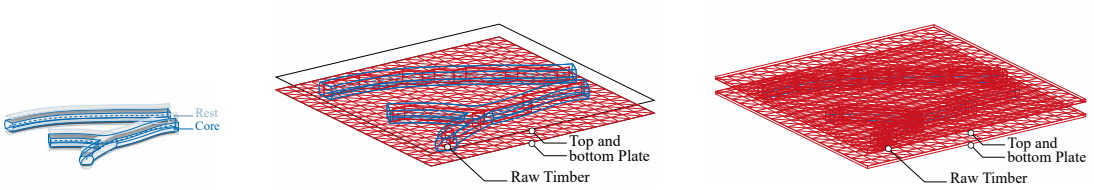

(a) Initial geometry (b) CAD design model (c) Discretized mesh

Figure 5.5: Structural modeling of board-based systems sandwich panels. Connections are modeled as pinned joints, analogous to fully threaded screws. Element thickness corresponds to minimum timber diameter D_{min}.

5.2 Structural Optimization Methods

The optimization processes addressed in this dissertation are implemented in two main stages. The first stage focuses on the geometric positioning of the raw timber elements based on their centerline curves c_g, aligned with the structural design requirements. This is know as Matching and is applicable whether for bar-type elements or planar assemblies (see Figure 5.6).

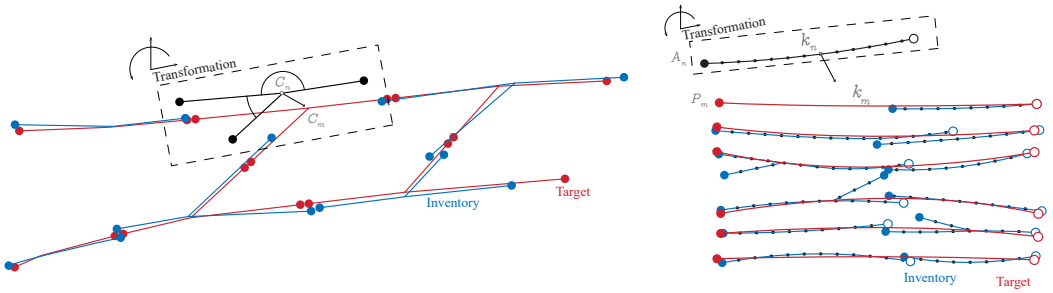

Figure 5.6: Matching positioning according to structural layout and centerline alignment.

The second optimization method targets the positioning of joints with respect to the connection points between elements. This step considers structural analysis data to minimize bending moments, axial forces, or shear stresses depending on the joint's location along the element. This is particularly relevant for the application of off-knot connector strategies (see Figure 5.7).

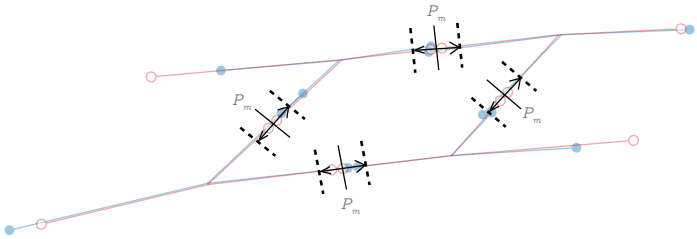

Figure 5.7: Joint positioning optimization.

5.2.1 Matching methodology

The design process must balance a high degree of flexibility in adapting structural systems to the available material library. Therefore, the next logical approach is based on the structural configurations and systems proposed in the previous section.

The procedure presented in the literature on matrix mismatch [68, 22] allows for the comparison of two geometric entities. The matrix geometry $\mathcal{G}$ refers to the geometric properties of the raw material, specifically timber branches, while the matrix $\mathcal{T}$ corresponds to the target geometric properties of the structural system.

In the next step, we will break down the geometric properties of both matrices. This process is divided into three phases. Here, the geometric properties of the matrices are defined, with $\mathcal{G}$ as Phase I and $\mathcal{T}$ as Phase II. This is further divided into two sections, which are executed in parallel.

Phase I: Breaking down raw timber gometry

Here, $\mathcal{G}$ is defined as the structured geometric matrix that organizes raw timber data into a mathematical framework for structural analysis. Additionally, the geometric inventories, referenced in Chapter 3, categorize timber elements into bifurcations or curved longitudinal elements, represented as c^i, with a start point A_0^i and stored as G.

Definition of G and $\mathcal{G}$:

- G represents a **geometric inventory**, a collection of raw timber elements characterized by fundamental properties such as curvature, segment length, and endpoint positions. These elements serve as the basic dataset for modeling.
- $\mathcal{G}$ is a **structured geometric matrix** that refines this dataset by incorporating additional parameters, such as admissible stresses σ_{adm} and shear stresses τ_{adm}, ensuring its applicability in structural analysis. While G provides a purely geometric description, $\mathcal{G}$ integrates mechanical properties into a system suited for load-bearing assessments.

Firstly, in the case of bifurcations, a set of three vectors can always be distinguished, originating from a central point and extending to three external points:

$$G^i = \{u_0^i, u_1^i, u_2^i, u_3^i\}, \quad i = 0, 1, 2, \dots$$

where u_0^i denotes the central point, also referred to as C_g in Chapter 3. The variable i represents the number of timber elements in the inventory, corresponding to the number of branches of the library.

The endpoints $\{u_1^i, u_2^i, u_3^i\}$, defined in geometric analysis as A_n, B_n, C_n, maintain a minimum threshold distance of 0.50 m from the center, which establishes the maximum span of the branches as structural elements. Therefore, u_1^i corresponds to the point located on curve a, u_2^i to the point on curve b, and u_3^i to the point on curve c. These points are later represented as the vectors $\vec{u}_n^i$, where:

$$\vec{u}_n^i, \quad n = 0, 1, 2$$

Additionally, curved and longitudinal elements can also be included in an inventory G:

$$G_n^i = \{k_n^i, l_n^i; k_{n+1}^i, l_{n+1}^i; k_{n+2}^i, l_{n+2}^i, \dots\}, \quad i = 0, 1, 2, \dots \quad \text{and} \quad n = 0, 1, 2, \dots$$

This structured approach allows the transition from raw timber data (G) to a more refined analytical framework ($\mathcal{G}$), integrating both geometric and mechanical considerations for further structural analysis.

These elements are further characterized by their primary curvature k_0^i over a segment of length l_0^i. Additionally, multiple curvatures can be considered with n, typically up to two additional segments for simplification purposes.

In cases where structural analysis or cross-sectional admissibility is required, parameters such as admissible stresses σ_{adm} and shear stresses τ_{adm} can be incorporated. Thus, these inventories can be structured into the geometric matrix $\mathcal{G}$ as follows:

$$\begin{aligned} &\mathcal{G} : \{\vec{u}_n^i, \sigma_{\text{adm},n}^i\}, \quad n = 0, 1, 2 \\ &\text{or} \quad \mathcal{G} : \{k_n^i, l_n^i, \sigma_{\text{adm},n}^i\}, \quad n = 0, 1, 2, ... \end{aligned} \tag{5.1}$$

Breaking Down Target Geometry in Phase II: Target Geometry

The target geometry c^j, as defined in structural systems, is decomposed into vectorial units that can be discretized according to the structural entity they belong to. Thus, the structural topology can be divided into the following element types, each of which is geometrically defined in terms of its corresponding vectors.

Longitudinal Elements (Bar-Type) for Node Connections

The primary structural elements are those positioned at specific locations within the structure, such as bars and nodes. These can be categorized into two main types: *Nodes* and *Longitudinal elements*, which do not form part of a node but serve to connect them, as illustrated in Figure 5.4.

Nodes (from tree bifurcations) must consist of three vectors and three angles summing to 360°, which correspond to branch bifurcations that naturally approximate this angular sum.

For proper concatenation with the branch library, these nodes are simplified into three co-planar vectors and represented by their skeletal centerline. As described in the literature, [22] defined the four terminal points of the skeletal representation and stored them as an inventory for each node:

$$T^j = \{v_0^j, v_1^j, v_2^j, v_3^j\}, \quad j = 0, 1, 2, \dots$$

where v_0^j denotes the central node points of the structure, and j represents the number of target curves. These central points are maintained at specific positions to facilitate the matching process in the subsequent phase. The endpoints points are later represented as the vectors $\vec{v}_m^j$, where:

$$\vec{v}_m^j, \quad m = 0, 1, 2$$

Longitudinal but curved elements can also be incorporated as alternatives to straight bars. In this case, the inventory is structured as follows:

$$T_m^j = \{k_m^j, l_m^j; k_{m+1}^j, l_{m+1}^j; k_{m+2}^j, l_{m+2}^j; \dots\}, \quad m = 0, 1, 2, \dots, \quad j = 0, 1, 2, \dots$$

where k_m^j represents an analyzed curvature within segment l_m^j. The number of segments is defined up to a maximum of three for simplification purposes, and m represents the segment index where k is located.

In a further breakdown, tensile stresses σ and shear stresses τ can be included within the inventories for each section to incorporate structural requirements.

This results in a set of target inventories, which can be formally defined within the matrix $\mathcal{T}$ as follows:

$$\begin{aligned} &\mathcal{T} : \{\vec{v}_m^j, \sigma_m^j\}, \quad m = 0, 1, 2 \\ &\text{or} \quad \mathcal{T} : \{k_m^j, l_m^j, \sigma_m^j\}, \quad m = 0, 1, 2, \dots \end{aligned} \tag{5.2}$$

Planar Elements

The planar structures defined as sandwich panel systems can be analyzed in a similar manner. In this case, target curves c^j can be generated to represent the reinforcements within the core of sandwich panels through an analysis of load paths, transverse shear forces, and principal moments. These values are obtained by performing a finite element analysis (FEA) using shell elements.

Unlike the previous approach based on structural systems or bar patterns, this procedure begins with the definition of the *load case*, where the reinforcements in the core will be integrated. Once the structural analysis is conducted, information such as the direction of the principal moment vectors can be extracted. Alternatively, these can be replaced by the resulting internal forces. These vectors are included in a vector field $\vec{M}$.

The target curves are generated through the vector field $\vec{M}$, which is extracted from the *moment transmission paths* within the shell analysis of a *reference panel*. In this process, only vectors whose modulus exceeds a reference threshold σ_R are considered.

This *reference panel* is determined by the thickness of a given timber panel. Consequently, target curves c_t^j will only be generated as reinforcements where necessary. The vector field $\vec{M}$ is defined by the scalar sum of the vectors $\vec{m1}$ and $\vec{m2}$, representing the first and second principal moments of the reference static analysis of the panel (see Eq. 5.3). The target curves are then stored in the target matrix $\mathcal{T}$ (see Eq. 5.2), which contains the curvature values (k_m^j), the length l_m^j, and their corresponding local stresses from the analysis (σ_m^j).

$$\vec{M} = \vec{m1} + \vec{m2} \tag{5.3}$$

Phase III: Matching and Design Approach

The process of comparing and matching multiple inventories is applied to the matrices defined in 5.1 in conjunction with 5.2. As cited in the literature, Huang et al. 2021 [68], developed a cost matrix $\mathcal{D}$ procedure, where elements from inventory i are matched with elements from inventory j.

Following this approach, the same method is applied to the curve inventories. Each element in both lists is compared, and the cost of pairing each curve from the timber inventory with a target curve is calculated within a 2D Euclidean space. This process, known as the *Linear Assignment Problem (LAP)*, is solved using the *Hungarian Algorithm*, a combinatorial optimization method. The outcome is a *Matching Score (MS)*, which quantifies how well the timber curves c^i align with the target curves c^j.

The assignment problem is formulated as follows, aiming to minimize the total cost of matching inventory curves c^i with target curves c^j:

$$\min \sum_{i=1}^{n} \sum_{j=1}^{n} d_{ij} x_{ij} \tag{5.4}$$

subject to:

$$\sum_{i=1}^{n} x_{ij} = 1, \quad \forall j, \quad \sum_{j=1}^{n} x_{ij} = 1, \quad \forall i \tag{5.5}$$

where:
- d_{ij} represents the *MS* between inventory curve c^i and target curve c^j,
- $x_{ij} = 1$ if c^i is assigned to c^j, otherwise $x_{ij} = 0$,
- The constraints ensure that each inventory curve is assigned to exactly one target curve.
- n represents the total number of elements in both the inventory and target sets. It defines

the size of the cost matrix $\mathcal{D}$, meaning that i and j range from 1 to n, ensuring a one-to-one correspondence between inventory and target curves.

To quantify the quality of the matching, the *MS* is computed by normalizing the total cost. The scale is adjusted so that *100 represents a perfect match* and 0 represents no match:

$$MS\% = \left(1 - \frac{\sum_{i=1}^{n}\sum_{j=1}^{n} d_{ij}x_{ij}}{\sum_{i=1}^{n}\sum_{j=1}^{n} d_{ij}^{\max}}\right) \times 100 \tag{5.6}$$

where $d_{ij}^{\max}$ is the maximum possible cost in the cost matrix $\mathcal{D}$, ensuring that $0 \leq MS \leq 100$. A higher *MS* indicates a better match.

Since the matrices $\mathcal{G}$ and $\mathcal{T}$ consider multiple factors—such as vectors defining bifurcated branches, measured curvatures, and stiffness requirements—it is possible to adjust a *variable slicer* to prioritize either geometric properties or structural strength, depending on the design constraints. This flexibility allows the *Matching Score* to be optimized further, providing a valuable parameter for future refinements.

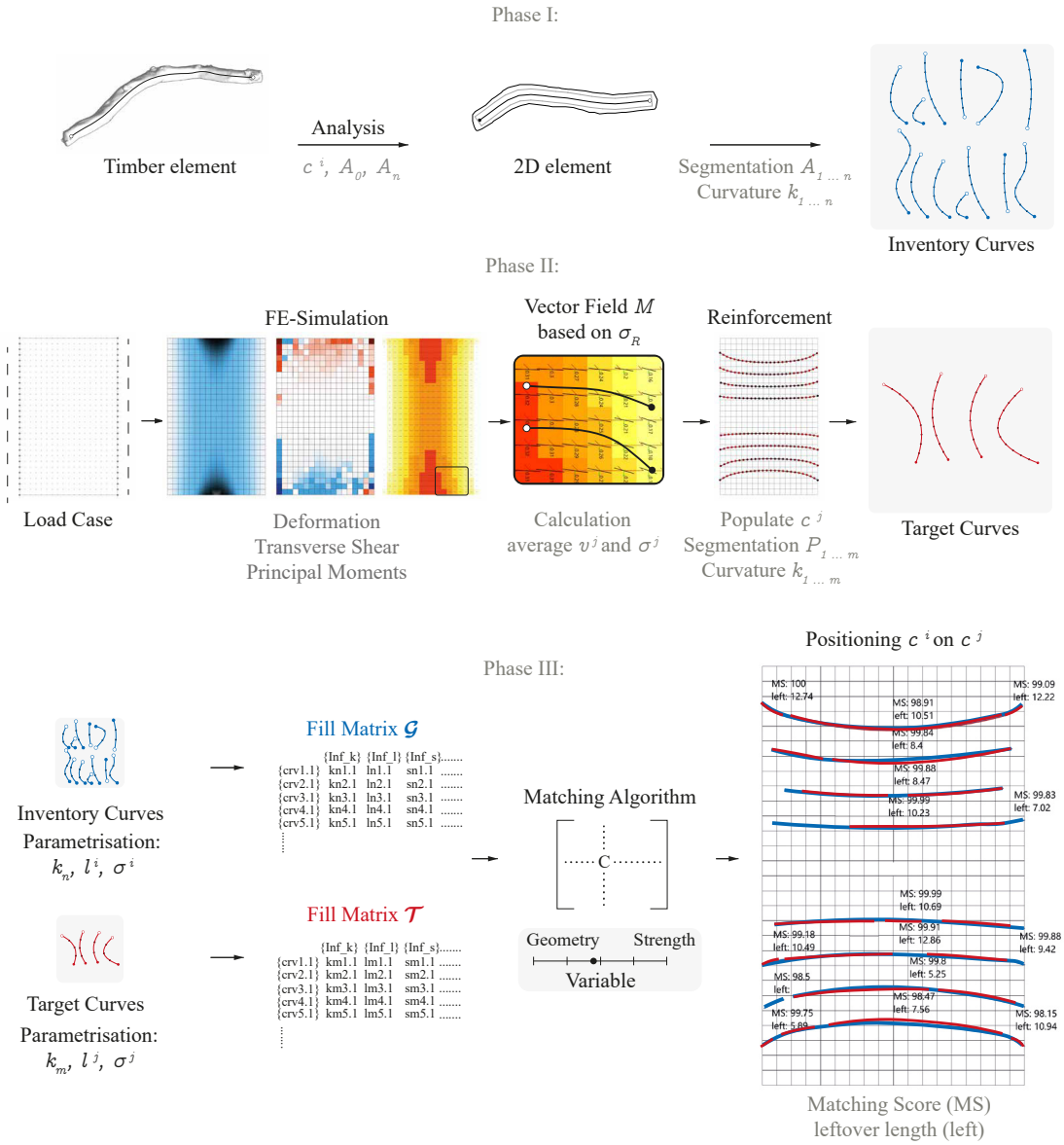

Figure 5.8: Workflow. Development of the parameterisation of inventory curves, through geometric analysis, and target curves, and FE analysis. Figure from [194].

Benchmarking

A benchmarking study has been conducted to evaluate the performance of the implemented matching algorithms across different structural configurations. This includes examples applied to bar-type assemblies [18] and plate-type systems [194]. The benchmarking framework assesses computational efficiency, geometric fitting accuracy, and element utilization rates. Selected results from this evaluation are presented in the supplementary material included in Appendix B.5 of this dissertation.

5.2.2 Joint Positioning Optimization For Bar-Type Structures

This section analyzes methods for improving the structural integrity of a system by adjusting the position of joints between raw timber components. Starting from a static diagram, the components may or may not be positioned using matching techniques. However, these methods do not precisely determine the optimal location of the joints. When joint positions can be shifted along the axis connecting structural nodes—as in the example shown in Fig. 5.9—this spatial flexibility can be utilized to improve performance.

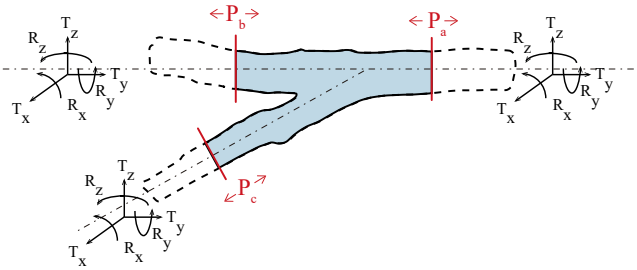

Figure 5.9: Component with conditions for joints.

As illustrated in the static diagrams in Fig. 5.10, these nodes can be positioned arbitrarily along the axes of the bar-type system. The joint requirements can vary: some may be articulated, allowing truss formation and the attachment of additional elements such as bars (highlighted in yellow in the figure); others may be semi-rigid, modeled as rotational spring joints. The latter configuration is feasible and will be discussed in greater detail in Chapter 6.2. In general, semi-rigidity can be achieved through form-fitting joints or by integrating fully threaded screws.

These diagrams are parametrized, distinguishing straight, curved, and bifurcated bars with their respective axes, derived from approximations of growth curves c_g adapted to the topology of the structure.

This section introduces the use of optimization and multi-objective optimization (MOO) methods to determine the optimal positioning of structural joints. By integrating static diagrams with automated evaluations of finite element (FE) simulation results for bar-type systems, the algorithm can iteratively shift node positions along the axis to identify configurations that best satisfy structural performance criteria such as moment transmission.

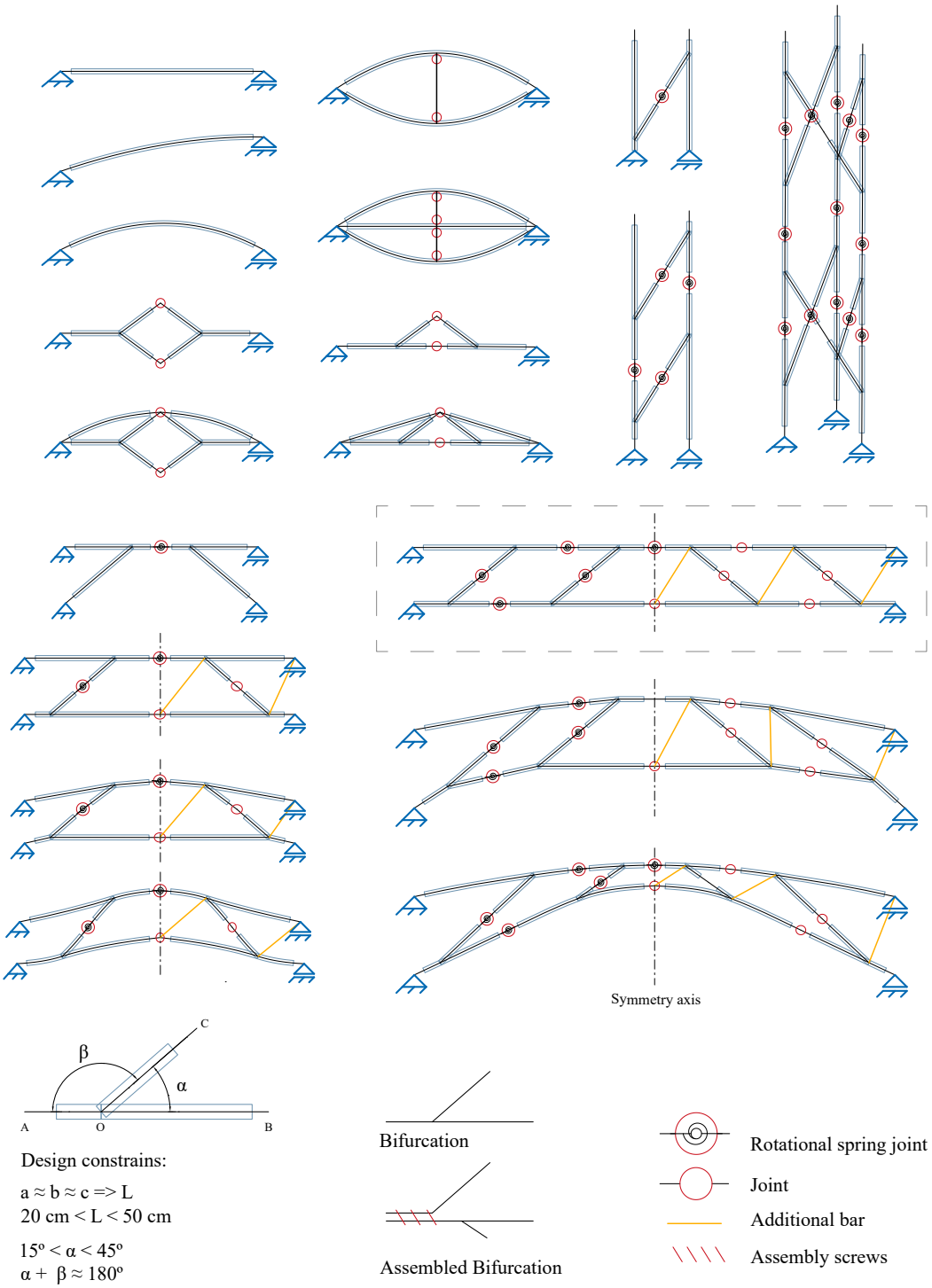

Figure 5.10: Examples of parametrized static diagrams showing articulated and semi-rigid joints. The bar types—straight, curved, and bifurcated—are defined by axes derived from approximated growth curves c_g adapted to the structural topology. Adaptation from [18].

Joint Methodology

To define the joint positioning strategy and apply it to a simplified topology, the joint location is treated as a variable along the axis of the bar member. This position is controlled by a parameter p within the range $0 < x_{\text{joint}} < L$, which serves as input to the model. The method applies multi-objective optimization, modeling joints as rotational springs. The geometric constraints that limit displacement are derived from the geometry of the raw timber elements themselves. For instance, displacement may be restricted to the interval $0.1L < x_{\text{joint}} < 0.9L$ to ensure feasible joint locations.

The optimization aims to minimize total deflection, maximum deflection, the sum of bending moments, or the maximum moment at critical points such as bifurcations.

To illustrate the methodology, a typical structural configuration—a Vierendeel truss—is subjected to multiple loading conditions, as shown in Fig. 5.11. These include vertical and 45° inclined loads to simulate asymmetrical loading scenarios. All load cases are considered during optimization.

In addition to lengths and angles, minimum cross-sectional dimensions—calculated from internal forces—can serve as input constraints within the data design space. This process is similar to typical cross-section optimization techniques, which operate within fixed dimensional ranges for each structural element.

The modeling workflow integrates Rhino & Grasshopper [71] for geometric modeling, the MOO engine Octopus [195, 196] for optimization, and Karamba [193] for structural analysis.

Optimization Results

To demonstrate the optimization workflow, a system previously studied and published in [18] was analyzed. Figure 5.11 shows a Vierendeel girder subjected to a vertical and a 45° inclined traveling load. Each of the 16 point loads (P01–P16) corresponds to an individual load case (LC01–LC16). The joint positions were optimized using three objective criteria: minimizing the sum of bending moments, minimizing total deflection, and minimizing maximum deflection of the girder.

As shown in Table 5.1, optimizing joint positions reduced total deflection (sum U) by up to 23% and maximum deflection (max U) by up to 21%. However, the total bending moment summed over the girder (sum My) increased by 7% to 78%. For systems or load cases with asymmetrical behavior, the optimization process leads to more favorable moment distributions and reduced deflections.

This method is particularly advantageous when using grown timber elements from the database, as they often do not allow joint placement precisely at the center of a member. In such cases, although fiber and load path eccentricities may occur, the reduction of bending moments causes the elements to primarily transmit axial forces. A subsequent iteration of the algorithm could incorporate additional constraints, such as minimizing eccentricities or reducing shear forces.

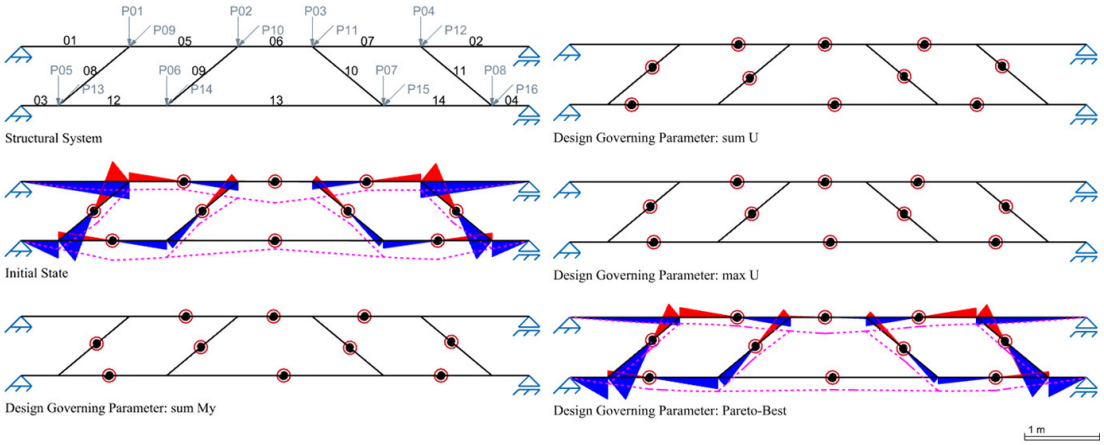

Figure 5.11: Optimization process of a Vierendeel girder system under multiple load cases. Adaptation from [18].

Table 5.1: Results: Joint location along each bar under different optimization criteria. Adaptation from [18].

Bar no.	Initial state	sum My	sum U	max U	Pareto-best*
01	-	-	-	-	-
02	-	-	-	-	-
03	-	-	-	-	-
04	-	-	-	-	-
05	0.50	0.52	0.53	0.52	0.52
06	0.50	0.52	0.54	0.54	0.54
07	0.50	0.52	0.47	0.53	0.52
08	0.50	0.54	0.62	0.59	0.62
09	0.50	0.52	0.56	0.53	0.48
10	0.50	0.53	0.53	0.52	0.52
11	0.50	0.57	0.64	0.59	0.60
12	0.50	0.53	0.78	0.58	0.62
13	0.50	0.54	0.53	0.51	0.52
14	0.50	0.53	0.35	0.52	0.52
sum My	100%	107%	178%	119%	126%
sum U	100%	84%	77%	80%	79%
max U	100%	84%	87%	79%	82%

The joint positioning obtained through the optimization process was tested by integrating raw timber elements to assess its applicability in the construction of physical prototypes. Figure 6.19 illustrates how this positioning can be translated geometrically into raw timber elements. Figures 6.20(a) and 6.20(b) depict a potential hybrid joint configuration for bifurcations in the Vierendeel girder introduced in the previous example.

5.3 Simulation of Structural System

This section outlines the structural simulation approaches used in this dissertation. The focus is on methods applicable to early design stages and compatible with parametric workflows, enabling the integration of design transformations.

Detailed simulation results are not presented here but are instead discussed in the construction demonstrations at the end of Chapter 6. Complementary results are available in the Appendix, covering both bar-type and planar systems.

5.3.1 Simulation of Structural Elements

This subsection briefly notes the simulation strategies for individual elements. Preliminary static assessments define boundary conditions for FEA. For more advanced analysis, collaboration with external partners enabled detailed simulations.

Workflow for Simulation Management

Mechanical properties obtained from raw timber test specimens allow for the assignment of specific material parameters to structural elements. Methodically, these properties are geometrically organized and applied to simulation models. This includes aligning growth direction with the centerline and assigning polar-distributed material parameters (see Chapter 4.3.1).

The geometric preparation consists of simplifying and formatting CAD models, including centerlines, NURBS surfaces, and bounding volumes (as defined in Chapter 3). These models are exported in formats compatible with FEA software, where meshing, boundary conditions, and loading scenarios are defined.

Mechanical Simulations

As a complementary contribution of this thesis, geometric data were used in various structural simulations to evaluate the behavior of raw timber elements under applied loads derived from architectural design.

The simulation workflow proceeds as follows: closed SubD volumes are converted to NURBS geometry. Connection types and load applications are modeled in CAD. These solid models are exported in ASCII-based formats such as `.IGES` or `.STEP` and imported into FEM software. Simulations include assembly definitions, cross-section properties, and meshing, typically using tetrahedral or quadrilateral elements depending on the model and structural connections. Results are then analyzed to identify stress concentrations and deformation patterns.

These examples serve as proof of concept, demonstrating the feasibility of using geometric analysis workflows for mechanical simulation. The results help identify critical stress regions and deformation zones that may not be evident through basic structural system analysis.

Application of Generalised Scaled Boundary Isogeometric Analysis (GSBIGA)

GSBIGA, as introduced in Spahn et al. [197], is applied in this research project to simulate the structural behavior of naturally grown timber. This method avoids internal meshing and is particularly effective for handling irregular morphologies. GSBIGA integrates with the NURBS-based geometric models developed in this thesis, enabling high-resolution simulation directly from the exact surface definitions. Material properties and analysis results are distributed volumetrically according to the NURBS formulation.

These techniques were applied to raw timber elements and published in [198, 197]. The figures 5.12 show results demonstrating surface continuity, stress distribution, and deformation behavior. This supports further development such as ongoing simulations of material growth [2].

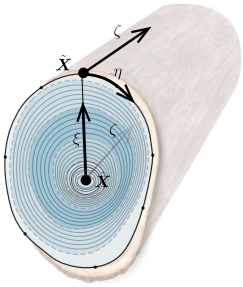

(a) SBIGA diagram with principal directions [197].

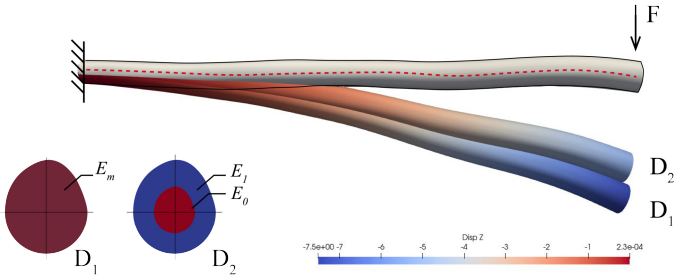

(b) Cantilever simulation with different material properties in the core [180].

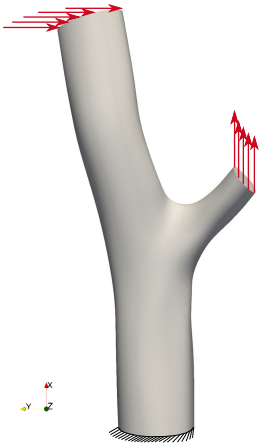

(c) Boundary conditions

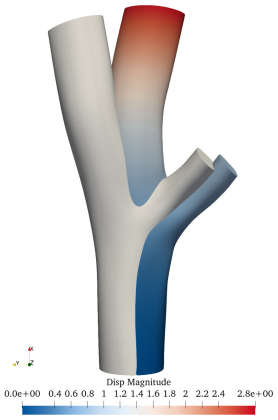

(d) Deformation.

Figure 5.12: Simulation results using SBIGA on raw timber geometries from Fig. 3.30. Figures extracted from [170].

5.4 Geometrical Growing Simulation

As a parallel project to the thesis, Appendix A.1 presents an initial approach to simulating geometric growth, based on form optimization using the criterion of stress homogenization in the tree stem. A cantilever-shaped simulation was developed.

5.5 Conclusion

This chapter has presented the methods used for analyzing and simulating applications related to raw timber construction. These processes were outlined in a workflow to support simplification and early-stage design strategies. Two optimization methodologies were introduced: first, the use of matching techniques—specifically a modified Hungarian algorithm—to organize timber elements; second, a strategy for joint positioning based on static studies aimed at minimizing bending moment transmission at the connections.

Additionally, this chapter clarified which methods are used for detailed mechanical simulations in parallel projects, where deeper material characterization is required. In doing so, it concludes the methodological foundation for analysis, which will be further applied and illustrated in the construction demonstrations presented in the following Chapter 6.

Chapter 6

Construction Methods

Raw Timber Potential Applications

This chapter explores various construction methodologies for integrating raw timber into building structures. It focuses on a classification of load-bearing structural systems, ranging from bar-type frameworks to planar elements such as slabs and walls. The emphasis lies in understanding how raw timber can be adapted both to highly individualized construction techniques and to approaches aimed at standardization for broader architectural applications. Additionally, the chapter investigates the design and optimization of connection systems. Special attention is given to digital fabrication processes and assembly strategies.

The chapter concludes with the presentation of two experimental constructions developed within an academic research environment. These full-scale prototypes—a pedestrian bridge based on a circular design strategy and a pavilion realized for an exhibition—serve as demonstrative examples of the construction potential outlined in this dissertation. They illustrate both individualized structural solutions and approaches toward standardized assembly using naturally grown timber in multiple structural applications.

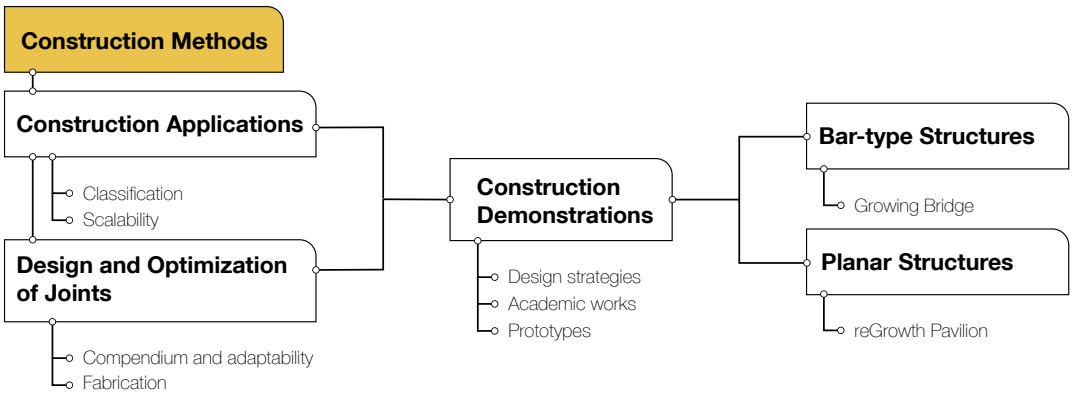

Figure 6.1: Chapter Diagram: Classification, joint strategies, and construction demonstrations.

6.1 Modeling Construction Applications

6.1.1 Classification of Construction Integration of Naturally Grown Timber

Unlike traditional timber construction, which primarily employs standardized rectangular sections in the form of beams, bars, and boards, integrating raw timber allows for more efficient use of naturally circular cross-sections. As discussed in Chapter 4, circular sections exhibit polar and tangential material distributions that reflect internal stress patterns. Preserving these sections in their natural form—particularly by retaining their circular geometry—enables structural applications that exploit the inherent properties aligned with the growth rings. Based on this principle, a classification of construction methods using naturally grown timber is proposed in this section. Preliminary classifications were introduced in Chapter 2, with basic structural systems using simple bars and metal joints (e.g., trusses and columns). A more recent framework is presented by Sun et al. [52], which explores computational design methods with a focus on material inventory upcycling, not limited to timber.

To develop a classification tailored to raw timber applications, this chapter draws on classical typologies of structural systems as outlined by Engel [199]. The classification emphasizes Section-Active Structural Systems, where load-bearing behavior depends on the cross-sectional properties of individual components to resist axial and bending forces.

Vertical-Linear

This category includes structures with a dominant vertical orientation, typically resolved through column-like assemblies. These can be subdivided into systems composed of single bar elements or composite vertical units such as sandwich columns, which integrate raw timber with planar components.

Vertical-Planar

This category includes applications that function as vertical planes or surfaces. These may include load-bearing walls, façade assemblies, or partition systems.

Horizontal-Linear

This category includes applications that primarily function as beams or trusses, typically configured with articulated or semi-rigid connections. These systems span in one axis.

Horizontal-Planar

This category includes solutions used to span surfaces. Systems may be unidirectional (e.g., beams or ribs) or bidirectional (e.g., spatial trusses or slabs) and typically serve as floor or roof structures.

Linear-Arches

This category includes arched systems composed of single or multiple interconnected arches.

Spatial or Shell

This category includes shell and spatial structures with one or multiple directions of span, designed to cover larger spaces.



(a) Three-point column connection using bifurcations



(b) Vertical sandwich column composed of planar layers

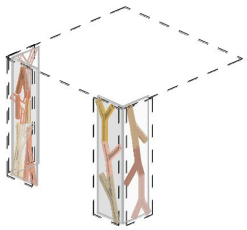

(c) Sandwich column with corner anchoring



(d) Three raw timber columns connected [40]

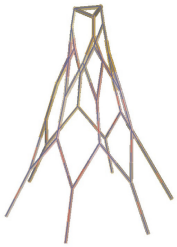

(e) Tower structure [200, 51]

Figure 6.2: Examples of vertical-linear structural systems.

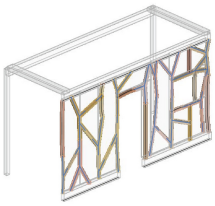

(a) Timber framing system [34]

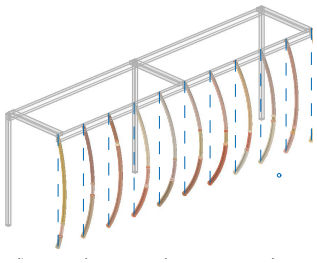

(b) Façade using raw timber as mullions

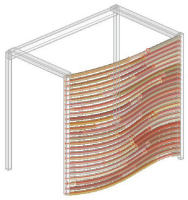

(c) Log-based construction [87]

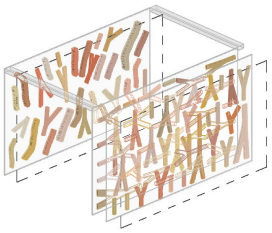

(d) Sandwich panel construction integrating raw timber

Figure 6.3: Examples of vertical-planar systems.

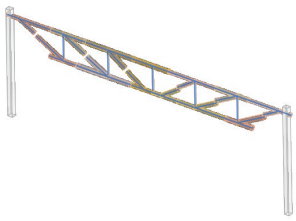

(a) Triangulated truss structure using articulated joints



(b) Vierendeel truss system with moment-resisting joints



(c) Sandwich beam configuration using layered elements

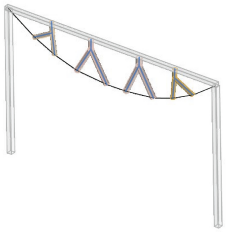

(d) Underspanned beam with a tied tension element

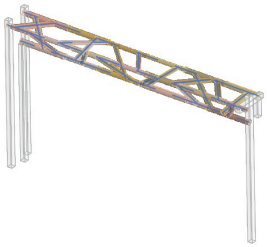

(e) Three-point truss with central bifurcation joint [43, 201]

Figure 6.4: Examples of horizontal-linear structural systems.

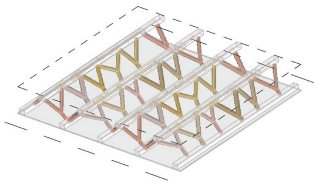

(a) Directional truss with bifurcations [202]

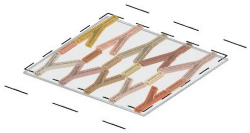

(b) Ribbed slab composed of connected bifurcations

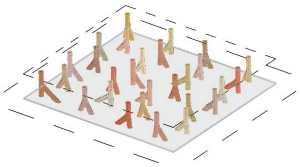

(c) Sandwich slab integrating planar layers and bifurcated elements

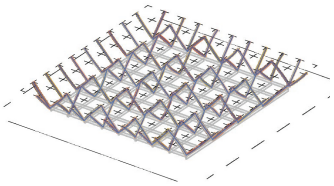

(d) Spatial bar system with curved elements [203]

Figure 6.5: Examples of horizontal-planar systems.



(a) Two-point arch using curved raw timber [204]

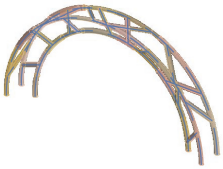

(b) Three-point arch system with bifurcated base elements

Figure 6.6: Examples of linear arch systems.

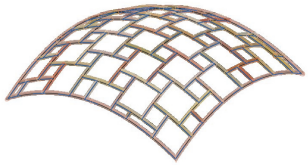

(a) Reticulated shell using interwoven bar elements [42]

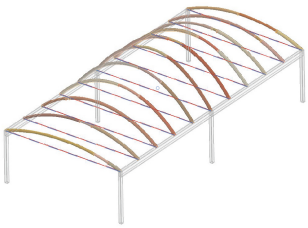

(b) Arched ribbing system for shell curvature

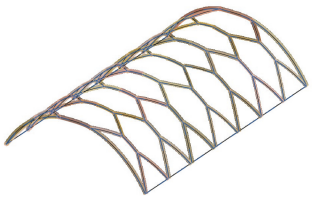

(c) Honeycomb-like vaulted shell with arched modules [65, 46]

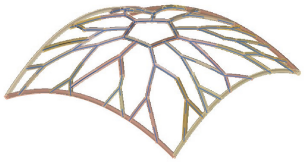

(d) Polar shell with radially distributed elements

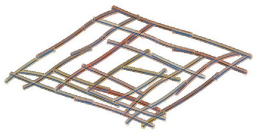

(e) Reciprocal frame shell using interlocked short members [205]

Figure 6.7: Examples of spatial and shell structures.

Off-knot Structures

One of the principal challenges in timber construction has historically been the joining of individual elements [206]. This limitation has led to the widespread use of metal fasteners, which provide the uniformity required for many types of joints that timber alone cannot achieve. Consequently, primary joints—particularly those involving axial intersections—are often executed using metal sheets.

This limitation, however, presents an opportunity: the integration of natural tree bifurcations as off-knot structural elements [180]. Owing to their natural node-like geometry, where three bars intersect, tree bifurcations can function as structural knots. This strategy shifts the structural connections away from the geometric nodes of the system, thereby simplifying structural interpretation and reducing stress concentrations at primary junctions. In this approach, joints and fasteners are positioned away from key structural nodes.

As a result, the overall geometry of the system depends heavily on the natural form of the bifurcations. This necessitates the use of optimization and matching algorithms (see Section 5.2.1) to align these irregular forms with the intended design configuration. This concept is integrated into the construction classification presented.

6.1.2 Scalability, Geometric Constraints, and Cross-Sectional Analysis

The availability of material cross-sections naturally limits the development of structural systems, which in turn determines the final design's possible scale. The investigated geometries indicate that *juvenile timber* suited for building has a clean cross-section diameter D range from 8 to 15 cm. In practice, feasible lengths L for *curved elements* are from 1.50 m, whereas those for *bifurcated elements* are often between 0.80 and 1.20 m. Because of practical and logistic limitations, elements that fall outside of these size limits have not been included. Smaller elements lack structural viability since the expenses of harvesting, drying, and processing are not justified by their small span capacity. Conversely, because of the difficulties involved in carrying, transporting, and felling trees, larger elements are also impracticable.

The key parameters for assessing scalability and feasibility in structural systems are:

- **Cross-Sectional Geometry**: Classification of elements based on shape, bending capacity, and fiber orientation.
- **Structural Load Capacity**: Computational simulations to evaluate moment resistance, axial loads, and overall mechanical performance.
- **Assembly Strategies**: Defining modular principles for integrating elements in large-scale applications.

The presented examples are designed for different span lengths. An initial feasibility assessment is conducted as a preparatory step using basic structural calculations. Following this, the optimization process enables the structural system to be adjusted accordingly.

6.2 Construction Design

This section presents joint typologies developed specifically for the structural integration of naturally grown timber elements. The aim is to address geometric variability and structural performance through custom joinery strategies adapted to irregular morphologies. The joint systems have been developed through iterative design and prototyping processes, considering fabrication constraints and load-bearing performance.

6.2.1 Modeling Joints

Given the layout and the requirements defined by axial, shear, or bending stress conditions, a complementary strategy can be developed to automate the modeling of joinery solutions.

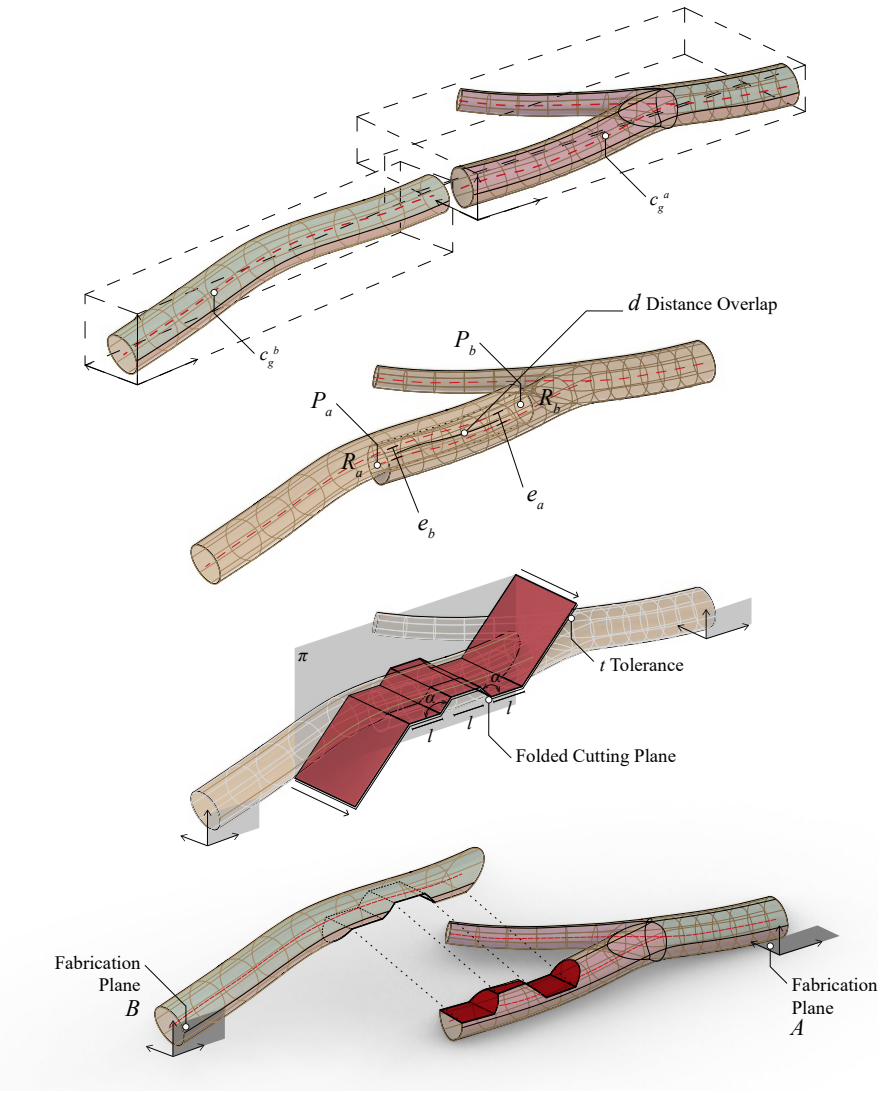

Figure 6.8: Automated joint modeling based on the structural and geometrical constrains.

The procedure begins by determining the static requirements, see Section 5.2.2. Then, the positioning of the timber elements is established, preserving their local coordinate references, and their respective centerline curves c_g are superimposed. This generates a variable eccentricity $e_a \rightarrow e_b$ along the joining length d. These parameters are compared with the end radii R of each element. Next, a plane π is defined, coplanar with the bounding boxes of both members, establishing the perpendicular cutting plane for the joint. To increase the overlap between the elements, a folded cutting plane is defined by a length l and an angle α. Finally, a tolerance parameter t is specified.

The process begins with the structural scheme and its integration into the geometric model, including the centerline curve, associated NURBS surfaces, and bounding box for each element. The position of the structural joint is transferred to the geometric model, where a cutting-plane strategy defines the joining concept.

As illustrated in Figure 6.8, this process is parametrically defined to accommodate two timber elements in an overlapping configuration. The example shows a longitudinal joint, constructed from a series of folded planes to increase the contact surface. Parameters such as D represent the diameter, w denotes the width (fixed to a predefined value), and l lenght and α define the horizontal joining surfaces and their respective angles.

Additionally, modified NURBS geometries are automatically extracted for digital fabrication tasks or for finite element analysis (FEA) to validate the structural performance of the joints. This method can be adapted to various joint types, including longitudinal, butt, splicing, and T-connections, as discussed in the next section.

6.2.2 Connections Catalogue: Custom Joinery for Naturally Grown Timber

To complement the development of digital joint modeling, a catalogue of joinery solutions has been compiled to address the geometric challenges of integrating irregular raw timber. This catalogue introduces a selection of joint strategies specifically tailored to the formal and structural variability of naturally grown timber components.

Each connection type addresses distinct spatial and structural conditions, including a variety of butt joints, splicing strategies, and panel-based assemblies. Figure 6.9 to Figure 6.13 show examples of splicing approaches developed for connecting linear timber elements with irregular geometries.

Butt Joints and Splicing Connections: These connections are designed for longitudinal assembly of timber elements. In the case of naturally grown timber, such joints are adapted to non-parallel surfaces and often include intermediate connectors such as metal rings or dowels to ensure structural alignment and load transfer.

Corner and T-Joints: enable orthogonal assembly of bifurcated or branched elements. Their geometry is adjusted to the natural curvature of the material and typically includes customized milling or adjustable fixtures to achieve precise fits in 3D space.

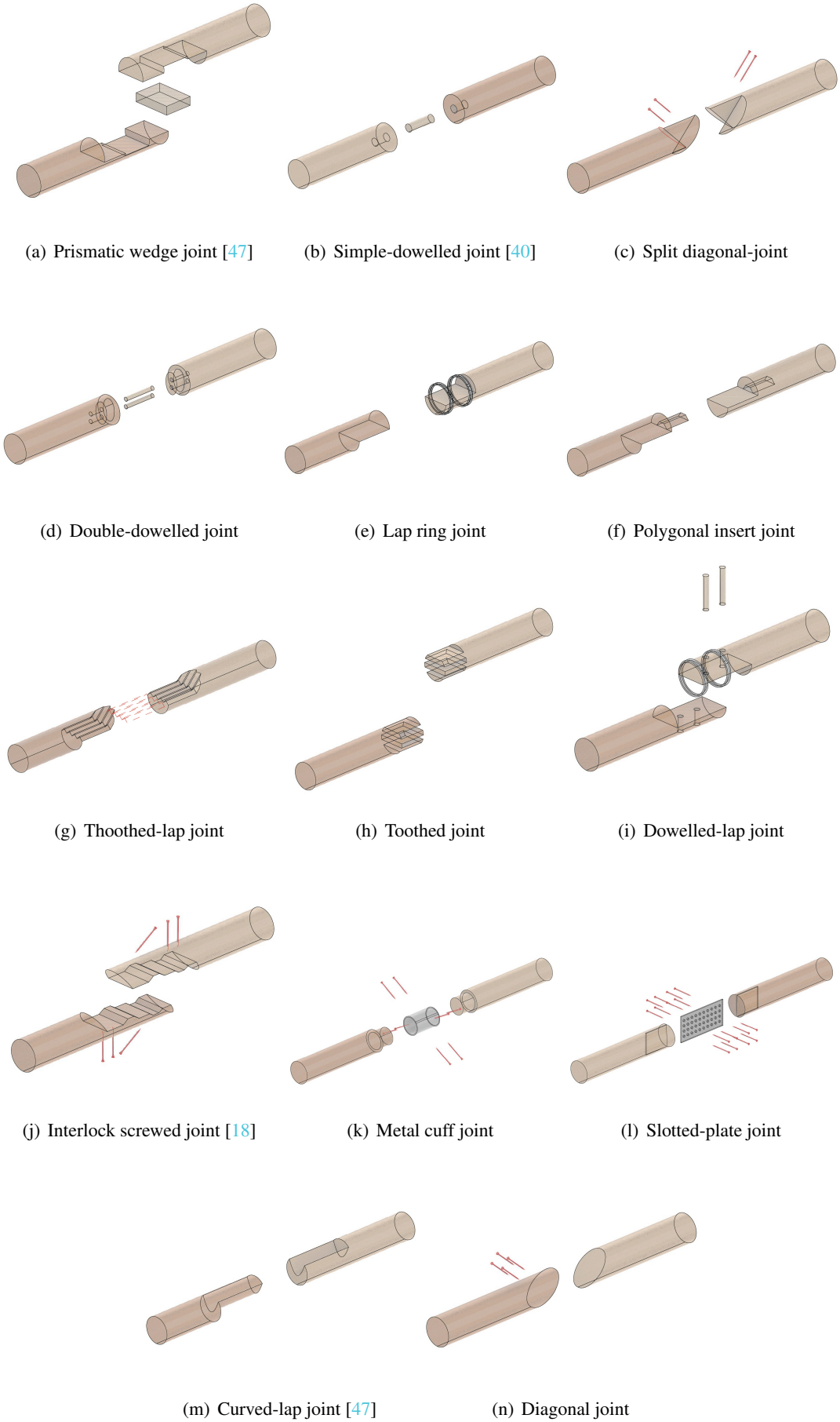

(a) Prismatic wedge joint [47] (b) Simple-dowelled joint [40] (c) Split diagonal-joint

(d) Double-dowelled joint (e) Lap ring joint (f) Polygonal insert joint

(g) Thoothed-lap joint (h) Toothed joint (i) Dowelled-lap joint

(j) Interlock screwed joint [18] (k) Metal cuff joint (l) Slotted-plate joint

(m) Curved-lap joint [47] (n) Diagonal joint

Figure 6.9: Splicing joint types for longitudinal timber connections.

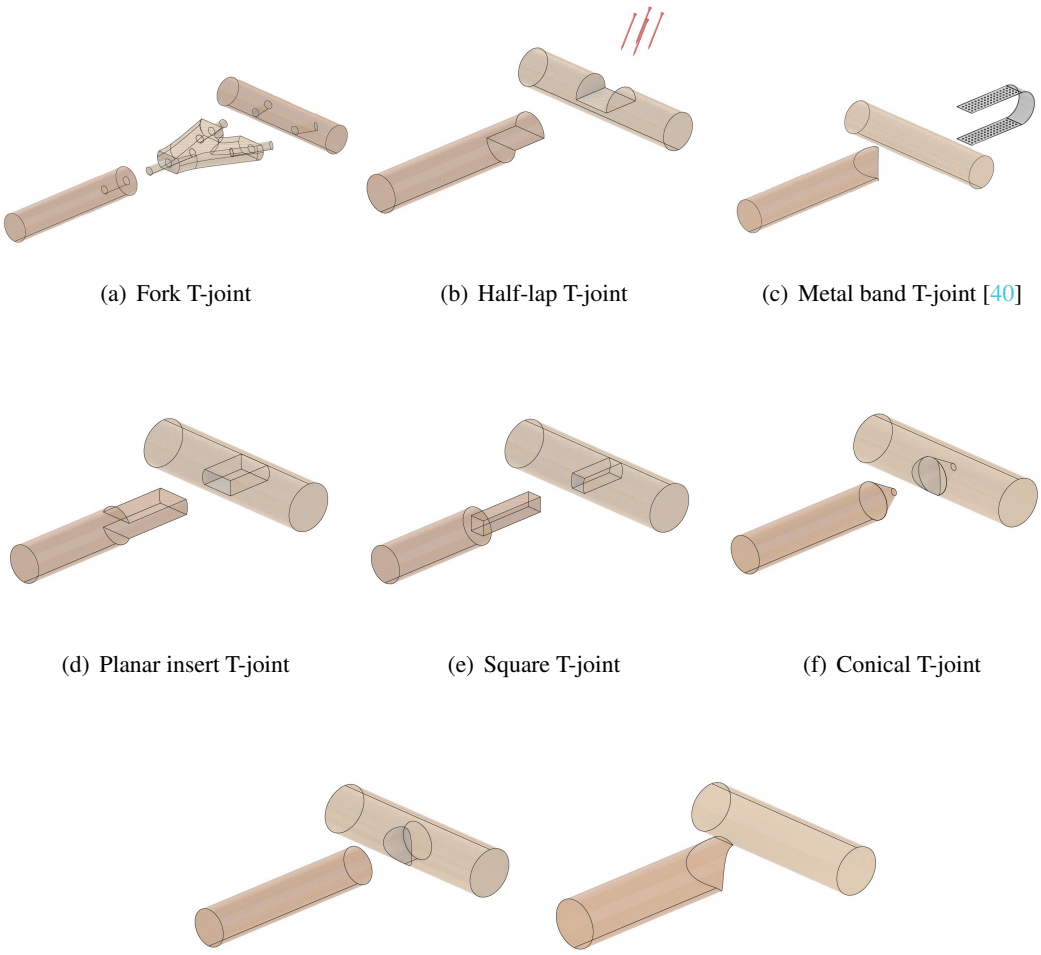

(a) Fork T-joint (b) Half-lap T-joint (c) Metal band T-joint [40]

(d) Planar insert T-joint (e) Square T-joint (f) Conical T-joint

(g) Insert T-joint (h) Simple T-joint

Figure 6.10: Corner and T-joint configurations for orthogonal timber connections.

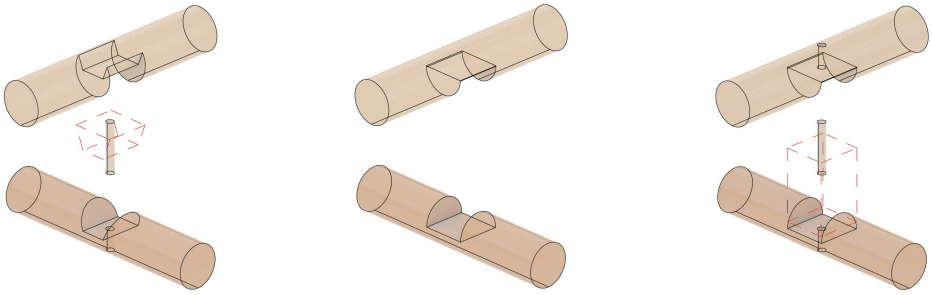

(a) Polygonal-dowelled cross joint [43] (b) Simple cross joint (c) Simple dowelled cross joint [207]

Figure 6.11: Cross joints for intersecting timber elements.

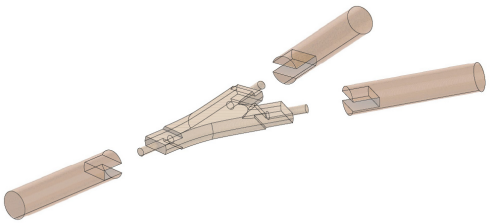

(a) 3-fork joint

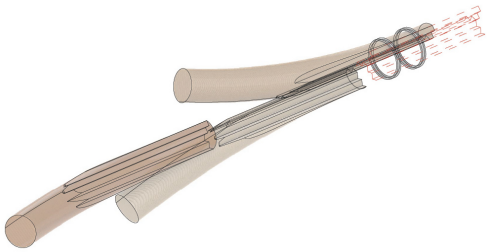

(b) 3-thoothed joint [208]

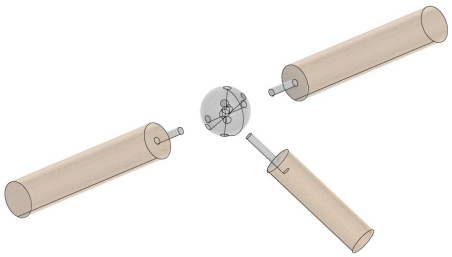

(c) Mero-type joint

Figure 6.12: Additional and experimental joints for specific configurations.

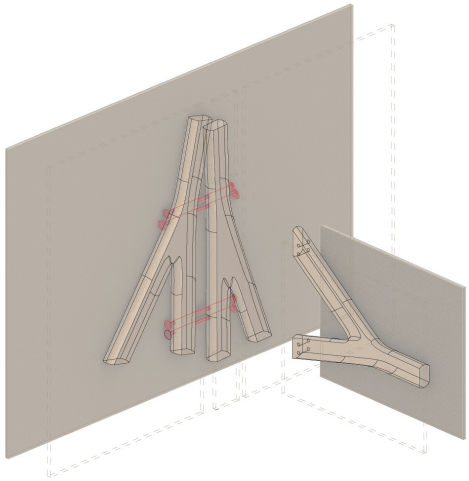

(a) Bolted sandwich-sandwich joint

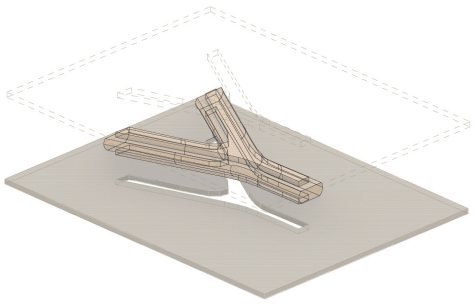

(b) Notched-sandwich joint

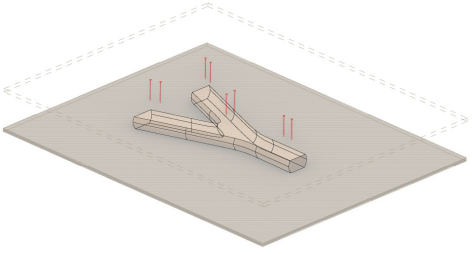

(c) Sandwich screwed joint

Figure 6.13: Joinery types for sandwich panel assemblies.

6.2.3 Design of Structural LRS Panels

This section further develops the thesis proposal to apply raw timber in the form of Leafy Raw Timber Sandwich Panels (LRS) (from the German: Laubrohholz Sandwichplatten). This is presented as an alternative design to standardized Cross-Laminated Timber (CLT) systems, proposing a transition towards the use of hardwoods as the core structural layer in sandwich-type panels. The concept aims to systematically integrate material circularity into a standardizable construction element, with various patterns depending on the type of load cases.

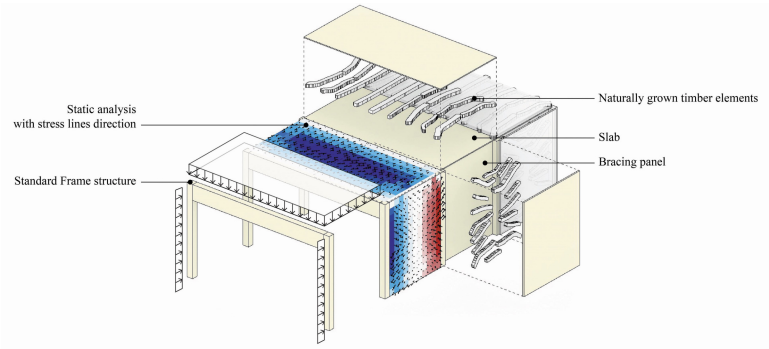

Figure 6.14: Example of the use of raw wood in structural panels.

Potential

The reduction in weight and the use of conifer wood present both opportunity and potential. The circular application of native hardwoods is a key aspect of this approach.

As a comparative approach, Fig. 6.15 illustrates a solid timber structure built with CLT alongside an alternative system using two-layer LRS panels. The raw timber elements in the LRS system are arranged crosswise to enhance load distribution and structural uniformity. Both configurations are designed to achieve similar structural performance and deformation behavior, with comparable cross-sectional properties and moments of inertia.

From this basic comparison, the following data can be derived: in a configuration with LRS panels, the volume of solid wood is drastically reduced. A basic cabin design (see Fig. 6.15) results in a solid wood volume of up to $5\,\mathrm{m}^3$. Based on tree growth analysis data, the crown of a single tree can yield approximately $4\,\mathrm{m}^3$ of raw wood. This demonstrates significant application potential. Additionally, this construction method can be combined with other types of recycled wood boards, resulting in a lower overall weight.

As a design application, a cabin construction is proposed to demonstrate the structural integration. It shows that this system can be combined with other elements, including finishes, flooring, façades, openings, and more—forming a complete structural system.

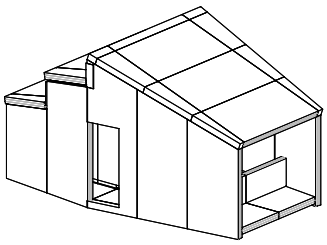

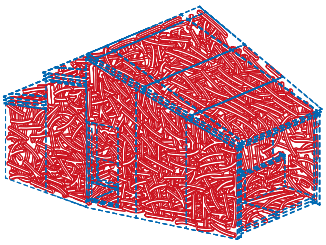

	Concept of a cabin with standarized solid CLT	**Concept of a cabin with structural panels in raw wood**
Material Origin:	Industrial laminated pine (non-native)	Local forest hardwood + OSB from recycled timber
Boards Material:	Cross-Laminated Timber (CLT, 18 cm)	3x OSB (12 mm) + 2x Raw hardwood core (70 mm)
Boards Area:	112.36 m²	462 m² (OSB)
Timber Volume:	20.23 m³	5.2 m³ (Raw hardwood)
Total Branch Length:	–	662 m
Total Weight:	10,112 kg	6,118 kg (OSB + hardwood)
Weight per m² built:	404 kg/m²	244 kg/m²

Figure 6.15: Comparison CLT and LRS Panels.

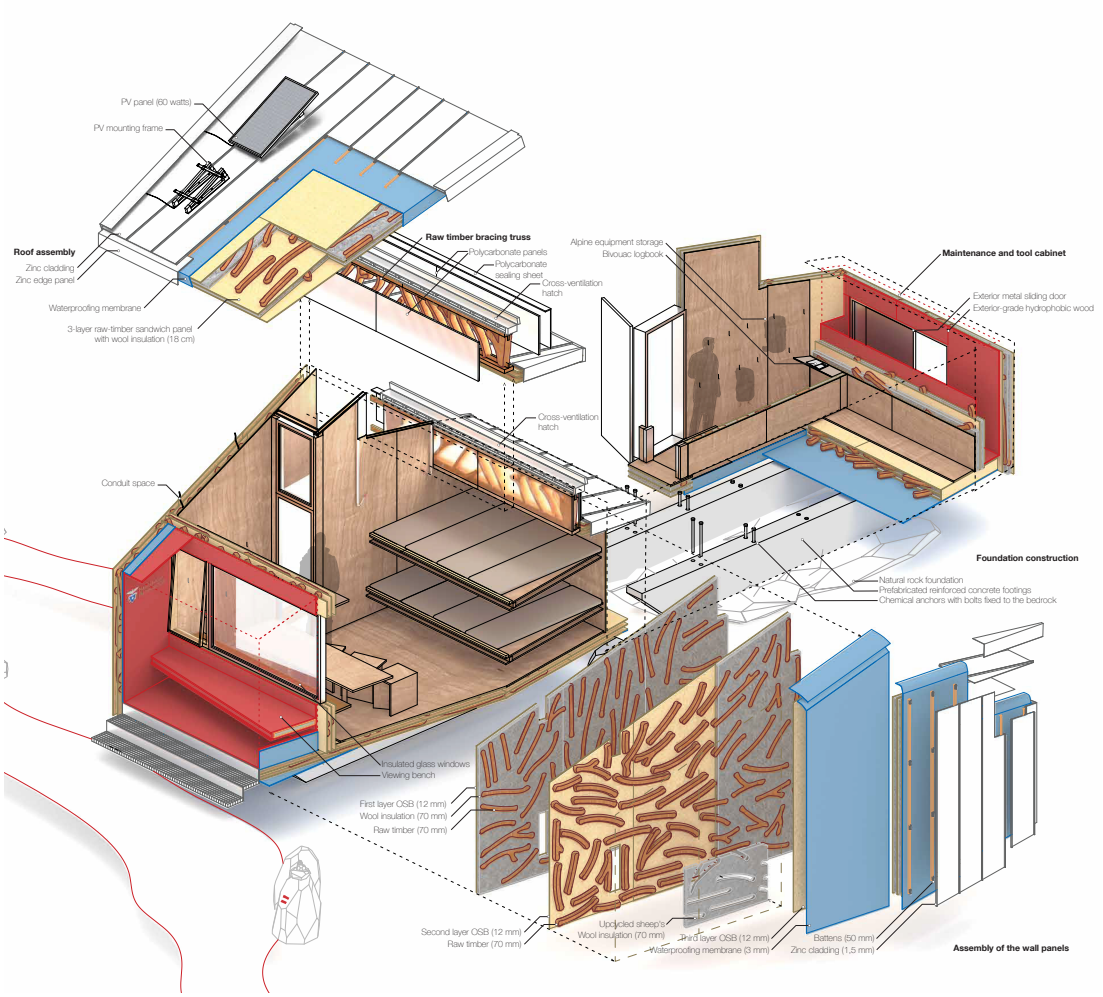

Figure 6.16: Assembly of a timber cabin based on LRS structural panels.

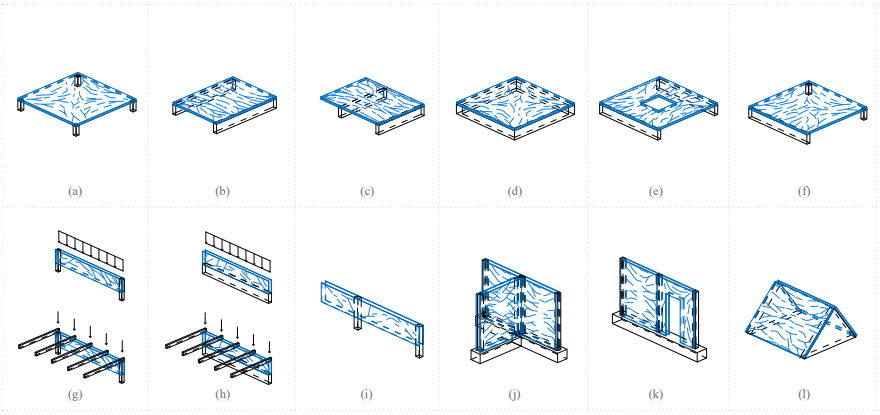

Figure 6.17: Construction methods catalog.

Construction Design

The construction design of these sandwich panels is studied across different structural scenarios, including single-axis plates, biaxial elements, cantilever integrations, and wall or bracing components. These configurations are illustrated in Figure 6.17, which outlines the possible element types.

The application of fully threaded screws is proposed for assembling the panel system. Due to their load-bearing capacity and versatility, they enable a fast and reversible method to join the top and bottom layers of the sandwich panel with the timber core, see Fig. 6.18(a).

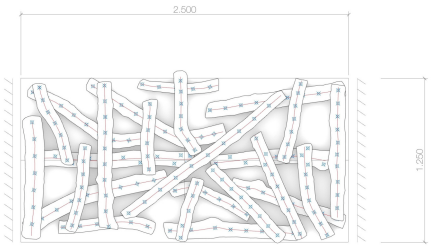

(a) Module (b) 2.40 m × 1.20 m



(b) Slab. Module (b) 2.40 m × 1.20 m



(c) Bending beam. Module (g) 3.60 m × 0.40 m

Figure 6.18: Built examples of modular prototypes in oak, birch, and birch with OSB, at scale 1:1, based on Fig. 6.17.

6.2.4 Fabrication and Assembly Techniques

Construction Development

This phase integrates structural design and optimization with the fabrication of custom connections. Once matching elements and joint positions are identified, detailed construction development is carried out, including geometry verification and preparation for fabrication. Figure 6.19 illustrates this process toward connection detailing. The development particularly focuses on the versatile use of fully threaded screws, as demonstrated in previous research, both for timber reinforcement and for reinforcement techniques using screws [209, 210].

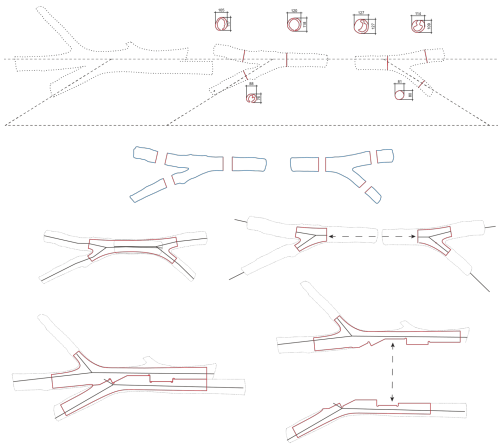

Figure 6.19: Layouting bar-type structure with optimized joint position to raw timber geometries.

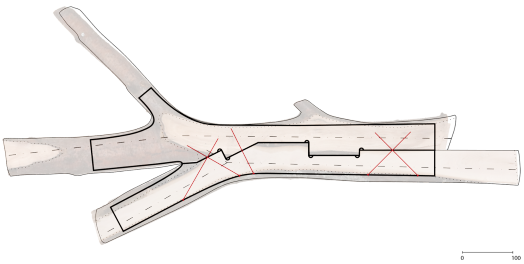

(a) Detail development of a bending-resistant connection from two elements of maple and beech in a hybrid bifurcation using fully threaded screws. Scale in cm.

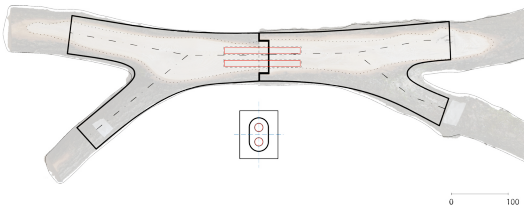

(b) Detail of a butt joint with two oak elements with inserted dowel. Scale in cm.

Figure 6.20: Transfer of structural design to construction details, showing hybrid connections for bifurcated nodes in a Vierendeel girder.

6.3 Case Studies and Built Demonstrations

The concepts discussed throughout this dissertation have been tested and validated through full-scale (1:1) built demonstrations. This section presents the description and development of two architectural applications: one based on bar-type raw timber elements—The Growing Bridge, built in 2023—and the other, a sandwich-type integration of raw timber into a pavilion constructed for the Pop-Up Campus Expo in 2022.

6.3.1 Case Study Design 1: Forest Pedestrian Bridge

Description

As a demonstration of circular construction using locally sourced raw timber, a pedestrian bridge was designed and built in a forest environment using material harvested from that very forest. The structure was conceived as a proof of concept integrating various species of timber, which were analyzed and fabricated to form a composite structural system. Drawing on the structural strategies previously examined in Section 5.2.2 and the analogical framework for bar-type assemblies in Fig. 5.11, a system resembling a Vierendeel truss was proposed. This design features off-knot rigid elements and semi-articulated joints, composed of tree branches.

The project was driven by an analysis of tree branch growth angles in the local forest of Aachen (Fig.3.14(a) and Fig.3.14). According to the geometric analysis detailed in Section 3.4.2, the most common branching angles (α) range from 22° to 54°. The resulting polygonal topology is designed to be modular and repeatable, based on geometric relationships among angles. Hence the name Growing Bridge, which reflects the use of branching patterns as a design principle. This angular logic is applied both longitudinally and transversely, forming square polygon modules where the four internal angles sum to approximately 360°. This configuration allows for planar fabrication and compatibility with 3D scanning and 2.5-axis CNC milling workflows.

For this first prototype, the topology was simplified to four primary nodes (16 total), each defined by symmetry and contextual constraints. Nodes 1–4, with respective angles of 34°, 54°, 22°, and 28° (see Fig. 6.22), were selected based on site-specific design studies. Timber was collected in spring 2022 from species including hornbeam, beech, oak, and birch.



Figure 6.21: Collecting raw material from a tree crown in the forest, followed by documentation.

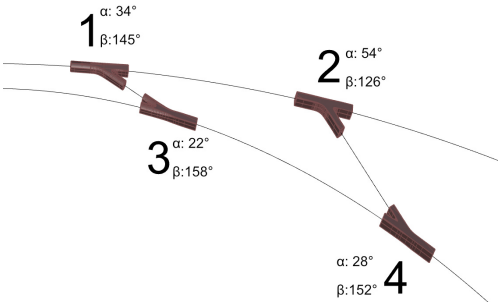

(a) Definition of main angles at the nodes

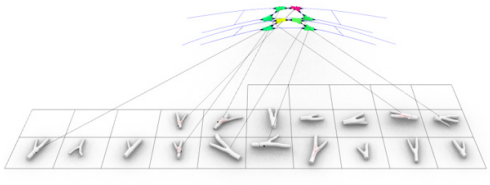

(b) Matching algorithm (see Section 5.2.1)



(c) Rendering of the site-specific structure

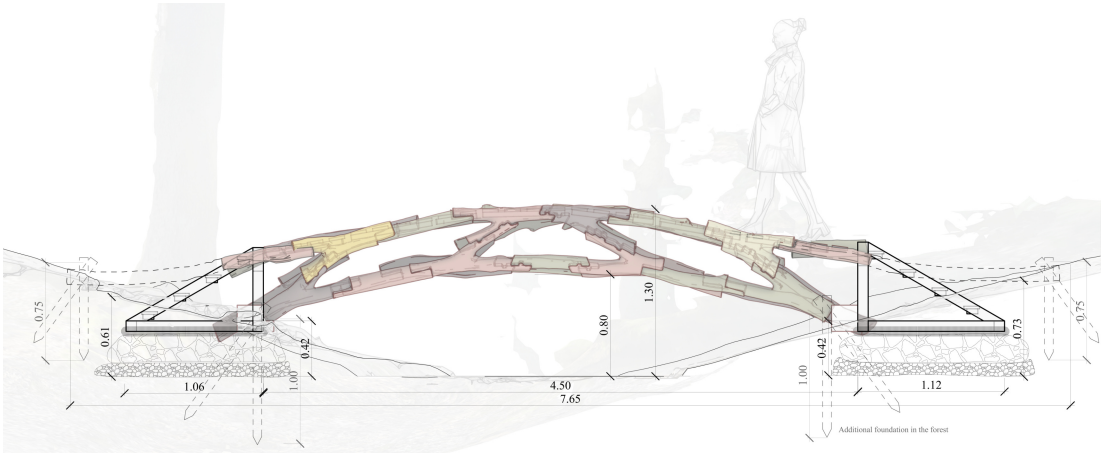

(d) Front view of the final structure

Figure 6.22: Structure design process based on raw material.

Site-Specific Bridge Design

In parallel with the structural development, a site study was conducted to define environmental and spatial constraints. A small stream located near the timber collection site was chosen as the test location. The stream—located at coordinates 50.683672, 6.157928—is a tributary of the Inde River, within the Eifel National Park. The waterway spans between $2\,\mathrm{m}$ and $6\,\mathrm{m}$ in width. A terrestrial laser scan was used to generate a 3D model of the terrain (see Fig. 6.22), which informed the structural span and determined a maximum clearance height of $1.20\,\mathrm{m}$.

The resulting structural system is a curved-arch Vierendeel-like truss, later adapted to accommodate the geometric variability of the collected timber. An initial analysis (Fig. 3.14) revealed that fork elements had segment lengths ranging from $20\,\mathrm{cm}$ to $60\,\mathrm{cm}$, with angle deviations between $16°$ and $46°$. These measurements were used to calculate average values of α and β, which guided the structural configuration. In the case of curved elements, length variations ranged from $70\,\mathrm{cm}$ to $170\,\mathrm{cm}$, with average angular deviations of $18°$ and linear deviations up to $10\,\mathrm{cm}$.

Material Matching for Circular Design

The methodology presented in Section 5.2.1 —adapted from the literature [68, 22]— was used to match the target geometry of the bridge with the library of timber specimens (see Fig. 3.14). Initially, the method achieved a 98% match with the collected elements. Later, during the structural design phase, the geometry was slightly modified in 3D. Heavier and stronger wood species, such as oak and birch, were intuitively placed around the supports, while lighter or thinner woods, such as hornbeam and beech, were placed toward the center of the bridge. The algorithm informed this modification process and provided feedback on the match score, resulting in an approximate 80% match. In this project, it was important to ensure consistency in the grain direction of all components, which required adjusting deviations in the structural topology to fit the specific specimen geometry at each node.

Static Analysis: Bar-Type Structural Analysis

The structural analysis was initially conducted using a bar-type analysis system (see Fig. 6.23). The structural model consists of 28 bars with rigid nodes, employing the off-knot construction method optimized in Section 5.2.2. In this construction scheme, the nodes are considered rigid due to the bending capacity of the timber bifurcations. This method is distinctive in that structural joints are shifted to the bars themselves. These bar joints are modeled as fixed (spring-like), and their specific locations are optimized to minimize bending moments. Subsequently, the joints are physically realized using Gerber-like connections.

The load cases (LC) studied include dead weight, a constant vertical load of $2\,\mathrm{kN\,m^{-1}}$ (LC1), and a variable *movable* load of $2\,\mathrm{kN\,m^{-1}}$ applied at $45°$ (LC2). In the next step, diagrams for

bending moments, shear forces, and normal stresses are calculated for each load case individually, as well as for all positions of the movable load in combination. The diagrams in Fig. 6.23 illustrate one such combination.

The normal stress analysis confirms that the main loads are compressive, thereby validating the use of compression joints, with compressive forces reaching up to $6.7\,\mathrm{kN}$ at the supports. The shear force diagram supports the joint design and determines the minimum timber section required, which is approximately $8\,\mathrm{cm}$ in the thinnest elements. The moment diagram is analyzed to evaluate the magnitude of bending at the joints, which reaches up to $0.3\,\mathrm{kN\,m}$ at the supports under load case 2. To ensure proper load transfer, fully threaded screws are employed in a triangular configuration at the joint areas.

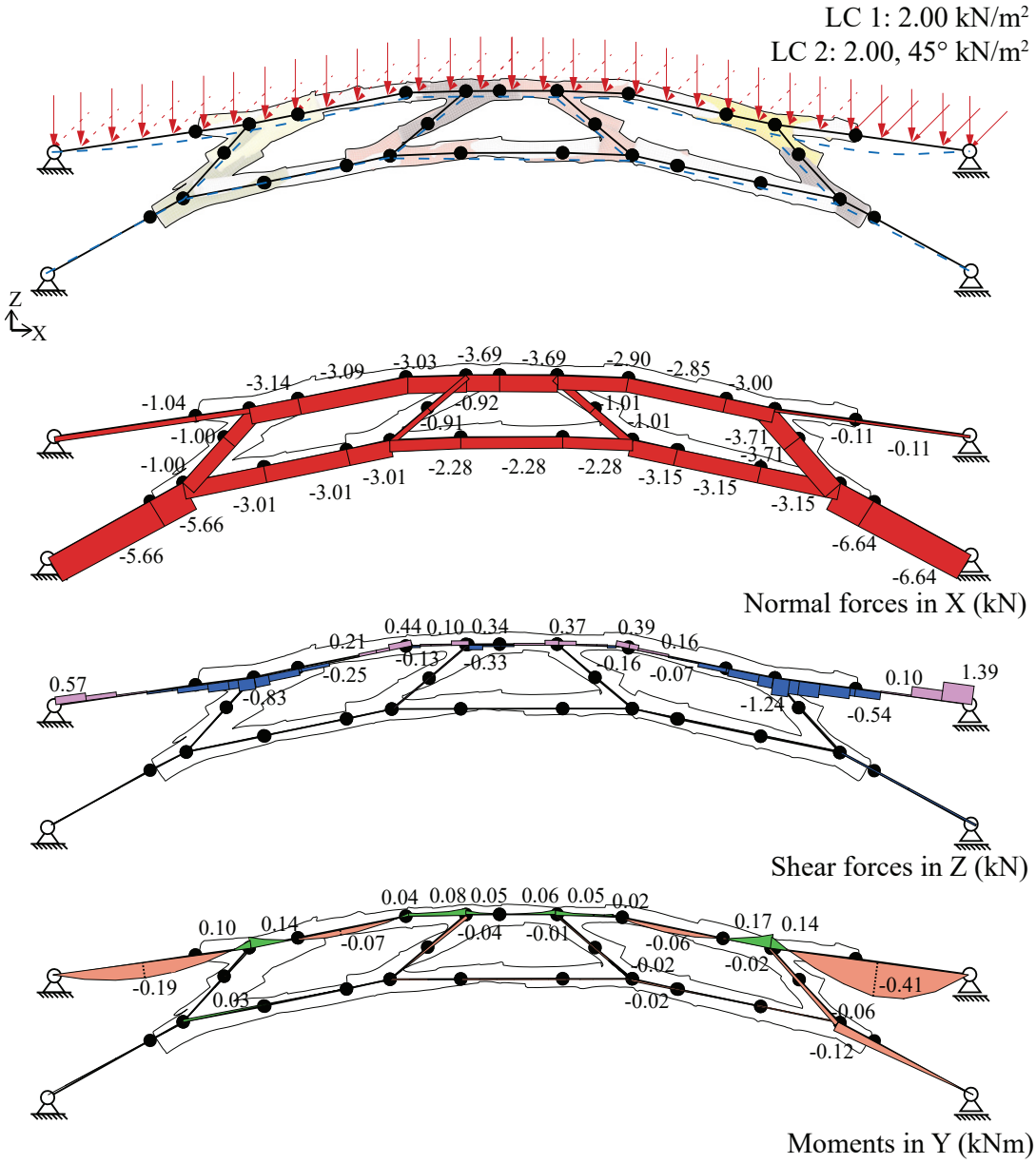

Figure 6.23: (LC) 1 and 2 with deformation, and moment, shear and normal forces diagrams.

The structural scheme is a curved arch where the top and bottom beams are not in the same plane, opening the structure toward the supports. This scheme is similar to the Vierendeel scheme in that the tree elements are resistant to bending. The curvature and opening of the structure, in addition to the bracing plates (also used as flooring), helps to resist horizontal loads that are not part of the static analysis. In this construction, all joints are bending resistant, but the degree of bending capacity varies depending on the load and the semi-rigid connection with Gerber-like joints and screws (see in Fig. 6.29). This however is not a problem and is taken into account by the oversized wooden elements.

Isogeometric Analysis Naturally curved timber elements are first 3D scanned and digitally converted into precise surface models. These models are then used in a special simulation method—called scaled-boundary isogeometric analysis (SBIGA) [211]—which analyzes the structural behavior of complex shapes using only their outer surfaces. For long and curved elements like tree branches, a more advanced version, GSBIGA [198], improves accuracy by focusing the analysis around a central line inside the wood. This approach is especially useful for modeling branch forks, where different curved parts connect. As shown in Fig. 6.24, the simulation results match the structural loads expected from simplified models. [212]

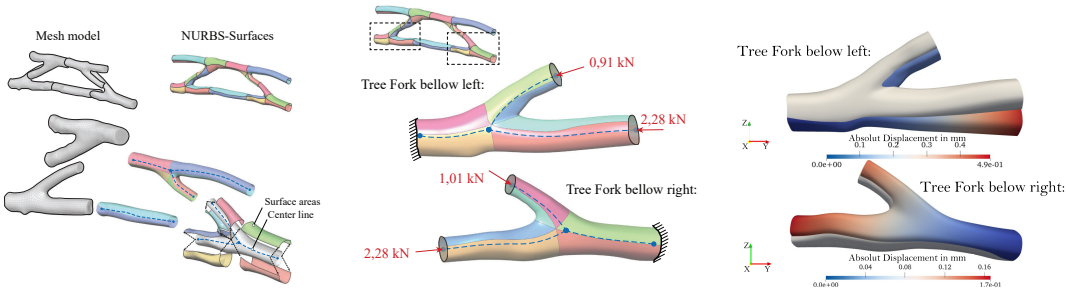

(a) Processing toward the NURBS model (b) Bifurcation model with loads and boundaries (c) Deformation plots vs. original geometry

Figure 6.24: Static analysis with SBIGA, extracted from [198].

Design to Fabrication

The construction design is directly influenced by the manufacturing process. The three-dimensional geometries of the scanned timber elements are automatically positioned at pre-defined locations using orientation methods derived from static analysis. Structural plots identifying zones with minimal bending moments and shear forces guide the segmentation of timber elements and determine joint positions.

Joint design follows classical carpentry principles, such as Gerber-like joints. Since axial stresses are primarily compressive, joints are shaped to match the structure's geometry, allowing components to slide into place during assembly. These joints are parametrically modeled (see Fig. 6.25(b)) and subsequently used in the fabrication process by exporting the NURBS volumes along with their defined bounding boxes for orientation.

Fully threaded screws are used to ensure joint stability and to counteract horizontal loads. The

two symmetrical parts of the bridge are later connected with planks for flooring and stairs, which also served as temporary foundations during initial assembly and testing (see Fig. 6.26).

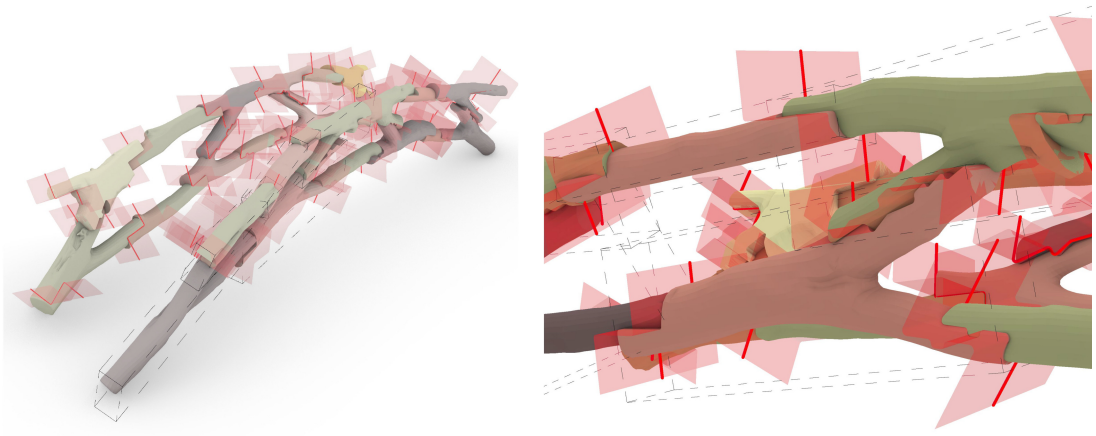

(a) Overall construction view with joint alignment and bounding boxes.

(b) Detailed view of a bifurcation with an adapted parametric joint.

Figure 6.25: Design-to-fabrication strategy with adapted joint detailing.

Fabrication process

The structural scheme determines the location of the joints, taking into account the final position of the timber elements. An algorithm is then used to customize the joint design for each element based on the thickness of the two elements being joined and the deviation of each element's geometric center-line from the structural design. This joint could potentially benefit from a simplified manufacturing process by using a CNC milling machine to cut the flat polygons in two axes. As shown in Fig. 6.28, the cutting surfaces that define the joint are highlighted in red. Prior to fabrication, each element is planed on one side using a planer, and positioned on a board. The final geometry is calibrated to determine the exact position of the timber element with the board. This step allows for precise placement on the CNC. The next step is machining, which cuts the joints with precision (see figure 6.29). The assembly process was completed within a few hours by clamping the elements together, while drilling and screwing them together. This method proved effective in achieving a strong and reliable final structure.

CAD was carried out in Rhinoceros 7.0 [71], automated with Grasshopper, and static calculation with Karamba 2022 [193]. Milling operations were carried out with a 3 axis CNC, with a 180mm lock case end mill, programmed with AlphaCAM 2022 [213].

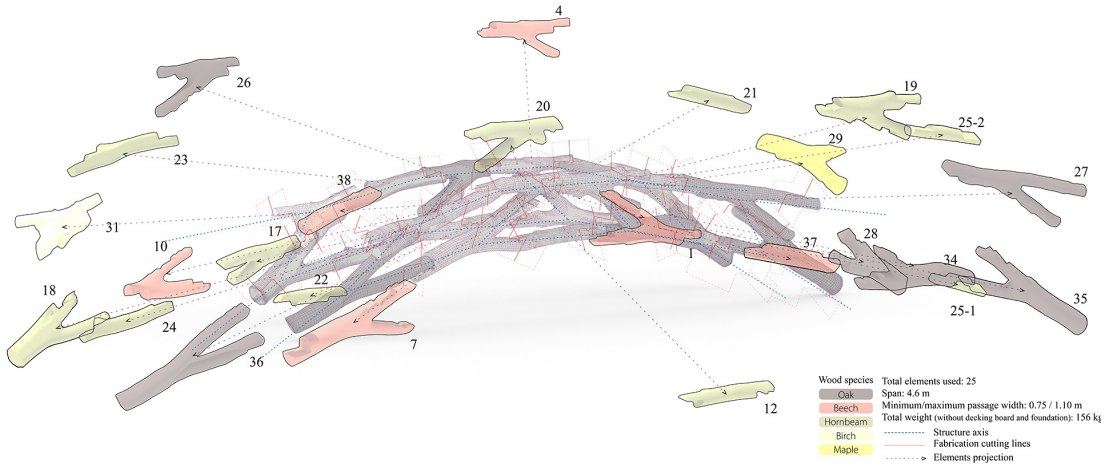

(a) Exploded axonometric view of the construction design, with different tree species in color

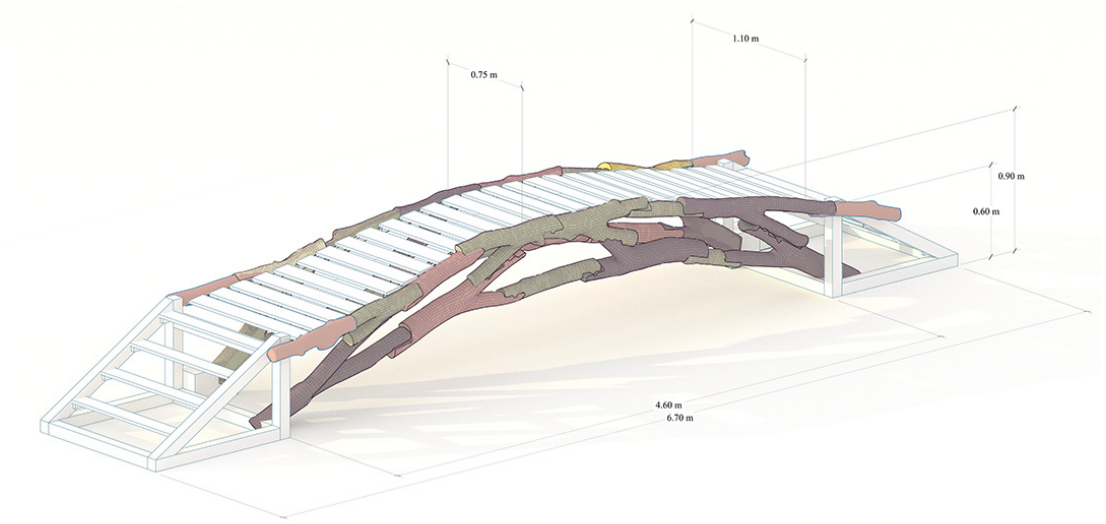

(b) Final construction

Figure 6.26: Construction diagrams of the Growing Bridge.

Installation

The timber bridge case study concludes with its public exhibition in Mausbach (Stolberg), following an initial display in the inner courtyard of the Faculty of Architecture at RWTH Aachen University (Fig. 6.30). The bridge is now permanently installed in Mausbach and serves as an ongoing case study for monitoring and experimentation with this construction system, as the timber has not been chemically treated. The structure has been inspected every 4–6 months, and the necessary maintenance has been carried out, primarily on the stair treads.

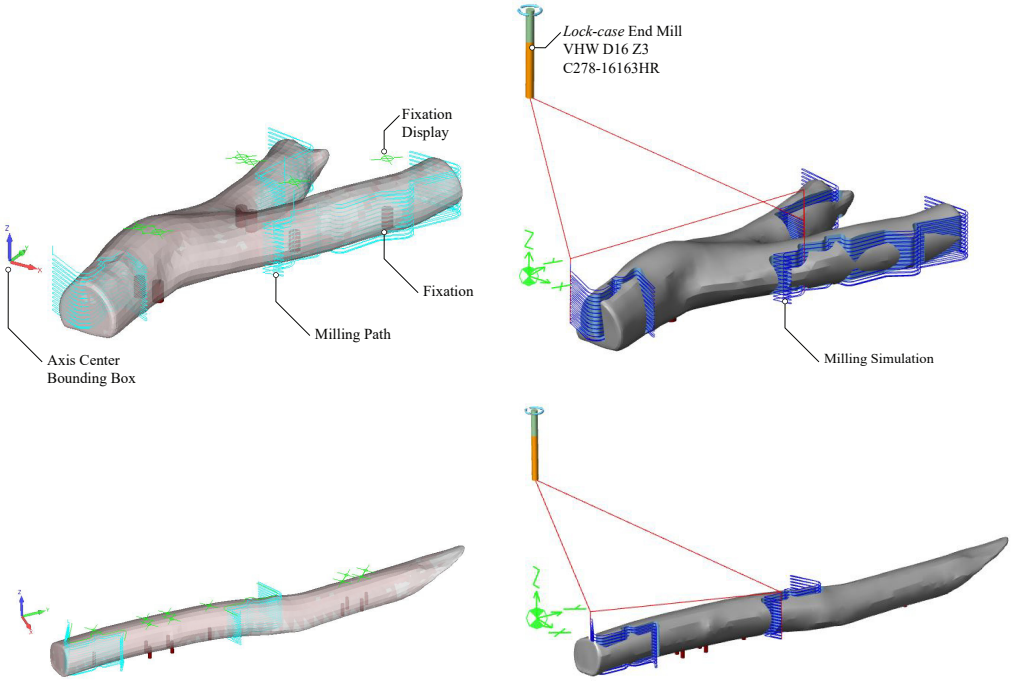

Figure 6.27: Fabrication preview.

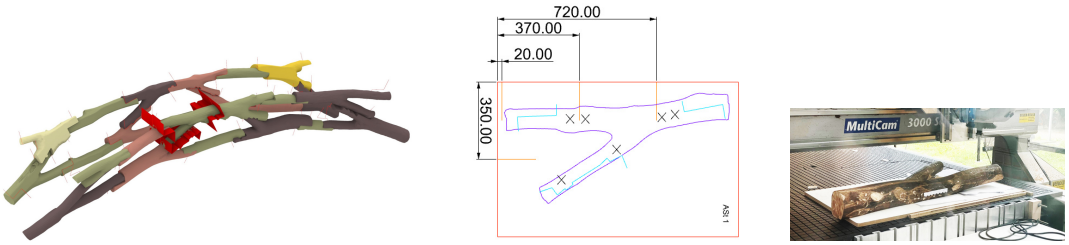

(a) Joint design automatization (b) CNC programming (c) CNC milling operation

Figure 6.28: Design to fabrication process.



(a) Form-fitting oak element (b) Interlocking joint (c) Fastening with fully threaded screws

Figure 6.29: Resulting fabrication of the interlocking joints for the off-knot connection.

The main structural system remains in excellent condition, and no significant structural changes have been observed since the year of installation. A detailed view of the current condition of the bridge in November 2025 is shown in Fig. 6.31.

The project illustrates how timber construction can adapt to locally sourced raw materials, emphasizing the importance of resource efficiency and environmentally responsible building practices. Employing naturally shaped timber highlights the feasibility of site-specific material sourcing, aligning with current trends in ecological construction and environmental protection.

Nevertheless, the morphological variability of natural timber elements demands individualized design and fabrication strategies. Since no two elements are identical, standardization remains a challenge. To address this, early-stage selection at the source—directly from the tree—is advised, focusing on the identification and pre-selection of geometrically appropriate components. This approach supports the creation of a digital timber geometry library, enabling efficient shape classification and optimized integration in structural design.



(a) Front detail view (b) Full bridge view

Figure 6.30: Final assembly showcasing the pedestrian bridge at its mid-term exhibition.



Figure 6.31: Detailed view of the Growing Bridge in Mausbach in November 2025.

6.3.2 Case Study 2: Sandwich Panel Application — The ReGrowth Pavilion

The integration of raw timber into sandwich panels has been proposed as a viable strategy to partially standardize construction processes. This approach facilitates the use of irregular materials within simplified structural systems, expanding the applicability of naturally grown timber in contemporary architecture.

To demonstrate this potential, a full-scale (1:1) prototype—the ReGrowth Pavilion—was developed as a circular structure incorporating naturally shaped timber into a panelized assembly.

The project investigates the use of irregular timber components in flat timber systems such as slabs, ceilings, and walls. Its primary objective is to assess how the inherent growth patterns of naturally grown timber can be integrated into sandwich panel construction, while also evaluating alternative digital and manual fabrication strategies.

The methodology is structured in two main phases. First, the geometry of the raw material is captured using image-based scanning and systematically cataloged. Second, a design workflow is implemented to parametrize stress-aligned reference panels. By aligning the centerlines of the irregular timber elements with precomputed stress trajectories, the system enables their integration into the core layer of sandwich panels.

ReGrowth Pavilion Description

As part of the *Zukunft Bau Pop-up Campus* exhibition, a pavilion was designed as a canopy to demonstrate the practical application of sandwich panels incorporating naturally grown timber, see Fig. 6.32. A total of 36 timber elements—sourced from the Aachen Forest—were utilized. These elements had previously been scanned, segmented, and planed (see Section 3.5.2).

The construction system consists of two outer layers of three-ply pine boards, each with a thickness of $16\,\mathrm{mm}$. The structural core comprises curved and bifurcated raw timber elements planed to a uniform thickness of $55\,\mathrm{mm}$, resulting in a total panel thickness of $87\,\mathrm{mm}$, see the assembly in Fig. 6.33. The panels are structurally supported by two V-shaped frames, each assembled from additional bifurcated timber components.

To facilitate transport and assembly, the panel system was subdivided into six modular segments. These segments were joined using mechanical fasteners, allowing for repeated disassembly and reinstallation.

For the purposes of this case study, structural performance was evaluated through static load-case analysis based on the intended canopy configuration. However, for the exhibition in September 2022, a modified layout was implemented to suit curatorial and spatial constraints. In this arrangement, one half of the panel was used as a canopy, while the other was repurposed as a horizontal surface, functioning as a table. This configuration exposed the internal layers of the panel, providing insight into the assembly process and construction detailing.

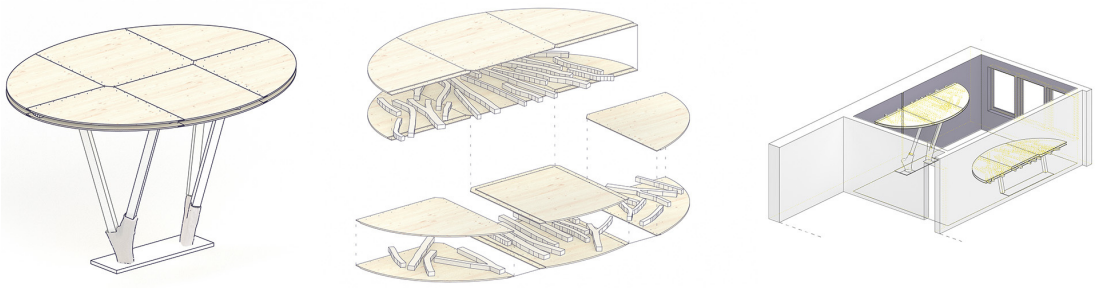

Figure 6.32: Design of the ReGrowth Pavilion.

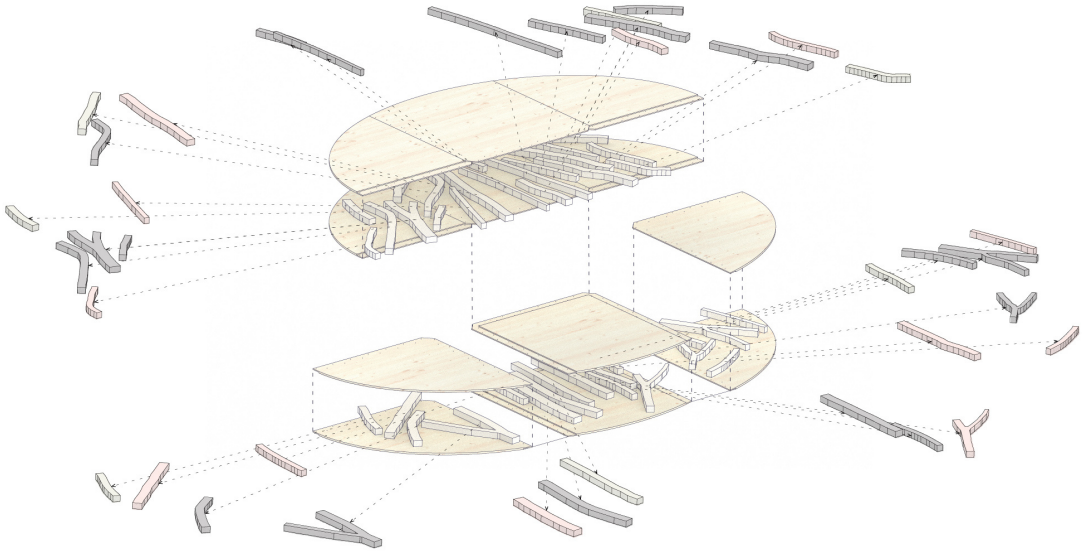

Figure 6.33: Assembly with the timber elements.

Structural Analysis and Design

The analysis process begins with a reference load-case setup of the elliptical panel from the case study. The simulation (see Fig. 6.35) reveals the direction of stress and moment lines, which allows for the assisted distribution of target curves. This provides the vector field $\vec{M}$, with the populated P_m points, c_t are generated. As an informative illustration, a range of colours (red-black) shows the proximity to higher moment values of the reference panel. This process is carried out iteratively, with some minor manual positioning assignments due to observations of results. Especially, shear calculations observed in the simulation suggest extra timber elements on the perimeter and the supports. To address the presence of multiple local directions in $\vec{M}$, it has been suggested that supplementary timber elements could be added to reinforce the required areas, especially with timber bifurcations.

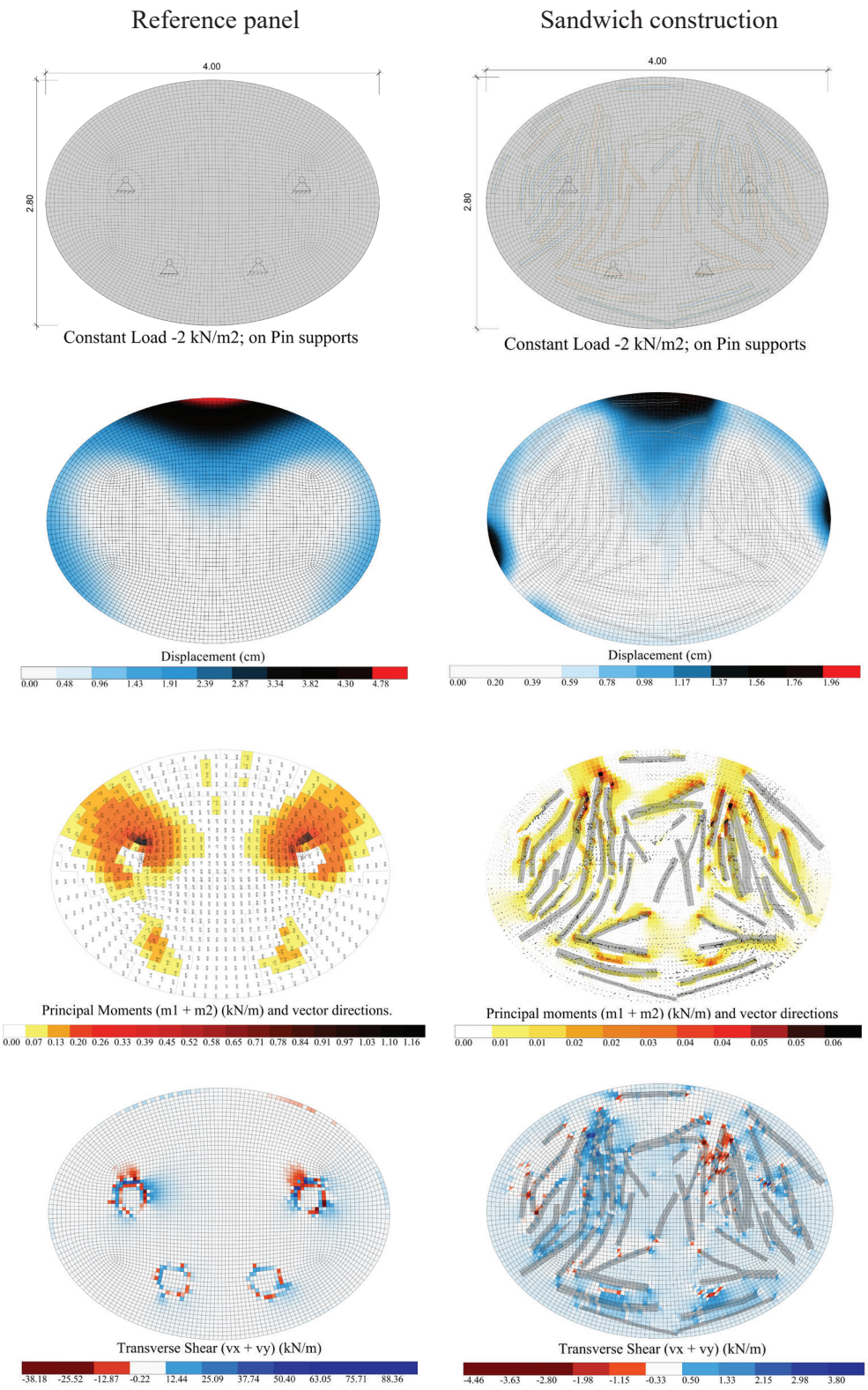

Figure 6.34: Static calculation: (Left) Reference panels with deformation, moment calculation, shear stresses. (Right) Resulting sandwich panels with deformation, moment calculation and shear stresses.

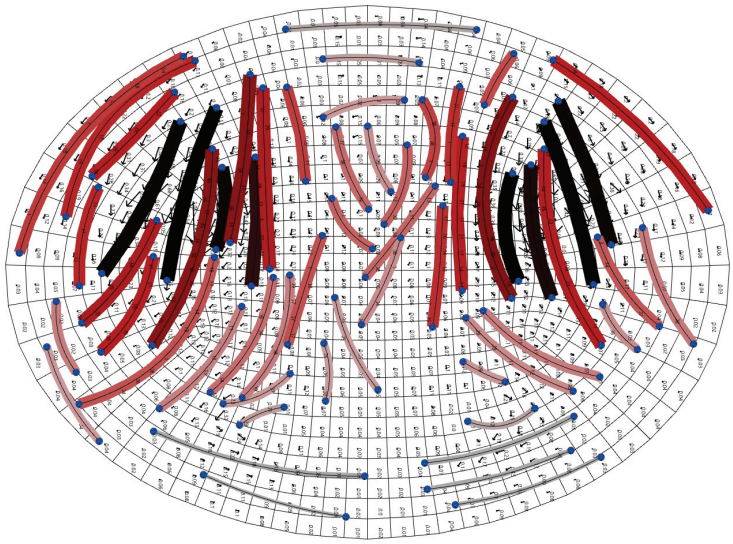

Populate points P_m for building c_t curves in vector field M

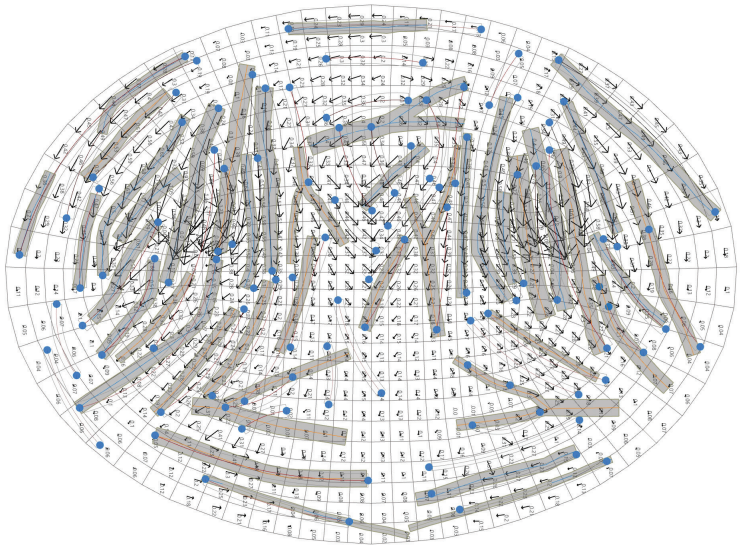

Positioning c_g curves according c_t

Figure 6.35: Overlap timber elements following stress directions: Target curves c_t generated from the vector fields $\vec{M}$, and the implementation of the timber elements c_g.

Application of Stress Lines and Matching

The process of matching and stress line distribution used to generate the reinforcement curves c_t, follows the method outlined in Section 5.2.1. In this procedure, a maximum number of points was defined and positioned in regions of highest absolute bending moments, resulting in the target reinforcement curves.

In relation to the timber element inventory, the generation of geometric curves c_g is informed

directly by the 2D geometric analysis procedure described in Section 3.5.1, based on data acquired from raw 2D photographs. The optimal matching is determined by minimizing the distance between matrices $\mathcal{G}$ and $\mathcal{T}$, corresponding respectively to the geometry of the available elements and the target reinforcement lines.

Preliminary Results Analysis

For a general comparison of the proposed systems, two simulation models with similar characteristics in terms of weight and deformation behavior were analyzed (see Fig. 6.34). Both share identical board material properties and moment of inertia. The simulation procedure is further defined in Section 5.1.1. In the graphic representation, displacements, moments, and transverse shear values close to zero are excluded for clarity.

A reference solid CLT panel was used for comparison. Its thickness was calculated using a rectangular cross section (see Eq. 6.1), resulting in a total of $77\,\mathrm{mm}$. The sandwich panel configuration, by contrast, has a total thickness of $85\,\mathrm{mm}$, consisting of two three-layer boards ($15\,\mathrm{mm}$ each) and a $55\,\mathrm{mm}$ timber core, see the analysis results in Appendix B.6.4.

$$EI: \quad I_r = I_s \quad \Rightarrow \quad \frac{b \cdot t^3_{\text{reference}}}{12} = \frac{b \cdot t^3_{\text{total}}}{12} - \frac{b \cdot t^3_{\text{panel}}}{12} \tag{6.1}$$

This setup enables a direct comparison between both systems, which share similar thicknesses and structural characteristics. First, their weights differ slightly: the reference panel weighs approximately $230\,\mathrm{kg}$, while the sandwich panel weighs about $214\,\mathrm{kg}$ (with each three-layer board at $48\,\mathrm{kg}$ and the timber core at $118\,\mathrm{kg}$). Second, the deformation diagrams reveal comparable patterns, with only a minor reduction in total deflection (approximately $2\,\mathrm{cm}$). More notably, the principal moment diagrams indicate that peak moments are not concentrated solely at the supports but are also distributed across the timber core—at lower magnitudes—resulting in a more uniform load distribution. The transverse shear diagrams further show that the core timber elements effectively carry shear forces, reducing demand at the supports.

Although the simulation provides a preliminary assessment, it suggests that the sandwich panel configuration offers a lighter alternative to the reference panel, achieves an organized load path, and relies on a greater proportion of naturally grown timber—making it structurally and materially efficient.

Fabrication

The fabrication process was relatively straightforward and involved the use of a CNC milling machine operating with a parallel toolpath strategy. The raw timber elements were initially fixed to an MDF board using screws. This setup enabled a consistent surfacing pass on one side of all elements (see Fig. 6.36). After the first pass, the elements—now flattened on one face—were placed in their final arrangement, and the opposite face was surfaced to complete the planarization process.

At this stage, a scaled prototype of a sandwich panel was produced. A form-fitting interlock was milled using multiplex panels to hold the irregular timber elements in position. In Fig. 6.36, subfigure (a) shows the CNC milling process with the elements positioned, while subfigure (b) displays the creation of custom joints for interlocking assembly.



(a) Planar surfacing of elements using CNC (b) Form-fitting milling for sandwich interlock

Figure 6.36: Fabrication steps using CNC milling: element surfacing and interlock milling.

To streamline the workflow, the form-fitting interlock feature was later omitted, as adhesive bonding was not chosen for panel assembly. Instead, mechanical fastening using screws was applied. Consequently, CNC surfacing was no longer required for both faces. A jointer was used to flatten one face of the 2D timber elements, followed by a thickness planer to calibrate the opposite face to a uniform thickness of $55\,\mathrm{mm}$, as defined in the construction design and simulation (see Fig. 6.37(a)).

This simplified approach offered a practical alternative to more complex robotic or automated fabrication systems. The final product can be seen in Figs. 6.37(b) and 6.37(c), where a curved timber element is shown undergoing the full preparation process. In this stage, bark removal was also performed, leaving the element ready for final assembly.



(a) Flattening process with jointer and planer (b) Processed (c) Final set of elements ready for assembly

Figure 6.37: Element processing.

Augmented Reality Assembly

Recent advances in automation within the Architecture, Engineering, and Construction (AEC) sector illustrate how craftsmanship and technology can be successfully integrated. Assembly tasks, in particular, can still be performed manually, while being enhanced through the use of Augmented Reality (AR). AR offers an effective solution by delivering real-time, in-situ instructions directly within the workspace. This approach has demonstrated significant potential, especially for non-repetitive assembly operations [214] and material manipulation tasks [215]. Numerous studies have validated the capability of AR systems to guide users through complex procedures with greater accuracy and efficiency.

In this project, the assembly process is carried out manually by affixing three-layer board panels to their corresponding timber elements using fully threaded screws. The entire operation is guided by AR, which overlays instructional graphics onto the physical workspace, thereby improving precision and reducing reliance on traditional documentation or workshop drawings.



(a) AR interface guiding the panel assembly.



(b) Real-time instruction during timber positioning.



(c) Screw insertion for internal load transfer.



(d) Securing shear-transmitting elements.



(e) Final fastener position before concealment.

Figure 6.38: Above: Augmented Reality guiding the assembly process. Below: Manual fastening of concealed structural connectors using screws.

This work was carried out in collaboration with colleagues from the ICD (Institute for Computational Design and Construction) at the University of Stuttgart, coordinated with Dr. Felix Amtsberg for the mapping and development of the collaborative augmented reality (AR) assembly system. The application Vizor, developed by doctoral researcher Xiliu Yang [216], was employed for this purpose.

Vizor [216] is a software framework designed to support human–robot collaboration and to extend the skillsets of craftspeople through the use of AR. It was used to facilitate the assembly of the sandwich panels (see Fig. 6.38). The system employs a QR code placed precisely on the workpiece for calibration. The position of the marker can be frequently updated to minimize inaccuracies due to camera drift or distraction.

A HoloLens II device projects the positions of the timber elements directly onto the user's field of vision, enabling rapid and accurate placement. Once the top panel is installed, the underlying structural elements remain visible through the AR overlay, allowing them to be easily fastened with screws.

During the exhibition, the AR glasses were also used to visualize the internal structural elements that would otherwise be hidden within the sandwich panel (see Fig. 6.39). In this way, AR functioned not only as an assembly aid but also as a didactic tool to explain the construction process to visitors.

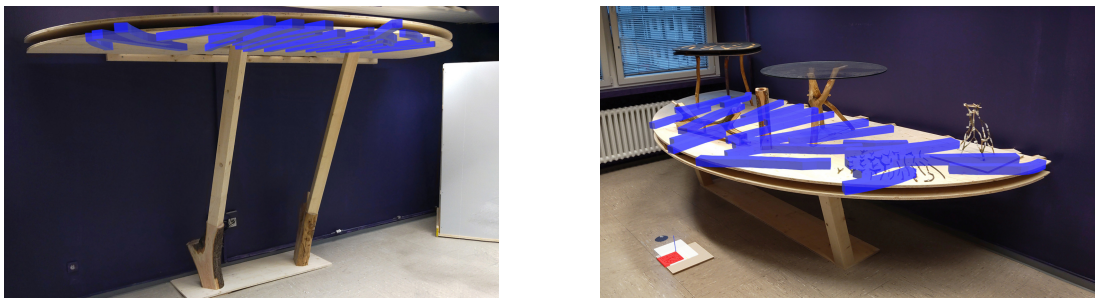

(a) AR projection during installation.

(b) User interaction with AR visualization.

Figure 6.39: Visualization of the timber elements using Augmented Reality during the exhibition.

Installation

This installation represents the first application of sandwich panel construction integrating raw timber elements guided by augmented reality assembly workflows. Beyond serving as a proof of concept, it demonstrates the feasibility of combining irregular, naturally grown components with precision-guided digital fabrication. The successful implementation of this system lays the groundwork for further explorations presented throughout this dissertation and supports the continued development of adaptable, resource-conscious construction strategies. Future research will build on these findings by exploring standardized applications of this construction system in diverse architectural scenarios, further integrating augmented reality workflows into scalable fabrication processes.

Chapter 7

Conclusion

7.1 Overview

This dissertation has addressed four main areas of interest concerning the use of naturally grown round timber in structural applications. These domains include: geometric analysis, material characterization, structural modeling, and construction methods. Each section outlines the key research directions and design considerations relevant to the use of non-standard timber components in architecture.

7.2 Restatement of Aims

This research outlines how the inherent geometry and material properties of naturally grown timber can be integrated into structural design and construction workflows. The main aims are as follows:

A central objective is to challenge the legacy of industrialized mass production in timber construction by promoting tailor-made design approaches. Rather than modifying timber to conform to standardized systems, this work advocates for using the material in its natural form—embracing irregularities such as curvature, asymmetries, and eccentricities found in tree-based elements.

This approach requires a thorough understanding of tree growth and geometry. One of the aims is therefore to analyze growth behavior and spatial patterns to develop methods for evaluating, classifying, and segmenting timber elements based on their geometric characteristics.

In parallel, current design trends and emerging research groups increasingly acknowledge the underutilized potential of naturally grown timber elements. This shift necessitates new interdisciplinary strategies that connect forestry, geometry, structural engineering, and fabrication. To support this, the research proposes methods for analyzing tree geometry—from data acquisition to the mapping of material features. It also addresses how forestry operations can be informed about optimal cutting positions, enhancing structural usability and minimizing waste

from improperly collected raw elements. In addition to tree fork bifurcations, the study includes curved and short timber elements and seeks to improve structural optimization methods to accommodate them.

Finally, this work supports the development of construction methods by reviewing existing literature and proposing a classification system for integrating naturally grown timber into architectural applications.

7.3 Summary of Findings

7.3.1 Geometrical Modeling

A direct relationship between geometry and structural design was demonstrated through the process of recording geometry and preparing it for structural purposes and cross-section analysis. Surface geometry data enables the approximation of intrinsic eccentricity. Several types of centerlines—geometric, growth-based, and center of mass—were introduced and compared. A practical workflow was developed to capture geometry from growing trees or harvested timber, in both 3D and 2D formats. This supports integration into material property mapping, simulation, and design detailing.

7.3.2 Material Mapping

A methodology based on computed tomography (CT) was established to map density variations across timber specimens. This technique provides insights into primary (longitudinal) and secondary (cross-sectional) biomass growth patterns. A research-based density evaluation also showed the location of reaction wood through CT visualization and tree static analysis, which helps in understanding material properties from visual data. A testing protocol for small-diameter, geometrically irregular elements was presented, along with analysis techniques for result interpretation.

7.3.3 Structural Design

An approach to early-stage structural assessment was developed, including transitions to mechanical analysis and finite element modeling (FEA). Two optimization strategies were proposed: one for geometric matching (for bar-type and plate-based structures) and another for joint positioning (for bar-type structures) to enhance structural performance. The benchmarking results enabled the evaluation of structural performance by comparing standardized solid timber systems with raw timber configurations. These comparisons demonstrated that integrating load distribution patterns facilitates load transmission along stress directions, allowing for lighter construction.

7.3.4 Construction Methods

Construction typologies were classified according to load transmission, supported by multiple examples both proposed and found in the literature. Additionally, a methodology for joint modeling was developed, automated through geometric constraints. Multiple prototypes were fabricated, and two full-scale demonstrations were showcased.

7.3.5 Demonstrative Constructions

The research was implemented in full-scale structures to demonstrate the application of the proposed methods. One project involved a circular-design pedestrian bridge, designed as a bar-type structure for a forest setting. This construction incorporated the developed joint methodology, matching algorithms, and joint position automation. A second project involved an exhibition pavilion functioning as a canopy, showcasing a plate-based structure with raw timber as the structural core. This construction applied the matching algorithm for element positioning and used augmented reality for automated assembly.

Both demonstrations highlight the potential of the proposed methods for future structural applications.

7.3.6 Interdisciplinary Workflow

The work integrates multiple disciplines, demonstrating how geometry, biology, simulation, and construction techniques can be combined to create viable engineered applications for non-standard timber.

7.4 Answering the Research Questions

- **Question 1:** *How can the irregularities and growth patterns be documented, analyzed and modeled for integration into load-bearing structures?*
  A strategy is applied that begins with image-based methods to acquire surface information. Based on segmentations, centerlines are generated, which serve as the basis for reconstructing the volumes using subdivision geometries in CAD. This modeling process not only enables the transition to structural elements but also allows for detailed geometrical analysis of the timber's irregularities and growth patterns.

- **Question 2:** *What design and simulation methodologies are most effective for evaluating the mechanical capabilities of naturally grown hardwood in structural applications?*
  On one hand, geometric acquisition of eccentricities makes it possible to identify growth paths, and thus to calculate moments of inertia and understand the behavior of cross-sections. On the other hand, both standard and non-standard testing methods for material characterization help determine the load-bearing capacity within the elastic range.

- **Question 3:** *How photogrammetry, 3D laser scanning, and finite element analysis facilitate the adaptation of non-standardized timber components into standardized construction workflows?*
  The image-based methods are used to generate principal axes around bounding boxes that define the elements in 2D planar geometries. These can be easily included in standardized construction methods such as trusses or plates. The geometry workflow facilitates the transition to FE that serves as a proofing method to assess the structural behavior.

- **Question 4:** *What are the specific structural advantages and limitations?*
  These elements offer structural advantages, particularly as off-knot components in bifurcations, where structural joints can be formed to transmit bending moments. In plate-based systems, curved elements can be oriented to distribute loads according to their geometry. However, limitations arise from their cross-sectional dimensions and restricted growth angles, which constrain direct implementation in large-span applications without duplicating members or in elements that tend to transmit orthogonal loads.

- **Question 5:** *How can tree crowns be incorporated into circular and sustainable design practices?*
  By evaluating the grown parts of the tree from the beginning, estimations can be made about how they can be applied in construction. A material cascade approach allows these elements to be used in their solid form with demountable joints for future reuse—whether as industrial wood, energy source, or for natural degradation, since the material remains unmodified.

- **Question 6:** *What fabrication and assembly techniques are necessary to accommodate the unique geometries?*
  Working with a system of local orthogonal coordinates (bounding boxes) enables transitions between processes while preserving consistent references. These references support 2D orientation and simplify calibration and positioning tasks during assembly.

7.5 Limitations

The main limitations identified are the difficulty to standardize these constructions for application in the building industry. However, this dissertation has presented methods to address this issue by proposing systematization strategies and specific applications. Therefore, the key limitation lies in scalability. On one side, large-scale applications have not yet been developed and will be addressed in future research. On the other side, there is the limitation of availability. Even if the material appears to be in good condition, it is always necessary to carry out an assessment in the workshop to ensure the raw timber elements are suitable.

Additionally, debarking and drying processes are required for scalability. These tasks must be revised with the aim of automation.

Another fundamental limitation is the cross-section size of the tree crown elements analyzed in the thesis. These sections are limited, which restricts the possible structural span. To overcome this, elements must be duplicated or combined in layered sandwich panels, increasing manual work and the number of joints—potentially reducing economic feasibility, which requires further evaluation.

Finally, the described process requires a certain level of expertise in digital tools and methods, which may constrain broader adoption.

7.6 Perspectives and Future Outlook

This work forms part of the ongoing research project [2], contributing to new applications and directions within a growing interdisciplinary research field. Future perspectives include improving the supply chain, integrating geometric analysis into material growth models, and scaling up construction applications—ultimately building a comprehensive agenda for raw timber integration.

7.6.1 Supply Chain

The supply chain should be developed across several stages. First, material acquisition must be optimized. Tree analysis can inform cutting strategies, and augmented reality could assist foresters in visualizing tree models to identify valuable sections before felling. Transport and labeling processes should support image-based automation. Drying and debarking also require streamlined protocols. Fabrication steps can be implemented using robotic and automated systems.

7.6.2 Tree Growth Model and Simulation

Static analysis of the tree can be extended toward modeling cross-section growth, introducing a material growth simulation that accounts for mechanical adaptation and biomass development.

7.6.3 Construction Demonstrations

The strongest proof of concept is to showcase more built examples. Although current implementations are limited to academic contexts, expanding these applications to larger-scale and industrial construction—with longer spans and broader structural types—would significantly enhance the field's credibility and acceptance.

7.6.4 Agenda for Naturally Grown Timber Research

Based on the findings presented, this agenda outlines future directions for research into the application of naturally grown hardwood—particularly crown wood—in Central European contexts. A key objective is to establish close collaboration with forestry professionals to develop an efficient and traceable supply chain.

The research should continue through iterative testing and refinement, including life-cycle assessments of the proposed construction and material systems. These evaluations are essential for understanding environmental performance and long-term viability.

Applications in education and prototyping should be further developed to promote a material-first mindset and to test the potential of irregular timber in real-world scenarios.

Furthermore, fabrication methods should evolve toward automated and adaptive systems. Investigating robot-assisted processes and custom joinery will support the scalability of raw timber use.

An additional goal is to build a collaborative network between academic researchers and construction professionals. This alliance would facilitate the practical implementation of raw timber systems, expand technical feasibility, and foster interdisciplinary innovation in architecture and construction.

Bibliography

[1] Otto, F. *Natürliche Konstruktionen: Formen und Konstruktionen in Natur und Technik und Prozesse ihrer Entstehung*. Deutsche Verlags-Anstalt, 1982. 144 pp. ISBN: 978-3-421-02591-3.

[2] Trautz, M., Klinkel, S. and Schurr, U. *DFG GEPRIS: Natürlich Gewachsene Holzelemente Als Basis Füur Tragende Konstruktionen – Statische Analyse Und Wachstumssimulation*. Research Project Nr. 512769030. Deutsche Forschungsgemeinschaft (DFG), 2022–2026. URL: https://gepris.dfg.de/gepris/projekt/512769030?context=projekt&task=showDetail&id=512769030& (visited on 18/04/2025).

[3] *Rureifel-Jülicher Börde*. Wald & Holz. URL: https://www.wald-und-holz.nrw.de/ueber-uns/einrichtungen/regionalforstaemter/rureifel-juelicher-boerde/kommune/Aachen?cHash=4f9bcb21ea8063b9aee2a51217657531 (visited on 14/11/2024).

[4] Morgan, M. H. *Vitruvius Pollio, On Architecture, Book II, in Vitruvius: Ten Books on Architecture*. London: Humbphrey Milford: Hardvard University Press, 1914. URL: https://penelope.uchicago.edu/Thayer/E/Roman/Texts/Vitruvius/2*.html (visited on 15/04/2025).

[5] Laugier, M.-A. *An Essay on Architecture*. London, Printed for T. Osborne and Shipton, 1755. 316 pp. URL: http://archive.org/details/essayonarchitect00laugrich (visited on 23/11/2023).

[6] Küreli, E. 'Laugier vs Durand: Revisiting Primitive Hut in the Classical Architectural Discourse'. In: *Dokuz Eylül Üniversitesi Güzel Sanatlar Fakültesi Dergisi* 15.15 (1st Jan. 2016), p. 111. ISSN: 1307-9840. DOI: 10.17484/yedi.60302. (Visited on 15/04/2025).

[7] Herrmann, W. *Gottfried Semper: In Search of Architecture*. The MIT Press, 5th Dec. 1984. ISBN: 978-0-262-36797-4. DOI: 10.7551/mitpress/3331.001.0001. (Visited on 15/04/2025).

[8] Ross, R. 'Wood Handbook: Wood as an Engineering Material'. In: *FPL-GTR-282* 282 (2021), pp. 1–543. URL: https://research.fs.usda.gov/treesearch/62200 (visited on 17/07/2024).

[9] Buchanan, A. H. and Levine, S. B. 'Wood-Based Building Materials and Atmospheric Carbon Emissions'. In: *Environmental Science & Policy* 2.6 (1st Dec. 1999), pp. 427–437. ISSN: 1462-9011. DOI: 10.1016/S1462-9011(99)00038-6. (Visited on 17/07/2024).

[10] Ramage, M. H. et al. 'The Wood from the Trees: The Use of Timber in Construction'. In: *Renewable and Sustainable Energy Reviews* 68 (1st Feb. 2017), pp. 333–359. ISSN: 1364-0321. DOI: 10.1016/j.rser.2016.09.107. (Visited on 24/12/2023).

[11] Hurmekoski, E., Jonsson, R. and Nord, T. 'Context, Drivers, and Future Potential for Wood-Frame Multi-Story Construction in Europe'. In: *Technological Forecasting and Social Change* 99 (1st Oct. 2015), pp. 181–196. ISSN: 0040-1625. DOI: 10.1016/j.techfore.2015.07.002. (Visited on 17/07/2024).

[12] Sathre, R. and O'Connor, J. 'Meta-Analysis of Greenhouse Gas Displacement Factors of Wood Product Substitution'. In: *Environmental Science & Policy* 13.2 (1st Apr. 2010), pp. 104–114. ISSN: 1462-9011. DOI: 10.1016/j.envsci.2009.12.005. (Visited on 17/07/2024).

[13] Kremer, P. D. and Symmons, M. A. 'Mass Timber Construction as an Alternative to Concrete and Steel in the Australia Building Industry: A PESTEL Evaluation of the Potential'. In: *International Wood Products Journal* 6.3 (1st Aug. 2015), pp. 138–147. ISSN: 2042-6445. DOI: 10.1179/2042645315Y.0000000010. (Visited on 17/07/2024).

[14] Ritter, M. A. 'TIMBER BRIDGES: DESIGN, CONSTRUCTION, INSPECTION, AND MAINTENANCE'. In: (June 1990). URL: https://trid.trb.org/View/344786 (visited on 17/07/2024).

[15] Brandner, R., Flatscher, G., Ringhofer, A., Schickhofer, G. and Thiel, A. 'Cross Laminated Timber (CLT): Overview and Development'. In: *European Journal of Wood and Wood Products* 74.3 (1st May 2016), pp. 331–351. ISSN: 1436-736X. DOI: 10.1007/s00107-015-0999-5. (Visited on 17/07/2024).

[16] Lobos Calquin, D. et al. 'Implementation of Building Information Modeling Technologies in Wood Construction: A Review of the State of the Art from a Multidisciplinary Approach'. In: *Buildings* 14.3 (3 Mar. 2024), p. 584. ISSN: 2075-5309. DOI: 10.3390/buildings14030584. (Visited on 17/07/2024).

[17] D'Amico, B., Pomponi, F. and Hart, J. 'Global Potential for Material Substitution in Building Construction: The Case of Cross Laminated Timber'. In: *Journal of Cleaner Production* 279 (Jan. 2021), p. 123487. ISSN: 09596526. DOI: 10.1016/j.jclepro.2020.123487. (Visited on 17/07/2024).

[18] Moreno Gata, K., Seiter, A., Grizmann, D. and Trautz, M. 'Development of Construction Methods with Naturally Grown Timber and Bending-Resistant Joints'. In: *Proceedings of World Conference on Timber Engineering*. WCTE 2023. Oslo, 2023. DOI: 10.52202/069179-0096.

[19] Mattheck, C. 'Engineering Components Grow like Trees'. In: *Materialwissenschaft und Werkstofftechnik* 21.4 (Apr. 1990), pp. 143–168. ISSN: 0933-5137, 1521-4052. DOI: 10.1002/mawe.19900210403. (Visited on 19/02/2020).

[20] Mattheck, C. *Design in Nature: Learning from Trees*. Berlin Heidelberg: Springer-Verlag, 1998. ISBN: 978-3-540-62937-5. DOI: 10.1007/978-3-642-58747-4. (Visited on 29/02/2020).

[21] Self, M. and Vercruysse, E. 'Infinite Variations, Radical Strategies'. In: *Fabricate 2017*. Ed. by A. Menges, B. Sheil, R. Glynn and M. Skavara. UCL Press, 2017, pp. 30–35. ISBN: 978-1-78735-000-7. DOI: 10.2307/j.ctt1n7qkg7.8. JSTOR: j.ctt1n7qkg7.8. (Visited on 13/11/2023).

[22] Amtsberg, F., Huang, Y., Marshall, D., Moreno Gata, K. and Mueller, C. 'Structural Up-cycling: Matching Digital and Natural Geometry'. In: *Advances in Architectural Geometry 2020*. Ed. by O. Baverel, C. Douthe, R. Mesnil, C. Mueller, H. Pottmann and T. Tachi. Paris: École des Ponts ParisTech & Université Gustave Eiffel, Presses des Ponts, 2021, pp. 486–504. ISBN: 978-2-85978-540-6. URL: thinkshell.fr/AAG2020.

[23] *USFS Wood Innovations Project Detail Report*. URL: https://apps.fs.usda.gov/nicportal/WOODINNOVATIONS/dspProjectDetailReport.cfm?id=410 (visited on 12/02/2025).

[24] Zamora-Pereira, J. C., Hanewinkel, M. and Yousefpour, R. 'Robust Management Strategies Promoting Ecological Resilience and Economic Efficiency of a Mixed Conifer-Broadleaf Forest in Southwest Germany under the Risk of Severe Drought'. In: *Ecological Economics* 209 (1st July 2023), p. 107825. ISSN: 0921-8009. DOI: 10.1016/j.ecolecon.2023.107825. (Visited on 12/03/2024).

[25] Holz, P. F.
bibinitperiod. *Rahmenvereinbarung für den Rohholzhandel in Deutschland (RVR)*. Deutschen Forstwirtschaftsrates e.V, 1st Dec. 2023. URL: https://rvr-deutschland.de/downloads/.

[26] Květina, P. and Hrnčíř, V. 'Between Archaeology and Anthropology: Imagining Neolithic Settlements'. In: *Anthropologie* 51 (1st Jan. 2013), pp. 323–347.

[27] Watson, J. *Lo-TEK: Design by Radical Indigenism*. Cologne: Taschen, 2020. 418 pp. ISBN: 978-3-8365-7818-9.

[28] Smil, V. *Growth: From Microorganisms to Megacities*. The MIT Press, 24th Sept. 2019. ISBN: 978-0-262-35451-6. DOI: 10.7551/mitpress/12074.001.0001. (Visited on 15/04/2025).

[29] 'The Archaeology of York. Fasc. 13: Vol. 17. The Small Finds Craft, Industry and Everyday Life: Wood and Woodworking in Anglo-Scandinavian and Medieval York / by Carole A. Morris'. In: ed. by C. A. Morris. London, 2000. ISBN: 978-1-902771-10-6.

[30] *Regia Anglorum*. URL: https://regia.org/research/ships/Ships1.htm (visited on 15/04/2025).

[31] Robert Greenhalgh Albion. *Forests And Sea Power*. 1926. URL: http://archive.org/details/ForestsAndSeaPower (visited on 15/04/2025).

[32] Guillet, P. *Timber Merchant's Guide:* J. Lovegrove, 1823. 256 pp.

[33] *Historische Entwicklung - Forstwirtschaft in Deutschland*. URL: https://www.forstwirtschaft-in-deutschland.de/waelder-entdecken/historische-entwicklung/ (visited on 15/04/2025).

[34] Weiss, W. *Fachwerk.: Bautraditionen in Mitteleuropa.* Stuttgart: Fraunhofer IRB Verlag, 1st Jan. 2019. 272 pp. ISBN: 978-3-7388-0184-2.

[35] Emmerich, D. G. (.-1. *Soft architecture : essais sur l'autoconstruction*. Paris : Institut de l'environnement, 1974. URL: http://archive.org/details/frapn02-soft-architecture-essais-sur-l-autoconstruction-1974 (visited on 15/04/2025).

[36] Mikurcik, G. *Visit to Hooke Park*. 30th Oct. 2015. URL: https://www.architype.co.uk/blog/visit-to-hooke-park/ (visited on 28/06/2025).

[37] *Hooke Park*. URL: https://www.aaschool.ac.uk/about/hookepark (visited on 28/06/2025).

[38] *Buildings-Workshop – Hooke Park*. URL: https://hookepark.aaschool.ac.uk/projects-workshop/ (visited on 28/06/2025).

[39] Wang, Y. 'Hooke Park Biomass Boiler House'. In: Menges, A., Schwinn, T. and Krieg, O. D. *Advancing Wood Architecture*. Ed. by A. Menges, T. Schwinn and O. D. Krieg. 1st ed. New York : Routledge, 2016.: Routledge, 22nd July 2016, pp. 169–183. ISBN: 978-1-315-67882-5. DOI: 10.4324/9781315678825-13.

[40] Bukauskas, A., Mayencourt, P., Shepherd, P., Sharma, B., Mueller, C., Walker, P. and Bregulla, J. 'Whole Timber Construction: A State of the Art Review'. In: *Construction and Building Materials* 213 (20th July 2019), pp. 748–769. ISSN: 0950-0618. DOI: 10.1016/j.conbuildmat.2019.03.043.

[41] *WholeTrees - Technology*. WholeTrees Structures. URL: https://wholetrees.com/technology/ (visited on 27/12/2023).

[42] Vestartas, P. and Weinand, Y. 'Joinery Solver for Whole Timber Structures'. In: WCTE 2020. 30th Nov. 2020. URL: https://infoscience.epfl.ch/handle/20.500.14299/173741 (visited on 20/08/2024).

[43] Vestartas, P. 'Design-to-Fabrication Workflow for Raw-Sawn-Timber Using Joinery Solver'. Lausanne: EPFL, 2021. 290 pp. DOI: 10.5075/epfl-thesis-8928.

[44] Zhou, Q.-Y., Park, J. and Koltun, V. *Open3D: A Modern Library for 3D Data Processing*. 30th Jan. 2018. DOI: 10.48550/arXiv.1801.09847. arXiv: 1801.09847 [cs]. URL: http://arxiv.org/abs/1801.09847 (visited on 30/11/2025). Pre-published.

[45] Cousin, T., Marshall, D., Pearl, N., Alkhayat, L. and Mueller, C. 'Integrating Irregular Inventories: Accessible Technologies to Design and Build with Nonstandard Materials in Architecture'. In: *Journal of Physics: Conference Series* 2600.19 (Nov. 2023), p. 192004. ISSN: 1742-6596. DOI: 10.1088/1742-6596/2600/19/192004. (Visited on 15/10/2024).

[46] Cousin, T., Alkhayat, L., Pearl, N., Dewart, C. B. and Mueller, C. 'Wild Wood Gridshells: Mixed-Reality Construction of Nonstandard Wood'. In: *Technology|Architecture + Design* 7.2 (3rd July 2023), pp. 216–231. ISSN: 2475-1448, 2475-143X. DOI: 10.1080/24751448.2023.2245725.

[47] Allner, L., Kroehnert, D. and Rossi, A. 'Mediating Irregularity: Towards a Design Method for Spatial Structures Utilizing Naturally Grown Forked Branches'. In: *Impact: Design With All Senses*. Ed. by C. Gengnagel, O. Baverel, J. Burry, M. Ramsgaard Thomsen and S. Weinzierl. Cham: Springer International Publishing, 2020, pp. 433–445. ISBN: 978-3-030-29828-9 978-3-030-29829-6. DOI: 10.1007/978-3-030-29829-6_34. (Visited on 06/05/2024).

[48] Kerezov, A. D., Koshihara, M. and Tachi, T. 'From Natural Tree Forks to Grid Shells: Towards a Self-forming Geometry'. In: *ICGG 2022 - Proceedings of the 20th International Conference on Geometry and Graphics*. Ed. by L.-Y. Cheng. Vol. 146. Cham: Springer International Publishing, 2023, pp. 418–430. ISBN: 978-3-031-13587-3 978-3-031-13588-0. DOI: 10.1007/978-3-031-13588-0_36. (Visited on 10/06/2024).

[49] Tamke, M., Gatz, S., Svilans, T. and Thomsen, M. *Tree-to-Product -Prototypical Workflow Connecting Data from Tree with Fabrication of Engineered Wood Structure - RawLam*. 27th Aug. 2021.

[50] Larsen, N. M. and Aagaard, A. K. 'Robotic Processing of Crooked Sawlogs for Use in Architectural Construction'. In: *Construction Robotics* 4.1 (1st June 2020), pp. 75–83. ISSN: 2509-8780. DOI: 10.1007/s41693-020-00028-7. (Visited on 24/10/2023).

[51] Chai, H., Zhou, X., Gao, X., Yang, Q., Zhou, Y. and Yuan, P. F. 'Integrated Workflow for Cooperative Robotic Fabrication of Natural Tree Fork Structures'. In: *Automation in Construction* 165 (Sept. 2024), p. 105524. ISSN: 09265805. DOI: 10.1016/j.autcon.2024.105524. (Visited on 09/10/2024).

[52] Sun, Q., Reisach, D., Langenberg, S. and Dillenburger, B. *Computational Design Methods for Upcycling Found Objects: A Review of Applications in Construction*. 23rd Aug. 2024. DOI: 10.2139/ssrn.4952086. Social Science Research Network: 4952086. URL: https://papers.ssrn.com/abstract=4952086 (visited on 15/03/2025). Pre-published.

[53] Wagner, H., Hua, C., Guo, Z., Menges, A. and Yuan, P. *Towards an On-site Fabrication System for Bespoke, Unlimited and Monolithic Timber Slabs*. 29th Oct. 2020. DOI: 10.13140/RG.2.2.14098.68802/1.

[54] Orozco, L., Krtschil, A., Skoury, L., Knippers, J. and Menges, A. 'Arrangement of Reinforcement in Variable Density Timber Slab Systems for Multi-Story Construction'. In: *International Journal of Architectural Computing* 20.4 (1st Dec. 2022), pp. 707–727. ISSN: 1478-0771. DOI: 10.1177/14780771221135003. (Visited on 11/03/2024).

[55] Krtschil, A. et al. 'Structural Development of a Novel Punctually Supported Timber Building System for Multi-Storey Construction'. In: *Journal of Building Engineering* 58 (15th Oct. 2022), p. 104972. ISSN: 2352-7102. DOI: 10.1016/j.jobe.2022.104972. (Visited on 11/03/2024).

[56] Chai, H., Zhou, X., Gao, T., Zhou, Y. and Yuan, P. F. 'Rationalizing Principal Stress Line Networks Using an Agent-Based Modelling Approach'. In: *Advances in Architectural Geometry 2023*. Ed. by K. Dörfler, J. Knippers, A. Menges, S. Parascho, H. Pottmann and T. Wortmann. De Gruyter, 18th Sept. 2023, pp. 441–454. ISBN: 978-3-11-116268-3. DOI: 10.1515/9783111162683-033. (Visited on 22/05/2024).

[57] Chai, H., Orozco, L., Kannenberg, F., Siriwardena, L., Schwinn, T., Liu, H., Menges, A. and Yuan, P. F. 'Agent-Based Principal Strips Modeling for Freeform Surfaces in Architecture'. In: *Nexus Network Journal* 26.2 (June 2024), pp. 369–396. ISSN: 1590-5896, 1522-4600. DOI: 10.1007/s00004-024-00765-0. (Visited on 22/05/2024).

[58] Svilans, T. 'Integrated Material Practice in Free-form Timber Structures'. UCL Press, 6th Apr. 2020. DOI: 10.2307/j.ctv13xprf6. JSTOR: 10.2307/j.ctv13xprf6. (Visited on 09/10/2024).

[59] Fukai, M. *Cathedral Square Complex*. Shigeru Ban. 28th Apr. 2017. URL: https://shigerubanarchitects.com/works/cathedral-square-complex/ (visited on 23/04/2025).

[60] Halpern, A., Billington, D. and Adriaenssens, S. 'The Ribbed Floor Slab Systems of Pier Luigi Nervi'. In: 54 (1st Sept. 2013), pp. 127–136.

[61] Musto, J. 'Formfindung und Potential beanspruchungsadaptiver Faltungen / vorgelegt von Juan Musto, M.Sc.' Aachen: Rheinisch-Westfälische Technische Hochschule Aachen, 2022. DOI: 10.18154/RWTH-2023-01104.

[62] Musto, J., Lyon, M., Trautz, M. and Kobbelt, L. 'Form Finding of Stress Adapted Folding as a Lightweight Structure under Different Load Cases'. In: 9. International Conference on Textile Composites and Inflatable Structures. Barcelona, Spain: International Centre for Numerical Methods in Engineering (CIMNE), 2019.

[63] Kaufmann, H., Krötsch, S. and Winter, S. *Atlas mehrgeschossiger Holzbau: Grundlagen - Konstruktionen - Beispiele*. 4. Auflage. München: Edition Detail, 2022. 311 pp. ISBN: 978-3-95553-556-8.

[64] BauNetz. *Möbel unter künstlichen Baumkronen - Holzbau-Showroom von Ludloff Ludloff in Bad Schönborn*. BauNetz. URL: https://www.baunetz.de/meldungen/Meldungen-Holzbau-Showroom_von_Ludloff_Ludloff_in_Bad_Schoenborn_7909579.html (visited on 23/04/2025).

[65] Amtsberg, F., Moreno Gata, K., Huang, Y., Marshall, D. and Mueller, C. 'DI-Terial – Development of Sensory-Informed Design-to-Fabrication Processes for the Efficient Use and Robotic Production of Discarded One-Off Hardwood Elements'. In: *12. World Conference on Timber Engineering*. Santiago, Chile: Red Hook, NY : Curran Associates, Inc, 2021, pp. 591–598. ISBN: 978-1-7138-4097-8.

[66] Larsen, N. M., Aagaard, A. K., Hudert, M. and Rahbek, L. W. 'Timber Structures Made of Naturally Curved Oak Wood: Prototypes and Processes'. In: *Architecture, Structures and Construction* 2.4 (1st Dec. 2022), pp. 493–507. ISSN: 2730-9894. DOI: 10.1007/s44150-022-00046-9. (Visited on 17/10/2024).

[67] Bukauskas, A., Shepherd, P., Walker, P., Sharma, B. and Bregulla, J. *Form-Fitting Strategies for Diversity-Tolerant Design*. 24th Sept. 2017.

[68] Huang, Y., Alkhayat, L., De Wolf, C. and Mueller, C. 'Algorithmic Circular Design with Reused Structural Elements: Method and Tool'. In: *Proceedings of the International Fib Symposium on the Conceptual Design of Structures*. Fib Conceptual Design of Structures 2021. Vol. 55. Fédération Internationale du Béton (fib), Sept. 2021, pp. 457–468. ISBN: 978-2-940643-12-7. DOI: 10.35789/fib.PROC.0055.2021.CDSymp.P056. (Visited on 29/12/2023).

[69] Tomczak, A., Haakonsen, S. M. and Łuczkowski, M. 'Matching Algorithms to Assist in Designing with Reclaimed Building Elements'. In: *Environmental Research: Infrastructure and Sustainability* 3.3 (1st Sept. 2023), p. 035005. ISSN: 2634-4505. DOI: 10.1088/2634-4505/acf341. (Visited on 09/10/2024).

[70] Warmuth, J., D'Acunto, P. and Fivet, C. 'Shaping Structures from Reclaimed Elements A Computational Framework for Stock-Constrained Design of Static Equilibrium'. In: *Scalable Disruptors*. Ed. by P. Eversmann, C. Gengnagel, J. Lienhard, M. Ramsgaard Thomsen and J. Wurm. Cham: Springer Nature Switzerland, 2024, pp. 42–56. ISBN: 978-3-031-68275-9. DOI: 10.1007/978-3-031-68275-9_4.

[71] McNeel, R. et al. *Rhinoceros 3D, Version 7.0*. Seattle, WA, USA: Robert McNeel & Associates, 2023.

[72] Trautz, M. *Wachstum und Konstruktion in der Natur als Vorbild und Prozess für innovative technische Lösungen*. RWTH-2017-04197. DWI an der RWTH Aachen e.V. Corporation, 2015. URL: https://publications.rwth-aachen.de/record/689035?ln=de (visited on 13/04/2020).

[73] Trautz, M., Grizmann, D., Seiter, A. J., Moreno Gata, K., Pranjic, A. and Saez, D. L. 'Design and Natural Materials – Innovative Approaches for a Sustainable Future Architecture and Structural Engineering'. In: *Proceedings Creative Construction Confer-*

ence 2023 : CCC 2023, Kezthely, Lake Balaton, 20-23 July 2023. Budapest: Diamond Congress Ltd, 2023. DOI: 10.3311/CCC2023-073.

[74] Knippers, J. 'From Minimal Surfaces to Integrative Structures – The SFB-TRR 141 in the Light of the Legacy of Frei Otto and the SFB 230 'Natürliche Konstruktionen''. In: *Biomimetic Research for Architecture and Building Construction: Biological Design and Integrative Structures*. Ed. by J. Knippers, K. G. Nickel and T. Speck. Biologically-Inspired Systems. Cham: Springer International Publishing, 2016, pp. 7–10. ISBN: 978-3-319-46374-2. DOI: 10.1007/978-3-319-46374-2_2. (Visited on 17/02/2022).

[75] Cervera Sardá, M. R. and Prieto, M. B. *ARQUITECTURA BIONICA: BIONIC ARCHITECTURE*. 1st edition. Sant Feliu del Racó, Castellar del Vallès: By Architect Publications, 1st Sept. 2015. 384 pp. ISBN: 978-84-947504-6-5.

[76] Pohl, G. and Nachtigall, W. *Biomimetics for Architecture & Design: Nature - Analogies - Technology*. Springer International Publishing, 2015. ISBN: 978-3-319-19119-5. DOI: 10.1007/978-3-319-19120-1. (Visited on 29/02/2020).

[77] Carpo, M. *The Digital Turn in Architecture 1992 - 2012 | Wiley*. 2013. URL: https://www.wiley.com/en-us/The+Digital+Turn+in+Architecture+1992+-+2012-p-9781119951759 (visited on 30/11/2025).

[78] Carpo, M. *The Second Digital Turn: Design Beyond Intelligence*. The MIT Press, 20th Oct. 2017. ISBN: 978-0-262-34124-0. DOI: 10.7551/mitpress/9976.001.0001. (Visited on 30/11/2025).

[79] Knippers, J., Schmid, U. and Speck, T., eds. *Biomimetics for Architecture: Learning from Nature*. 1st edition. Basel/Berlin/Boston: Birkhäuser, 17th June 2019. 208 pp. ISBN: 978-3-0356-1786-3.

[80] *DFG - GEPRIS - EXC 2120: Integratives Computerbasiertes Planen Und Bauen Für Die Architektur*. 2019. URL: https://gepris.dfg.de/gepris/projekt/390831618?context=projekt&task=showDetail&id=390831618& (visited on 30/11/2025).

[81] Mattheck, C. *Bionik - Bionische Strukturoptimierung*. ISO 18459:2015. Beuth Verlag GmbH, Aug. 2016, p. 27. DOI: 10.31030/2500339. (Visited on 17/02/2022).

[82] Pranjic, A., Della Puppa, G. and Trautz, M. 'Structural Tree Growth Optimization'. In: World Conference on Timber Engineering. Seoul, 2018. URL: https://publications.rwth-aachen.de/record/731678 (visited on 29/01/2024).

[83] Lindenmayer, A. 'Mathematical Models for Cellular Interactions in Development I. Filaments with One-Sided Inputs'. In: *Journal of Theoretical Biology* 18.3 (1st Mar. 1968), pp. 280–299. ISSN: 0022-5193. DOI: 10.1016/0022-5193(68)90079-9. (Visited on 29/01/2024).

[84] Prusinkiewicz, P. and Lindenmayer, A. *The Algorithmic Beauty of Plants*. New York: Springer-Verlag, 1990.

[85] Jirasek, C., Prusinkiewicz, P. and Moulia, B. 'Integrating Biomechanics into Developmental Plant Models Expressed Using L-systems'. In: *Plant biomechanics* (Proceedings of the 3rd Plant Biomechanics Conference, Freiburg-Badenweiler 2000), pp. 615–624.

[86] Ludwig, F., Schwertfreger, H. and Storz, O. 'Living Systems: Designing Growth in Baubotanik'. In: *Architectural Design* 82.2 (Mar. 2012), pp. 82–87. ISSN: 00038504. DOI: 10.1002/ad.1383. (Visited on 19/02/2020).

[87] Wang, X. 'Build with Nature'. 2024. URL: https://repository.tudelft.nl/record/uuid:8557da44-3a73-4c6b-a32a-0e9dd3c1ae73 (visited on 22/04/2025).

[88] Quan, L. *Image-Based Modeling*. Boston, MA: Springer US, 2010. ISBN: 978-1-4419-6678-0 978-1-4419-6679-7. DOI: 10.1007/978-1-4419-6679-7. (Visited on 18/04/2025).

[89] Kang, S. B. *Image-Based Modeling of Plants and Trees /*. 1st ed. 2010. Synthesis Lectures on Computer Vision. Cham: Springer International Publishing, 2010. x+74. ISBN: 978-3-031-01808-4. DOI: 10.1007/978-3-031-01808-4.

[90] Quan, L. 'Tree Modeling'. In: *Image-Based Modeling*. Ed. by L. Quan. Boston, MA: Springer US, 2010, pp. 149–175. ISBN: 978-1-4419-6679-7. DOI: 10.1007/978-1-4419-6679-7_8. (Visited on 18/04/2025).

[91] Seidel, D. 'Terrestrial Laser Scanning : Applications in Forest Ecological Research'. GOEDOC, Dokumenten- und Publikationsserver der Georg-August-Universität Göttingen, 2011, Bd. 6. DOI: 10.3249/WEBDOC-2782. HDL: 11858/00-1735-0000-0006-B3A6-9. (Visited on 18/03/2025).

[92] Mildenhall, B., Srinivasan, P. P., Tancik, M., Barron, J. T., Ramamoorthi, R. and Ng, R. *NeRF: Representing Scenes as Neural Radiance Fields for View Synthesis*. 3rd Aug. 2020. DOI: 10.48550/arXiv.2003.08934. arXiv: 2003.08934 [cs]. URL: http://arxiv.org/abs/2003.08934 (visited on 20/08/2024). Pre-published.

[93] Kerbl, B., Kopanas, G., Leimkühler, T. and Drettakis, G. *3D Gaussian Splatting for Real-Time Radiance Field Rendering*. 8th Aug. 2023. DOI: 10.48550/arXiv.2308.04079. arXiv: 2308.04079. URL: http://arxiv.org/abs/2308.04079 (visited on 14/10/2024). Pre-published.

[94] *Luma AI - Fields Dashboard*. Luma AI - Fields Dashboard. URL: https://lumalabs.ai/dashboard/captures (visited on 14/10/2024).

[95] *Cross-Platform 3D Scanning Floor Plans & Drone Mapping*. URL: https://poly.cam/ (visited on 20/03/2025).

[96] *Scaniverse | Free 3D Scanner | Capture & Explore with Gaussian Splatting*. Scaniverse. URL: https://scaniverse.com/ (visited on 30/11/2025).

[97] Steininger, D., Simon, J., Trondl, A. and Murschitz, M. *TimberVision: A Multi-Task Dataset and Framework for Log-Component Segmentation and Tracking in Autonomous Forestry Operations*. 13th Jan. 2025. DOI: 10.48550/arXiv.2501.07360. arXiv: 2501.07360 [cs]. URL: http://arxiv.org/abs/2501.07360 (visited on 25/02/2025). Pre-published.

[98] *CT WOOD | Luleå Tekniska Universitet*. 16th Aug. 2024. URL: https://www.ltu.se/en/research/research-subjects/wood-science-and-engineering/ct-wood (visited on 18/04/2025).

[99] Huber, J. A. J., Abdeljaber, O., Oja, J. and Olsson, A. *EVALUATION OF MODELS OF FIBRE ORIENTATION IN SAWN TIMBER USING SYNCHRONISED COMPUTED TOMOGRAPHY AND OPTICAL SCANNING DATA*. 1st Jan. 2023, p. 427. 421 pp. DOI: 10.52202/069179-0057.

[100] Huber, J. A. J. and Forsberg, F. *Local Stiffness of Softwood Based on Micro- Macroscale Computed Tomography*. 7th July 2023.

[101] *Innovating Wood*. MiCROTEC. URL: https://www.microtec.com/de (visited on 18/04/2025).

[102] Peng, Y.-S., Cheng, B.-Y. and Liu, T.-C. 'Mechanical Properties and Optimization Strategies of Tree Fork Structures'. In: *Plants* 14.2 (9th Jan. 2025), p. 167. ISSN: 2223-7747. DOI: 10.3390/plants14020167. (Visited on 10/01/2025).

[103] Metzner, R., van Dusschoten, D., Bühler, J., Schurr, U. and Jahnke, S. 'Belowground Plant Development Measured with Magnetic Resonance Imaging (MRI): Exploiting the Potential for Non-Invasive Trait Quantification Using Sugar Beet as a Proxy'. In: *Frontiers in Plant Science* 5 (2014), p. 469. ISSN: 1664-462X. DOI: 10.3389/fpls.2014.00469. PMID: 25278947.

[104] Metzner, R., Eggert, A., van Dusschoten, D., Pflugfelder, D., Gerth, S., Schurr, U., Uhlmann, N. and Jahnke, S. 'Direct Comparison of MRI and X-ray CT Technologies for 3D Imaging of Root Systems in Soil: Potential and Challenges for Root Trait Quantification'. In: *Plant Methods* 11 (2015), p. 17. ISSN: 1746-4811. DOI: 10.1186/s13007-015-0060-z. PMID: 25774207.

[105] *State of Europe's Forests - FOREST EUROPE*. FOREST EUROPE - Ministerial Conference on the Protection of Forests in Europe. 27th Sept. 2021. URL: https://foresteurope.org/state-of-europes-forests/ (visited on 24/03/2025).

[106] *Waldstrategie 2020*. BMEL. URL: https://www.bmel.de/SharedDocs/Downloads/DE/_Wald/waldstrategie-2020.pdf?__blob=publicationFile&v=4 (visited on 24/03/2025).

[107] *Ergebnisse der Waldzustandserhebung 2023*. BMEL. 13th May 2024. URL: https://www.bmel.de/DE/themen/wald/wald-in-deutschland/waldzustandserhebung.html (visited on 24/03/2025).

[108] WUH, W. u. H. N. *Eingeführte Baumarten in Nordrhein-Westfalen: Neue Baumarten an neuen Orten – Chancen und Möglichkeiten im Fokus des Klimawandels, PDF*. URL: https://www.waldwissen.net/de/waldwirtschaft/waldbau/neue-broschuere-zu-eingefuehrten-baumarten (visited on 24/03/2025).

[109] Nocetti, M. and Brunetti, M. 'Advancements in Wood Quality Assessment: Standing Tree Visual Evaluation—A Review'. In: *Forests* 15 (30th May 2024), p. 943. DOI: 10.3390/f15060943.

[110] Bosela, M. et al. 'Stem Quality Assessment in European National Forest Inventories: An Opportunity for Harmonised Reporting?' In: *Annals of Forest Science* 73.3 (3 Sept. 2016), pp. 635–648. ISSN: 1297-966X. DOI: 10.1007/s13595-015-0503-8. (Visited on 04/04/2025).

[111] *DIN EN 1316-1:2013-01, Laub-Rundholz_- Qualitäts-Sortierung_- Teil_1: Eiche und Buche; Deutsche Fassung EN_1316-1:2012*. DOI: 10.31030/1889825. (Visited on 04/04/2025).

[112] Ruano, A. et al. 'Improving Stem Quality Assessment Based on National Forest Inventory Data: An Approach Applied to Spanish Forests'. In: *Annals of Forest Science* 80.1 (10th May 2023), p. 20. ISSN: 1297-966X. DOI: 10.1186/s13595-023-01187-7. (Visited on 04/04/2025).

[113] Wang, S., Yang, T. and Ouyang, S. 'A New Perspective of Trees Competition Network Research'. In: *E3S Web of Conferences* 478 (2024), p. 01015. ISSN: 2267-1242. DOI: 10.1051/e3sconf/202447801015. (Visited on 06/08/2024).

[114] Morin, X., Fahse, L., Scherer-Lorenzen, M. and Bugmann, H. 'Tree Species Richness Promotes Productivity in Temperate Forests through Strong Complementarity between Species'. In: *Ecology Letters* 14.12 (Dec. 2011), pp. 1211–1219. ISSN: 1461-0248. DOI: 10.1111/j.1461-0248.2011.01691.x. PMID: 21955682.

[115] Jin, S., Zhang, W., Shao, J., Wan, P., Cheng, S., Cai, S. and Yan, G. *Estimation of Larch Growth at the Stem, Crown and Branch Levels Using Ground-based LiDAR Point Cloud*. 28th Sept. 2021. DOI: 10.21203/rs.3.rs-910503/v1. URL: https://www.researchsquare.com/article/rs-910503/v1 (visited on 06/08/2024). Pre-published.

[116] Tang, X., Lei, P., You, Q., Liu, Y., Jiang, S., Ding, J., Chen, J. and You, H. 'Monitoring Seasonal Growth of Eucalyptus Plantation under Different Forest Age and Slopes Based on Multi-Temporal UAV Stereo Images'. In: *Forests* 14.11 (11 Nov. 2023), p. 2231. ISSN: 1999-4907. DOI: 10.3390/f14112231. (Visited on 06/08/2024).

[117] Hoppen, M. et al. 'Smart Forestry – a Forestry 4.0 Approach to Intelligent and Fully Integrated Timber Harvesting'. In: *International Journal of Forest Engineering* 35.2 (3rd May 2024), pp. 137–152. ISSN: 1494-2119. DOI: 10.1080/14942119.2024.2323238. (Visited on 26/04/2025).

[118] De Miguel-Díez, F. and Purfürst, T. 'Shaping the Future of Forestry in Germany: Stakeholder Perspectives on Optimizing Forest Management through Augmented Reality'. In: *Journal of Environmental Management* 385 (6th May 2025). DOI: 10.1016/j.jenvman.2025.125601.

[119] De Miguel-Díez, F. and Purfürst, T. 'Automatization of the Measurement Process of Stacked Roundwood - Past Milestones, Current Status and Perspectives'. In: *26th IUFRO World Congress*. International Union of Forest Research Organizations. 27th June 2024. DOI: 10.13140/RG.2.2.11379.13605. (Visited on 24/05/2025).

[120] Zhu, J., Shi, Y., Fang, L., Liu, X. and Ji, C. 'Patterns and Determinants of Wood Physical and Mechanical Properties across Major Tree Species in China'. In: *Science China Life Sciences* 58.6 (1st June 2015), pp. 602–612. ISSN: 1869-1889. DOI: 10.1007/s11427-015-4847-y. (Visited on 08/02/2024).

[121] Tissari, M. J. 'MONITORING THE TECHNICAL AND ENVIRONMENTAL STANDARDS OF TROPICAL TIMBER PRODUCTS IN INTERNATIONAL MARKETS'. In: *FOOD AND AGRICULTURE ORGANIZATION OF THE UNITED NATIONS* (2010).

[122] Teischinger, A., Huber, C. and Hansmann, C. 'Hardwood Resources, Process Chains, Challenges and Solutions'. In: 25th Oct. 2018, p. 8. ISBN: 978-963-359-096-6.

[123] Bouchard, E. et al. 'Global Patterns and Environmental Drivers of Forest Functional Composition'. In: *Global Ecology and Biogeography* 33.2 (2024), pp. 303–324. ISSN: 1466-8238. DOI: 10.1111/geb.13790. (Visited on 12/03/2024).

[124] United Nations Economic Commission for Europe. *The Outlook for the UNECE Forest Sector in a Changing Climate: A Contribution to the Forest Sector Outlook Study 2020-2040*. Geneva Timber and Forest Discussion Papers. United Nations, 8th June 2023. ISBN: 978-92-1-002373-3. DOI: 10.18356/9789210023733. (Visited on 08/02/2024).

[125] Teischinger, A., Ritter, S., Huber, C. and Hansmann, C. 'Laubholzaufkommen, Laubholzverarbeitung in Österreich Und Ansätze Für Konzepte von Innovationsstrategien'. In: 1st Mar. 2019, p. 3.

[126] *Arboa Tree Safety: Tree Protection -Tree Bracing System, Tree Cabling System, Plant Securing, Securing Trees, Taproot of Iron, Soil Dike for Trees, Tree Care Products - Home (En)*. URL: https://arboa.com/en/sia-calculator (visited on 14/11/2024).

[127] Niklas, K. J. 'Responses of Hollow, Septate Stems to Vibrations: Biomechanical Evidence That Nodes Can Act Mechanically as Spring-like Joints'. In: *Annals of Botany* 80.4 (1st Oct. 1997), pp. 437–448. ISSN: 0305-7364. DOI: 10.1006/anbo.1997.0463. (Visited on 14/11/2024).

[128] Siegert, B. 'Comparative Analysis of Tools and Methods for the Evaluation of Tree Stability'. In: *Arborist News*. Apr. 2013. URL: www.isa-arbor.com.

[129] Uzquiano, S., Barbeito, I., San Martín, R., Ehbrecht, M., Seidel, D. and Bravo, F. 'Quantifying Crown Morphology of Mixed Pine-Oak Forests Using Terrestrial Laser Scanning'. In: *Remote Sensing* 13.23 (23 Jan. 2021), p. 4955. ISSN: 2072-4292. DOI: 10.3390/rs13234955. (Visited on 16/03/2024).

[130] Neudam, L. C., Höwler, K. and Seidel, D. 'Stem Shape and Structural Complexity Change in Beech Forests along a Management Gradient'. In: *Forest Ecology and Management* 549 (1st Dec. 2023), p. 121473. ISSN: 0378-1127. DOI: 10.1016/j.foreco.2023.121473. (Visited on 16/03/2024).

[131] Alméras, T., Jullien, D. and Gril, J. 'Modelling, Evaluation and Biomechanical Consequences of Growth Stress Profiles Inside Tree Stems'. In: *Plant Biomechanics: From Structure to Function at Multiple Scales*. Ed. by A. Geitmann and J. Gril. Cham: Springer International Publishing, 2018, pp. 21–48. ISBN: 978-3-319-79099-2. DOI: 10.1007/978-3-319-79099-2_2. (Visited on 06/08/2024).

[132] Salmén, L. 'Wood Cell Wall Structure and Organisation in Relation to Mechanics'. In: *Plant Biomechanics: From Structure to Function at Multiple Scales*. Ed. by A. Geitmann and J. Gril. Cham: Springer International Publishing, 2018, pp. 3–19. ISBN: 978-3-319-79099-2. DOI: 10.1007/978-3-319-79099-2_1. (Visited on 06/08/2024).

[133] Prusinkiewicz, P. and Runions, A. 'Computational Models of Plant Development and Form'. In: *New Phytologist* 193.3 (2012), pp. 549–569. ISSN: 1469-8137. DOI: 10.1111/j.1469-8137.2011.04009.x. (Visited on 06/08/2024).

[134] Palubicki, W., Horel, K., Longay, S., Runions, A. and Lane, B. 'Self-Organizing Tree Models for Image Synthesis'. In: *ACM Transactions on Graphics* 28 (1st Apr. 2009), pp. 1–10. DOI: 10.1145/1531326.1531364.

[135] Routier-Kierzkowska, A.-L. and Runions, A. 'Modeling Plant Morphogenesis: An Introduction'. In: *Plant Biomechanics: From Structure to Function at Multiple Scales*. Ed. by A. Geitmann and J. Gril. Cham: Springer International Publishing, 2018, pp. 165–192. ISBN: 978-3-319-79099-2. DOI: 10.1007/978-3-319-79099-2_8. (Visited on 06/08/2024).

[136] *PEFC - Programme for the Endorsement of Forest Certification*. URL: https://www.pefc.org/ (visited on 13/11/2024).

[137] States, F. S. C.-U. *FSC Certification*. FSC United States. URL: https://us.fsc.org:443/en-us/certification (visited on 13/11/2024).

[138] *Regulation - 995/2010 - EN - EU Timber Regulation - EUR-Lex*. URL: https://eur-lex.europa.eu/eli/reg/2010/995/oj/eng (visited on 23/05/2025).

[139] Wilson, K. (*The Anatomy of Wood, Its Diversity and Variability*. London : Stobart, 1986. 330 pp. ISBN: 978-0-85442-033-9 978-0-85442-034-6. URL: http://archive.org/details/anatomyofwoodits0000wils (visited on 15/11/2024).

[140] Wagenführ, R. *Anatomie des Holzes: Unter besonderer Berücksichtigung der Holztechnik*. Leinfelden-Echterdingen, 1999. 190 pp. ISBN: 978-3-87181-351-1.

[141] Spatz, H.-C. and Bruechert, F. 'Basic Biomechanics of Self-Supporting Plants: Wind Loads and Gravitational Loads on a Norway Spruce Tree'. In: *Forest Ecology and Management* 135 (1st Jan. 2000), pp. 33–44. DOI: 10.1016/S0378-1127(00)00296-6. (Visited on 06/08/2024).

[142] Niklas, K. J. *Plant Biomechanics: An Engineering Approach to Plant Form and Function*. Chicago, IL: University of Chicago Press, Aug. 1992. 622 pp. ISBN: 978-0-226-58631-1. URL: https://press.uchicago.edu/ucp/books/book/chicago/P/bo3631132.html (visited on 06/08/2024).

[143] Fritts, H. *Tree Rings and Climate*. Academic Press, London, 1976. 567 pp.

[144] Braun, H. *Bau und Leben der Bäume*. Freiburg im Breisgau: Rombach, 1998. 303 pp.

[145] Bamber, R. K. 'A General Theory for the Origin of Growth Stresses in Reaction Wood: How Trees Stay Upright'. In: *IAWA Journal* 22.3 (2001), pp. 205–212. ISSN: 0928-1541, 2294-1932. DOI: 10.1163/22941932-90000279. (Visited on 19/02/2020).

[146] Kwon, M., Bedgar, D. L., Piastuch, W., Davin, L. B. and Lewis, N. G. 'Induced Compression Wood Formation in Douglas Fir (Pseudotsuga Menziesii) in Microgravity'. In: *Phytochemistry* 57.6 (July 2001), pp. 847–857. ISSN: 00319422. DOI: 10.1016/S0031-9422(01)00145-5. (Visited on 19/02/2020).

[147] Goetz, K. *Die innere Optimierung der Bäume als Vorbild für technische Faserverbunde - eine lokale Approximation*. Wissenschaftliche Berichte FZKA 6552. Karlsruhe: Forschungszentrum Karlsruhe GmbH, 2000. DOI: 10.5445/IR/7502000. (Visited on 17/02/2022).

[148] Moreno Gata, K., Musto, J. and Trautz, M. 'Growing Construction Components - Design and Simulation Strategy for Self-Formation Following Tree Growth'. In: *Werner, L and Koering, D (Eds.), Anthropologic: Architecture and Fabrication in the Cognitive Age - Proceedings of the 38th eCAADe Conference - Volume 2, TU Berlin, Berlin, Germany, 16-18 September 2020, Pp. 51-59*. CUMINCAD, 2020. URL: http://papers.cumincad.org/cgi-bin/works/paper/ecaade2020_312 (visited on 10/02/2021).

[149] Wessolly, L. and Erb, M. *Handbuch der Baumstatik und Baumkontrolle*. Berlin-Hannover: Patzer Verlag, 2014. ISBN: 978-3-87617-128-9.

[150] Sterken, P. *A Guide For Tree-stability Analysis_First Print Edition*. 1st Jan. 2005. ISBN: 978-90-90-19377-9.

[151] *Inside Wood - Modern Hardwood Menu*. URL: https://insidewood.lib.ncsu.edu/menu/type/MH?3 (visited on 17/11/2024).

[152] Catmull, E. and Clark, J. 'Recursively Generated B-spline Surfaces on Arbitrary Topological Meshes'. In: *Computer-Aided Design* 10.6 (1st Nov. 1978), pp. 350–355. ISSN: 0010-4485. DOI: 10.1016/0010-4485(78)90110-0. (Visited on 15/03/2025).

[153] Loop, C. 'Smooth Subdivision Surfaces Based on Triangles'. In: (1st Jan. 1987). URL: https://www.microsoft.com/en-us/research/publication/smooth-subdivision-surfaces-based-on-triangles/ (visited on 15/03/2025).

[154] *Doo–Sabin Subdivision Surface*. In: *Wikipedia*. 23rd July 2022. URL: https://en.wikipedia.org/w/index.php?title=Doo%E2%80%93Sabin_subdivision_surface&oldid=1099884170 (visited on 15/03/2025).

[155] *NX-Software | Siemens Software*. Siemens Digital Industries Software. URL: https://plm.sw.siemens.com/de-DE/nx/ (visited on 15/03/2025).

[156] *Autodesk Fusion | 3D CAD, CAM, CAE, & PCB Cloud-Based Software | Autodesk*. URL: https://www.autodesk.com/products/fusion-360/overview (visited on 15/03/2025).

[157] *CATIA*. Dassault Systèmes. 13th Dec. 2023. URL: https://www.3ds.com/products/catia (visited on 15/03/2025).

[158] Piegl, L. and Tiller, W. *The NURBS Book*. Monographs in Visual Communications. Berlin, Heidelberg: Springer, 1995. ISBN: 978-3-642-97387-1 978-3-642-97385-7. DOI: 10.1007/978-3-642-97385-7. (Visited on 25/03/2025).

[159] Grimson, E. L. W. *From Images to Surfaces: A Computational Study of the Human Early Visual System*. Cambridge, MA, USA: MIT Press, Oct. 1981. 274 pp. ISBN: 978-0-262-07083-6.

[160] Debevec, P. E., Taylor, C. J. and Malik, J. 'Modeling and Rendering Architecture from Photographs: A Hybrid Geometry- and Image-Based Approach'. In: *Proceedings of the 23rd Annual Conference on Computer Graphics and Interactive Techniques*. SIGGRAPH '96. New York, NY, USA: Association for Computing Machinery, 1st Aug. 1996, pp. 11–20. ISBN: 978-0-89791-746-9. DOI: 10.1145/237170.237191. (Visited on 25/03/2025).

[161] Habbecke, M. and Kobbelt, L. 'An Intuitive Interface for Interactive High Quality Image-Based Modeling'. In: *Comput. Graph. Forum* 28 (1st Oct. 2009), pp. 1765–1772. DOI: 10.1111/j.1467-8659.2009.01553.x.

[162] Moreno Gata, K. and Echeverría Valiente, E. 'The Use of Digital Tools for the Preservation of Architectural, Artistic and Cultural Heritage, through Three-Dimensional Scanning and Digital Manufacturing'. In: *The International Archives of the Photogrammetry, Remote Sensing and Spatial Information Sciences* (8th Feb. 2019). ISSN: 1682-1750. DOI: 10.5194/isprs-archives-XLII-2-W9-501-2019.

[163] Seidel, D., Ehbrecht, M., Dorji, Y., Jambay, J., Ammer, C. and Annighöfer, P. 'Identifying Architectural Characteristics That Determine Tree Structural Complexity'. In: *Trees* 33.3 (June 2019), pp. 911–919. ISSN: 0931-1890, 1432-2285. DOI: 10.1007/s00468-019-01827-4. (Visited on 19/09/2024).

[164] Seidel, D., Ehbrecht, M., Annighöfer, P. and Ammer, C. 'From Tree to Stand-Level Structural Complexity—Which Properties Make a Forest Stand Complex?' In: *Agricultural and Forest Meteorology* 278 (2019), p. 107699. URL: https://www.sciencedirect.com/science/article/pii/S0168192319303156 (visited on 19/09/2024).

[165] Messier, C., Puettmann, K. J. and Coates, K. D., eds. *Managing Forests as Complex Adaptive Systems: Building Resilience to the Challenge of Global Change*. London: Routledge, 11th Feb. 2013. 368 pp. ISBN: 978-0-203-12280-8. DOI: 10.4324/9780203122808.

[166] Lindenmayer, D. B. and Franklin, J. F. *Conserving Forest Biodiversity: A Comprehensive Multiscaled Approach*. Island Press, 10th Apr. 2013. 368 pp. ISBN: 978-1-59726-853-0. Google Books: gOQq4jcEvTQC.

[167] *PEFC in Nordrhein-Westfalen*. URL: https://pefc.de/waldbesitzende/pefc-in-meiner-region/pefc-in-nordrhein-westfalen/ (visited on 18/03/2025).

[168] *Normals\Compute - CloudCompareWiki*. URL: https://cloudcompare.org/doc/wiki/index.php?title=Normals%5CCompute (visited on 24/10/2024).

[169] Kazhdan, M., Bolitho, M. and Hoppe, H. 'Poisson Surface Reconstruction'. In: (Eurographics Symposium on Geometry Processing 2006). URL: https://github.com/mkazhdan/PoissonRecon.

[170] Moreno Gata, K., Spahn, F., Klinkel, S. and Trautz, M. 'Geometrical Analysis of Naturally Grown Timber for the Design of Load-Bearing Structures'. In: *Research Directions: Biotechnology Design* 2.e19 (2024). ISSN: 2752-9452. DOI: 10.1017/btd.2024.12.

[171] Adobe Inc. *Adobe Photoshop*. Version CC 2019. 6th Mar. 2019. URL: https://www.adobe.com/products/photoshop.html.

[172] Niemz, P. and Sonderegger, W. U. *Holzphysik: Eigenschaften, Prüfung und Kennwerte*. Carl Hanser Verlag GmbH Co KG, 6th Sept. 2021. 590 pp. ISBN: 978-3-446-47010-1.

[173] Niemz, P., Teischinger, A. and Sandberg, D., eds. *Springer Handbook of Wood Science and Technology*. Springer Handbooks. Cham: Springer International Publishing, 2023. ISBN: 978-3-030-81314-7 978-3-030-81315-4. DOI: 10.1007/978-3-030-81315-4. (Visited on 05/03/2024).

[174] Michajlova, K., Gejdoš, M., Gergeľ, T. and Gretsch, D. 'Evaluation of the Quality of Standing Trees Using an Arbotom Acoustic Stress Tomograph'. In: *Central European Forestry Journal* 71 (6th Feb. 2025), pp. 65–72. DOI: 10.2478/forj-2024-0019.

[175] Huber, J. A. J., Broman, O., Ekevad, M., Oja, J. and Hansson, L. 'A Method for Generating Finite Element Models of Wood Boards from X-ray Computed Tomography Scans'. In: *Computers & structures* 260 (2022). URL: https://urn.kb.se/resolve?urn=urn:nbn:se:ltu:diva-84593 (visited on 27/12/2023).

[176] Zipse, A. *Untersuchungen zur lastgesteuerten Festigkeitsverteilung in Bäumen*. Forschungszentrum Karlsruhe: Institut für Materialforschung, 1997, p. 109.

[177] Kleinschmit von Lengefeld, A. N. 'Untersuchungen Zur Hochauflösenden Bestimmung von Qualitätsbeeinflussenden Rundholzmerkmalen Am Beispiel von Fichten- Und Buchenholz'. Technische Universität München, 2005. URL: https://mediatum.ub.tum.de/603660 (visited on 30/03/2022).

[178] Matsuo-Ueda, M. et al. 'Comprehensive Study of Distributions of Residual Stress and Young's Modulus in Large-Diameter Sugi (Cryptomeria Japonica) Log'. In: *Wood Science and Technology* 56.2 (Mar. 2022), pp. 573–588. ISSN: 0043-7719, 1432-5225. DOI: 10.1007/s00226-022-01360-7. (Visited on 31/10/2023).

[179] Dupré, S. *Experimentelle Untersuchung zur schadensfreienErmittlung relevanter Materialkenngrößennatürlich gewachsener Holzelemente*. Bachelor Thesis. Aachen: RWTH Aachen University: Publikationsserver der RWTH, 2025.

[180] Trautz, M., Moreno Gata, K., Spahn, F. and Klinkel, S. 'Bauen mit Rohholz'. In: Baustatik – Baupraxis 15. Technische Universität Hamburg: Institut für Baustatik, 2024, pp. 447–455. ISBN: 978-3-00-077808-7. URL: https://www.bb15.baustatik-baupraxis.de/Anmeldung/Upload/PDF/945879d9.pdf.

[181] Mattheck, C. 'DESIGN AND GROWTH RULES FOR BIOLOGICAL STRUCTURES AND THEIR APPLICATION TO ENGINEERING'. In: *Fatigue & Fracture of Engineering Materials & Structures* 13.5 (Sept. 1990), pp. 535–550. ISSN: 8756-758X, 1460-2695. DOI: 10.1111/j.1460-2695.1990.tb00623.x. (Visited on 05/11/2024).

[182] *DIN 52186 - Testing of Wood; Bending Test*. 1978. URL: https://nautos.de/7TE/search/item-detail/DE00005342 (visited on 24/05/2025).

[183] *DIN EN 14251 - Structural Round Timber - Test Methods;* 2022. URL: https://nautos.de/7TE/search/item-detail/DE30095616 (visited on 24/05/2025).

[184] *DIN EN 408 - Timber Structures – Structural Timber and Glued Laminated Timber – Determination of Some Physical and Mechanical Properties*. 2012. URL: https://nautos.de/7TE/search/item-detail/DE30050071 (visited on 24/05/2025).

[185] *DIN 68364 - Properties of Wood Species - Density, Modulus of Elasticity and Strength*. 2003. URL: https://nautos.de/7TE/search/item-detail/DE30005463 (visited on 24/05/2025).

[186] Schober, K.-U., Hörnel-Metzger, B., Müller, M. L., Schütz, U. and Bender, T. *Teilvorhaben 3: Mechanische Versuche, Sortierung und Zuordnung zu Festigkeitsklassen der Rohholzressource Laubschwachholz*. Forschungsgruppe Holz und Kunststoffe: Hochschule Mainz - University of Applied Sciences, 2023.

[187] Blaß, H. J. and Frese, M. *Dauerhaftes Laubrundholz Für Holzbauwerke - Grundlagen Für Die Bemessung*. KIT Scientific Publishing, 5th Aug. 2013. ISBN: 978-3-7315-0062-9. DOI: 10.5445/KSP/1000035706. (Visited on 15/11/2024).

[188] Rais, A., Kovryga, A., Pretzsch, H. and Van De Kuilen, J.-W. G. 'Timber Tensile Strength in Mixed Stands of European Beech (Fagus Sylvatica L.)' In: *Wood Science and Technology* 56.4 (July 2022), pp. 1239–1259. ISSN: 0043-7719, 1432-5225. DOI: 10.1007/s00226-022-01398-7. (Visited on 27/03/2025).

[189] *Azure Kinect GH*. Food4Rhino. 22nd Jan. 2022. URL: https://www.food4rhino.com/en/app/azure-kinect-gh (visited on 24/05/2025).

[190] Senalik, C. A. and Farber, B. 'Chapter 5: Mechanical Properties of Wood'. In: *Wood Handbook—Wood as an Engineering Material*. General Technical Report FPL-GTR-282. Madison, WI: U.S.: Department of Agriculture, Forest Service, Forest Products Laboratory, 2021, pp. 5–46. URL: https://research.fs.usda.gov/treesearch/62244 (visited on 15/11/2024).

[191] Watanabe, U., Norimoto, M., Ohgama, T. and Fujita, M. 'Tangential Youngs Modulus of Coniferous Early Wood Investigated Using Cell Models'. In: *Holzforschung* 53.2 (1st Mar. 1999), pp. 209–214. ISSN: 0018-3830. DOI: 10.1515/HF.1999.035. (Visited on 15/11/2024).

[192] Niklas, K. J. and Spatz, H.-C. 'Worldwide Correlations of Mechanical Properties and Green Wood Density'. In: *American Journal of Botany* 97.10 (Oct. 2010), pp. 1587–1594. ISSN: 0002-9122, 1537-2197. DOI: 10.3732/ajb.1000150. (Visited on 15/11/2024).

[193] Preisinger, C. and Heimrath, M. 'Karamba—A Toolkit for Parametric Structural Design'. In: *Structural Engineering International* 24 (1st May 2014). DOI: 10.2749/101686614X13830790993483.

[194] Moreno Gata, K., Amtsberg, F., Stephens, S. W., Menges, A. and Trautz, M. 'Integrating Naturally Grown Timber in Sandwich Timber Panels'. In: *Scalable Disruptors*. Ed. by P. Eversmann, C. Gengnagel, J. Lienhard, M. Ramsgaard Thomsen and J. Wurm. Cham: Springer Nature Switzerland, 2024, pp. 81–93. ISBN: 978-3-031-68275-9. DOI: 10.1007/978-3-031-68275-9_7.

[195] *Octopus*. Food4Rhino. 6th Dec. 2012. URL: https://www.food4rhino.com/en/app/octopus (visited on 02/05/2025).

[196] Vierlinger, R. 'Multi Objective Design Interface'. 22nd Apr. 2013. DOI: 10.13140/RG.2.1.3401.0324.

[197] Spahn, F., Moreno Gata, K., Trautz, M. and Klinkel, S. 'Generalised Scaled Boundary Isogeometric Analysis – a Method for Structural Analysis of Naturally Shaped Timber Structures'. In: *Wood Material Science & Engineering* 0.0 (2024), pp. 1–13. ISSN: 1748-0272. DOI: 10.1080/17480272.2024.2323590.

[198] Spahn, F., Moreno Gata, K., Trautz, M. and Klinkel, S. 'Einsatz von Rohholzelementen Für Tragende Strukturen Und Mechanische Analyse Mittels Bildbasierter Simulationsverfahren/Application of Raw Wood Elements for Load-Bearing Structures and Mechanical Analysis Using Image-Based Simulation Methods'. In: *Bauingenieur* 99 (1st Jan. 2024), pp. 109–116. DOI: 10.37544/0005-6650-2024-04-41.

[199] Engel, H. and Rapson, R. *Tragsysteme / Structure Systems*. 1st edition. Ostfildern: Hatje Cantz Verlag, 4th Oct. 2006. 352 pp. ISBN: 978-3-7757-1876-9.

[200] Wages, V. R. *Baumbasierte Holzkonstruktionen*. Bachelor Thesis RWTH-2023-12156. Lehrstuhl für Tragkonstruktionen, 2022. URL: https://publications.rwth-aachen.de/record/975652 (visited on 22/12/2023).

[201] Schepers, J., Herscu, M. and Brandis, J. *IKON | Robotic Timber Studio*. 2025. URL: https://ikon-institute.com/lehre/robotic-timber-studio (visited on 23/05/2025).

[202] Vercruysse, E., Davies, K. and Solly, J. 'A FOREST DATUM The Use of Crown Timber in a Structural System'. In: *IASS Annual Symposium 2025: The Living Past as a Source of Innovation*. IASS. Mexico City: UNAM, Nov. 2025.

[203] *Field Station – Hooke Park*. URL: https://hookepark.aaschool.ac.uk/portfolio/field-station/ (visited on 23/05/2025).

[204] *Hooke Park – AA School's Woodland Campus*. URL: https://hookepark.aaschool.ac.uk/ (visited on 23/05/2025).

[205] Gujejiani, K., Frieling, O., Boldt, J. and Melzer, L.-M. *IKON | Robotic Timber Studio*. 2025. URL: https://ikon-institute.com/lehre/robotic-timber-studio (visited on 23/05/2025).

[206] Bell, P. W. R. 'Wooden Structures by G. G. Karlsen and the Derevyagin Beam'. In: *History of Construction Cultures Volume 1*. CRC Press, 2021. ISBN: 978-1-003-17335-9.

[207] Stephens, S. W. 'Holzbauremapped.' Aachen: RWTH Aachen University, 2024. 1 p.

[208] Suliman, R. *Strukturelle Knoten aus zusammengesetzten Astgabeln: Untersuchung und Entwicklung eines adaptiven Bausystems aus natürlich gewachsenen Rohholzteilen*. Aachen: RWTH Aachen University, 2024.

[209] Trautz, M. and Koj, C. 'Self-Tapping Screws as Reinforcement for Timber Structures'. In: *Evolution and Trends in Design, Analysis and Construction of Shell and Spatial Structures*. IASS Symposium 2009: Evolution and Trends in Design, Analysis and Construction of Shell and Spatial Structures. Valencia: Ed. UPV, 2009.

[210] Koj, C. and Trautz, M. 'Mit Schrauben fügen und bewehren – Langzeitversuche an biegesteifen Rahmenecken im Außenklima'. In: *Bautechnik* 91.1 (2014), pp. 38–45. ISSN: 1437-0999. DOI: 10.1002/bate.201300077. (Visited on 01/07/2025).

[211] Chen, L., Simeon, B. and Klinkel, S. 'A NURBS Based Galerkin Approach for the Analysis of Solids in Boundary Representation'. In: *Computer Methods in Applied Mechanics and Engineering* 305 (June 2016), pp. 777–805. ISSN: 00457825. DOI: 10.1016/j.cma.2016.03.019. (Visited on 29/12/2023).

[212] Zschäbitz, T., Vaculik, S., Matschei, T., Seiter, A., Trautz, M., Cooman, K. D. and Bekemans, L. 'Bond Behaviour of Wood Reinforcement in a Clay Matrix'. In: *Structures and Architecture*. CRC Press, 2025. ISBN: 978-1-003-65864-1.

[213] *Alphacam Version 2022*. Neu-Isenburg, Germany: Hexagon. URL: https://de.alphacam.com/.

[214] Mitterberger, D., Dörfler, K., Sandy, T., Salveridou, F., Hutter, M., Gramazio, F. and Kohler, M. 'Augmented Bricklaying: Human–Machine Interaction for in Situ Assembly of Complex Brickwork Using Object-Aware Augmented Reality'. In: *Construction Robotics* 4 (2020), pp. 151–161.

[215] Jahn, G., Newnham, C. and van den Berg, N. 'Augmented Reality for Construction from Steam-Bent Timber'. In: *Proceedings of the 27th Conference on Computer Aided Architectural Design Research in Asia (CAADRIA)*. Vol. 2. 2022, pp. 191–200.

[216] Yang, X., Amtsberg, F., Skoury, L., Wagner, H. J. and Menges, A. 'VIZOR: Facilitating Cyber-Physical Workflows in Prefabrication through Augmented Reality'. In: *Proceedings of the 27th Conference on Computer Aided Architectural Design Research in Asia (CAADRIA)*. Vol. 2. 2022, pp. 141–150.

[217] Spahn, F., Kolisch, F., Praster, M., Balmayor, E. R. and Klinkel, S. 'Isotropic Growth Model for Generalized Scaled Boundary Isogeometric Analysis on Slender Structures'. In: *PAMM* 24.2 (Aug. 2024), e202400200. ISSN: 1617-7061, 1617-7061. DOI: 10.1002/pamm.202400200. (Visited on 15/05/2025).

[218] Moreno Gata, K., Musto, J., Pranjic, A. and Trautz, M. 'STUDY AND SIMULATION OF SELF-FORMATION FOR LOCAL TREE GROWTH'. In: *World Conference on Timber Engineering*. WCTE 2021. Curran Associates, Inc., pp. 2726–2732. ISBN: 978-1-7138-4097-8.

[219] Mattheck, C. and Kubler, H. *Wood - The Internal Optimization of Trees*. Springer Series in Wood Science. Berlin, Heidelberg: Springer Berlin Heidelberg, 1997. ISBN: 978-3-540-62019-8 978-3-642-61219-0. DOI: 10.1007/978-3-642-61219-0. (Visited on 12/12/2023).

[220] *Eurocode 5: Design of Timber Structures | Eurocodes: Building the Future*. URL: https://eurocodes.jrc.ec.europa.eu/EN-Eurocodes/eurocode-5-design-timber-structures (visited on 08/02/2024).

[221] Moreno Gata, K., Grizmann, D. and Trautz, M. 'Guiding the Tree Growth for Timber Structures Design'. In: World Conference on Timber Engineering 2021, WCTE 2021. 2021, pp. 345–350. URL: https://www.proceedings.com/61811.html.

[222] Suliman, R., Moreno Gata, K. and Trautz, M. 'Structural Nodes from Composite Tree Bifurcations: Investigation and Development of an Adaptive Construction System from Naturally Grown Raw Wood Members'. In: *The 7th International Conference on Computational Design and Robotic Fabrication (CDRF2025)*. Shanghai, 2025.

List of Figures

1.1 Interaction between disciplines. The themes are addressed at varying levels of depth throughout the thesis. . . . 5

1.2 Forest and material acquisition. . . . 14

1.3 Stages in dumping site recycling. . . . 14

2.1 Chapter Diagram: Overview of the domains covered in the state-of-the-art review. 15

2.2 Integration of the thesis (in blue) into the existing supply chain to optimize the use of raw wood in the construction industry. . . . 39

3.1 Chapter Diagram: Determination of areas and the connection. . . . 41

3.2 From raw timber branch geometry to structural application. Transition from natural form acquisition to construction-oriented modeling. . . . 42

3.3 Illustration of primary and secondary growth types in trees, including volume growth. Adapted from [148]. . . . 43

3.4 Illustration of primary growth logic based on the L-System defined in [84]. . . . 44

3.5 Secondary growth illustrated through thickening of the cross-section based on the moment of inertia for each segment of the tree. . . . 44

3.6 Tension and compression wood distribution across a tree cross-section, illustrating shifts in center of mass and structural adaptation as biomass increases. . 45

3.7 Observation of growth areas related to tree statics in a "Conifer-like" scheme. Picture adapted from [148]. . . . 46

3.8 Comparison visible reaction wood growth zones in trees. . . . 46

3.9 Classic tree diagram: differentiation of *knots/forks* or bifurcations, *crooked* or curved, and straight branches. . . . 48

3.10 Integration of Image-Based Data Acquisition and NURBS Modeling. . . . 50

3.11 Point cloud database from Hainich [163, 164], visualized with color height map. 51

3.12 Mixed forest study locations. . . . 53

3.13 Point cloud dataset of edge trees. 53
3.14 Overview of raw timber specimens used in modeling and construction studies. . 54
3.15 Example of a state of the art process of 3d acquisition of a pine tree (*Example 01*) in the Entrepeñas reservoir using the Photogrammetry NeRFs Luma software [94] (date July 9, 2024). 54
3.16 Scan of the oak tree *Edge Tree06*, located in the Zweifall forest, obtained using Polycam software [95] and visualized through Gaussian Splattings (date March 19, 2025). 55
3.17 Poisson surface mesh computation of *Example 01* in Fig. 3.15. 57
3.18 Mesh retopology and packed faces hierarchy. 57
3.19 Hierarchical retopology based on packed faces. 58
3.20 Processed NURBS from the QSM hierarchy applied to of *Example 01* in Fig. 3.15 with basic modeling. 59
3.21 Design workflow of the tree modeling process. 60
3.22 Computation of forest trees. Example from PointCloud in Figure 3.13. 61
3.23 Hierarchical structure of the tree 62
3.24 Geometric reference calculations: branch-level segmentation and curvature; cross-sectional diameter and eccentricity. 64
3.25 Workflow diagram of the analysis algorithm for geometry segmentation and metric extraction. 65
3.26 Comparison of extracted volumes from point cloud data using QSM for branch volume calculation. 67
3.27 Visualization of growth vectors projected onto the horizontal plane, scaled according to tree volume. The figure displays directional growth tendencies extracted from forest quadrat analysis. 68
3.28 Automation of Bounding Boxes with Minimal Volume and 2D Realignment. Global and local coordinates. 70
3.29 Geometric analysis workflow of a naturally curved timber element. 71
3.30 Geometric analysis workflow a naturally bifurcated timber element. 73
3.31 3D Timber element segmentation for 2D elements, followed by planning their top and bottom. 75
3.32 Geometric analysis applied to multiple timber elements c_g^i and conforming the image-based library, where the names S mean straight, C is curved, and K is knot. 75
3.33 Process for macro editing the raw photos. 77
3.34 2D Automation. 77

3.35 Segmentation of branch T-16 (beech specimen) based on bounding box computation. The geometry is divided into two elements using a plane aligned with the working XY plane. This plane, derived from the minimal bounding box, defines 2D working geometry for further analysis and modeling. 78

3.36 Subdivision modeling of a curved timber element 80

3.37 Subdivision modeling of a bifurcated timber element 82

4.1 Chapter Diagram: Linking geometry, growth patterns, and material properties. . 85

4.2 Representative macroscopic features relevant to timber geometry. 86

4.3 Workflow from geometry to material exploration. 88

4.4 Example of a bifurcated specimen exhibiting reaction wood. Left: density distribution from CT imaging. Right: CT longitudinal section showing internal density variation along the diameter. 88

4.5 Adapted model included in the research proposal 89

4.6 Definition of the three centers of the cross-section: Geometric center – centroid–, Growth center, and Center of mass. Polar ray (r) positioning for cross-section analysis. 90

4.7 Visualization of the bifurcation of a small specimen of oak. In red: reference tangent circular geometry with c_G, assuming the tree grows straight. In blue: grown geometry with eccentric displacement of c_g. The production of tension wood can be seen in blue. c_M calculated after applying the derived polynomial density function. 91

4.8 CT material density variation λ along the radius R. λ_i corresponding to every r_i, and λ_m represents the resulting density in the cross-section. Using a polynomial, a formula can be derived, which can then be reapplied to the cross-section from C_G to R_i. 92

4.9 Symmetrized variation of the E-modulus over the cross-section according to [178], in a softwood. Picture extracted from [180]. 93

4.10 From tree geometry to growth analysis and cross-section analysis. 94

4.11 Directional growth and internal stress zones —tension and compression— leading to reaction wood formation in a tree structure. 96

4.12 Testing workflow: From raw timber geometry to specimen properties. 97

4.13 Selection of specimens for testing. Above: the global timber element divided into two specimens for non-destructive testing and off-cuts. Below: extraction of testing samples for material characterization from different zones. 98

4.14 Photographs of the acquired samples. 98

4.15 Material characterization tests. Specimen in Zone 2. 99

4.16 Axonometric view of the testing machine setup, illustrating movable parts and load application points. . . . 101
4.17 Geometric constraints of the bending setup. . . . 102
4.18 Four-point bending test configurations. . . . 102
4.19 Three-point bending and three-point bending testing for bifurcations. . . . 103
4.20 Testing setup with adjustable supports and loading components. . . . 104
4.21 Parametric configuration of the testing setup, including bounding box alignment and load pin positioning. . . . 105
4.22 Point cloud-based calibration of the testing setup. . . . 105
4.24 Testing setup with digital gauges placed at defined cross-section locations. . . . 105
4.23 Photographs of the testing setup. . . . 106
4.25 Three-point bending setup applied to a bifurcated timber specimen. . . . 106
4.26 Volumetric data acquisition setup using Azure Kinect sensor for real-time displacement tracking. . . . 107
4.27 Workflow for point cloud deformation analysis. . . . 107

5.1 Chapter Diagram: Structural Design and Simulation. . . . 111
5.2 Workflow of the structural design process. . . . 112
5.3 Element definitions: straight, curved, and bifurcated. Parameters include endpoints P (modeled as rotational springs), axes (A, B, C), and angles α, β. . . . 113
5.5 Structural modeling of board-based systems sandwich panels. Connections are modeled as pinned joints, analogous to fully threaded screws. Element thickness corresponds to minimum timber diameter D_{min}. . . . 115
5.6 Matching positioning according to structural layout and centerline alignment. . 115
5.7 Joint positioning optimization. . . . 115
5.8 Workflow. Development of the parameterisation of inventory curves. . . . 120
5.10 Examples of static diagrams with articulated or semi-rigid joints . . . 122
5.11 Optimization process of a Vierendeel girder system under multiple load cases. Adaptation from [18]. . . . 124
5.12 Simulation results using SBIGA on raw timber geometries from Fig. 3.30. Figures extracted from [170]. . . . 126

6.1 Chapter Diagram: Classification, joint strategies, and construction demonstrations. . . . 129
6.2 Examples of vertical-linear structural systems. . . . 131

6.3 Examples of vertical-planar systems. . . . 131
6.4 Examples of horizontal-linear structural systems. . . . 132
6.5 Examples of horizontal-planar systems. . . . 132
6.6 Examples of linear arch systems. . . . 133
6.7 Examples of spatial and shell structures. . . . 133
6.8 Automated joint modeling based on the structural and geometrical constrains. . . 135
6.9 Splicing joint types for longitudinal timber connections. . . . 137
6.10 Corner and T-joint configurations for orthogonal timber connections. . . . 138
6.11 Cross joints for intersecting timber elements. . . . 138
6.12 Additional and experimental joints for specific configurations. . . . 139
6.13 Joinery types for sandwich panel assemblies. . . . 139
6.14 Example of the use of raw wood in structural panels. . . . 140
6.15 Comparison CLT and LRS Panels. . . . 141
6.16 Assembly of a timber cabin based on LRS structural panels. . . . 141
6.17 Construction methods catalog. . . . 142
6.18 Built examples of modular prototypes in oak, birch, and birch with OSB, at scale 1:1, based on Fig. 6.17. . . . 142
6.19 Layouting bar-type structure with optimized joint position to raw timber geometries. . . . 143
6.20 Transfer of structural design to construction details, showing hybrid connections for bifurcated nodes in a Vierendeel girder. . . . 143
6.21 Collecting raw material from a tree crown in the forest, followed by documentation. . . . 144
6.22 Structure design process based on raw material. . . . 145
6.23 (LC) 1 and 2 with deformation, and moment, shear and normal forces diagrams. 147
6.24 Static analysis with SBIGA, extracted from [198]. . . . 148
6.25 Design-to-fabrication strategy with adapted joint detailing. . . . 149
6.26 Construction diagrams of the Growing Bridge. . . . 150
6.28 Design to fabrication process. . . . 151
6.29 Resulting fabrication of the interlocking joints for the off-knot connection. . . . 151
6.30 Final assembly showcasing the pedestrian bridge at its mid-term exhibition. . . 152
6.31 State of the bridge in November 2025 . . . 152
6.32 Design of the ReGrowth Pavilion. . . . 154

6.33 Assembly with the timber elements. . . . 154
6.34 Static calculation: (Left) Reference panels with deformation, moment calculation, shear stresses. (Right) Resulting sandwich panels with deformation, moment calculation and shear stresses. . . . 155
6.35 Overlap timber elements following stress directions: Target curves c_t generated from the vector fields $\vec{M}$, and the implementation of the timber elements c_g. . . . 156
6.36 Fabrication steps using CNC milling: element surfacing and interlock milling. . . 158
6.37 Element processing. . . . 158
6.38 Above: Augmented Reality guiding the assembly process. Below: Manual fastening of concealed structural connectors using screws. . . . 159
6.39 Visualization of the timber elements using Augmented Reality during the exhibition. . . . 160

A.1 Workflow for simulating geometrical growth through iterative FEA and geometry adjustment. . . . 200
A.2 Steps in the digital growth simulation pipeline: geometric base generation and corresponding finite element mesh. . . . 201
A.3 FE simulation outputs from Ansys: evaluation of different configurations and loading conditions. . . . 202
A.4 Self-formation results based on internal stress distribution. . . . 202
A.5 Moment in the central region. . . . 203
A.6 Overview of guided growth strategy and system setup used to manipulate young Paulownia trees. . . . 205
A.7 Indoor guided growth experiments demonstrating curvature generation in response to phototropism and passive constraints. . . . 205
A.8 Outdoor observations of three-year-old Paulownia specimens showing base deformation and growth-induced asymmetry. . . . 206

B.1 Tools developed in Grasshopper . . . 207
B.2 Analysis Dataset 1 3.2.3: Global growth vector $\vec{p}$ and main growth by hierarchy. 209
B.3 Analysis Dataset 1 3.2.3: Global growth vector $\vec{p}$ and main growth by hierarchy. 210
B.4 Tree Growth Analysis Dataset 2 3.2.3. . . . 211
B.5 Tree Growth Analysis Dataset 2 3.2.3. . . . 212
B.6 Tree Growth Analysis Dataset 2 3.2.3. . . . 213
B.7 Tree Growth Analysis Dataset 2 3.2.3. . . . 214
B.8 Tree Growth Analysis Dataset 2 3.2.3. . . . 215

B.9 Tree Growth Analysis Dataset 2 3.2.3. 216

B.10 Growing Bridge timber library, dataset 3 3.2.3. Mesh automation showing eccentricities with color grading. $\|\vec{\delta}_i\|$ evaluate curvature deviation from pith for each specimen. See Section 3.6. 217

B.11 reGrowth Pavilion timber library, dataset 4 3.2.3. Mesh automatization with dimensions and growth vector. See Section 3.5. 218

B.12 Micro-CT scans of timber specimens, showing outer surfaces and internal high-density structures across 8 samples. 219

B.13 Macro-CT image set (1/2) showing outer surfaces and internal high-density structures of specimens. 220

B.14 Macro-CT image set (2/2) showing outer surfaces and internal high-density structures of specimens. 221

B.15 Prototype tests and construction: material experiments, joinery detailing, and assembly phases. 223

B.16 Design concept for a sandwich base table. 224

B.18 Axonometric view of the custom jig for end-joint fabrication. 225

B.19 End-joint milling for bifurcated components. Result shown in Fig. B.15(a). . . 225

B.20 Bridge assembly. 227

B.21 Axonometric view. 228

B.22 Views of the Growing Bridge installation: axonometric and site perspectives. . 229

B.23 Final photos of the Growing Bridge: installation, preparation, transport (Nov 24), and winter condition (Jan 25). 231

B.24 Referent plate analysis. 233

B.25 Assembly plans of the exhibition *reGrowth* at Pop-up Campus, September 2022. 234

B.26 Assembly plans of the exhibition *reGrowth* at Pop-up Campus, September 2022. 235

B.27 Stephens et al. (2024) [207]. Developing a modern half-timbered house using raw timber modeling. 236

B.28 Suliman et al. (2024) [208, 222]. Exploration of non-standard joints in spatial structures. 236

List of Tables

1.1 Overview of domains and associated projects. 10

2.1 Key Concepts in Tree Biomechanics: 34
2.2 Overview of Plant Growth Modeling Approaches: 34
2.3 Quality Classes for Timber Sorting according to RVR: 35
2.4 Timber Supply Chain Based on RVR: 36

5.1 Results: Joint location along each bar under different optimization criteria. Adaptation from [18]. 124

C.1 Research projects conducted during the thesis period. 237
C.2 Submitted research proposals related to raw timber construction. 238
C.3 Supervised Student Works and Thesis Related to the Dissertation. 239
C.4 Supervised Student Works and Thesis Non-related to the Dissertation. 239

Appendix A

Appendix

Project Extensions of the Dissertation

This appendix includes complementary sections related to projects and research branches that extend beyond the core thematic of this dissertation. These explorations maintain relevance to the central focus but have been organized separately to preserve a cohesive narrative throughout the main body of the work.

A.1 Geometrical Growth Simulation

This section introduces a complementary approach that integrates structural design with the study of growth processes through geometric growth simulation. Various material growth models discussed in the literature serve as a conceptual foundation for this method.

A preliminary implementation of a geometric approach to material growth was explored in [217], where isotropic growth—i.e., homogeneous expansion in all directions—was simulated. A potential extension of this approach incorporates directionally defined geometric vectors, offering an alternative interpretation of growth behavior.

In earlier work [148, 218], a basic simulation was carried out by thickening the cross-section of a branch, which is further elaborated here.

A.1.1 Self-Formation Geometry Optimization

The process described here simulates the biological phenomenon of self-formation observed in trees, specifically the thickening of the trunk in response to mechanical stress—commonly referred to as reaction wood. In conifers, this typically occurs in compression zones, whereas in hardwood species it develops in tension zones, corresponding to localized increases in lignin and cellulose production, respectively. This behavior has been studied for decades, with preliminary simulations assuming that the tree internally tends to equalize stress. As shown in [219],

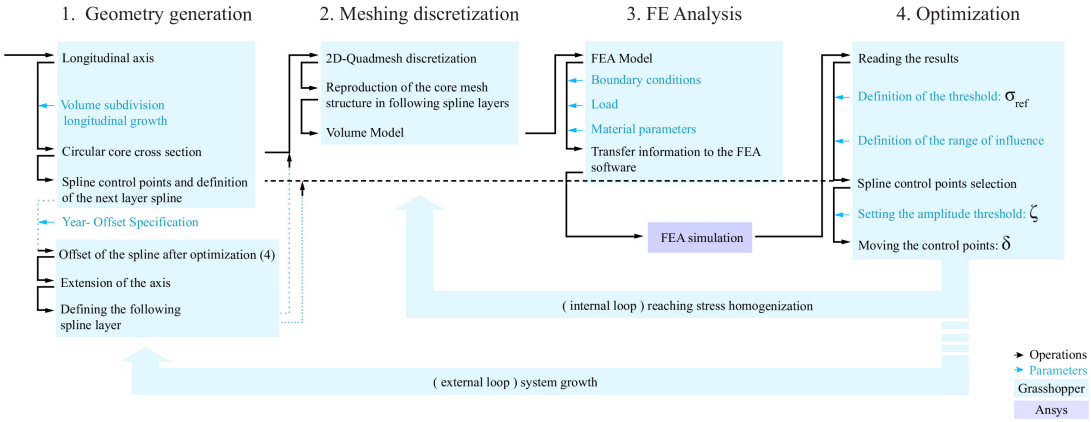

Figure A.1: Workflow for simulating geometrical growth through iterative FEA and geometry adjustment.

previous studies have demonstrated that this adaptive mechanism can be analyzed numerically through simplified mechanical hypotheses.

The simulation workflow consists of the following steps:

1. **Geometry Generation**: Starting from a longitudinal axis (representing the tree stem), a geometric model is created using splines with circular cross-sections, positioned at regular intervals.

2. **Mesh Discretization**: These cross-sectional profiles are used to generate a solid mesh composed of volumetric elements (e.g., parallelepipeds).

3. **Finite Element Analysis (FEA)**: The mesh, including nodes, connectivity, material properties, loads, and support conditions, is imported into the FEA software.

4. **Optimization Loop**: Based on the FEA results, nodes exceeding a predefined stress threshold σ_{ref} are identified. The corresponding control points in the local cross-section are displaced outward by a factor δ, increasing the local geometry to reduce stress. This iterative loop continues until stress is homogenized across the structure.

$$\min_{x \in \Omega} \left\| \frac{\sigma_{\text{vMises}} - \sigma_{\text{ref}}}{\sigma_{\text{ref}}} \right\| \tag{A.1}$$

$$\delta = \left\| \frac{\sigma_{\text{vMises}} - \sigma_{\text{ref}}}{\sigma_{\text{ref}}} \right\| \cdot \zeta \tag{A.2}$$

Optimization criteria, where σ_{vMises} is the von Mises stress result, δ is the displacement of control points, and ζ is the vector amplitude applied to the control points. Once this internal loop converges, the process restarts with new geometry (external loop). Figures A.2 illustrate the geometry and mesh generation stages:

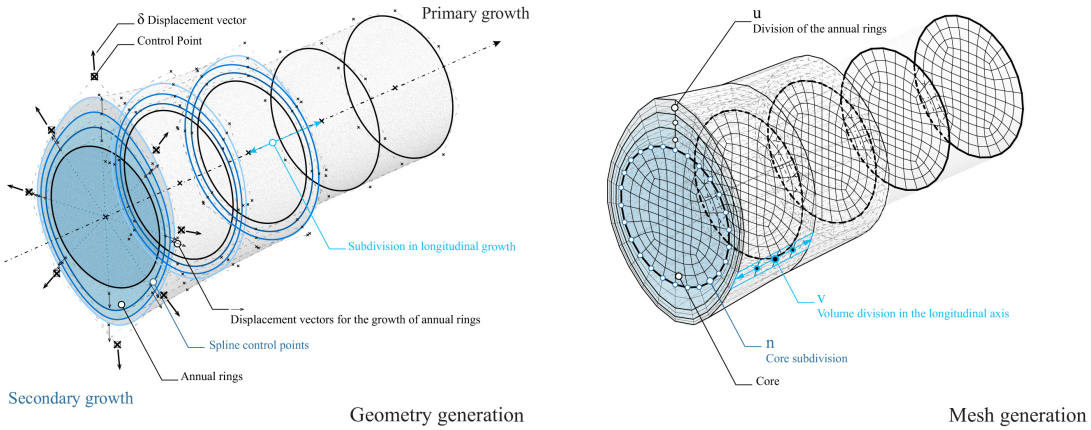

(a) Geometry generation. (b) Mesh generation.

Figure A.2: Steps in the digital growth simulation pipeline: geometric base generation and corresponding finite element mesh.

Following the proposed workflow, two configurations are simulated: one simulating growth based purely on static stress distribution (Fig. A.4(a)) and another simulating reaction wood behavior by restricting geometric expansion to one side of the cross-section (Fig. A.4(b)). Later simulations using this method can incorporate variable material densities—e.g., changing modulus of elasticity E—to reflect more realistic biological composition.

Results Analysis Geometrical Growth Simulation

Static Shape Optimization

The first test simulates pure static shape optimization. Control points are free to move in the plane of each cross-section. Using a model with a 30 mm core and 1000 mm length, the algorithm restricts growth to three cross-sectional rings and a longitudinal extension of 100 mm per external loop. The final geometry assumes an oval shape tending toward rectangularity, with flattened upper and lower faces. Comparing FEA results from the initial and optimized states reveals a significant reduction in peak stress, particularly along the edges.

Reaction Wood-Based Optimization

The second test simulates asymmetric growth, mimicking the behavior of reaction wood in conifers. In this case, geometric expansion is restricted to the lower half of the cross-section, allowing only the control points in that region to move. This produces a material distribution biased toward the compression zone, as illustrated in the asymmetric cross-section in Fig. A.4(b), where the eccentricity between the centerline and the outer geometry becomes visible.

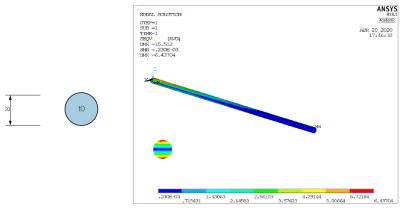

(a) Simulation start: Only the core.

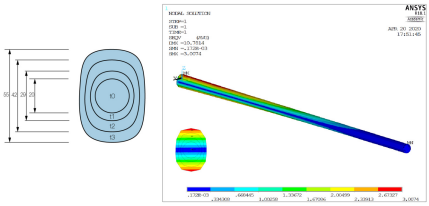

(b) Simulation result 1: Static simulation allow to grow in all directions.

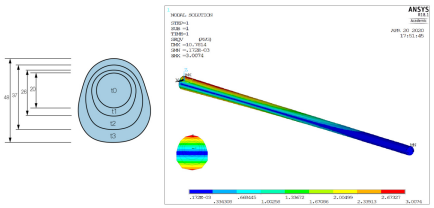

(c) Simulation result 2: "Reaction wood" allow to grow only in compression zone

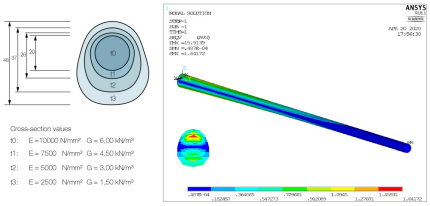

(d) Simulation result 3: Internal stress variability due to different E-Modulus for each section.

Figure A.3: FE simulation outputs from Ansys: evaluation of different configurations and loading conditions.

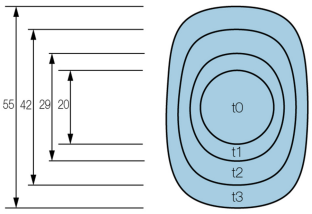

(a) Self-formation mechanism in branches.

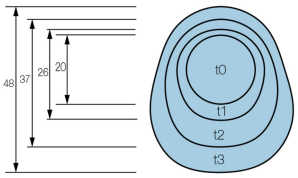

(b) Reaction wood distribution in conifers.

Figure A.4: Self-formation results based on internal stress distribution.

Comparing the two sections, it can be observed that at iteration $t = 3$, the area expands laterally, resulting in an egg-like cross-sectional shape. This change in eccentricity corresponds to a redistribution of material aimed at reducing internal stresses.

A comparative analysis (Fig. A.3) shows that at iteration $t = 3$, maximum cross-sectional stress was reduced by up to 67% in the symmetric case (Fig. A.4(a)) and 54% in the asymmetric case (Fig. A.4(b)), compared to the initial state ($t = 1$), despite a slight increase in overall stress due to lengthening of the geometry.

A.2 Design of a Testing Machine

A.2.1 Calculation of Test Span and Diameter Limits

The following provides a step-by-step derivation used to define span length l and maximum specimen diameter D for four-point bending tests under elastic loading conditions, summarized in Section 4.4.2.

The bending stress in the region of constant moment is defined as:

$$\sigma = \frac{M}{W_y}$$

where M is the bending moment and W_y is the section modulus for a circular cross-section:

$$W_y = \frac{\pi r^3}{4} = \frac{\pi D^3}{32}$$

Substituting into the stress expression:

$$\sigma = \frac{M}{W_y} = \frac{32M}{\pi D^3}$$

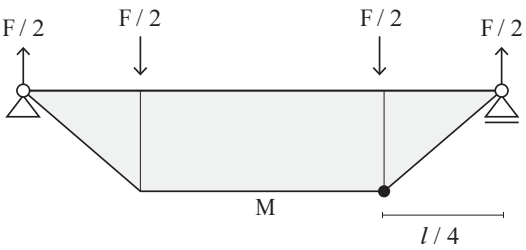

Figure A.5: Moment in the central region.

For a symmetric four-point bending configuration, see Fig. A.5, the moment in the central constant-moment region is:

$$M = \frac{F \cdot l}{8}$$

Substituting into the stress formula:

$$\sigma = \frac{32F \cdot l}{8\pi D^3} = \frac{4F \cdot l}{\pi D^3}$$

Solving for the required span:

$$l = \frac{\pi D^3 \sigma}{4F}$$

To define a design limit within the elastic range, the stress σ is based on:

$$\sigma = \frac{f_m}{\gamma_M} \cdot k_{\text{mod}}$$

where:

- $f_m = 6.0\,\text{kN}\,\text{cm}^{-2}$ is the characteristic bending strength for European beech [188],
- $\gamma_M = 1.5$ is the partial safety factor [220],
- $k_{\text{mod}} = 0.8$ accounts for short-term load duration and moisture content.

This yields:

$$\sigma = \frac{6.0}{1.5} \cdot 0.8 = 3.2\,\text{kN}\,\text{cm}^{-2}$$

Using $D = 10\,\text{cm}$ and $F = 5\,\text{kN}$, the span becomes:

$$l = \frac{\pi \cdot 10^3 \cdot 3.2}{4 \cdot 5000} = 0.50\,\text{m}$$

To evaluate the maximum diameter supported by the system, the test setup constraints are:

$$F_{\text{Max}} = 50\,000\,\text{N}, \quad l = 150\,\text{cm}, \quad \sigma = 320\,\text{N}\,\text{cm}^{-2}$$

Solving the span equation for D:

$$D = \left(\frac{4F \cdot l}{\pi\sigma}\right)^{1/3} = \left(\frac{4 \cdot 50000 \cdot 150}{\pi \cdot 320}\right)^{1/3} = \left(\frac{30000000}{1005.31}\right)^{1/3} = (29837.8)^{1/3} \approx 31.1\,\text{cm}$$

Thus, the maximum admissible diameter for a specimen that can be tested under the given conditions, without exceeding load or span limits, is approximately:

$$D_{\text{max}} < 30\,\text{cm}$$

A.3 Growing Experiments

Guided Growth Research: Tree-Based Structural Formation

The paper [221] presents an experimental framework for guiding tree growth to produce structurally useful components. By manipulating growth conditions—through applied loads, constraints, and environmental parameters—the research aims to generate curvature and branching geometries aligned with structural design needs. The study focuses on *Paulownia Artemis* due to its rapid growth and low density and distinguishes between passive and active guided growth conditions. Passive manipulation leverages natural tropisms (light and gravity), while active strategies apply defined static interventions using mechanical constraints. As shown in Figure A.7, various configurations were implemented using custom positioners and fixtures to influence growth direction, shape, and curvature development. The experiment categorizes structural responses and introduces a methodology to manipulate and classify growth typologies for future architectural applications.

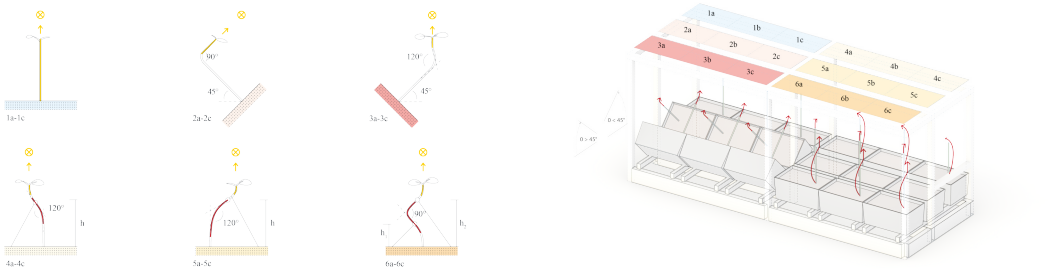

(a) Diagram of guided growth geometries, showing manipulation process

(b) Experimental setup: anchoring, guides, and structural frame

Figure A.6: Overview of guided growth strategy and system setup used to manipulate young Paulownia trees.

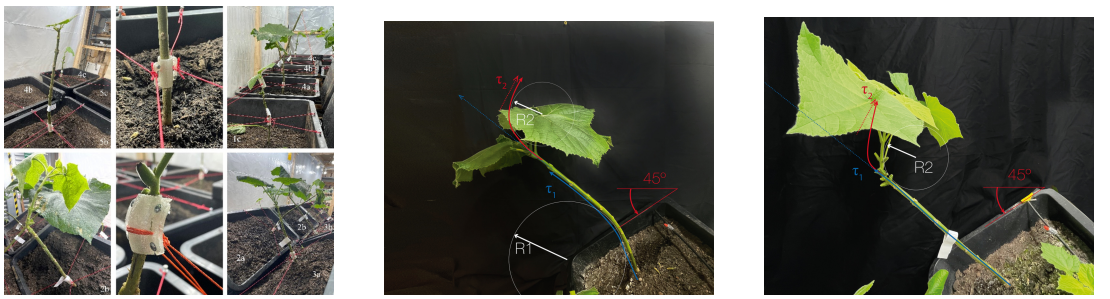

(a) Photographs of various specimens with distinct growth paths

(b) Curvature induced by phototropic behavior under controlled lighting

(c) Comparison of curvature after growth period under controlled deviation

Figure A.7: Indoor guided growth experiments demonstrating curvature generation in response to phototropism and passive constraints.

Subsequent experiments extended the methodology outdoors, monitoring three-year-old Paulownia trees for long-term curvature, section deformation, and cross-sectional deviation. Regular perimeter and height measurements revealed an evolution toward elliptical trunk profiles due to self-weight, asymmetrical growth, and static adaptation. As illustrated in Figure A.8(a), the study documented how natural self-formation processes lead to directional mass redistribution and ovalization of the stem base (Figure A.8(b)). These morphological changes suggest that mild static intervention during early growth stages can influence future material characteristics and structural performance. This approach offers a modeling-based plant growth strategy for producing custom-shaped structural elements.



(a) Outdoor growth setup with older trees

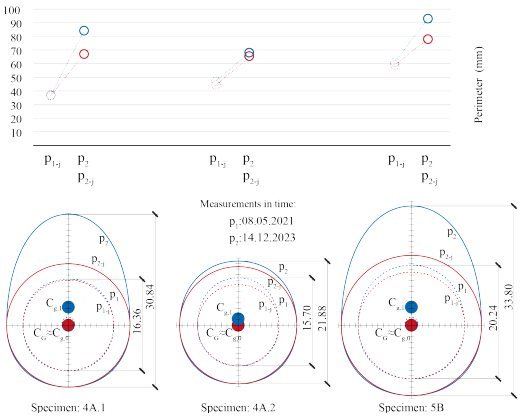

(b) Perimeter deformation indicating base ovalization

Figure A.8: Outdoor observations of three-year-old Paulownia specimens showing base deformation and growth-induced asymmetry.

Appendix B

Technical Material

B.1 Overview

This appendix presents additional developments related to the research, including scripting tools, geometric analysis workflows, supporting pages linked to chapter content, a raw timber element library, experimental setups, and supplementary diagrams.

B.2 List of Technical Applications and Plugins

Overview of tools and scripts developed to automate the geometric processing:

- **Tree QSM Analysis Tool for Grasshopper** Performs hierarchical analysis of trees.
- **Geometric Analysis Tool** Extracts central axes and performs basic segmentation using NURBS.
- **2D Geometric Analysis Tool** Segments 3D splines in 2D, assigning them to individual elements.
- **2D Automation: Data Acquisition for Flat Elements** Nearly flat timber image-based.
- **SubD to NURBS** Converts SubD geometry into segmented NURBS using explicit control.

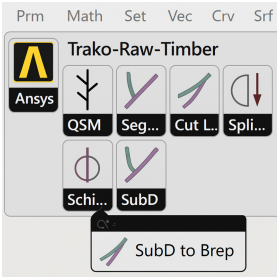

Figure B.1: Tools developed in Grasshopper using C# scripting. The scripts will be made available after the publication of this thesis and its chapters at: github.com/kevinmg12.

B.3 Attached in Chapter 3

B.3.1 Results of Tree Global Growth Analysis

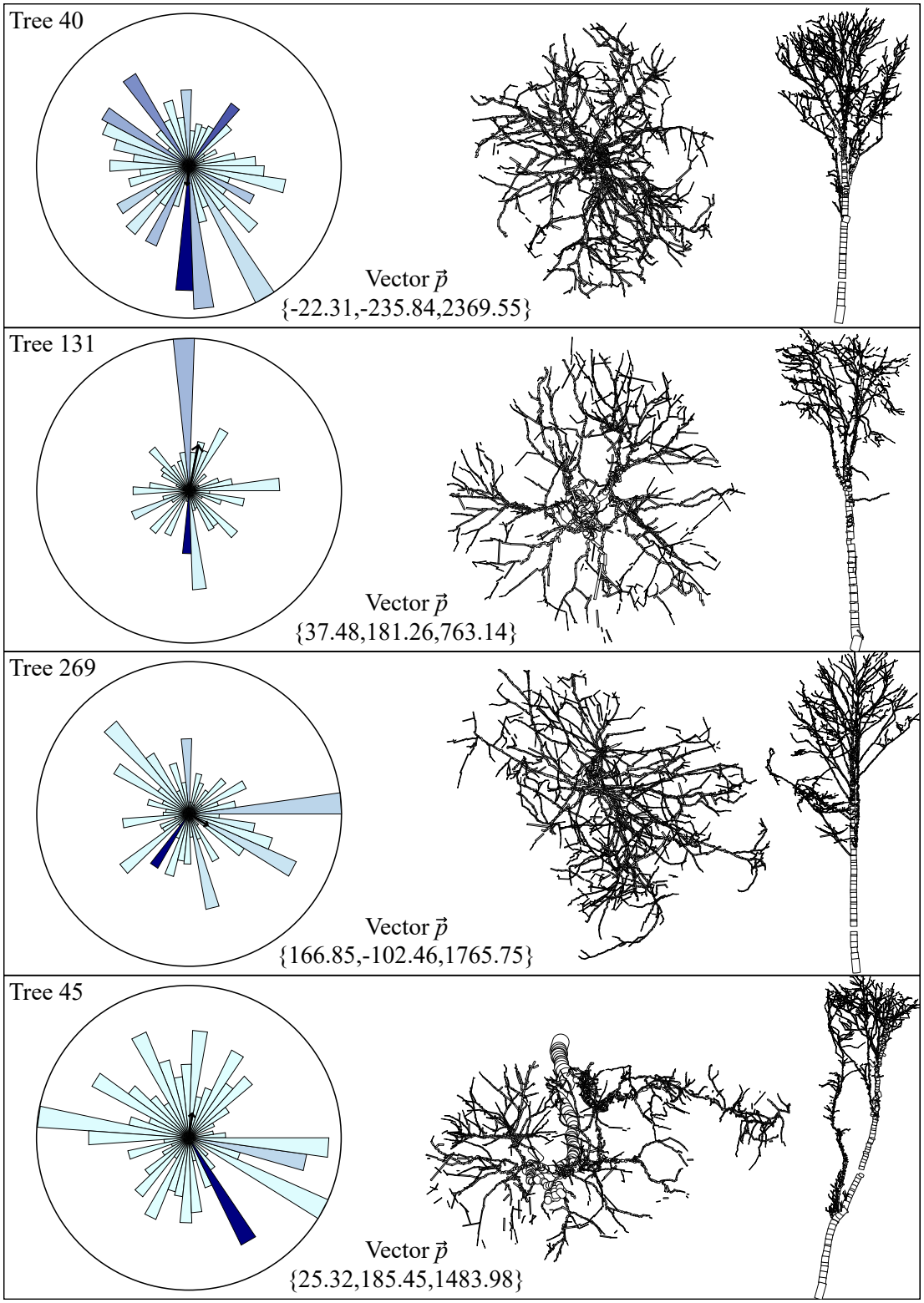

Figure B.2: Analysis Dataset 1 3.2.3: Global growth vector $\vec{p}$ and main growth by hierarchy.

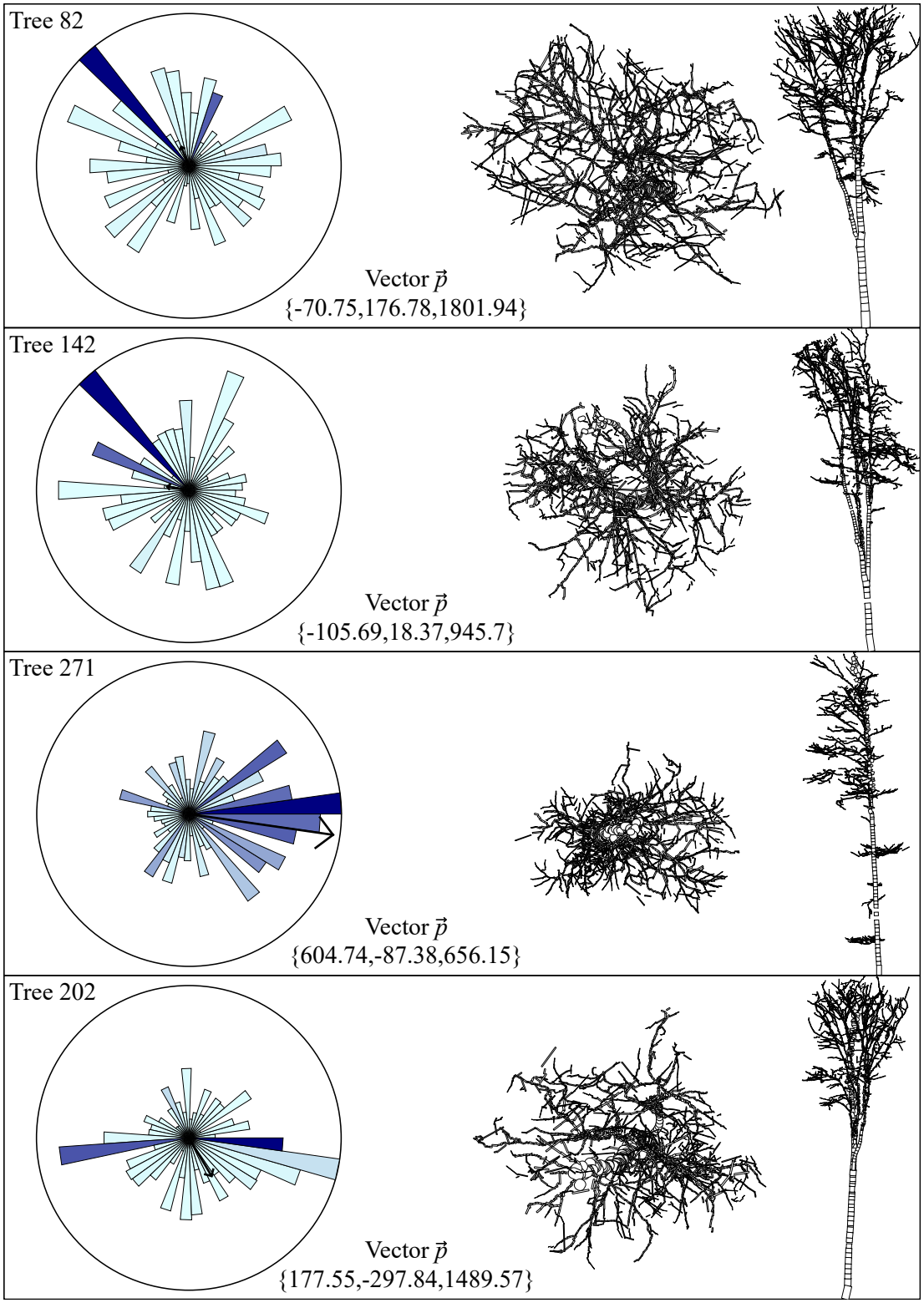

Figure B.3: Analysis Dataset 1 3.2.3: Global growth vector $\vec{p}$ and main growth by hierarchy.

B.3.2 Results of Tree Geometry Analysis and Library

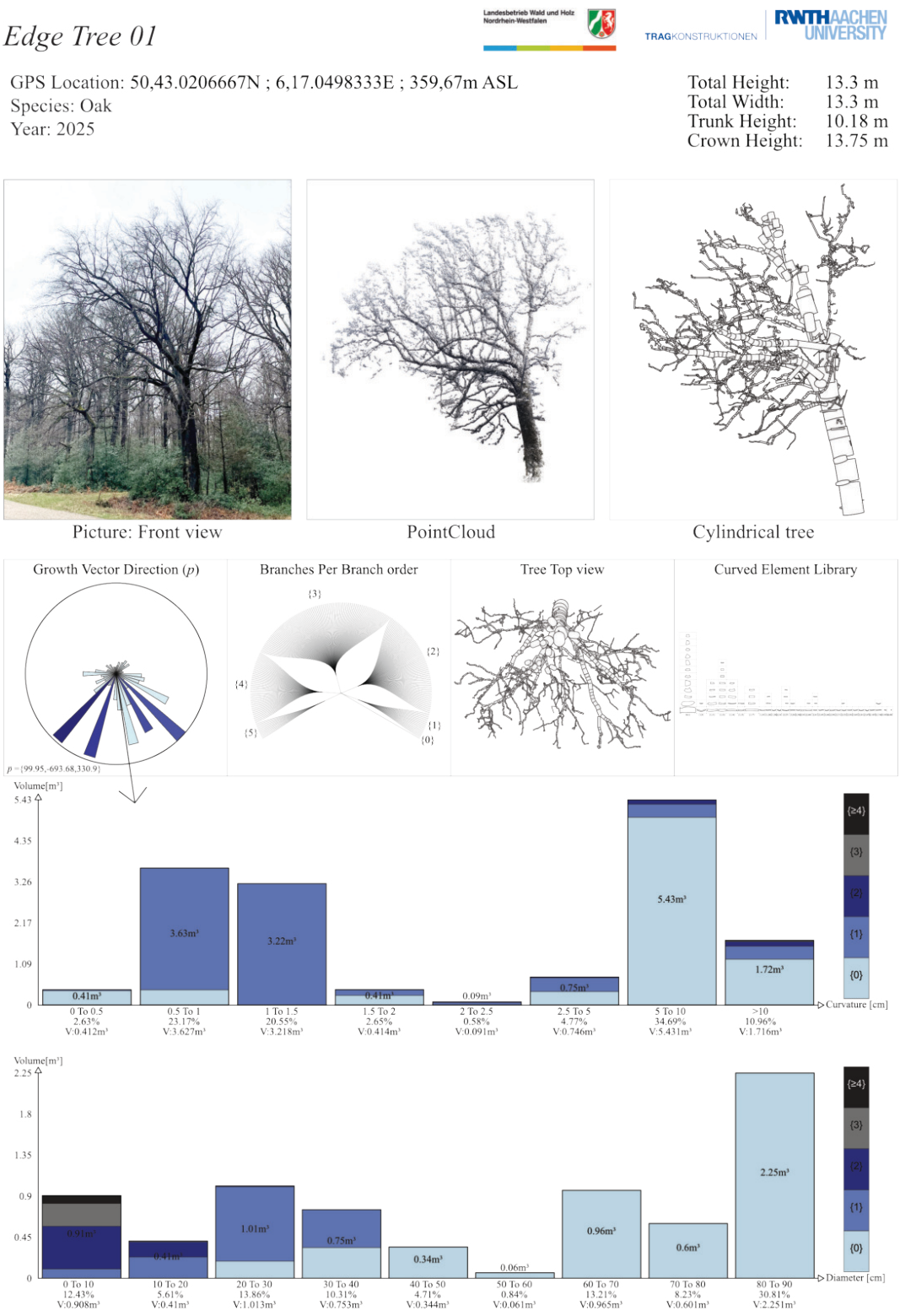

Figure B.4: Tree Growth Analysis Dataset 2 3.2.3.

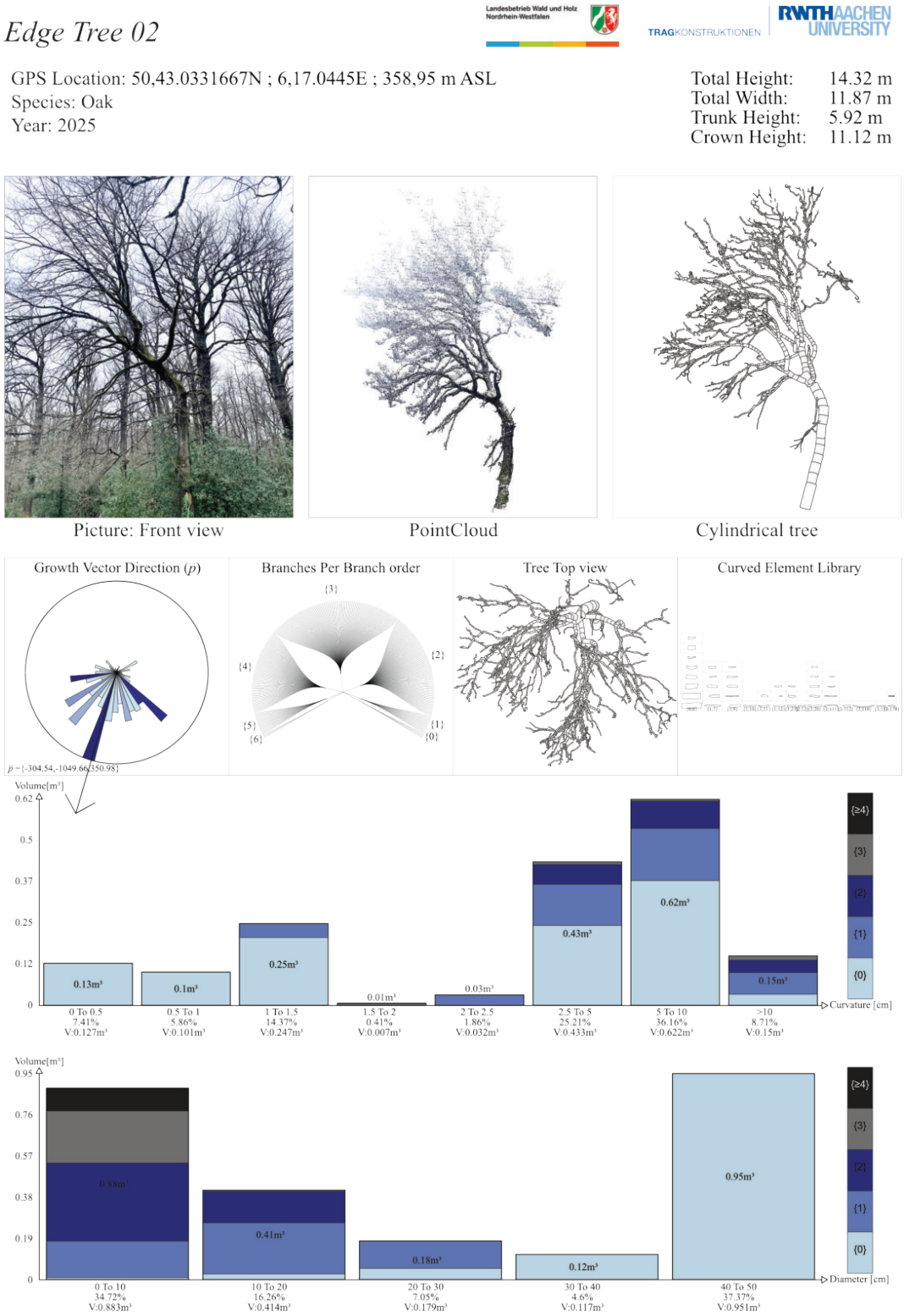

Figure B.5: Tree Growth Analysis Dataset 2 3.2.3.

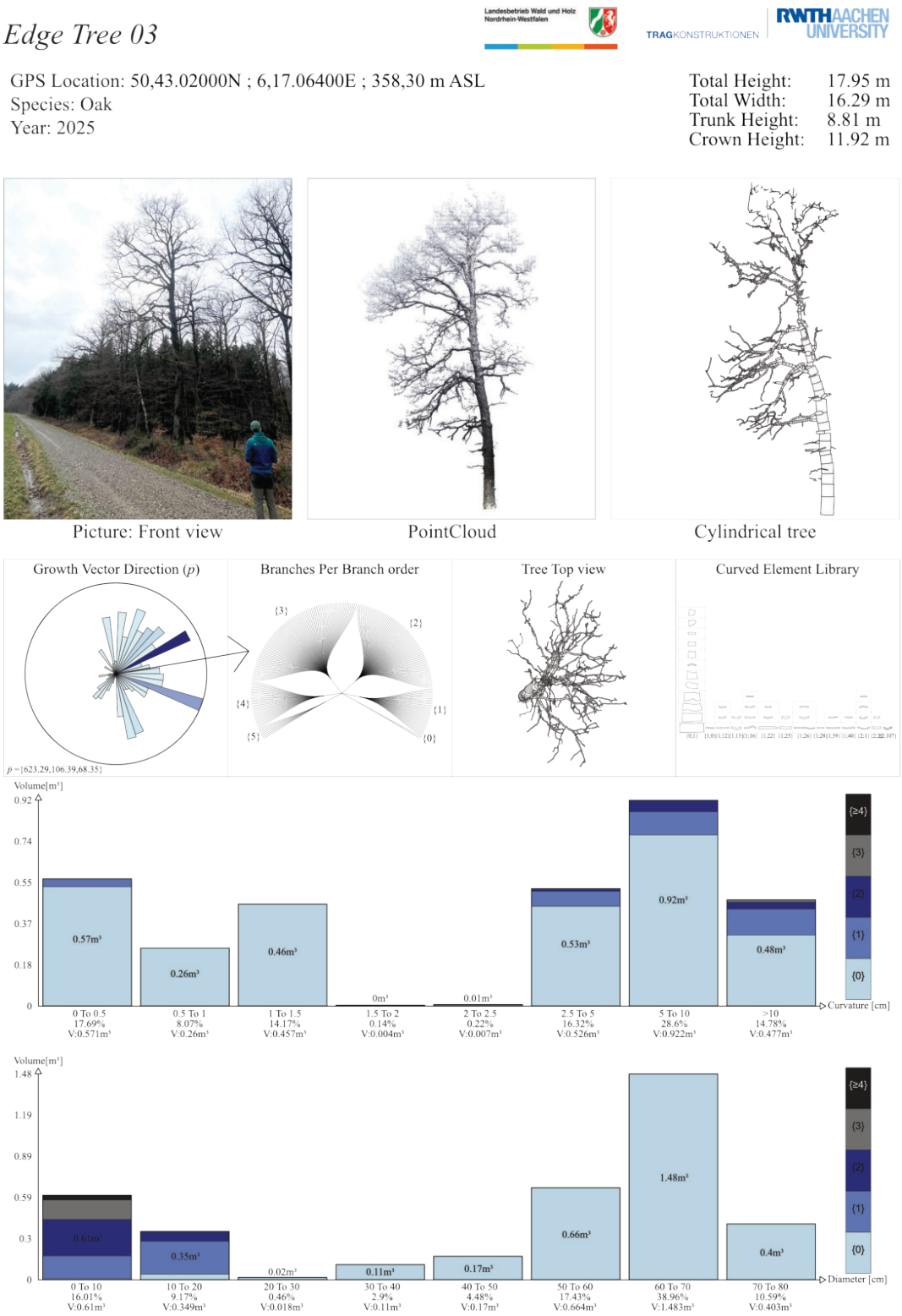

Figure B.6: Tree Growth Analysis Dataset 2 3.2.3.

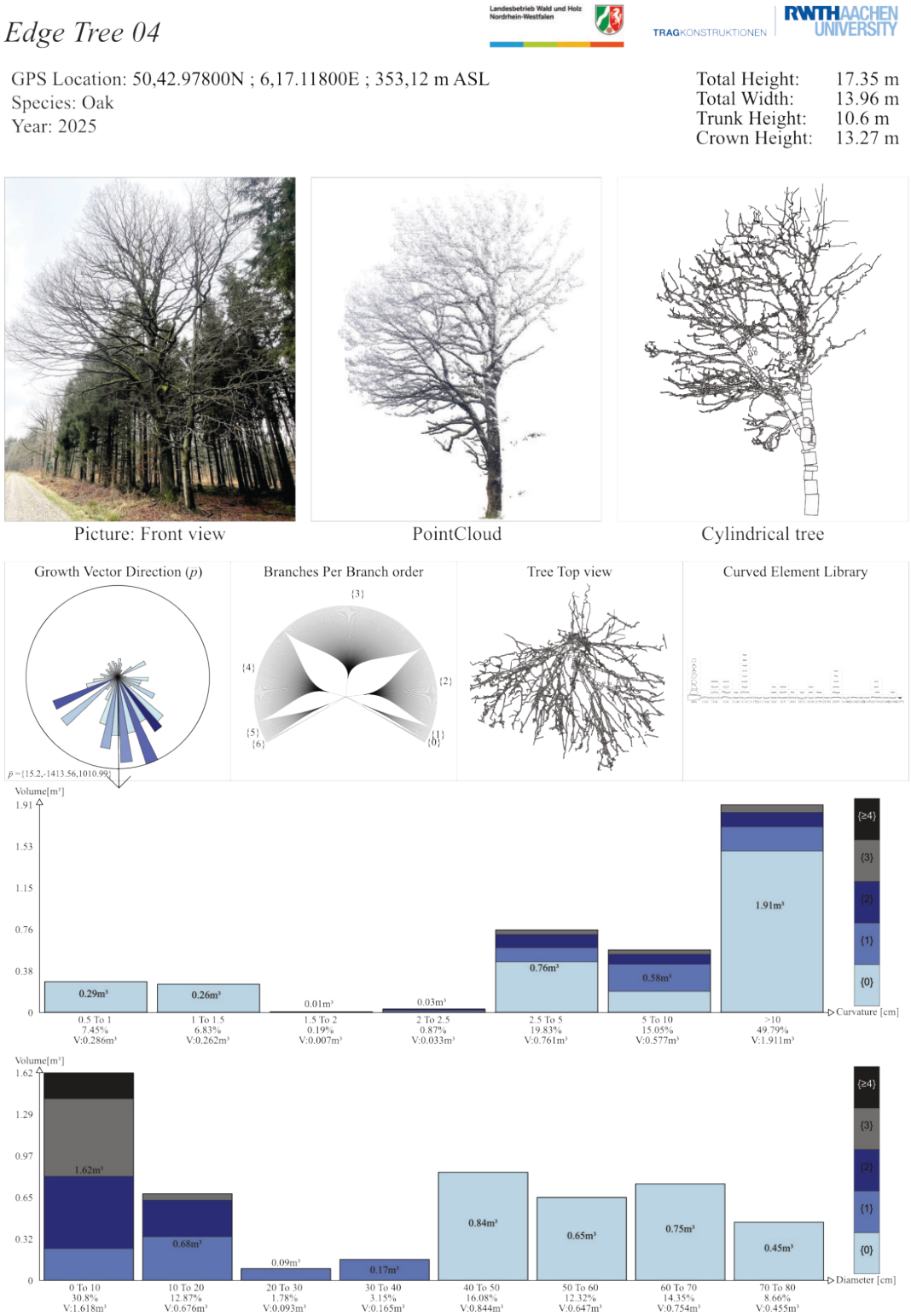

Figure B.7: Tree Growth Analysis Dataset 2 3.2.3.

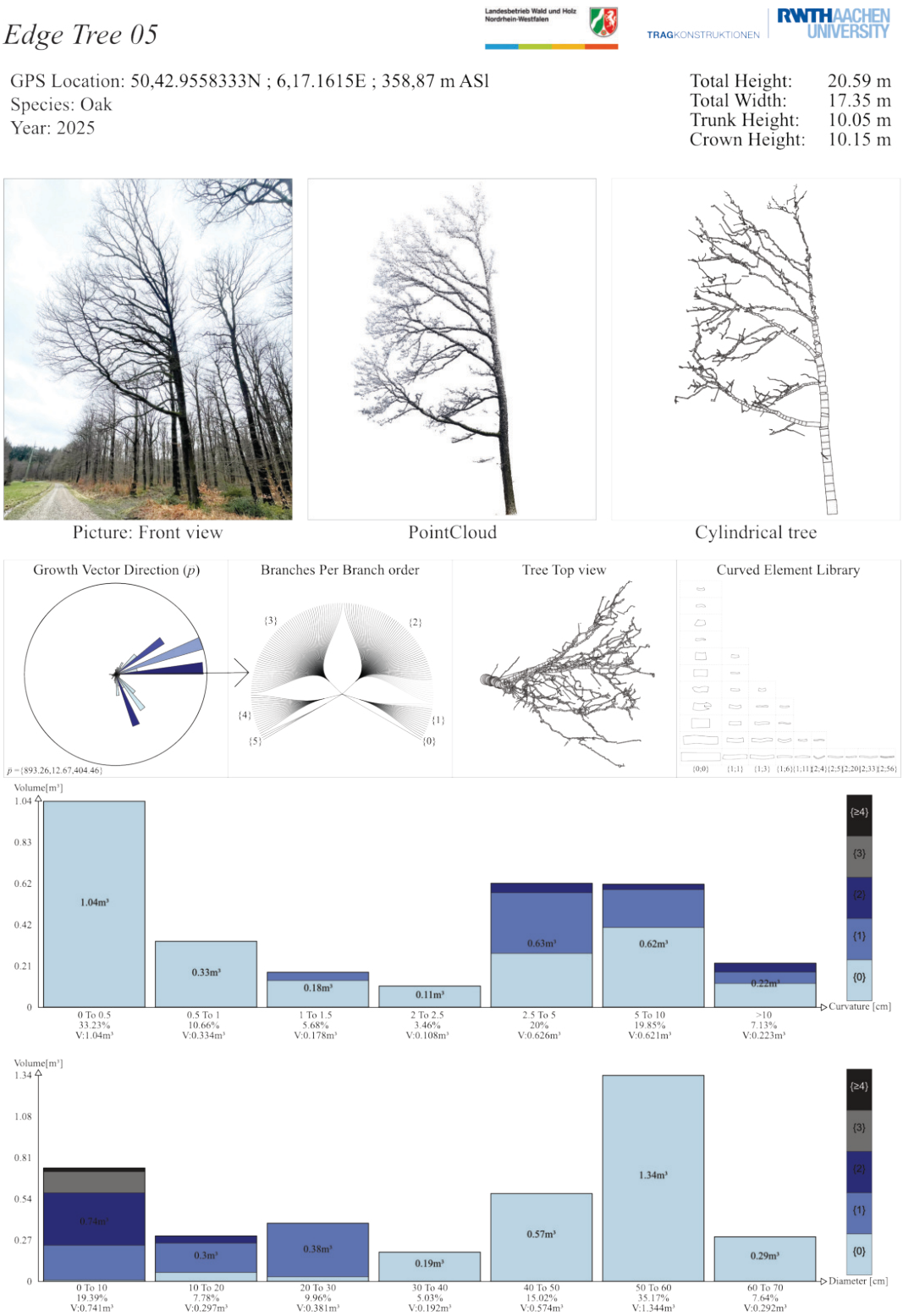

Figure B.8: Tree Growth Analysis Dataset 2 3.2.3.

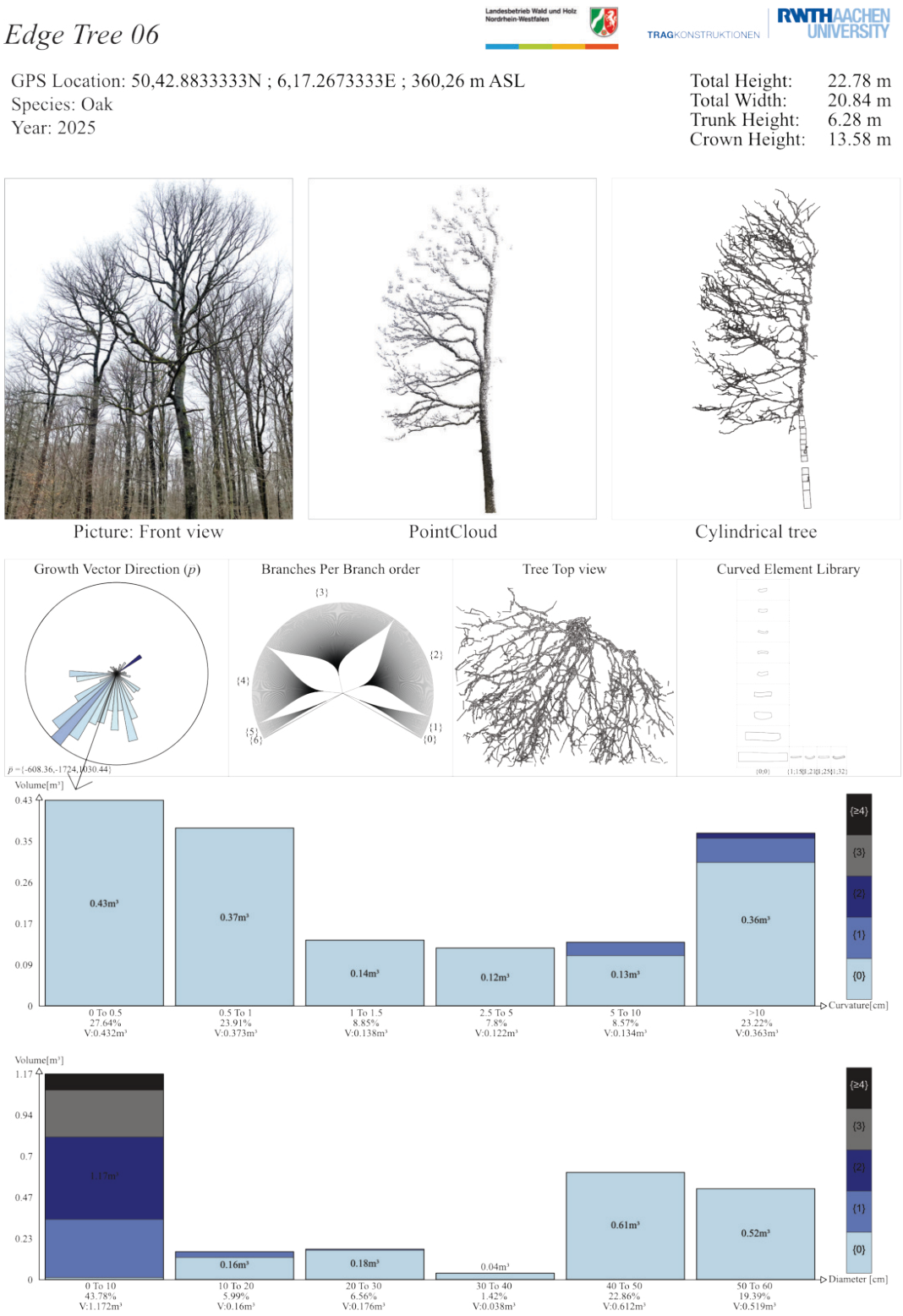

Figure B.9: Tree Growth Analysis Dataset 2 3.2.3.

B.3.3 Raw Timber Library. Geometrical Analysis

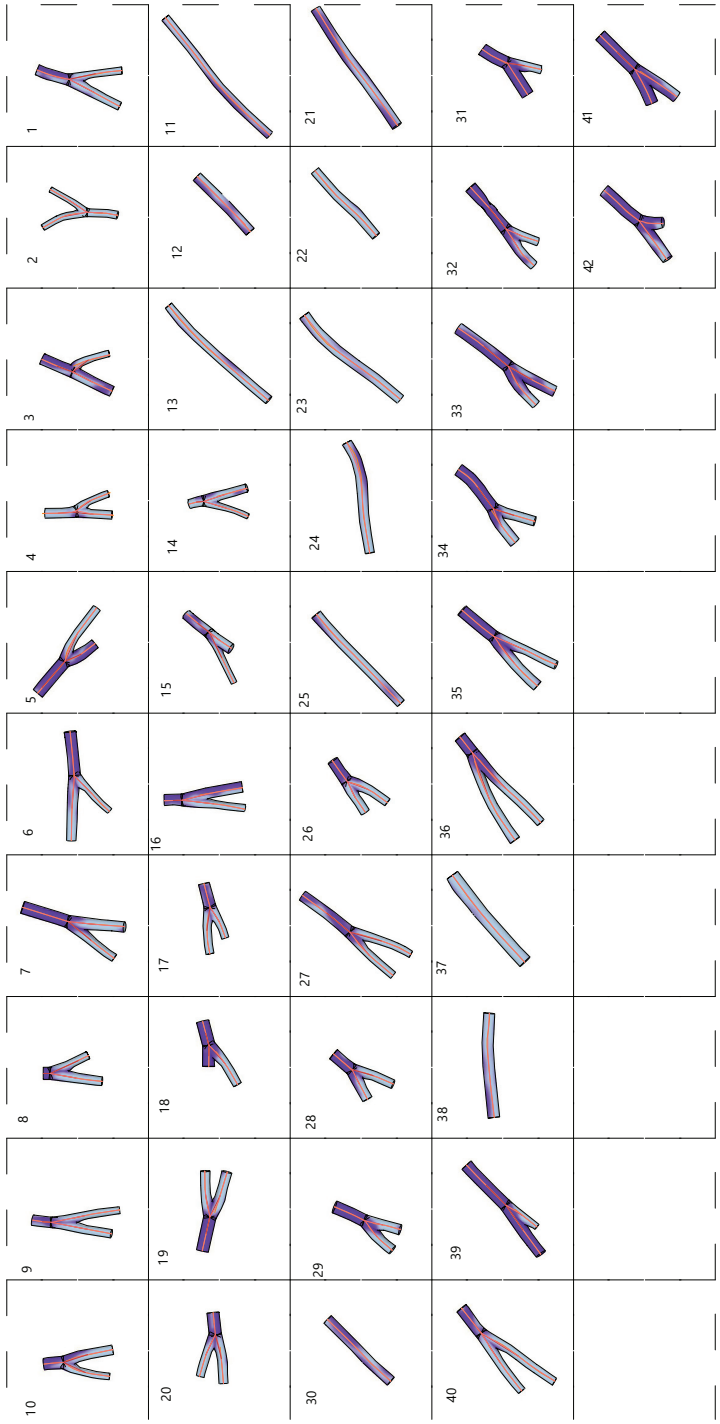

Figure B.10: Growing Bridge timber library, dataset 3 3.2.3. Mesh automation showing eccentricities with color grading. $\|\vec{\delta_i}\|$ evaluate curvature deviation from pith for each specimen. See Section 3.6.

B.3.4 Raw Wood Library 2D Segmentation

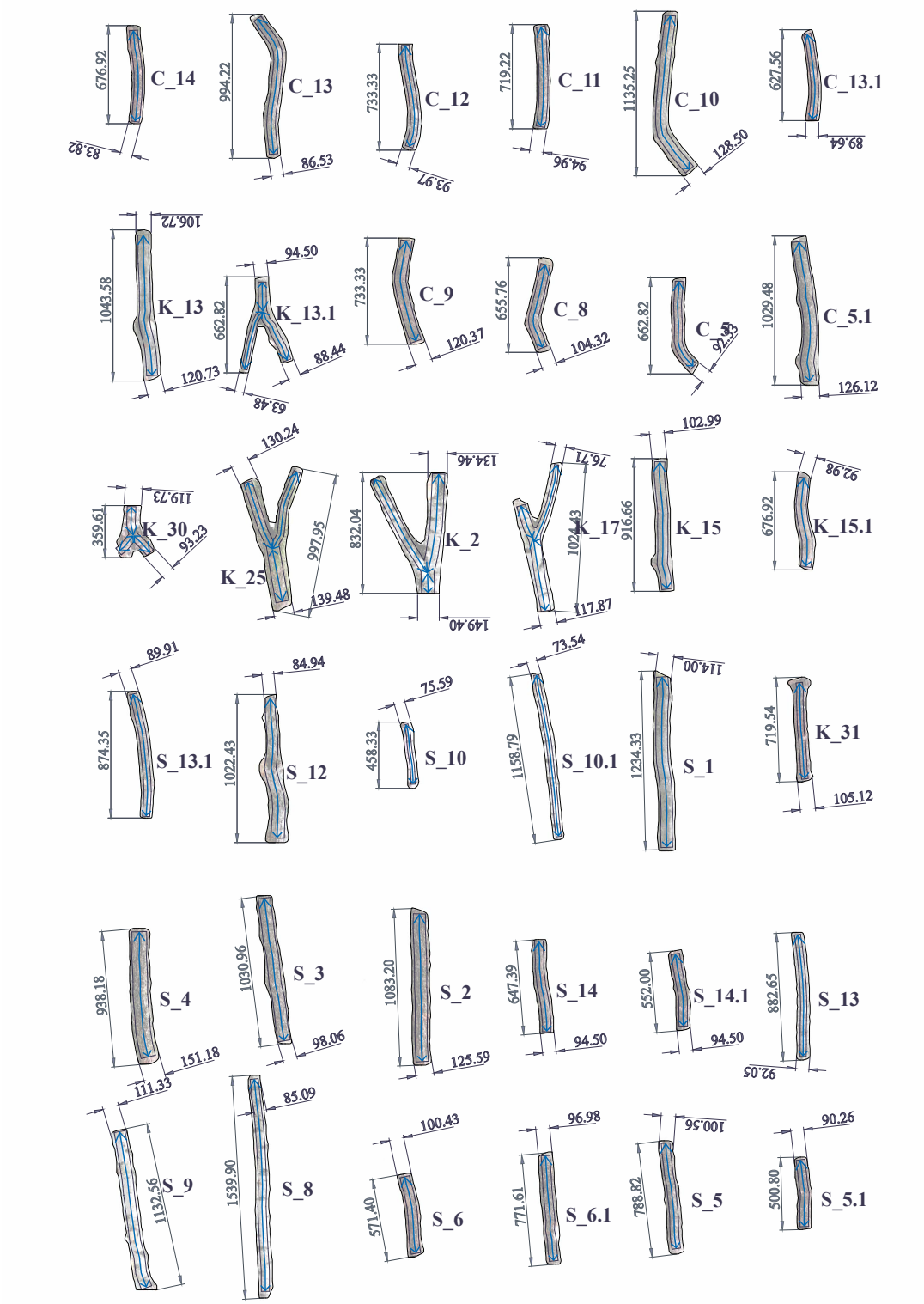

Figure B.11: reGrowth Pavilion timber library, dataset 4 3.2.3. Mesh automatization with dimensions and growth vector. See Section 3.5.

B.4 Attached in Chapter 4

B.4.1 Micro-CT Scan Overview

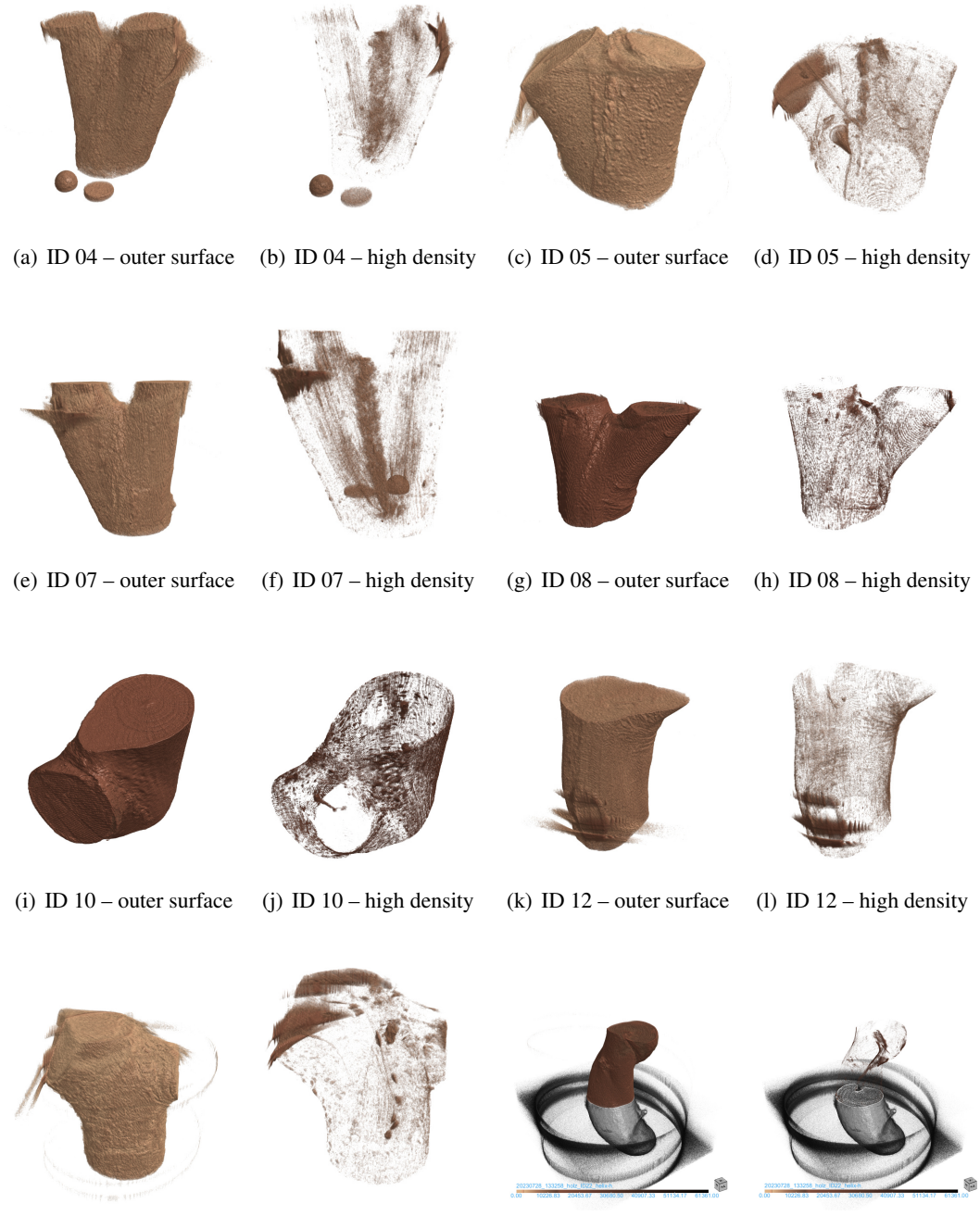

(a) ID 04 – outer surface (b) ID 04 – high density (c) ID 05 – outer surface (d) ID 05 – high density

(e) ID 07 – outer surface (f) ID 07 – high density (g) ID 08 – outer surface (h) ID 08 – high density

(i) ID 10 – outer surface (j) ID 10 – high density (k) ID 12 – outer surface (l) ID 12 – high density

(m) ID 21 – outer surface (n) ID 21 – high density (o) ID 22 – outer surface (p) ID 22 – high density

Figure B.12: Micro-CT scans of timber specimens, showing outer surfaces and internal high-density structures across 8 samples.

B.4.2 Macro-CT Scan Overview

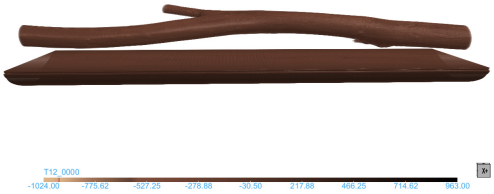

(a) T12 – outer surface

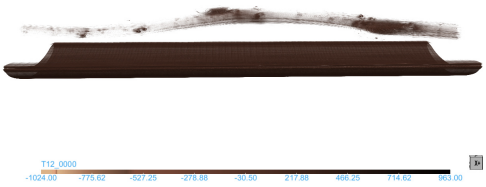

(b) T12 – high density



(c) T16 – outer surface

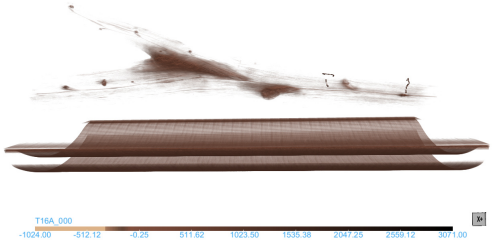

(d) T16 – high density

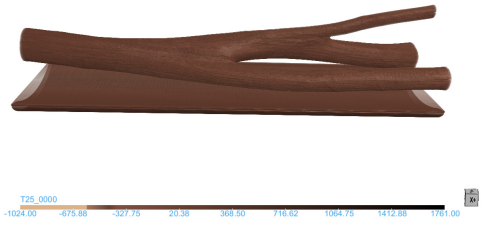

(e) T25 – outer surface

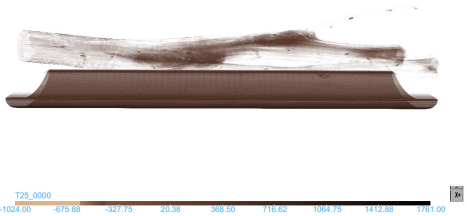

(f) T25 – high density



(g) T26 – outer surface

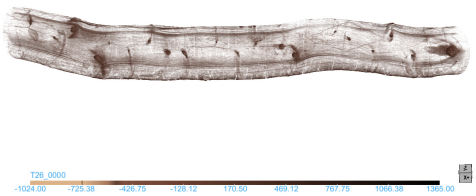

(h) T26 – high density

Figure B.13: Macro-CT image set (1/2) showing outer surfaces and internal high-density structures of specimens.



(a) T27 – outer surface



(b) T27 – high density



(c) T1 – outer surface

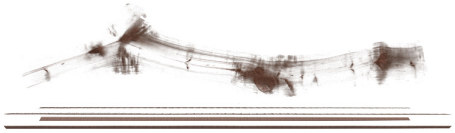

(d) T1 – high density

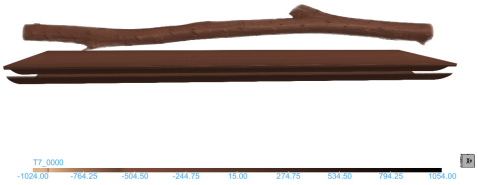

(e) T7 – outer surface

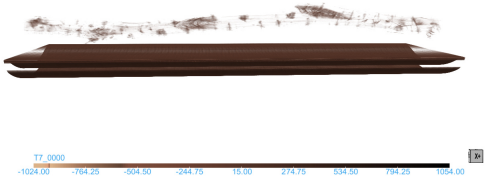

(f) T7 – high density

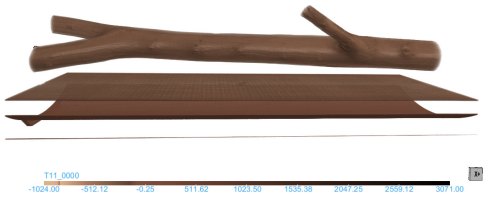

(g) T11 – outer surface

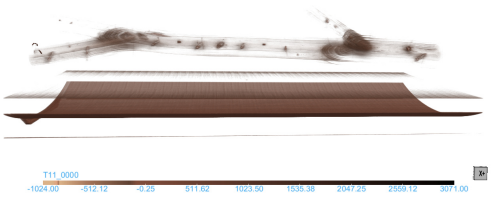

(h) T11 – high density

Figure B.14: Macro-CT image set (2/2) showing outer surfaces and internal high-density structures of specimens.

B.5 Attachments in Chapter 5

No additional attachments are provided for Chapter 5. The corresponding material is presented in the publications [18, 170, 194, 197].

B.6 Attached in Chapter 6

B.6.1 Construction Details



(a) (b) (c) (d) (e) (f) (g) (h)

Figure B.15: Prototype tests and construction: material experiments, joinery detailing, and assembly phases.

B.6.2 Built Prototypes

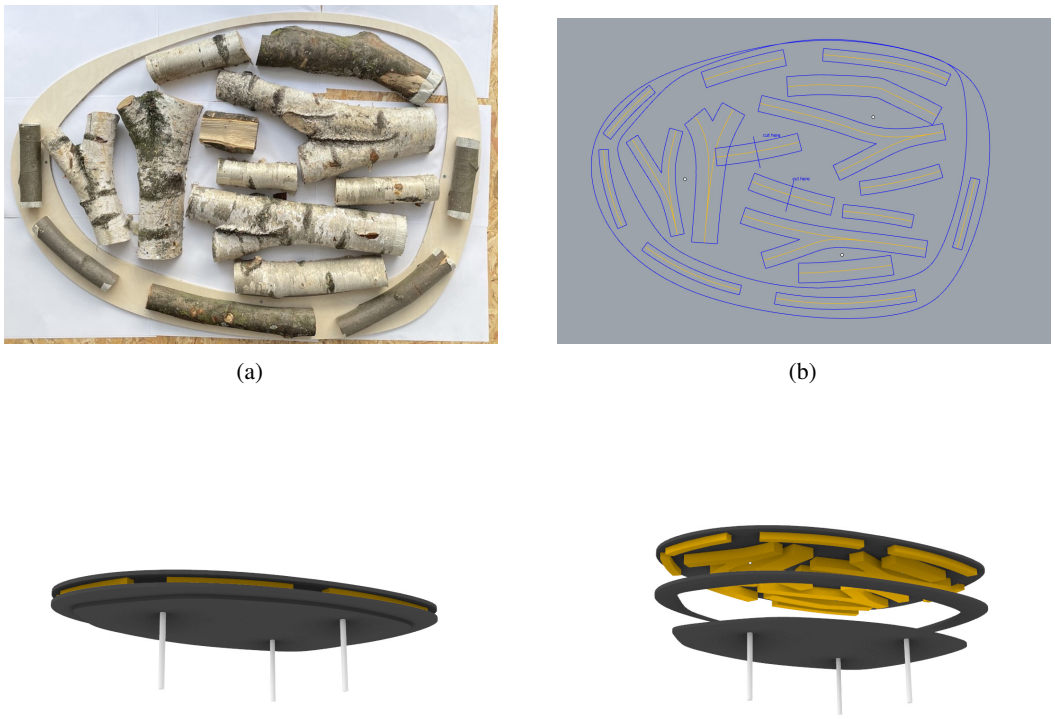

(a) (b)

(c) (d)

Figure B.16: Design concept for a sandwich base table.



Figure B.17: Final product.

End-Joint Fabrication

A custom jig was developed for end-joint fabrication using the Shaper Origin. Designed to support dowel or metal ring connections, the jig securely holds irregular timber elements within a rigid, adjustable fixture (Fig. B.18). This setup enables precise milling operations, particularly for components aligned along a single axis. The process follows a CAD-based workflow: each

element is positioned, and reference distances are automatically plotted to ensure alignment. Additional support and safety measures are applied according to the weight and geometry of the timber element. To demonstrate the method, a rigid ring joint connecting two bifurcated timber elements was fabricated. This configuration can be integrated into a larger truss system. The elements are fixed in the jig (Fig. B.19) using adjustable components that conform to the raw timber geometry. A milling operation is performed on the exposed joint surface.

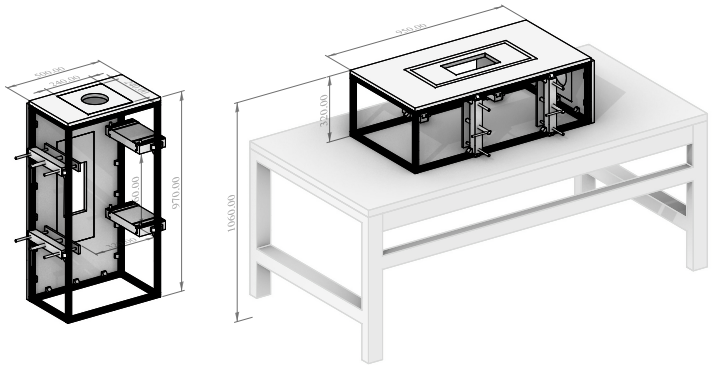

Figure B.18: Axonometric view of the custom jig for end-joint fabrication.

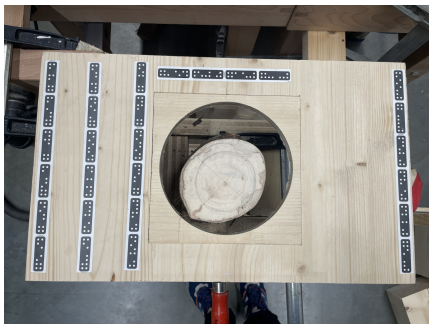

(a) Area to mill



(b) Element fixed



(c) Milling operation on the butt joint

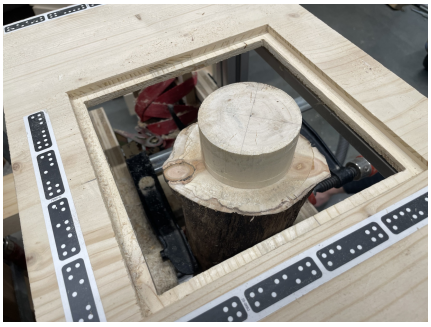

(d) Final connection using a ring insert

Figure B.19: End-joint milling for bifurcated components. Result shown in Fig. B.15(a).

B.6.3 Growing Bridge

Assembly

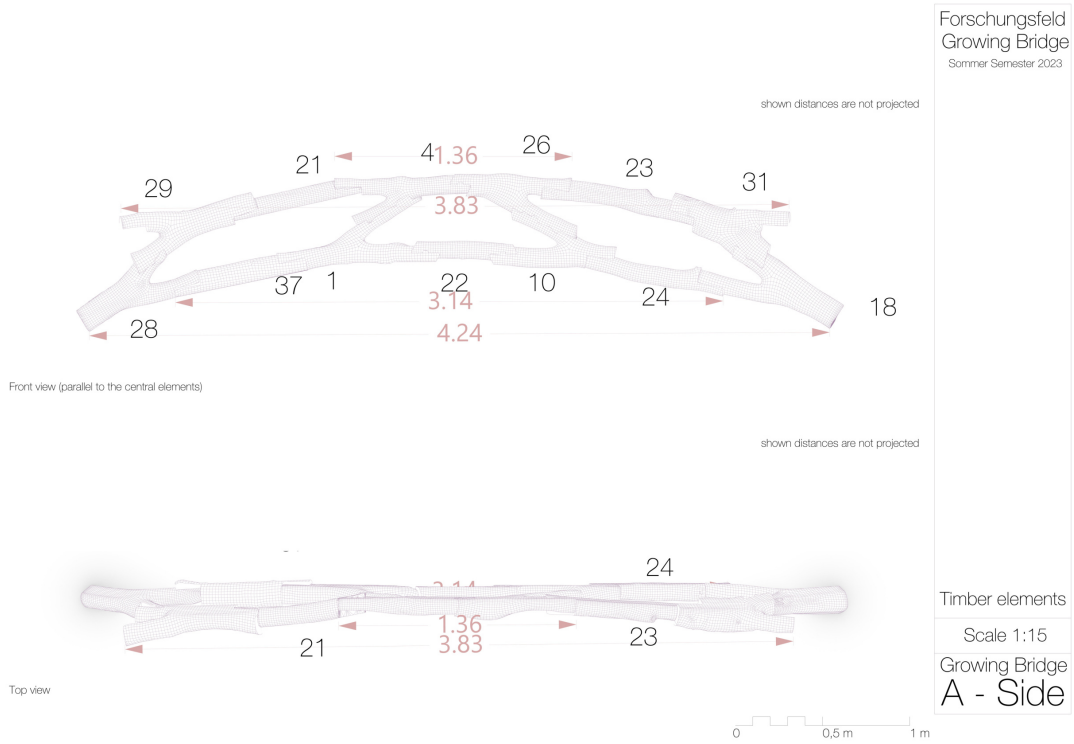

(a) Side A

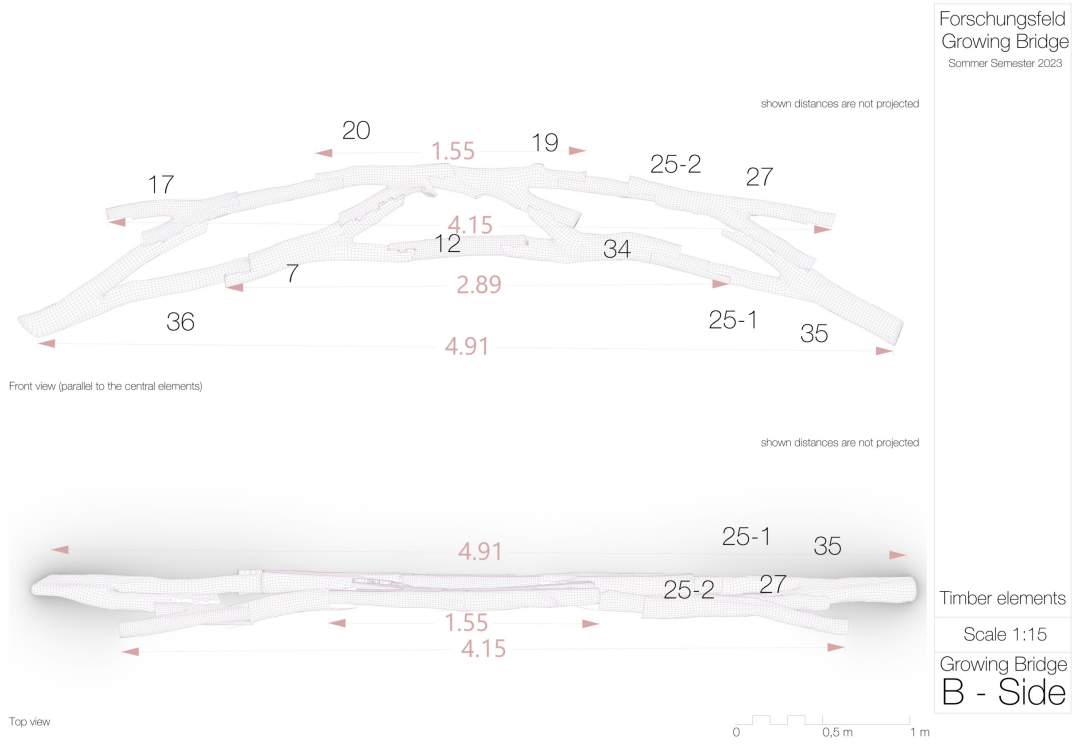

(b) Side B

Figure B.20: Bridge assembly.

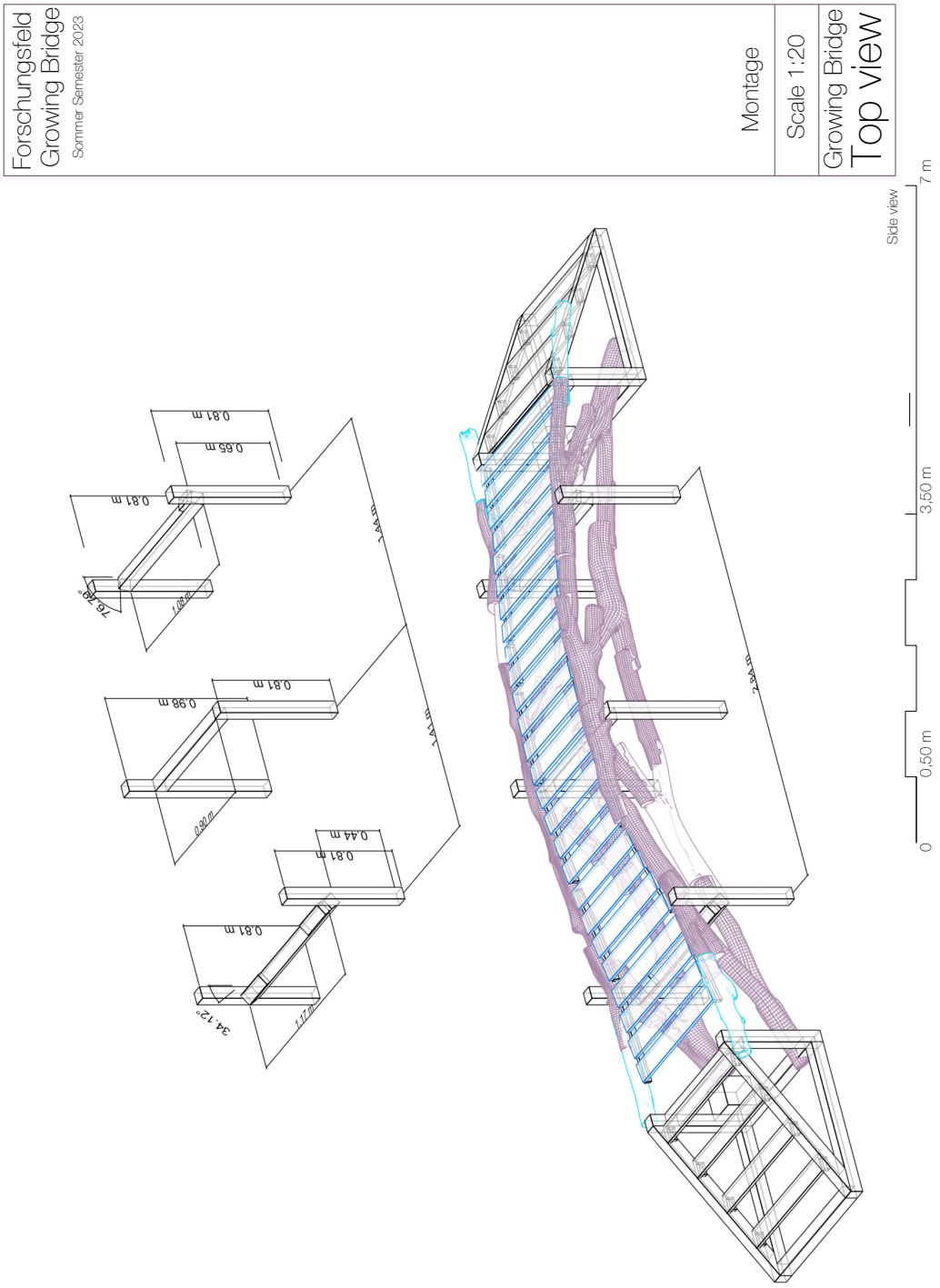

Figure B.21: Axonometric view.

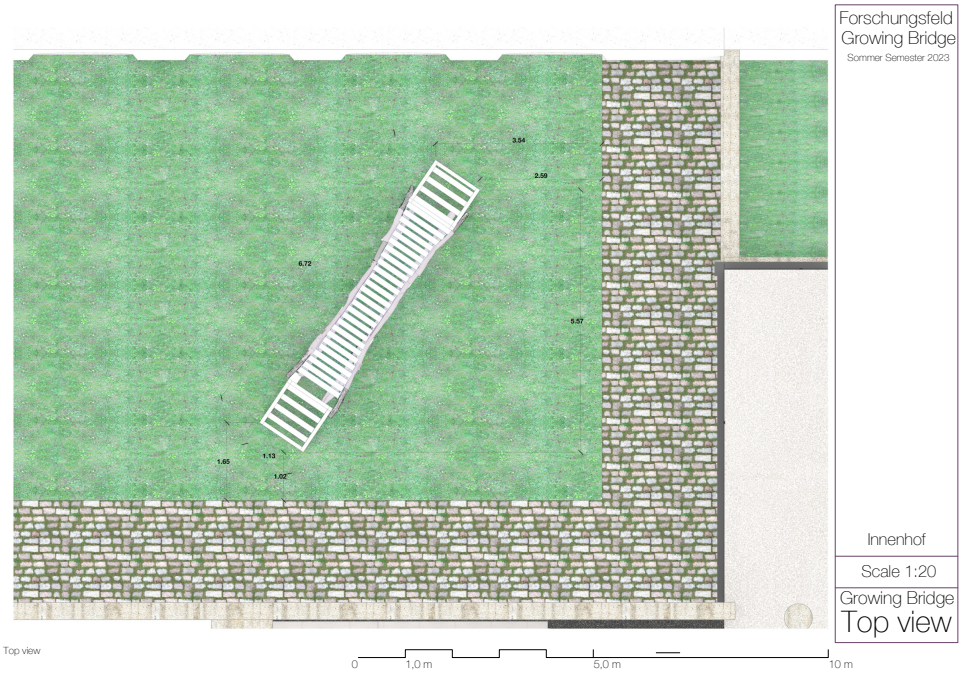

(a) Top view

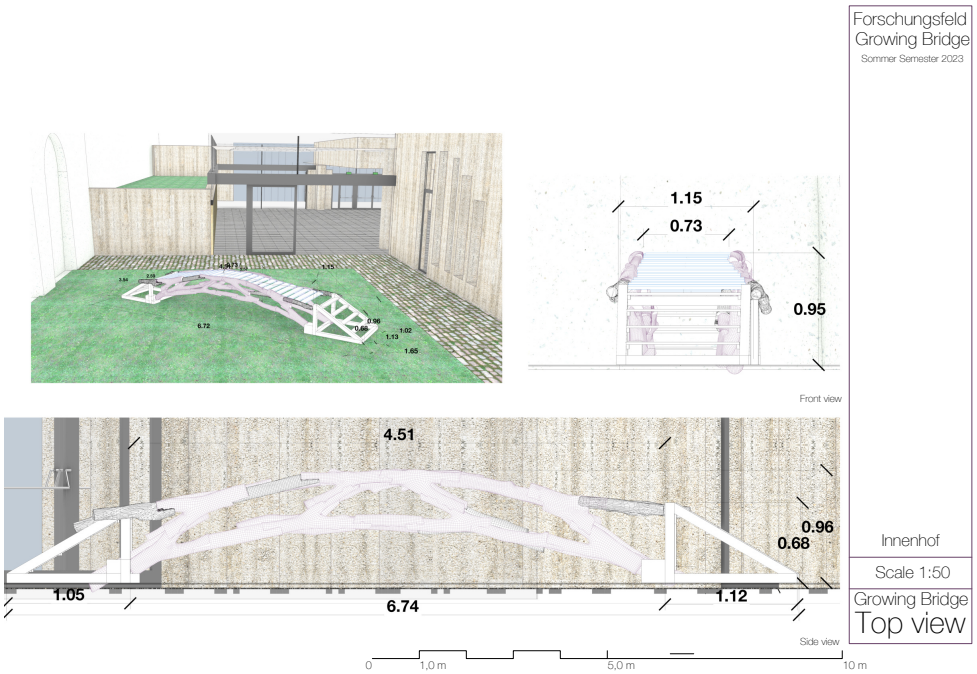

(b) Perspective

Figure B.22: Views of the Growing Bridge installation: axonometric and site perspectives.

Final Photos



(a)



(b)

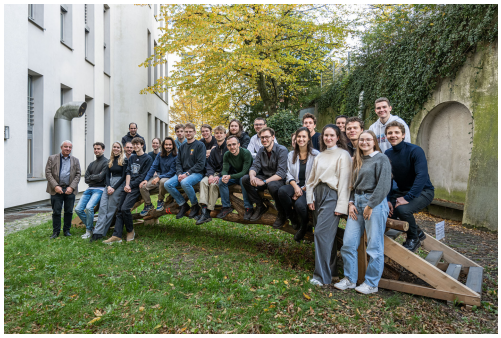

(c) Team Trako 2023-24



(d) Replacing flooring and debarking



(e) Transport, Nov 24



(f) Transport, Nov 24



(g) Winter view, Jan 25



(h) Winter detail, Jan 25

Figure B.23: Final photos of the Growing Bridge: installation, preparation, transport (Nov 24), and winter condition (Jan 25).

B.6.4 reGrowth Pavilion

Static diagrams

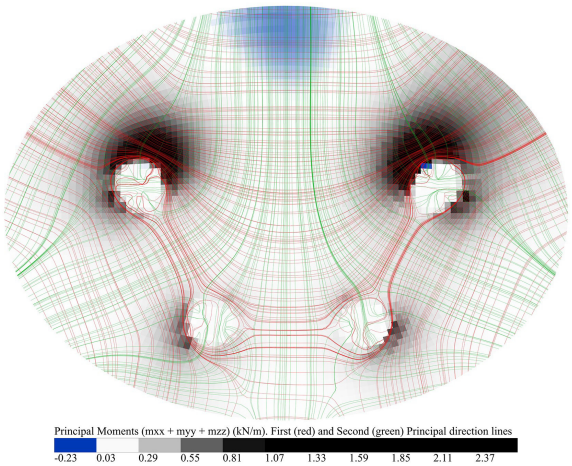

(a) Principal moments

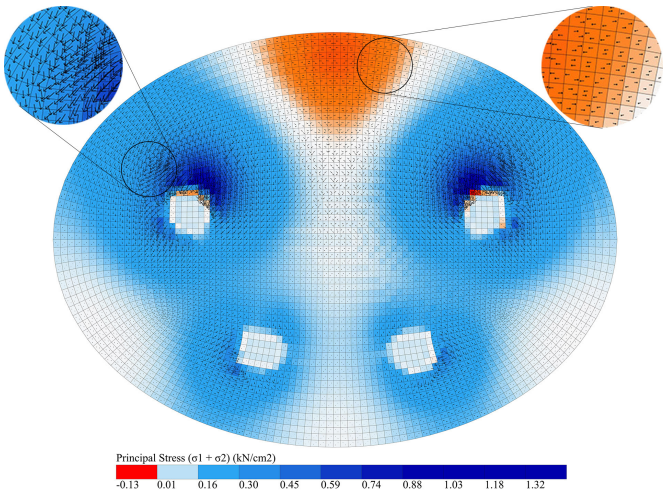

(b) Principal stress displayed as vector field by module

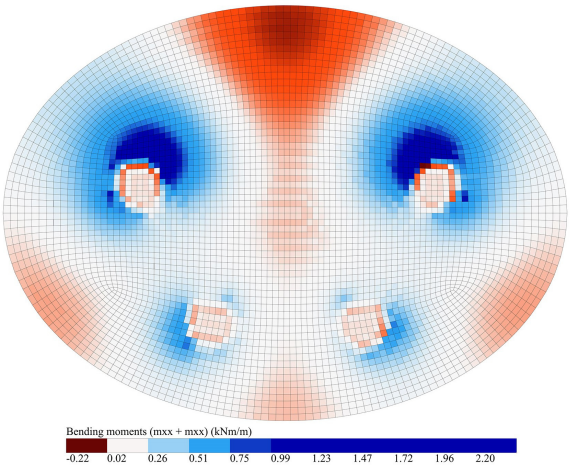

(c) Bending moment distribution

Figure B.24: Referent plate analysis.

Assembly diagrams

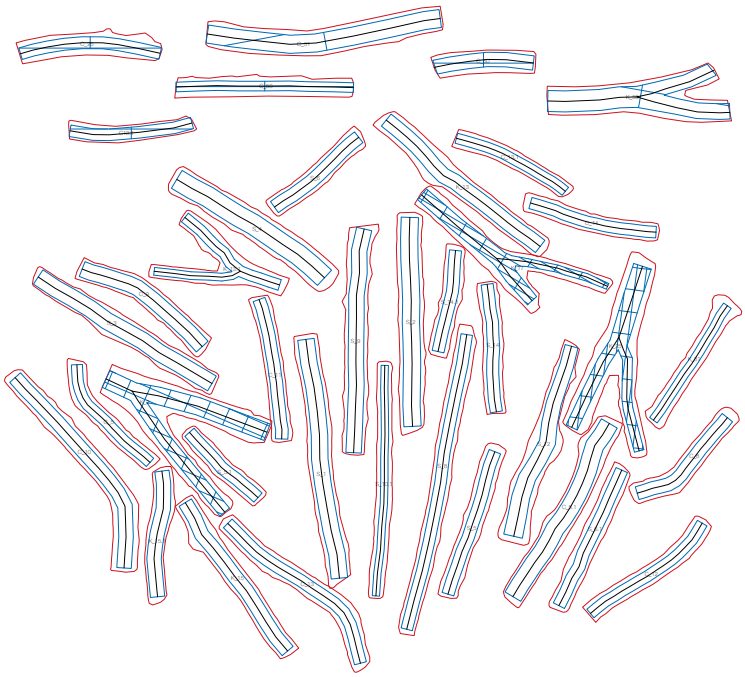

(a) Parts overview

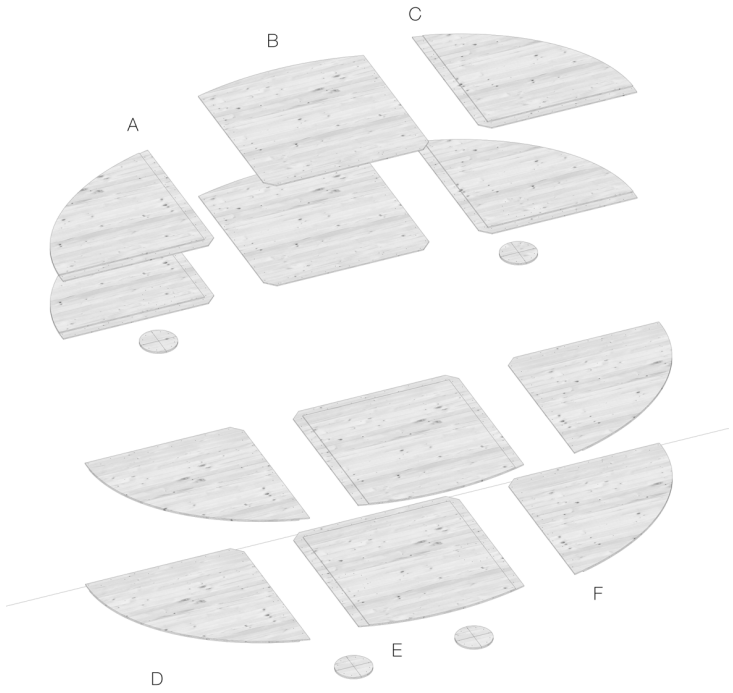

(b) Plates layout

Figure B.25: Assembly plans of the exhibition *reGrowth* at Pop-up Campus, September 2022.

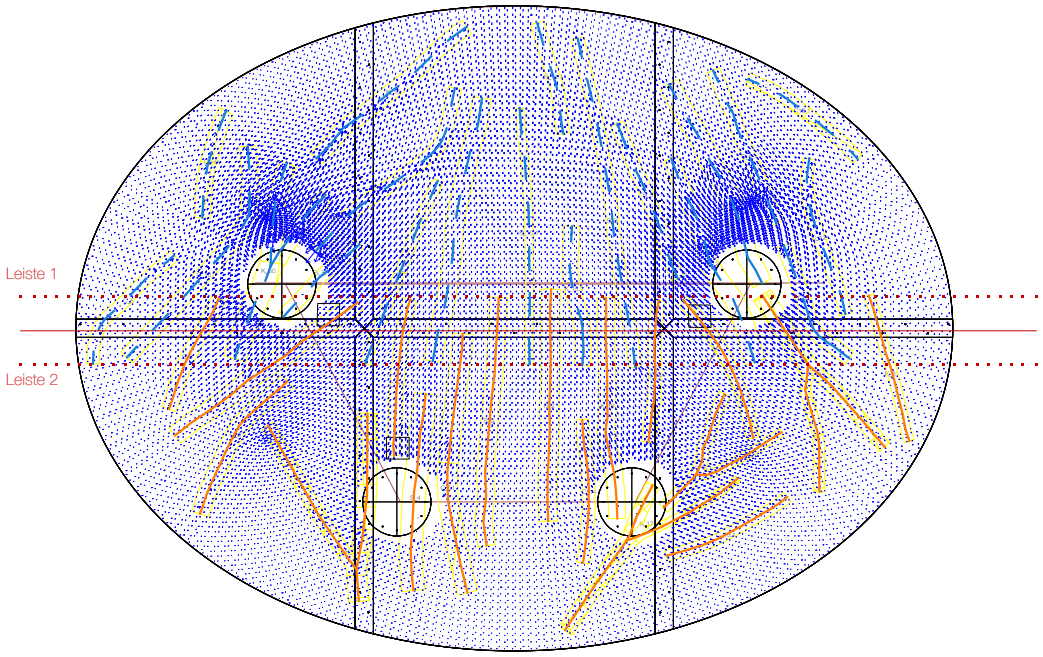

(a) Assembly plan

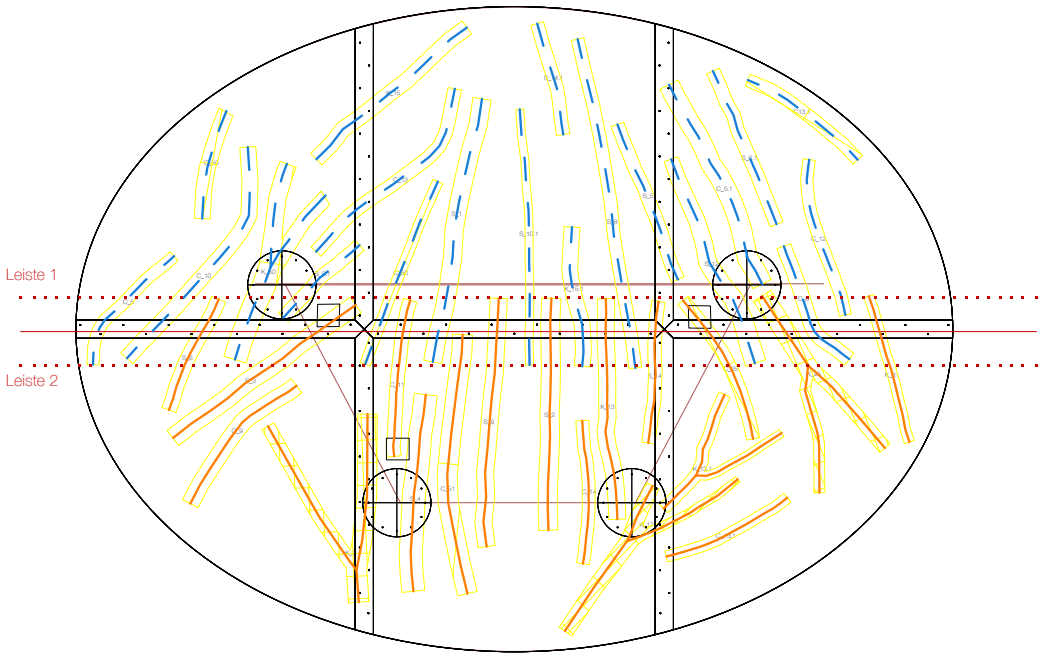

(b) Construction phase

Figure B.26: Assembly plans of the exhibition *reGrowth* at Pop-up Campus, September 2022.

B.6.5 Academic Works

Research Application in Student Works

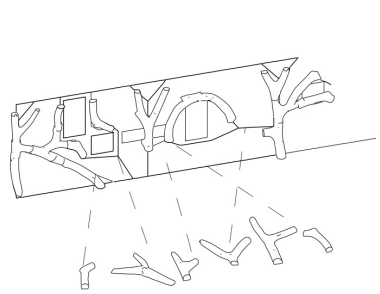

(a) Raw timber facade integration

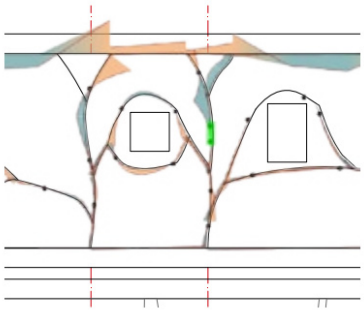

(b) Static analysis

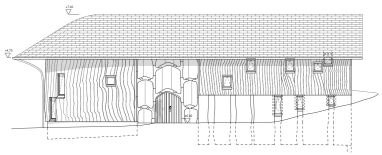

(c) Design of a forest hut using raw timber (front view)

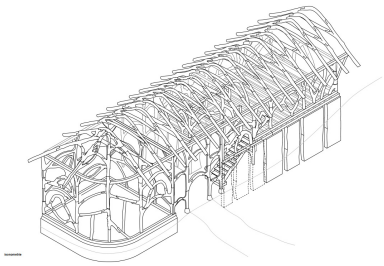

(d) Axonometric drawing

Figure B.27: Stephens et al. (2024) [207]. Developing a modern half-timbered house using raw timber modeling.

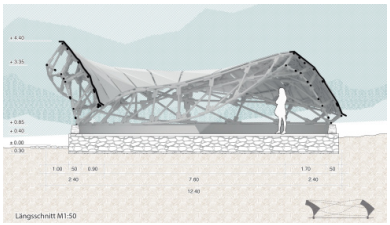

(a) Design of a spatial truss with raw timber

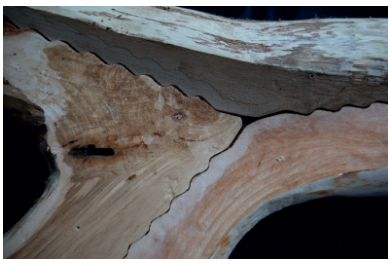

(b) Connection detail in raw timber

Figure B.28: Suliman et al. (2024) [208, 222]. Exploration of non-standard joints in spatial structures.

Appendix C

Research & Academic Projects

C.1 Research Projects

During the thesis period, full-time work was dedicated to several research projects that directly contributed to the understanding and development of the dissertation. In addition, the author participated in the co-drafting and submission of research proposals focusing on design, prototyping, and basic research in timber construction with naturally grown raw timber.

Research Project	**Period**	**Type**	**Link**
Design Folding Mechanisms	2020–2022	DFG: Basic Research	https://gepris.dfg.de/gepris/projekt/289387994?context=projekt&task=showDetail&id=289387994&
reGrowth in Pop-up Campus	2022	BBSR Zukunft Bau: Applied Research	https://www.zukunftbau.de/projekte/forschungsfoerderung/pop-up-campus/1008183-2215
Naturally Grown Timber Elements as Basis for Load-Bearing Structures: Structural Analysis and Growth Simulation	2023–2026	DFG: Basic Research	https://gepris.dfg.de/gepris/projekt/512769030?context=projekt&task=showDetail&id=512769030&

Table C.1: Research projects conducted during the thesis period.

Submitted Research Proposals

In parallel, the author was actively involved in the preparation and submission of research proposals. These proposals aim to extend the investigation of raw timber applications in structural and architectural design.

Proposal Title	Year	Funding Body	Status
Wachstumssimulation von pflanzlichen Organismen unter Berücksichtigung der strukturellen Selbstbildung (v1-3)	2019-21	DFG	Declined
reGrowth – Tragkonstruktionen aus ungenutzten Holzabschnitten	2022	BBSR Zukunft Bau: Applied Research	Approved
Naturally grown timber elements as basis for load-bearing building structures - structural analysis and growth simulation (v4)	2022	DFG	Approved
Living lab „Natürlich gewachsene Holzkonstruktionen“ Entwicklung eines Konstruktionsprinzips und Numerische Strukturanalyse natürlich gewachsener Holzelemente in tragenden Baukonstruktionen	2022	RWTH ERS Living lab	Declined
Laubrohholz-Sandwichplatten für modulare Wandscheiben- und Deckenplattenkonstruktionssysteme	2024	FNR BMEL	Submitted
RawTimber Structures: Structural Innovations, Market Integration, and Implementation Strategies	2025	RWTH ERS Start-up Postdoc	Approved

Table C.2: Submitted research proposals related to raw timber construction.

C.2 Contributions to Academic Projects and Thesis

In addition, contributions were made to the development and co-supervision of several master's theses, bachelor's theses, and other academic projects during the dissertation period. The following list includes related work. In parallel, additional projects—while not directly linked to the main topic—were carried out in the fields of sustainable construction, geometric modeling, and lightweight structures, influencing the broader application context.

Author	Year	Type	Title
Multiple students	2020	Master's Studio Project M1	M1: The Growing Tower
Multiple students	2021	Master's Studio Project M2	M2: Bionic Tower I and II
Multiple Students	2022	Research Field Seminar	Tree-based Constructions
Viktor Wages	2022	Bachelor's Thesis Architecture	Baumbasierte Konstruktionen [1]
Multiple Students	2023	Research Field Seminar	Growing Bridge
Victor Ramirez	2023	Master's Thesis Construction Robotics	Computational Validation of the Structural Efficiency of Slabs with Stress-Aligned Ribs [2]
Multiple Students	2024	Research Field Seminar / Arch + Civil Eng.	Shaped in the Forest
Sheldon Stephens	2024	Master's Thesis Architecture	Holzbau Remapped
Raman Suliman	2024	Master's Thesis Architecture	Strukturelle Knoten aus zusammengesetzten Astgabeln [3]
Simon Dupre	2025	Bachelor's Thesis Civil Eng.	Experimentelle Untersuchung zur schadensfreien Ermittlung relevanter Materialkenngrößen natürlich gewachsener Holzelemente [4]
Multiple Students	2025-	Master course Impromptu	Bench in the Forest
Tobias Grüters	2025-	Master's Thesis Construction Robotics	*Timber Pavilion Design for the Büchel, Aachen*
Marc Kreimendahl	2025-	Bachelor's Thesis Civil Eng.	*Modeling and Simulating LRS Panels*
Gregor Wehberg	2025-	Bachelor's Thesis Civil Eng.	*Experimental Assesement of Volumetric Visualization for Non-destructive testing in raw timber*

Table C.3: Supervised Student Works and Thesis Related to the Dissertation.

Author	Year	Type	Title
Multiple Students	2019	Master's Studio Project M1	Metal shell structures
Multiple Students	2020	Research Field Seminar	IASS Pavilion Contest: Curved Folded Dome
Multiple Students	2020	Master course Impromptu	Transformers
Multiple Students	2021	Research Field Seminar	Transformable Constructions I
Multiple Students	2022	Master course Impromptu	Transformable Constructions II
Julia Buhr	2020	Master's Thesis	Spannbandbrücke Kamper Straße: Fuß- und Radweg mit Eisenbahnaussicht in Aachens Süden
Sigrid Neffgen	2022	Bachelor's Thesis Architecture	Campus-Tower: Aachens erstes Holzhochhaus
Bahaaedin Abduljawad	2021	Master's Thesis	Vorgefertigte Holzbauweise im Gesundheitswesen
Kateryna Babiichuk	2023	Master's Thesis	Ein neuer internationaler Flughafen für Winnyzja
Eva Beule	2024	Master's Thesis	Gefaltete Formen: Entwurf eines beweglichen Tragwerks

Table C.4: Supervised Student Works and Thesis Non-related to the Dissertation.

C.3 Scientific Results

The following list includes peer-reviewed journal articles, book chapters, and conference contributions authored or co-authored during the doctoral research period at the Chair of Structures. While not all are directly included in the core of this dissertation, they reflect the broader research context and collaborative work developed in parallel.

C.3.1 Peer-Reviewed Journals and Book Chapters

P-1 Moreno Gata, K., Spahn, F., Klinkel, S. and Trautz, M. 'Geometrical Analysis of Naturally Grown Timber for the Design of Load-Bearing Structures'. In: *Research Directions: Biotechnology Design* 2.e19 (2024). ISSN: 2752-9452. DOI: 10.1017/btd.2024.12

P-2 Moreno Gata, K., Amtsberg, F., Stephens, S. W., Menges, A. and Trautz, M. 'Integrating Naturally Grown Timber in Sandwich Timber Panels'. In: *Scalable Disruptors*. Ed. by P. Eversmann, C. Gengnagel, J. Lienhard, M. Ramsgaard Thomsen and J. Wurm. Cham: Springer Nature Switzerland, 2024, pp. 81–93. ISBN: 978-3-031-68275-9. DOI: 10.1007/978-3-031-68275-9_7

P-3 Spahn, F., Moreno Gata, K., Trautz, M. and Klinkel, S. 'Generalised Scaled Boundary Isogeometric Analysis – a Method for Structural Analysis of Naturally Shaped Timber Structures'. In: *Wood Material Science & Engineering* 0.0 (2024), pp. 1–13. ISSN: 1748-0272. DOI: 10.1080/17480272.2024.2323590

P-4 Spahn, F., Moreno Gata, K., Trautz, M. and Klinkel, S. 'Einsatz von Rohholzelementen Für Tragende Strukturen Und Mechanische Analyse Mittels Bildbasierter Simulationsverfahren/Application of Raw Wood Elements for Load-Bearing Structures and Mechanical Analysis Using Image-Based Simulation Methods'. In: *Bauingenieur* 99 (1st Jan. 2024), pp. 109–116. DOI: 10.37544/0005-6650-2024-04-41

P-5 Moreno Gata, K., Seiter, A., Musto, J., Merz, J., Wieja, F., Jacobs, G., Corves, B. and Trautz, M. 'Design and Development of a Foldable and Transformable Hemispherical Enclosure for Robotic Manufacturing'. In: *Origami 8*. 8th International Meeting on Origami in Science, Mathematics and Education (8OSME). Melbourne, Australia, 16th July 2024

P-6 Amtsberg, F., Huang, Y., Marshall, D., Moreno Gata, K. and Mueller, C. 'Structural Up-cycling: Matching Digital and Natural Geometry'. In: *Advances in Architectural Geometry 2020*. Ed. by O. Baverel, C. Douthe, R. Mesnil, C. Mueller, H. Pottmann and T. Tachi. Paris: École des Ponts ParisTech & Université Gustave Eiffel, Presses des Ponts, 2021, pp. 486–504. ISBN: 978-2-85978-540-6. URL: thinkshell.fr/AAG2020

P-7 Wieja, F. A., Jacobs, G., Stürmer, S., Boelsen, K., Konrad, C., Merz, J., Moreno Gata, K. and Seiter, A. J. 'Function-Oriented Applicability Evaluation of Technical Folding Based on Expert Knowledge'. In: *Applied Sciences* (2024). DOI: 10.3390/app142311417

P-8 Suliman, R., Moreno Gata, K., Trautz, M. 'Structural nodes from composite tree bifurcations: Investigation and development of an adaptive construction system from naturally grown raw wood members'. In: *The 7th International Conference on Computational Design and Robotic Fabrication (CDRF2025)*, Shanghai, Jul. 2025. *"Best Paper Award 1st Place"*.

C.3.2 Peer-Reviewed Conference Papers

P- (*under review*)Moreno Gata, K., Spahn, F., Wintraken, A., Klinkel, S. and Trautz, M. 'From Tree Growth to Structural Design'. In: *Proceedings of IASS Annual Symposia*. The Living Past as a Source of Innovation. Mexico City, 2025

P-9 Moreno Gata, K., Spahn, F., Wehren, C., Klinkel, S. and Trautz, M. 'Building with Naturally Grown Timber: Circular Design in Forest Construction – A Pedestrian Bridge Case Study'. In: *Proceedings of IASS Annual Symposia*. Redefining the Art of Structural Design. Zürich, 2024

P-10 Moreno Gata, K., Seiter, A., Grizmann, D. and Trautz, M. 'Development of Construction Methods with Naturally Grown Timber and Bending-Resistant Joints'. In: *Proceedings of World Conference on Timber Engineering*. WCTE 2023. Oslo, 2023. DOI: 10.52202/069179-0096

P-11 Moreno Gata, K., Grizmann, D. and Trautz, M. 'Guiding the Tree Growth for Timber Structures Design'. In: World Conference on Timber Engineering 2021, WCTE 2021. 2021, pp. 345–350. URL: https://www.proceedings.com/61811.html

P-12 Amtsberg, F., Moreno Gata, K., Huang, Y., Marshall, D. and Mueller, C. 'DI-Terial – Development of Sensory-Informed Design-to-Fabrication Processes for the Efficient Use and Robotic Production of Discarded One-Off Hardwood Elements'. In: *12. World Conference on Timber Engineering*. Santiago, Chile: Red Hook, NY : Curran Associates, Inc, 2021, pp. 591–598. ISBN: 978-1-7138-4097-8

P-13 Moreno Gata, K., Musto, J., Pranjic, A. and Trautz, M. 'STUDY AND SIMULATION OF SELF-FORMATION FOR LOCAL TREE GROWTH'. in: *World Conference on Timber Engineering*. WCTE 2021. Curran Associates, Inc., pp. 2726–2732. ISBN: 978-1-7138-4097-8

P-14 Moreno Gata, K., Musto, J. and Trautz, M. 'Growing Construction Components - Design and Simulation Strategy for Self-Formation Following Tree Growth'. In: *Werner, L and Koering, D (Eds.), Anthropologic: Architecture and Fabrication in the Cognitive Age - Proceedings of the 38th eCAADe Conference - Volume 2, TU Berlin, Berlin, Germany, 16-18 September 2020, Pp. 51-59*. CUMINCAD, 2020. URL: http://papers.cumincad.org/cgi-bin/works/paper/ecaade2020_312 (visited on 10/02/2021)

P-15 Trautz, M., Moreno Gata, K., Spahn, F. and Klinkel, S. 'Bauen mit Rohholz'. In: Baustatik – Baupraxis 15. Technische Universität Hamburg: Institut für Baustatik, 2024, pp. 447–455. ISBN: 978-3-00-077808-7. URL: https://www.bb15.baustatik-baupraxis.de/Anmeldung/Upload/PDF/945879d9.pdf

P-16 Moreno Gata, K., Seiter, A. J., Musto, J. and Trautz, M. 'Design and Development of a Hybrid Deployable Spherical Shield Based on Foldable Plate Structures and Scissor Systems'. In: *Integration of Design and Fabrication : Proceedings of the International Association for Shell and Spatial Structures*. International Association for Shell and Spatial Structures Annual Symposium 2023. Melbourne , Australia: IASS, 2023, pp. 2600–2609. ISBN: 978-0-646-87830-0

P-17 Moreno Gata, K., Mueller, C. and Echeverria Valiente, E. 'Designing Strategies for Topological Interlocking Assemblies in Architecture. Flat Vaults'. In: *7-10 October 2019*. Vol. FORM & FORCE 2019 Conference Proceeding. 2019, pp. 2701–2708. URL: https://iass-structures.org/event-2791848

C.3.3 Conference Proceedings and Other Contributions

P-18 Moreno Gata, K., Grizmann, D. and Trautz, M. 'Bauen mit Rohholz – Entwurfs- und Konstruktionsmethoden'. In: *2. Fachkongress Konstruktiver Ingenieurbau: Entwurf und Planung nachhaltiger Bestands- und Neubauten*. Technische Akademie Esslingen e. V: Narr Francke Attempto Verlag GmbH + Co. KG, 2024, pp. 145–148. ISBN: 978-3-381-12781-8

P-19 Moreno Gata, K. 'Experimental Constructions, from Prototypes to Demonstrations'. In: *Strukturen, Formen Und Prinzipien -Festschrift Zum 60. Geburtstag von Univ.-Prof. Dr.-Ing. Martin Trautz*. 1st ed. Aachen: Lehrstuhl für Tragkonstruktionen, 2023, pp. 167–191. ISBN: 978-3-95886-500-6 978-3-95886-503-7

P-20 Moreno Gata, K., Amtsberg, F., Menges, A. and Trautz, M. 'reGrowth — Tragkonstruktionen Aus Ungenutzten Holzabschnitten'. In: *Zukunft Bau Pop-up Campus Aachen*. Vol. 1. Bundesinstitut für Bau-, Stadt-, und Raumforschung (BBSR) im Bundesamt für Bauwesen und Raumordnung (BBR), 2023, pp. 210–213. ISBN: 978-3-98655-049-3. URL: https://www.bbsr.bund.de/BBSR/DE/veroeffentlichungen/sonderveroeffentlichungen/2023/pop-up-campus-aachen-dl.pdf?__blob=publicationFile&v=2 (visited on 13/11/2023)

P-10 Spahn, F., Moreno Gata, K., Trautz, M. and Klinkel, S. 'Image-Based Modelling of Wooden Structures for Structural Computation'. In: *3rd ECCOMAS Thematic Conference on Computational Methods*. Wood Mechanics (CompWood 2023). Dresden, 5–8th Sept. 2023

P-22 Qdeimat, M., Moreno Gata, K. and Trautz, M. *Solidified Natural Rubber Latex (NRL) as a Joint Material in Foldable and Kinetic Structures*. Zurich: ETH Zurich, 2024. 1 p.

P-23 Ramirez, V., Moreno Gata, K., Pranjic, A. and Trautz, M. 'Slabs with Stress-Aligned Ribs: Computational Validation of Their Structural Efficiency'. In: *Proceedings of IASS Annual Symposia*. Redefining the Art of Structural Design. Zürich, 2024

P-24 Saez, D. L., Moreno Gata, K. and Trautz, M. *Repair It with Additive Manufacturing: An Approach to the Circular Economy in Architectural Education*. Guildford: Spatial Structures Research Centre of the University of Surrey, 2021. 278 pp.

P-25 Trautz, M., Grizmann, D., Seiter, A. J., Moreno Gata, K., Pranjic, A. and Saez, D. L. 'Design and Natural Materials – Innovative Approaches for a Sustainable Future Architecture and Structural Engineering'. In: *Proceedings Creative Construction Conference 2023 : CCC 2023, Kezthely, Lake Balaton, 20-23 July 2023*. Budapest: Diamond Congress Ltd, 2023. DOI: 10.3311/CCC2023-073

Posters and Exhibitions

P-26 Moreno Gata, K. 'Naturally grown timber elements as a base for load-bearing structures', Ph.D. Poster, In: *Advance AEC Autumn School 2022*. Stuttgart: Cluster of Escellence IntCDC, Oct. 2022; *"Best Poster Award 1st Place"*

P-27 Moreno Gata, K., Trautz, M., Spahn, F., Klinkel, S. 'Natürlich gewachsene Holzelemente / Bauen mit Rohholz' In: *RWTH Transparent*. Aachen, Jan. 2025

P-28 Moreno Gata, K. 'Building with Raw Timber' In: *Material Flows / Building within Planetary Boundaries; International Symposium / Exhibition: Scales and Practices of Sustainable Development*. Curators: Axel Sowa and Murielle Hladik. Chidori Bunka, Osaka, Apr. 2025

Curriculum Vitae

Personal Data

Title:	M. Sc. & Architect
Last name, first name:	Moreno Gata, Kevin
Current position:	Research Associate, *Trako*
Current institution, country:	RWTH-Aachen University, Germany
ORCID:	0009-0006-3901-8410

Qualifications and Career

Stages	**Periods and Details**
B. Sc. & M. Sc.	*Architecture, 2011–2017, Universidad de Alcalá, Spain*
M. Sc. Exchange	*Architecture, 2014–2015, RWTH Aachen University, Germany*
Advanced Studies	*Advanced Architecture and City, 2017–2018, Universidad de Alcalá, Spain*
Doctorate	*(Dr.-Ing.), 2019–2025, RWTH Aachen University, Germany*

Professional Experience

Position	**Periods and Details**
Research Associate	at *Trako, RWTH Aachen University, Germany, 05.2019–05.2026*
Independent Architect	*Freelance, 09.2018–Present*
Visiting Researcher	at *Digital Structures Research Group, MIT, USA, 08.2018–05.2019*
Product and CAD Designer	*TreeDdesign S.L. for wood artist Jorge Palacios, Spain and USA, 11.2017–08.2018*
Architectural Collaborator	*Ministry of Development, Spain, 02.2017–02.2018*
Research Student Assistant	*Department of Architecture, Universidad de Alcalá, Spain, 01.2016–10.2017*
Research Student Assistant	at *Trako, RWTH Aachen University, Germany, 03.2015–09.2015*

Activities in the Research System: Member of the *International Association for Shell and Spatial Structures (IASS)*, Working Group on *Timber and Bio-based Materials*. Reviewer for *The Royal Society Journal* and participant in international conferences on sustainable and timber construction, *World Conference on Timber Engineering (WCTE)*. Alumni of the *Solar Decathlon Europe (SDE)*. Member of the Madrid's Chamber of Architects *(COAM, N.23332)*.

University and Faculty Committees: At the faculty of architecture, RWTH Aachen University, serving as representative for research associates (*WM-Sprecher*), member of the examination board for the master's program *Construction and Robotics*, deputy representative on the *Faculty Tenure Commission* and on the *Professorship for Construction*.

Academic Distinctions: Gast lecturer at *TU Braunschweig (2025)* in the *Master of Architecture: Robotic Timber Studio* program; and gast lecturer at *Robot Lab*, *Amsterdam University of Applied Sciences (2025)*. *MIT Scholarship (2018)* from Universidad de Alcalá for research at the Massachusetts Institute of Technology (MIT). *Arquia Scholarship (2016)* as one of Spain's top 20 architecture students. Graduated first in class in *Architecture (2017)*, with a final thesis shortlisted for the *2018 Young Architects* competition.